ANTIBIOTIC ADJUVANTS FOR RESISTANT GRAM-NEGATIVE PATHOGENS

SYNTHESIS AND DEVELOPMENT OF ANTIBIOTIC ADJUVANTS TO RESTORE ANTIMICROBIAL ACTIVITY AGAINST RESISTANT GRAM-NEGATIVE PATHOGENS

By MADELAINE ROSE MAI LING COLDEN LEUNG, B.Sc.H.

A Thesis Submitted to the School of Graduate Studies in Partial Fulfilment of the Requirements for the Degree Doctor of Philosophy

McMaster University DOCTOR OF PHILOSOPHY (2019) Hamilton, Ontario (Chemical Biology)

TITLE: Synthesis and Development of Antibiotic Adjuvants to Restore Antimicrobial Activity Against Resistant Gram-Negative Pathogens

AUTHOR: Madelaine Rose Mai Ling Colden Leung, B.Sc.H. (Queen's University)

SUPERVISOR: Professor Alfredo Capretta NUMBER OF PAGES: xix, 229

LAY ABSTRACT

Antibiotics, such as aminoglycosides and carbapenems, are losing their effectiveness against bacteria responsible for deadly diseases. This is often due to resistance enzymes such as aminoglycoside N-acetyltransferase-3 (AAC(3)) and O-nucleotidyltransferase-2" (ANT(2")), which inactivate aminoglycosides, and the New Delhi metallo-β-lactamase-1 (NDM-1), which destroys carbapenems. If these enzymes are blocked, the antibiotics should work against bacteria again.

In order to develop compounds that will inhibit these enzymes, sets of similar compounds are made and tested. Patterns of what chemical groups improve or worsen inhibitory activity are noted and used to make another set of compounds in an iterative process. This thesis describes the development of inhibitors of AAC(3)-Ia and ANT(2")-Ia by this process. Additionally, a specific compound was made to test if a particular chemical group has a role in inhibiting NDM-1.

ABSTRACT

Widespread antimicrobial resistance, particularly in Gram-negative pathogens, is a serious threat facing the global community. Aminoglycosides are inactivated by enzymes such as aminoglycoside N-acetyltransferase-3 (AAC(3)) and O-nucleotidyltransferase-2" (ANT(2")), while the New Delhi metallo-β-lactamase-1 (NDM-1) degrades carbapenems. Inhibition of these enzymes should result in bacteria becoming once again susceptible to aminoglycosides and carbapenems. This thesis describes the development of inhibitors to these enzymes, in an effort to rescue the utility of aminoglycoside and carbapenem drug classes through adjuvant therapy.

High-throughput screening of protein kinase libraries identified two AAC(3)-Ia inhibitors with a common 3-benzylidene-2-indolinone core. New methods for purification of AAC(3)-Ia and monitoring its activity were developed. A chemical library was built around this scaffold and assessed for SAR. It was found that the initial hit (*Z*)-methyl 3-(3,5-dibromo-4-hydroxybenzylidene)-2-oxoindoline-5-carboxylate was the most active against AAC(3)-Ia, and alterations to either the 3,5-dibromo-4-hydroxybenzyl warhead or methyl ester substituent resulted in a decrease in activity.

Previous whole-cell screening had identified two protein kinase inhibitors with a biphenyl isonicotinamide scaffold as inhibitors of ANT(2")-Ia. A convergent parallel synthesis was developed, involving Suzuki and amide couplings and protecting group strategies. This methodology was used to assemble

a focused chemical library for SAR analysis. Stepwise removal of extraneous complexity from the initial hits yielded a selective ANT(2")-Ia inhibitor which demonstrated *in vivo* synergy with gentamicin.

Aspergillomarasmine A (AMA) is a natural product with activity against NDM-1. Several derivatives of AMA have been synthesized to assess SAR, but the specific contributions of individual carboxylic acids have yet to determined due to difficulties accessing position 6. A synthetic approach was developed *via* reductive amination using Garner's aldehyde as a serine equivalent. This strategy was used to synthesize an AMA analog with a hydroxyl group in place of the carboxylic acid in position 6. Additionally, an imine-promoted isomeric resolution was discovered.

ACKNOWLEDGMENTS

I am so grateful to the many people who have supported and guided and encouraged me throughout the years, including:

My supervisor, Dr. Fred Capretta, who struck a perfect balance between letting me learn through experience and passing on his impressive wealth of chemistry knowledge. I am especially appreciative of his support as I navigated the MD/PhD program, and explored where the degree could take me after graduation.

The members of my supervisory committee, Drs. Gerry Wright and Peter Margetts, for their unique expertise and guidance, both in their respective fields and in the overlap of chemistry, microbiology, and medicine.

The past and present members of the Capretta, Wright, and Brennen groups, and the Biointerfaces Institute. In particular, Dr. Mehdi Keramane, for imparting chemistry skills and career advice, while keeping me from accidentally blowing up the lab; Linda Ejim and Dawn White, for their patient instruction as I fumbled assay after assay; and Dr. Kalinka Koteva for sharing her extensive knowledge of natural product synthesis.

Also, thank-you to Dr. Yuichi Terazono, an honorary group member who responded to every "is this bad…?" with a smile and calm demeanor.

Tammy Feher, who has gone above and beyond so many times for me and the rest of the chemical biology department.

Dr. Mackenzie Elliot FitzSimmons, for his lionizing support, proof-reading, and apt, if somewhat biting, commentary.

My colleagues both in medicine and in chemistry, who were always there to encourage and lend a hand when I got overwhelmed, and made feel a part of both communities.

My mother, Ruth Hackett, who taught me my first chemistry lessons as I covered the kitchen ceiling with my chocolate chip cookie dough “reaction” (not much has changed in that regard as the orange splotch on the roof of my fumehood can attest), and has been putting up with my science experiments ever since.

And the rest family and friends, for their encouragement and support and nodding and smiling as I rambled on about something that made no sense. I would not be where I am today without you.

TABLE OF CONTENTS

1.0 Introduction 1
1.1 Medicinal Chemistry and Drug Discovery 1
1.1.1 Combinatorial Chemistry 6
1.1.2 Antimicrobial Chemistry 11
1.2 Antimicrobial Resistance 13
1.2.1 Mechanisms of Resistance 15
1.2.2 The ESKAPE Pathogens 17
1.3 Resistance in Gram-Negative Pathogens 20
1.3.1 Aminoglycoside Antibiotic Mechanisms of Action and Resistance 21
1.3.1.1 Aminoglycoside N-Acetyltransferase-3 24
1.3.1.2 Aminoglycoside O-Nucleotidyltransferase-2" 25
1.3.2 β-Lactam Antibiotic Mechanisms of Action and Resistance 26
1.3.2.1 New Delhi Metallo-β-Lactamase-1 37
1.4 Combination Therapy 38
1.4.1 Antimicrobial Combination Therapy 40
1.4.2 Adjuvant Therapy 41
1.4.2.1 Serine β-Lactamase Inhibitors 42
1.4.2.2 Metallo-β-Lactamase Inhibitors 44
1.4.2.3 Aminoglycoside Modifying Enzyme Inhibitors 47
1.5 Statement of Thesis 48
1.6 References 49

2.0 Development and Structure-Activity Relationship Analysis of Substituted Indolinones as Aminoglycoside 3-N-Acetyltransferase AAC(3)-IA Inhibitors 71
2.1 Background 71
2.2 Screening and Target Identification 73
2.3 Indolinone Library Synthesis 76
2.4 Structure-Activity Relationship Analysis 79
2.5 Implications and Future Work 83
2.6 Experimental 84
2.6.1 Synthesis 84
2.6.2 Biological Testing 95
2.7 References 98
2.8 Supplementary Data 103

3.0 Development and Structure-Activity Relationship Analysis of Biphenyl Isonicotinamides as Aminoglycoside 2"-O-Nucleotidyltransferase ANT(2")-IA Inhibitors 127
3.1 Background 127

3.2 Parallel Synthesis Methodology 130
3.3 Structure-Activity Relationship Analysis 139
3.4 Implications and Future Work 145
3.5 Experimental 147
3.5.1 Synthesis 147
3.5.2 Biological Testing 163
3.6 References 165
3.7 Supplementary Data 169

4.0 Synthesis of Aspergillomarasmine A (AMA) Analogs and Inhibitors of the New Delhi Metallo-β-Lactamase-1 (NDM-1) 190
4.1 Background 190
4.2 Previous Total Syntheses and SAR Analysis 191
4.3 Synthetic Strategy to Access Position 6 of AMA 196
4.4 Attempted Total Synthesis of AMA Using Garner's Aldehyde 199
4.5 Kinetic Resolution of (*S,R*)-Stereoisomer 200
4.6 Implications and Future Work 203
4.7 Experimental 203
4.8 References 209
4.9 Supplementary Data 212

5.0 Conclusions and Future Directions 222
5.1 References 227

LISTS OF FIGURES AND TABLES

List of Figures

Figure 1-1 Aminoglycoside Antibiotics…… 22
Figure 1-2 Mechanisms of Aminoglycoside Inactivation…….... 26
Figure 1-3 β-Lactam Antibiotics……..…….... 27
Figure 1-4 Mechanism of Carbapenem Hydrolysis by New Dehli Metallo-β-Lactamase-1…… 38
Figure 1-5 Inhibitors of β-Lactamases……... 43
Figure 1-6 Inhibitors of Aminoglycoside-Modifying Enzymes ……....…… 48

Figure 2-1 Mechanism of Gentamicin Inactivation by AAC(3)-Ia ...……..... 72
Figure 2-2 AAC(3)-Ia-Coupled Ellman Assay …….... 74
Figure 2-3 Confirmed Hits from GlaxoSmithKline and Bio Screen-Well Kinase Inhibitor Libraries ……..... 75
Figure 2-4 Synthetic Scheme for Parallel Synthesis of AAC(3)-Ia Inhibitor Library ……... 76
Figure 2-5 Mechanism of Imine-Promoted Knoevenagel Aldol Condensation …… 77
Figure 2-6 Indolinone Library with Reaction Conditions and Isomeric Ratios ……..... 78
Figure 2-7 AAC(3)-Ia Inhibitors with IC_{50} Values ……. 82
Figure 2-8 Checkerboard Assay for Interaction of **II-1** and Gentamicin in *E. coli* BW25113 Δ*tolC*Δ*bamB* pGDP:*aac(3)-Ia* …….…… 83
Figure 2-9 Checkerboard Assay for Interaction of **II-11** and Gentamicin in *E. coli* BW25113 Δ*tolC*Δ*bamB* pGDP:*aac(3)-Ia* ……...……... 83

Figure 3-1 Mechanism of Gentamicin Inactivation by ANT(2”)-Ia ……. 128
Figure 3-2 Hits from Cell-Based ANT(2”)-Ia Screen with the Common Biphenyl Isonicotinamide Scaffold ……. 129
Figure 3-3 Initial Parallel Synthetic Route ……... 131
Figure 3-4 Suzuki Mechanism …….. 131
Figure 3-5 Possible Suzuki Coupling Partners ……. 132
Figure 3-6 Suzuki Ligand Structures ……..... 133
Figure 3-7 Formation of 5’-Amino-2’-Methyl-[1,1’-Biphenyl]-4-Carboxylic Acid (**III-17**) ……..... 135
Figure 3-8 HATU/HBTU Coupling Combination …… 136
Figure 3-9 Sample Amide Coupling *via* Thionyl Chloride Activation and Reaction Mechanism…… 136
Figure 3-10 Sample Amide Coupling Using EDC …….. 137
Figure 3-11 Revised Parallel Synthesis Strategy ……..... 138
Figure 3-12 S_NAr Reaction of Isonicotinic Acid in Morpholine ……. 138
Figure 3-13 ANT(2”)-Ia Inhibitor Library …….. 140
Figure 3-14 *E. coli* BW25113 Δ*tolC*Δ*bamB* pGDP:*ant(2”)-Ia* Screening Results ……..... 141

Figure 3-15 *E. coli* BW25113 Δ*tolC*Δ*bamB* Screening Results and MICs …. 142
Figure 3-16 Dose-Dependency and MIC Determinations for **III-21** and **III-30** in *E. coli* BW25113 Δ*tolC*Δ*bamB* pGDP:*ant(2")-Ia*……. 143
Figure 3-17 Checkerboard Assays for Interaction of **III-21** and Gentamicin in *E. coli* BW25113 Δ*tolC*Δ*bamB* pGDP:*ant(2")-Ia* ……... 144
Figure 3-18 Checkerboard Assays for Interaction of **III-30** and Gentamicin in *E. coli* BW25113 Δ*tolC*Δ*bamB* pGDP:*ant(2")-Ia* ……... 144
Figure 3-19 Pyrophosphatase-Coupled ANT(2")-Ia Assay ……... 146

Figure 4-1 Deconstruction of Aspergillomarasmine A (AMA) …… 192
Figure 4-2 Koteva's Synthesis of AMA *via* Aziridine Ring-Opening Reactions …… 193
Figure 4-3 Liao's Synthesis of AMA *via* Reductive Amination of Acetonide-Diols …….. 194
Figure 4-4 Albu's Synthesis of AMA *via* Sulfamidate Ring-Opening Reactions …… 194
Figure 4-5 Zhang's Synthesis of AMA *via* Mitsunobu Couplings …… 195
Figure 4-6 Summary of SAR Analysis of AMA Derivatives Performed by Koteva, Albu, and Zhang, and Colleagues …….. 195
Figure 4-7 Synthetic Route to 6-Hydroxy AMA Analog **IV-8** ……. 197
Figure 4-8 Planned Total Synthesis of Aspergillomarasmine A Using Garner's Aldehyde …….. 200
Figure 4-9 X-Ray Crystallographic Structure of **IV-3** …….. 202
Figure 4-10 Possible Mechanism of Reductive Amination and Kinetic Resolution …….. 203

Figure 5-1 Lead AAC(3)-Ia Inhibitor **II-1** ……... 224
Figure 5-2 Lead ANT(2")-Ia Inhibitor **III-30** ……... 225
Figure 5-3 AMA Analog **IV-8** and Other Potential Analogs That Could Be Synthesized *via* Reductive Amination of Garner's Aldehyde-Like Building Blocks ……. 227

List of Tables

Table 1-1 Commonly Used Absorption-Distribution-Metabolism-Excretion-Toxicity (ADMET) Assays ……..……. 4

Table 2-1 Methyl Ester Hydrolysis Conditions Tested …….. 79

Table 3-1 Suzuki Coupling Conditions Screened ……... 134

Table 4-1 Reaction Conditions Tried for Second Reductive Amination …. 201

LISTS OF ABBREVIATIONS AND SYMBOLS

–Ar	Aromatic Group
Δ	Heated
2,2-DMP	2,2-Dimethoxypropane
AAC	Aminoglycoside Acetyltransferase
ABC	ATP-Binding Casette
ACE	Angiotensin-Converting Enzyme
Acetyl-CoA or Ac-CoA	Acetyl Coenzyme A
ACN	Acetonitrile
AcOH or HOAc	Acetic Acid
ACT	Artemisinin-Based Combination Therapy
ADMET	Absorption-Distribution-Metabolism-Excretion-Toxicity
AIDS	Acquired Immune Deficiency Syndrome
Ala	Alanine
ALT	Alanine Aminotransferase
AMA	Aspergillomarasmine A
AMB	Aspergillomarasmine B
AME	Aminoglycoside-Modifying Enzyme
anh	Anhydrous
ANT	Aminoglycoside Nucleotidyltransferase
APH	Aminoglycoside Phosphotransferase
aq	Aqueous
Ar	Argon
Asp	Aspartic Acid
AST	Aspartate Aminotransferase
ATP	Adenosine Triphosphate
AU	Absorbance Units
B-thuj	β-Thujaplicinol
BIOS	Biology-Oriented Synthesis
Boc	*tert*-Butoxycarbonyl
Boc_2O	Di-*tert*-Butyl Dicarbonate
BODIPY FL	Boron-Dipyrromethene (4,4-Difluoro-4-Bora-3a,4a-Diaza-s-Indacene) Fluorophore
BZT	Bisthiazolidine
Caco-2	Caucasian Colon Adenocarcinoma-2
CbzCl	Benzyl Chloroformate
CCK	Cholecystokinin
$CDCl_3$	Deuterated Chloroform
CF_3SO_3H	Triflic Acid
cLogP	Corrected Partition Coefficient

COSY	Correlation Spectroscopy
cP450 or CYP	Cytochrome P450
CrO_3	Chromium Trioxide
Cs_2CO_3	Cesium Carbonate
CSA	Camphorsulfonic Acid
CtD	Complexity-to-Diversity
D_2O	Deuterium
DAA	Direct-Acting Antiviral Agents
dba	Dibenzylideneacetone
DCE	1,2-Dichloroethane
DCM	Dichloromethane
DEAD	Diethyl Azodicarboxylate (Mitsunobu Reagent)
DEM	Disodium 2,3-Diethylmaleate
DEPT Q	Distortionless Enhancement by Polarization Transfer Including Detection of Quaternary Nuclei
DIBAL	Diisobutylaluminum Hydride
DIPEA	N,N-Diisopropylethylamine (Hunig's Base)
DME	1,2-Dimethoxyethane
DMF	Dimethylformamide
DMP	Dess-Martin Periodinane
DMSO	Dimethyl Sulfoxide
DMSO-d_6	Deuterated Dimethyl Sulfoxide
DNA	Deoxyribonucleic Acid
DNase	Deoxyribonuclease
DNTB	5,5'-Dithiobis-(2-Nitrobenzoic Acid) (Ellman's reagent)
DOS	Diversity-Oriented Synthesis
DTS	Diverted Total Synthesis
ECE	Endothelin-Converting Enzyme
EDC	1-Ethyl-3-(3-Dimethylaminopropyl)carbodiimide
eDNA	Environmental DNA
EDTA	Ethylenediamine-*N,N,N',N'*-Tetracetic Acid
EMB	Ethambutol
ESBL	Extended-Spectrum β-Lactamase
ESI	Electrospray Ionization
ESKAPE	*Enterococcus faecium*, *Staphylococcus aureus*, *Klebsiella pneumoniae*, *Acinetobacter baumannii*, *Pseudomonas aeruginosa*, and *Enterobacter* species
EtOAc	Ethyl Acetate

EtOH	Ethanol
FBDD	Fragment-Based Drug Design
FDA	Federal Drug Administration
FIC	Fractional Inhibitory Concentration
FOS	Function-Oriented Synthesis
Gent	Gentamicin
GTP	Guanosine Triphosphate
H_2	Hydrogen Gas
H_2O	Water
H_2SO_4	Sulfuric Acid
HAART	Highly-Active Anti-Retroviral Treatment
HATU	1-[Bis(dimethylamino)methylene]-1*H*-1,2,3-Triazolo[4,5-*b*]pyridinium 3-Oxid Hexafluorophosphate
HBTU	*N,N,N′,N′*-Tetramethyl-*O*-(1*H*-Benzotriazol-1-yl)uronium Hexafluorophosphate
HCl	Hydrochloric Acid
HCV	Hepatitis C Virus
Hep G2	Hepatoma G2
HEPES	4-(2-Hydroxyethyl)-1-Piperazineethanesulfonic Acid
hERG	Human Ether-a-go-go Related Gene
hex	Hexanes
His	Histidine
HIV	Human Immunodeficiency Virus
HPLC	High Performance Liquid Chromatography
HRMS	High Resolution Mass Spectrometry
HTS	High-Throughput Screening
IC_{50}	Half Maximal Inhibitory Concentration
IDSA	Infectious Disease Society of America
IMP	Imipenemase
INH	Isoniazid
INSTI	Integrase Strand Transfer Inhibitor or Integrase Inhibitor
iPrOH	Isopropanol
IPTG	Isopropyl b-d-1-Thiogalactopyranoside
IV	Intravenous
K_2CO_3	Potassium Carbonate
K_3PO_4	Potassium Phosphate
$KMnO_4$	Potassium Permanganate
KPC	*K. pneumoniae* Carbapenemase
Lac	Lactate

LB	Lysogeny Broth
LC	Liquid Chromatography
LDH	Lactate Dehydrogenase
LiBr	Lithium Bromide
LiOH	Lithium Hydroxide
LPS	Lipopolysaccharide
MAP	Mitogen-Activated Protein
MATE	Multidrug and Toxin Compound Extrusion
MBL	Metallo-β-Lactamase
MDCK	Madin-Darby Canine Kidney
MDR	Multidrug Resistant
MDR1	Multidrug Resistance Protein 1 (P-Glycoprotein 1, ATP-Binding Cassette B1)
Me_3SnOH	Trimethyl Tin Hydroxide
MeOH	Methanol
MFS	Major Facilitator Superfamily
MHB	Mueller Hinton Broth
MIC	Minimum Inhibitory Concentration
mRNA	Messenger Ribonucleic Acid
MRSA	Methicillin-Resistant *S. aureus*
MS	Mass Spectrometry
MsCl	Methanesulfonyl Chloride
MTT	3-(4,5-Dimethyl-Thiazol-2-yl)-2,5-Diphenyl Tetrazolium Bromide
N_2	Nitrogen Gas
$NaBH_3CN$	Sodium Cyanoborohydride
NaCl	Sodium Chloride
NADPH	Dihydronicotinamide-Adenine Dinucleotide Phosphate
$NaHCO_3$	Sodium Bicarbonate
$NaIO_4$	Sodium Periodate
NaOH	Sodium Hydroxide
NDM	New Delhi Metallo-β-Lactamase
NEt_3	Triethylamine
NH_4	Ammonium
NMR	Nuclear Magnetic Resonance
NNRTI	Non-Nucleoside Reverse-Transcriptase Inhibitor
NOE or NOESY	Nuclear Overhauser Effect Spectroscopy
NOTA	1,4,7-Triazacyclo- Nonane-1,4,7-Triacetic Acid
NRTI	Nucleoside Reverse-Transcriptase Inhibitor
NsCl	2-Nitrobenzenesulfonyl Chloride

O_3	Ozone
OAc	Acetate
OD	Optical Density
OXA	Oxacillinase
$PAPh(OMe)_2$	2,4-Dimethoxyphenyl Phosphaadamantane
PBP	Penicillin-Binding Protein
Pd	Palladium
Pd/C	Palladium on Carbon
PhSH	Thiophenol
PMSF	Phenylmethylsulfonyl Fluoride
PPh_3	Triphenyl Phosphine
PRP	Pentapeptide Repeat Protein
PXRE	Pregnane-X-Receptor Response Element
PyBop	Benzotriazole-1-yl-Oxy-Tris-Pyrrolidino-Phosphonium Hexafluorophosphate
PZA	Pyrazinamide
R_f	Retention Factor
RFU	Relative Fluorescence Units
RIF	Rifampin
RND	Resistance-Nodulation-Cell Division
RO5	Rule of Five
RT	Room Temperature
R_t	Retention Time
$RuCl_3$	Ruthenium (III) Chloride
SAR	Structure-Activity Relationship
SBL	Serine β-Lactamase
SDS-PAGE	Sodium Dodecyl Sulfate Polyacrylamide Gel Electrophoresis
Ser	Serine
SMR	Small Multidrug Resistance
S_NAr	Nucleophilic Aromatic Substitution
$SOCl_2$	Thionyl Chloride
SOSA	Selective Optimization of Side Activities
SPR	Surface Plasmon Resonance
STAB	Sodium Triacetoxyborohydride
^{t}BuXPhos	2-Di-*tert*-Butylphosphino-2',4',6'-Triisopropylbiphenyl (Buchwald ligand)
TFA	Trifluoroacetic Acid
THF	Tetrahydrofuran
TLC	Thin Layer Chromatography
TNB^{2-}	2-Nitro-5-Thiobenzoate

TOF	Time of Flight
tol	Toluene
TPA	Tris-Picolylamine
TSA	Thermal Shift Assay
TsOH	p-Tolenesulfonic Acid
UV	Ultraviolet Light
VISA	Vancomycin-Intermediate *S. aureus*
VRE	Vancomycin-Resistant Enterococci
VRSA	Vancomycin-Resistant *S. aureus*
WHO	World Health Organization
XDR	Extensively Drug Resistant
μW	Microwave

DECLARATION OF ACADEMIC ACHIEVEMENT

CHAPTER 2 CONTRIBUTIONS

I optimized a bead-based purification method for AAC(3)-Ia. I developed a fluorescence-based AAC(3)-Ia assay protocol with which I performed SAR analysis of the indolinone library, and I followed up promising compounds with cell-based synergy assays. Marisa Azad performed initial screens. Kyle Leckett developed the synthetic strategy, and together with Xiaomeng Li and I, built the chemical library tested. Linda Ejim provided the preliminary screening and IC_{50} results using the AAC-coupled Ellman assay. I am indebted to Dawn White and Dr. Juliana Milojevic for their assistance in developing the AAC(3)-Ia purification methodology.

CHAPTER 3 CONTRIBUTIONS

I developed the synthetic methodology and assembled the chemical library. I tested the library on enzyme and cell-based assays, including synergy assays. Dr. Georgina Cox purified ANT(2")-Ia enzyme and performed the initial screens. Horace Huang assisted with library synthesis.

CHAPTER 4 CONTRIBUTIONS

I optimized the reductive amination and product purification and completed the rest of the synthesis. Dr. Silvia Albu developed the initial reductive amination of Garner's aldehyde protocol. Dr. Kalinka Koteva provided valuable expertise

regarding the aziridine ring-opening reaction and subsequent deprotections. Drs. James Britten and Chris Frampton provided X-ray crystallographic analysis.

1.0 INTRODUCTION

1.1 MEDICINAL CHEMISTRY AND DRUG DISCOVERY

Though medical prescriptions have been recorded since before 1500 BC,[1] a systematic approach to drug discovery really only began in 1907 with Paul Ehrlich's screening of arsenic compounds (initially against trypanosomes), and subsequent identification anti-syphilitic arsphenamine (Salvarsan) in 1909.[2] The drug discovery and development process of modern times is even more intensive. Theoretically, before work on a specific drug can even begin, a target must be identified and validated.[3–5] This process often starts with bioinformatics, followed up with basic science research and integration of clinical feedback to ensure that the target is relevant, without obvious safety concerns, and "druggable": accessible to and able to bind a potential drug with high affinity in order to provoke a measurable response.[3,6,7] A vast and expanding assortment of tools are available to aid in target validation, including antibodies, recombinant proteins, inducible gene knock-outs and knock-ins, RNA interference, and small molecule probes.[3,6]

Once there is a validated target, an assay can be developed. There are two main types of assay: cell-based, where the target is overexpressed to assess functional response, and biochemical, where the target protein is purified; results from biochemical assays usually give a measure of the affinity of the hit for its target.[3] The type and features of the assay chosen depend on the target and desired modification (activation, modulation, or inhibition), but relevance, reproducibility, cost, and quality need to be considered.[3,8,9] Positive and negative controls are

tested to determine the screening window and quality of the assay for high-throughput screening.[3,10] This is done through calculation of the Z' factor, which compares the data variability to the relative signal intensity; Z' $\geq$ 0.5 indicates a robust screening assay.[10]

There are various approaches to screening: high-throughput screens (HTS) are usually only done by large pharmaceutical companies due to the cost of building and maintaining the huge compound collections required, although there has been a movement towards collaborations with academic centres for screening as a cost-cutting measure.[3,11,12] The average pharmaceutical library houses 1 million compounds and can screen up to 200 (384- or 1536-well) plates a day, with hit rates ranging from 0.01% (or less) to 3%.[3,6,13–15] Antagonist screens typically have higher hit rates due to false positives from signal interference.[3] Focused (or knowledge-based) screens involve subsets of libraries with higher probabilities of interacting with the target, based on previous screens of related targets and other insights found in the literature.[3,9,11] Adjunct screening strategies include fragment-based screens (where compound fragments added to crystalized proteins and visualized by X-ray or NMR are linked to build molecules with desired binding properties), virtual screens (virtual compounds are docked into the protein crystal structure), and physiological or phenotypic screens (effects of the drug are tested at the tissue rather than cellular or biochemical level).[3]

Once "hits" are identified through primary screens, and confirmed with follow-up assays, medicinal chemistry- the development of molecules to treat disease states, begins. Structure-activity relationships (SAR) are explored by

adding or removing various parts of the molecule and analyzing the effect on potency, selectivity, and physicochemical properties.[3,4,6,11] This is an iterative process resulting in one or more leads which can go on to pre-clinical testing.[3–5]

Pre-clinical testing is often done in tandem with hit-to-lead optimization to give early feedback regarding toxicity and pharmacokinetics, as poor bioavailability, metabolic instability, drug-drug interactions, and other toxicity issues are responsible for up to 90% of drug candidate failure.[4,5,16] There are many *in vitro* assays available to assess these ADMET (absorption-distribution-metabolism-excretion-toxicity) properties (Table 1-1), though ultimately these parameters must be evaluated in animal models.[3,4,16] The choice of animal model is dependent on the therapy indication, but the Federal Drug Administration (FDA) and other regulatory bodies generally require safety data from two different species, at least one of which must be non-rodent.[4,5] Mice, rats, dogs, and primates are the most commonly used models.[4] These studies provide important information about the pharmacodynamic, pharmacokinetic, and safety profiles, allowing predictions of the dosing levels and regimens required for efficacy (via allometric scaling), drug metabolism and interactions with food or other drugs, and toxicity (including neurological, cardiovascular, hepatic, pulmonary, and reproductive toxicity and carcinogenicity).[4,5] Animal studies should include higher doses and longer durations than those expected for human testing, and pharmaceutical-grade purity is not required at this step, though the formulation and production methods should be established by this point, with all impurities identified and no single impurity present at greater than 0.5%.[4,5]

Table 1-1. Commonly Used Absorption-Distribution-Metabolism-Excretion-Toxicity (ADMET) Assays (Summarized from references 3, 4, and 16)

Absorption	Caco-2 cells ± verapamil (intestinal)
	MDR1-MDCK cells (intestinal and CNS permeability, efflux)
Drug metabolism	Liver microsomes and NADPH (Phase I)
	S9 fraction (Phase I and II)
	Hepatocytes
Inhibitory drug-drug interaction (increased toxicity)	Genetically-engineered microsomes with one human cP450 isoform and fluorescent substrates
	Liver microsomes with isoform-specific cP450 substrates: ex. testosterone for isoform CYP3A4 and dextromethorphan for CYP2D6
	Pooled hepatocytes and isoform-specific cP450 substrates
Inductive drug-drug interaction (therapeutic failure)	PXRE-luciferase assay (CYP3A4)
	Hepatocytes and isoform-specific cP450 substrates
	Hepatocytes and Western or northern blotting (to detect P450 isoform proteins or mRNA respectively)
Toxicity	hERG channel activity (cardiac effects)
	Hep G2 cells (hepatotoxicity)
	ATP measurement via luciferin-luciferase assay
	MTT assay (mitochondrial activity)
	Cytoplasmic enzyme release (membrane integrity): LDH, ALT, AST
	Neutral red uptake (lysosomal activity)
	Radiolabeled precursors (DNA, RNA, or protein synthesis)
	Glutathione measurement using *O*-phthaldehyde (toxic metabolites)
	Caco-2: Caucasian colon adenocarcinoma-2; MDR1: multidrug resistance protein 1 (p-glycoprotein 1, ATP-binding cassette B1) ; MDCK: Madin-Darby canine kidney; NADPH: dihydronicotinamide-adenine dinucleotide phosphate; cP450 or CYP: cytochrome P450; PXRE: pregnane-X-receptor response element; hERG: human Ether-a-go-go Related Gene; Hep G2: Hepatoma G2; MTT: 3-(4,5-dimethyl-thiazol-2-yl)-2,5-diphenyl tetrazolium bromide; LDH: lactate dehydrogenase; ALT: alanine aminotransferase; AST: aspartate aminotransferase

It is only after robust animal studies that an Investigational New Drug

application can be filed for the compounds (now called drug candidates) to be tested in humans. There are four stages of clinical trials. Phase 1 trials involve 10-50 healthy subjects (unless the drug carries significant risk of adverse effects or involves invasive procedures for administration, in which case they are tested in patients most likely to benefit), looking for adverse drug effects not picked up in pre-clinical testing and to establish the pharmacokinetic profile in humans. Phase 2 trials test the drug candidate on a small group (50-250) of affected patients, looking for efficacy and to establish dosing regimens before the large, expensive Phase 3 trials commence. Phase 2 trials are randomized, controlled, and blinded, but surrogate rather than clinical endpoints are usually used due to the size. Phase 3 are massive studies (up to 1500 patients over various time points) assessing clinical endpoints to confirm that the drug is safe and effective for its given indication; the FDA generally requires two Phase 3 trials demonstrating efficacy at $p < 0.05$.[4] Phase IV trials are longitudinal studies after drug approval looking for long-term complications.[17]

This is a costly process, with the average drug taking 12 years and costing $1 billion USD.[4] Pre-clinical studies alone can cost $1 million. Along the way, many compounds are discarded, with only 10% of leads making it through preclinical development, and 80-90% of those failing during clinical development, especially in Phase 2 trials.[3–5] Approved drugs can also be pulled off the market for toxicity issues.[16] In addition, the regulatory environment is extremely complex, with stringent requirements for compound manufacturing and testing, although there are procedures in place to fast-track desperately needed drugs.[4]

1.1.1 COMBINATORIAL CHEMISTRY

Combinatorial chemistry is a method of synthesizing large numbers of compounds using combinations of interchangeable building blocks, generally for the purpose of building libraries for screening.[18] There are two main subsets of combinatorial chemistry: split-pool synthesis and parallel synthesis. In the split-pool method, a set of reactions are conducted using different reagents, the products of which are pooled and divided for the next synthetic step.[19] Compounds are screened in mixtures, and mixtures containing hits are then de-convoluted.[12,19] In contrast, during parallel synthesis, each reaction is set up separately, and the identity of hits does not need to be determined following screening.[12]

Geysen *et al.* was one of the earliest groups to use a combinatorial approach. Building off the broad applicability of Merrifield's solid phase peptide synthesis,[20] a library of 400 peptide analogs was made and screened against monoclonal antibodies to deduce the sequence of viral epitopes.[21] Solid phase synthesis was rapidly adapted to small molecules, and the first small molecule combinatorial library followed in 1992.[22,23] Coupled with technological advances in high-throughput screening around the same time (implemented between 1989 and 1991), the popularity of this methodology skyrocketed.[8,24,25] However, as intensive but indiscriminate screening yielded few useable drug leads (no drugs from purely combinatorial origins were approved until 2005, and only two since), people began look for ways of focusing screening efforts.[6,9,25–27]

After studying orally-available compounds that reached phase II clinical trials, Lipinski noted that approximately 90% of them shared similar

physicochemical properties, thus engendering his famous Rule of Five (RO5) for druglikeness:[24]

- No more than 500 Da
- No more than 5 hydrogen-bond donors
- No more than 10 hydrogen-bond acceptors
- cLogP not greater than 5

A fifth rule- no more than ten freely-rotatable bonds, is usually added to round them out.[28] Follow-up criteria were later added for lead-likeness, to compensate for the fact that mass and complexity are habitually added during the drug optimization process:[29,30]

- No more than 350 Da
- cLogP not greater than 3
- Affinity of approximately 0.1 μM

Benjamin Evans coined the term "privileged" to describe scaffolds that were over-represented in unrelated, biologically-active drug families (for example, indoles, biphenyls, quinolines, and benzoxazoles) and surmised that they must be in possession of distinctive properties not found by the majority of compounds populating chemical space.[6,12,31,32]

Camille Wermuth built on this idea with her selective optimization of side activities (SOSA) approach. SOSA involves screening libraries of already approved drugs against new targets then optimizing their activity and selectivity using medicinal chemistry techniques.[15,33] Since only compounds that had already been shown to be biologically-relevant (and had compiled human pharmacokinetic

and safety data) were included, libraries could be much smaller (approximately 1000 compounds) and any hits would be unlikely to have significant toxicity or bioavailability issues.[15,33] This approach is not uncommon, as pharmaceutical screening libraries are often populated by compounds made during previous optimization campaigns.[30] An early example of this approach was the use of a sulfonamide antibiotic as a lead for phase II drug for congestive heart failure by Bristol-Myers-Sqibb.[34] More recently, Pollinger *et al*. combined this approach with computational modeling to derive a PPARα modulator.[35]

Stuart Schreiber proposed a different a solution: diversity-oriented synthesis (DOS).[36] DOS uses short (three- to five-step) synthetic strategies to build libraries with as much diversity (in terms of appendages, functional groups, stereochemistry, and the underlying scaffolds) as possible.[11,12,18,37] Diversity is developed in one of two ways: in the reagent-based approach is a differentiating process, where a common starting material is subjected to different reaction conditions.[11,37] The starting material chosen must either have many functional groups, or one functional group with versatile reactivity.[11] In the substrate-based approach, the starting material is pre-modified by σ-elements so that the same reaction conditions produce different products; this is termed a "folding process" in reference to the analogous folding of amino acid chains into proteins.[11,37] Library members are typically three-dimensional, natural product-like compounds with abundant chiral centres, and cascade, multicomponent, and pericyclic or ring-closing reactions are commonly employed in their synthesis.[9,11,18] Although DOS is often saddled with the auspicious goal of developing small molecule probes for every biological target, in

reality DOS libraries tend to be much smaller than traditional combinatorial libraries, while still accessing much more chemical space.[6,11,12,18] This strategy is especially useful for poorly characterized or undruggable targets, multi-target pathways, and exploring biological systems.[9,12,18]

Complexity-to-diversity (CtD) is an off-shoot of this strategy, where the natural product starting material provides initial complexity, and the various functional groups present are treated with one or more reaction conditions to increase diversity in a combinatorial fashion.[38,39]

Samuel Danishefsky's approach was somewhere in between. Noting the widespread therapeutic success of natural products (over half of drugs on the market at that time were natural product or natural product-derived, and even with the advent of biologics and vaccines, natural products and their derivatives account for approximately a third of approved drugs, nearly two thirds in enriched areas such as antibacterial drugs),[26,27,40] he proposed a method that involves diverting total synthesis of natural products to allow simultaneous development and testing of analogs: diverted total synthesis (DTS).[25,36,41] In this way, evolutionary pressures are exploited as an intensive preliminary screening, followed by SAR analysis to enhance activity and remove unnecessary complexity.[25,36,41]

Biology-oriented synthesis (BIOS), proposed by Herbert Waldman, similarly takes note of the small subset of chemical space occupied by natural products, and likens it to the conservation of protein folds.[42,43] Waldman posited that, as nature selected for three-dimensional structures of proteins, it also selected for chemical compounds to interact with them; therefore, proteins with similar folds

should interact with the same scaffold.[43] Just as chemical scaffolds are tuned by the addition of different functional groups, the binding site set by the protein fold is modified by the specific amino acid sequence.[43] Thus, in this approach, natural products are deconstructed down into their base, single-ringed parent scaffolds that will interact with the members of the protein structure cluster, and then built up into simplified analogs that retain the activity of the more complex molecules but with better selectivity for the target.[42,43] Known inhibitors of the related proteins can instruct scaffold deconstruction and analog development, and may be useful in predicting drug side effects.[43]

Fragment-based drug design (FBDD), first theorized by William Jencks in 1981[44] and reported by Abbott researchers in 1996,[45] takes the reductionist approach to the extreme. Simple molecular "fragments" (compounds with molecular masses less than 300 Da, less than three rotatable bonds, less than three hydrogen-bond donors or acceptors, cLogP no greater than three, and with generally less than 20 non-hydrogen atoms) are screened at high concentrations against a protein target.[11,45,46] Initial hits have very poor affinities for the protein of interest (micro- or even millimolar concentrations), but they can quickly and easily be optimized to high-affinity (nanomolar) leads by "linking" multiple low-affinity fragments, "merging" their features, or "growing" the fragment based on knowledge about the binding site.[11,45,46] This method has wide applicability, targeting even the notoriously difficult protein-protein interactions as the streamlined fragments can identify and bind tiny pockets inaccessible to larger compounds, and binding site information is built into the screening process.[45,46]

Additionally, due to the combinatorial nature of linking fragment building blocks, a large number of possible inhibitors are represented in a small collection ($n_{compounds} = (n_{linkers}) \times (n_{fragments})^{n_{binding\ sites}}$).[45] Nuclear magnetic resonance (NMR), surface plasmon resonance (SPR) and X-ray crystallization techniques are the traditional screening methods, leading to the nickname "SAR by NMR", but there have been many technical advances in recent years, including thermal shift assays (TSAs), weak affinity chromatography, computational docking, off-rate screening, and even cell assays, to the point where structural knowledge of the binding site is no longer essential for optimization of hit fragments.[45–47]

Function-oriented synthesis (FOS), while not a new or strictly-combinatorial method, can also be appropriated for medicinal chemistry. FOS involves designing a molecular structure to perform a desired function, and doing so in an efficient way.[48,49] Paul Wender used this approach to develop novel inhibitors of protein kinase C by comparing the special orientations of key oxygen atoms of two unrelated protein kinase C inhibitor ligands and building functional, but not structural, analogs.[48–50]

1.1.2 Antimicrobial Chemistry

Though antimicrobials were instrumental in the establishment of our current drug development procedures, they also present some unique challenges due to both their intrinsic chemical properties as well as their indications for use.[2] First of all, antibiotics have traditionally been natural products, which do not follow Lipinski's

RO5, despite many of them being orally dosed (the synthetic sulfonamide class is a notable exception).[24,51,52] Antimicrobials targeting Gram-positive bacteria do not appear to be size-limited (members up to 2000 Da were found), but must be more lipophilic relative to Gram-negative-targeting antibiotics to allow them to pass through bacterial membranes.[52] Gram-negative-targeting compounds are almost exclusively under 600 Da (450 Da for orally-available), but require much greater polarity in order to displace the hydration shell guarding the entrance to porins.[52] It is thought that many antimicrobials utilize cellular transporters.[24,52–55] Nevertheless, intracellular accumulation can be problematic, especially for drugs targeting the notoriously impermeable Gram-negative pathogens.[56–58] Some groups are working on ways to circumvent this through the use of siderophores or liposomes.[59–61] Also, much higher exposure levels are needed to stop bacterial growth and prevent resistance (compare the maximum serum concentration of amoxicillin (12 μg/mL) with that of atorvastatin (55 ng/mL)), resulting in issues involving tolerability and toxicity.[56,62]

Prescription practices compound the scientific difficulties. Antibiotics are often prescribed empirically (ie. before the causative organism is known), but treatment regimens are short (often less than two weeks).[56,63,64] The widespread success of antibiotics has not only resulted in resistance, but also in market saturation with low-cost generics, limiting the price of new drugs, which in any case are reserved to delay resistance onset.[56,62,65] Resistance development is unpredictable, and may appear as a sudden outbreak that society is unprepared for, or as a slow accumulation adding time and cost to clinical trials.[56] There are also

regulatory issues to overcome in clinical trials, such as recruitment of patients (larger numbers are required since it is unknown at onset which patients are infected with the target bacteria, and traditionally patients were required to be antibiotic-free for 24 hours before trial commencement) and setting endpoints (obviously, it is unethical to withhold treatment from the control group).[56,62] This, coupled with technical challenges and the low return on investment has resulted in a well-documented retreat from this area by major pharmaceutical companies and a slowing of the antimicrobial pipeline.[56,62,66] Only five new classes have been approved since the 1960s - linezolid (2000), daptomycin (2003), retapamulin (2007), fidaxomyxin (2011), and bedaquiline (2012), and all of them targeting Gram-positive pathogens.[67,68] However, there has been considerable effort in recent years to address these concerns, through academic-industrial-government partnerships, regulatory changes, and financial incentives.[4,51,56,62]

1.2 ANTIMICROBIAL RESISTANCE

Since the discovery of penicillin by Sir Alexander Fleming in 1928,[69] antimicrobial therapy has become a cornerstone of modern medicine, with indications ranging from prophylaxis to acute resuscitation to chronic complications (such as diabetic foot infections), and everything else in between.[63,70–72] Unfortunately, their widespread use (and misuse) has selected for bacteria carrying resistance genes, who survive and multiply.[62,73,74] Currently, there are bacterial species resistant to all known classes of antibiotics, and multidrug

resistant organisms are found with alarming frequency.[62,75,76] It is estimated that antibiotic-resistant organisms are responsible for 700 000 deaths each year, and that number is predicted to explode to 10 million by 2050 and cost the global community $100 trillion.[66] In response to this threat, the World Health Organization (WHO) launched the Global Action Plan on Antimicrobial Resistance, which highlights the need for education, appropriate and efficient antibiotic use, and development of new technologies.[77] Of particular concerns are the ESKAPE pathogens: *Enterococcus faecium*, *Staphylococcus aureus*, *Klebsiella pneumoniae*, *Acinetobacter baumannii*, *Pseudomonas aeruginosa*, and *Enterobacter* species.[78,79]

Resistance arises through spontaneous mutations over time. If the change results in a survival advantage, it will be passed on. Nature is replete in genes with the potential to confer resistance, even in the absence of human involvement.[62,80–82] Many resistance mechanisms (for example efflux and β-lactamases) are adaptation of normal physiological roles such as signaling, detoxification, and peptidoglycan homeostasis.[80,83–85] Antimicrobial producing organisms may be a source of resistance, as they must develop means of protecting themselves from the compounds they produce, and competition with neighbouring microbes potentiates the development of resistance genes.[80,81] Nevertheless, the selective pressure imposed by human activity has greatly accelerated this process.[81] In addition to problematic prescription practices (approximately half of antibiotics are improperly prescribed), millions of kilograms of antimicrobials are used every year for pest control, agricultural/aquacultural prophylaxis, animal growth promotion, plant cloning, and cleaning products, not to mention scientific applications in research

and industry.[62,81] Run-off and improper waste treatment also create perfect conditions for resistance development and dissemination.[62,81] Resistance elements are easily spread within and between species by conjugation, transformation, and rarely, transduction and cellular fusion.[58,73,81]

1.2.1 Mechanisms of Resistance

Resistance is categorized as intrinsic, adaptive, or acquired. Intrinsic resistance refers inherent characteristics, such as the outer membrane of Gram-negative species, that protect against the actions of antimicrobial drugs.[81,83,86] Adaptive resistance is a temporary change in protein expression that protects against an environmental trigger.[83] Acquired resistance is the archetypal resistance: decreased susceptibility to the actions of antibiotics as result of new genetic material either through mutations or horizontal gene transfer.[83,86] Often, transient adaptive changes are followed by sequential mutations until breakthrough or high-level resistance is realized.[83] Multidrug resistant (MDR) species have acquired defenses to at least three or more antimicrobial classes, extensively drug resistant (XDR) species have resistance to all but one or two classes, and pandrug-resistant species are resistant to all classes.[58]

There are five main mechanisms of antibiotic failure: drug inactivation, target modification, porin alteration, efflux upregulation, and biofilm formation.[80,83,86,87] Most species employ multiple mechanisms. Antibiotics are typically inactivated one of two ways: they are destroyed by hydrolytic enzymes (for example β-lactamases, macrolide esterases, and fosfomycin epoxidases) or

they are covalently modified by chemical groups that prevent them from binding to their targets (*O*- or *N*-acetylation, *O*-glycosylation, *O*-nucleotidylation, *O*-phosphorylation, and *O*-ribosylation); there are also examples of lyase- or redox-associated degradation.[80] Antimicrobials can also be prevented from binding to their target by modification of the target itself, through structure changes (as in the PBP2a peptidase in MRSA)[88,89], post-translational modifications (for example methylation of the ribosome by *erm* and *rmt* methylases which interferes with macrolide and aminoglycoside binding respectively)[90,91], alternative substrates (substitution of terminal D-Ala-D-lac or D-Ala-D-Ser for D-Ala-D-Ala in Lipid II prevents recognition by vancomycin)[92], or shielding proteins (PRPs provide protection from quinolones).[86,93]

Because they both reduce intracellular antibiotic concentration, porin and efflux changes have a synergistic effect, and they are often the first steps in the gradual progression of resistance.[83,86,94] Porins provide size- and charge-selective entry points for antibiotics and other substrates to enter the cell, particularly the relatively impenetrable Gram-negative bacteria.[57,83,86] Mutations that delete, down-regulate expression, or constrict the lumen of porins therefore prevent drugs from accessing their target, leading to (usually low-level) resistance.[83] Efflux pumps evolved to protect cells (both eukaryotic and prokaryotic) against toxins in their environment. Mutations related to efflux are most commonly in the regulatory regions, typically at a fitness cost.[83,86] ATP-binding cassette (ABC) transporters use primary active transport, while resistance-nodulation-cell division (RND), major facilitator superfamily (MFS), multidrug and toxic compound extrusion

(MATE), and small multidrug resistance (SMR) superfamilies use secondary active transport.[83] The MDR RND pumps are the most widely distributed in clinically-relevant Gram-negative species, while Gram-positive species tend to use MFS antiporters.[83,94] Efflux also plays a role in biofilm-associated resistance.[83,87]

Biofilms are groups of physiologically heterogeneous cells, adherent to a surface and surrounded by an extracellular matrix.[87] They have increased resistance and tolerance to antimicrobial compounds relative to their planktonic states, resulting from multifaceted and interconnected factors, including physical sequestration by polysaccharides, cyclic glycans, and environmental DNA (eDNA) in their extracellular matrix, peptidoglycan modification via the PhoPQ and PrmAB resistance pathways, decreased antibiotic uptake from changes to their outer membrane potential (due to hypoxia and spermidine synthesis), reduced oxidative stress from hypoxia and nutrition-limited stringent response activation, and lowered metabolic activity, resulting in a greater proportion of dormant persister cells.[87] They also utilize other resistance mechanisms such as secreted β-lactamases and other resistance enzymes, porin alterations, and increased efflux, and their close proximity facilitates increased horizontal gene transfer and hypermutability.[83,87]

1.2.2 The ESKAPE Pathogens

In 2008, the Infectious Disease Society of America (IDSA) coined the "ESKAPE" acronym to describe problematic group of bacteria on the leading edge of resistance development.[95] These pathogens: *Enterococcus faecium*, *Staphylococcus aureus*, *Klebsiella pneumoniae*, *Acinetobacter baumannii*,

Pseudomonas aeruginosa, and *Enterobacter* species, are a major cause of nosocomial infections in both the developed and developing world.[78,79,95] Of the six pathogens, four (*K. pneumonia, A. baumannii, P. aeruginosa,* and *Enterobacter*) are Gram-negative, and two are Gram-positive.

Enterococcus faecium are Gram-positive, catalase-negative, facultatively anaerobic cocci that are part of the normal bowel flora in healthy individuals.[73] However, nearly all isolates are resistant to β-lactam antibiotics, and over 60% are resistant to the second line agent vancomycin *via* alternative peptidoglycan precursors.[78,96] Vancomycin-resistant enterococci (VRE) can cause severe infections in immune-compromised patients, and the responsible genes (*van A-E*) have spread to other species.[73,78,79] They can also form biofilms.[78]

Staphylococcus aureus are catalase-positive, Gram-positive cocci present on the skin of about half the population at any time.[73,79] They are generally benign, but can cause endocarditis, meningitis, osteomyelitis, pneumonia, septic arthritis, and urinary tract infections.[63,73,79] They also produce exotoxins (responsible for gastroenteritis and Toxic Shock Syndrome), and have a proclivity for forming biofilms.[63,73,78] Development of an alternative PBP, PBP2a, confers resistance to β-lactam antibiotics, resulting in the notorious methicillin-resistant *S. aureus* (MRSA).[78,79,88] Some species then go on to develop glycopeptide resistance, through changes to their peptidoglycan thickness and composition (vancomycin-intermediate *S. aureus*, VISA) or acquisition of the *van* genes from enterococci (vancomycin-resistant *S. aureus*, VRSA).[78,79]

Klebsiella pneumoniae is a Gram-negative, encapsulated enteric pathogen that usually only affects hospitalized patients, though it causes violent pneumonia in diabetic and alcoholic patients.[63,73,78,79] It is the second leading cause of sepsis (after *E. coli*), and the initial source of two carbapenemases: the *K. pneumonia* carbapenemase (KPC) and the New Delhi metallo-β-lactamase (NDM).[73,97,98]

Acinetobacter baumannii is an opportunistic, facultatively anaerobic Gram-negative pathogen wreaking havoc in intensive care units due to its environmental persistance.[62,78,79] Its thick peptidoglycan cell wall allows it to survive in dry conditions for up to five months, while its Omp38 exotoxin promotes colonization.[62,78] It has intrinsic resistance conferred by constitutively-expressed efflux pumps and restrictive porins.[78,83] Additionally, most of the OXA-type carbapenemases originated in this species.[78,99,100]

Pseudomonas aeruginosa are rod-shaped, facultatively anaerobic, Gram-negative pathogens with impressive arsenal of intrinsic resistance mechanisms, including the pro-adherent pili, substrate-specific or closed porins, constitutive efflux, siderophores and pigments, and biofilm formation.[53,62,78,79,83,87] While relatively innocuous in immune-competent individuals, this bacteria causes a host of infections in immune-compromised patients, including chronic cystic fibrosis lung infections, ventilator-associated pneumonia, osteomyelitis and malignant external otitis in diabetic patients, catheter-associated pyelonephritis, acute endocarditis in IV drug users, burn wound infections, and high-mortality sepsis.[63,73,101,102] Furthermore, the first reported metallo-β-lactamase, imipenemase (IMP), was found in this species.[100,103,104]

Enterobacter species are Gram-negative rods that are part of the normal gut bacteria.[73] However, they can acquire resistance elements and cause opportunistic infections.[78,79] Strains of this species, like *A. baumannii* and *P aeruginosa*, have also been found to harbor the NDM carbapenemases.[105]

1.3 Resistance in Gram-Negative Pathogens

Gram-negative bacteria have two membranes separated by a thin layer of peptidoglycan. The outer membrane is composed of lipopolysaccharide (LPS) and is a source of intrinsic drug resistance and virulence.[57,73] Lipid A (a component of LPS) acts as an endotoxin, triggering a severe immune response, while the tightly-packed lipopolysaccharides form a non-fluid barrier to large and hydrophobic molecules.[57,58,73] Intracellular antimicrobial concentration is further decreased by the presence of efflux pumps, such as the RND transporters.[83,94] As a result, only a limited number of classes of antibiotics have activity against these pathogens: select β-lactams (ureidopenicillins, later-generation cephalosporins, carbapenems, and aztreonam), aminoglycosides, fluoroquinolones, polymyxins, tetracyclines and glycylcycline, amphenicols, sulphonamides, and fosfomycin.[58,63,64,106] The β-lactams and fosfomycin interfere with peptidoglycan synthesis.[73,107–109] Polymyxins (colistin) disrupt the outer membrane and neutralize endotoxin.[63,64] Aminoglycosides, chloramphenicol and tetracyclines bind the ribosome.[63,64,73] Fluoroquinolones block DNA replication by inhibiting DNA gyrase, while sulfonamides block folate synthesis.[63,64,73,106] These antimicrobials employ a

variety of mechanisms to cross the outer membrane. β-lactams and amphenicols diffuse through porins.[53,55] Tetracyclines and fluoroquinolones primarily use porins, but are also able to diffuse through the membrane in their charge-neutral state.[53] Polymyxins and aminoglycosides promote their own uptake, by binding to negatively-charge LPS and replacing stabilizing cations,[110,111] while fosfomycin utilizes sugar transporters.[109]

Gram-negative pathogens are a major source of infections in critically-ill patients.[112] Acquisition of resistance elements have made pathogenic species such as *K. pneumoniae*, *A. baumannii*, *P. aeruginosa*, *Enterobacter* spp, and *Neisseria* spp much more problematic. While there has been some success in recent years to develop new classes of Gram-positive-targeting antimicrobials following the emergence of methicillin-resistant *S. aureus* (MRSA), vancomycin-intermediate and vancomycin-resistant *S. aureus* (VISA and VRSA), and vancomycin-resistant enterococcus (VRE) in the 1990s, there have been no new classes effective against Gram-negative pathogens since the discovery of the fosfomycin in 1969.[62,67,68,109]

1.3.1 Aminoglycoside Antibiotic Mechanisms of Action and Resistance

Aminoglycosides are historically tri-ringed structures, each containing double-ringed neamine ((2R,3S,4R,5R,6R)-5-amino-2-(aminomethyl)-6-[(1R,2R,3S,4R,6S)-4,6-diamino-2,3-dihydroxycyclohexyl]oxyoxane-3,4-diol), with the substitution pattern of the third ring on 2'-deoxystreptamine differentiating neomycin/paromomycin (4,6-substitution, Figure 1-1) and gentamicin/kanamycin families (5,6-substitution).[113] They are active against Gram-negative pathogens

(aerobic or facultative anaerobic, especially bacilli), as well some Gram-positive (streptococci and enterococci) and Mycobacteria species, usually as part of a combination therapy.[63,64,114] They block the A-site of bacterial ribosomes by binding to the S12 protein of the 30S subunit, with the conserved lock-and-key interaction of the ribosome to the neamine rings supplemented by fuzzy interactions to the third ring.[113,115] Aminoglycosides' concentration-dependent bactericidal activity is due to corruption of the genetic code, resulting in the incorporation of misfolded proteins in the bacterial cell membrane.[63,64,114–116] The subsequent effect on membrane integrity promotes increased uptake of aminoglycosides until a sufficient concentration is reached to block all ribosomes.[115]

The first aminoglycoside, streptomycin, was isolated from *Streptomyces griseus* by Schatz and Waksman at Rutgers University in 1943 and brought to clinic the following year.[106,116] Several others followed quickly: neomycin in 1949,[117]

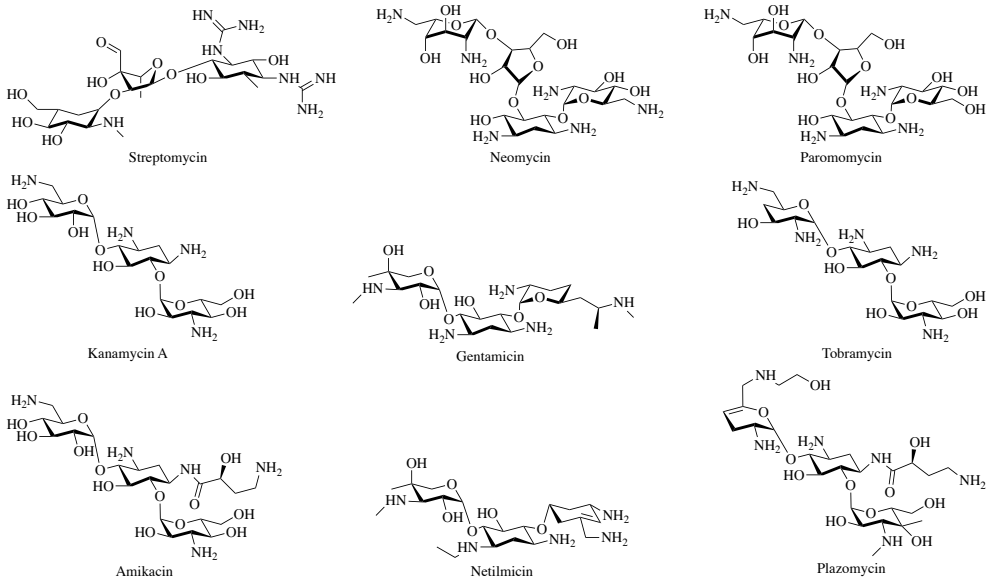

Figure 1-1. Aminoglycoside Antibiotics

paromomycin in 1956,[118] kanamycin in 1958,[119] gentamicin in 1963,[114,120] tobramycin in 1968,[121] and semisynthetic amikacin and netilmicin in 1972 and 1983 respectively.[116,121–123] The newest aminoglycoside, plazomicin, was approved in 2018.[60,124] While initially very successful, particularly against tuberculosis, aminoglycosides have largely fallen out of favour, mostly due to their toxicity profile (nephrotoxicity, audiovestibular toxicity, and prolongation of neuromuscular blockade).[63,64,106,114,116] There are several possible reasons for this toxicity, including the inherent structure of the drug, its ability to generate reactive oxygen species, and the single base pair difference between eukaryotic and prokaryotic ribosomes at the A-site.[116,125,126] Nevertheless, aminoglycosides are still used in select circumstances: gentamicin is used for sepsis of unknown origin (in combination with a third-generation cephalosporin), intra-abdominal abscesses (with metronidazole), neonatal meningitis (with penicillin), and endocarditis (with vancomycin or a penicillin).[63,64] Tobramycin is also used for sepsis of unknown origin, and where *P. aeruginosa* is suspected (ventilator-associated pneumonia, cystic fibrosis, burns).[63,64,78,101] Amikacin is used for bowel perforations (with clindamycin),[63] and when organisms are resistant to tobramycin or gentamicin.[63,64,106,114] Neomycin is used to treat hepatic encephalitis.[63,64] Aminoglycosides remain first-line treatments for exotic diseases such as plague, brucellosis (in combination with doxycycline), tularemia, and verruga peruana, and second-line treatment for tuberculosis .[63,64,106,127] They also have a role in surgical prophylaxis[63,64,70] and treatment of protozoal infections, and are being investigated as potential cancer, cystic fibrosis, and muscular dystrophy therapies.[125,126,128]

High-level resistance in aminoglycosides results primarily from drug modification by aminoglycoside-modifying enzymes (AMEs).[116,129] The three broad categories of AMEs are aminoglycoside acetyltransferases (AACs), aminoglycoside nucleotidyltransferases (ANTs), and aminoglycoside phosphotransferases (APHs).[125,126,129] AACs use acetyl-coenzyme A (acetyl-CoA) to acetylate an amine of the aminoglycoside; ANTs and APHs transfer adenyl-phosphate and phosphate groups respectively from ATP (or GTP) to a hydroxyl substituent (Figure 1-2).[125,126,129,130] These resistance enzymes may be encoded chromosomally or on plasmids, and originate from the self-protective mechanisms of producing bacteria or from genes involved in normal cellular function through mutation.[129]

1.3.1.1 Aminoglycoside N-Acetyltransferase-3

In 1973, aminoglycoside N-acetyltransferase-3-Ia (AAC(3)-Ia, or gentamicin acetyltransferase-I) was found in resistant *P. aeruginosa* isolates.[131] AAC(3)-Ia uses acetyl-CoA to acetylate the 3-amino substituent of aminoglycosides *via* a random mechanism, where the order of substrate binding does not matter, as binding of either aminoglycoside or acetyl-CoA will promote the binding of the other, but both must be bound before catalysis can occur.[132,133] The aminoglycoside interacts via the amines on its two outer rings (2', 3', and 6"), and the rate-limiting step is dependent on which aminoglycoside is used.[132–134]

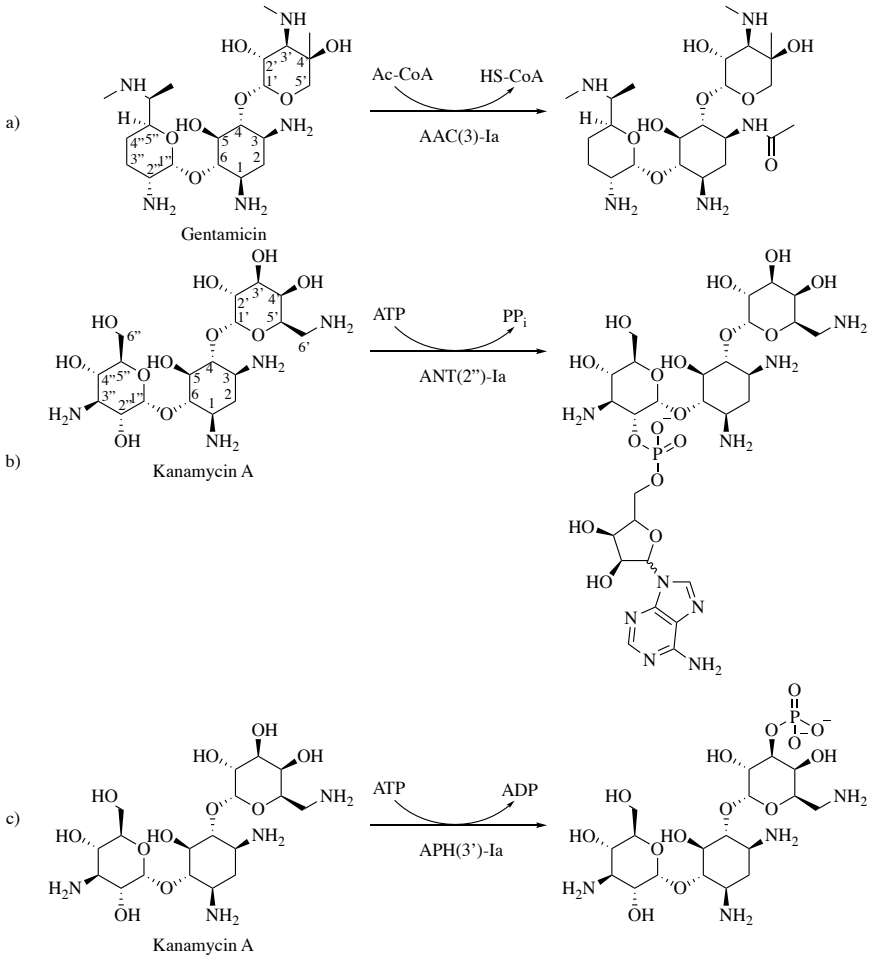

Figure 1-2. Mechanisms of Aminoglycoside Inactivation by a) Aminoglycoside Acetyltransferaes-3, AAC(3), b) Aminoglycoside Nucleotidyltransferase-2", ANT(2"), and c) Aminoglycoside Phosphotransferase-3', APH(3')

1.3.1.2 Aminoglycoside O-Nucleotidyltransferase-2"

Aminoglycoside O-nucleotidyltransferase-2"-Ia (ANT(2")-Ia) is an aminoglycoside-modifying enzyme found in *K. pneumonia*, *P. aeruginosa*, *A. baumanii*, and *Enterobacter*.[135] First described in 1971, it catalyzes the transfer of an adenylphosphate group from ATP to the 2"-hydroxyl group of gentamicin,

tobramycin, and kanamycin.[129,135,136] Adenylation proceeds by an ordered Theorell-Chance mechanism, where ATP binds to the active site first, stabilized and oriented by the two magnesium ions, followed by the aminoglycoside.[135,137] The 2"-hydroxyl is then activated by an aspartic acid for nucleophilic attack on the α-phosphate of ATP, pyrophosphate is released, followed by the rate-limiting exit of the adenylated aminoglycoside.[135,137]

1.3.2 β-Lactam Antibiotic Mechanisms of Action and Resistance

The β-lactam class was the initial antibiotic class, and is still the most commonly prescribed class.[106,108,138] It consists of four main subclasses- penicillins, cephalosporins, carbapenems, and monobactams (Figure 1-3), with multiple subgroups. The β-lactam core is required for antimicrobial activity; however, within the subclasses and subgroups, structural modifications have been used to tailor coverage to specific pathogens.[139–141] The penicillins have a thiazolidine as the second ring in the bicyclic structure, the cephalosporins a dihydrothiazine, and the carbapenems a 2-pyrroline, while monobactams have only the single β-lactam ring N-substituted with a sulfonic acid.

Penicillin G (benzylpenicillin) was famous contaminating antibiotic.[62,69,106,108,142] Although first reported in 1929, purification and scale-up issues delayed clinical use until 1941.[62,69,106,108,143,144] Both penicillin G and penicillin V (phenoxymethylpenicillin- also a natural product, approved in 1968), suffer from extensive resistance; however, they are still effective against spirochetes such as *Treponema pallidum* (syphilis) and group A β-hemolytic

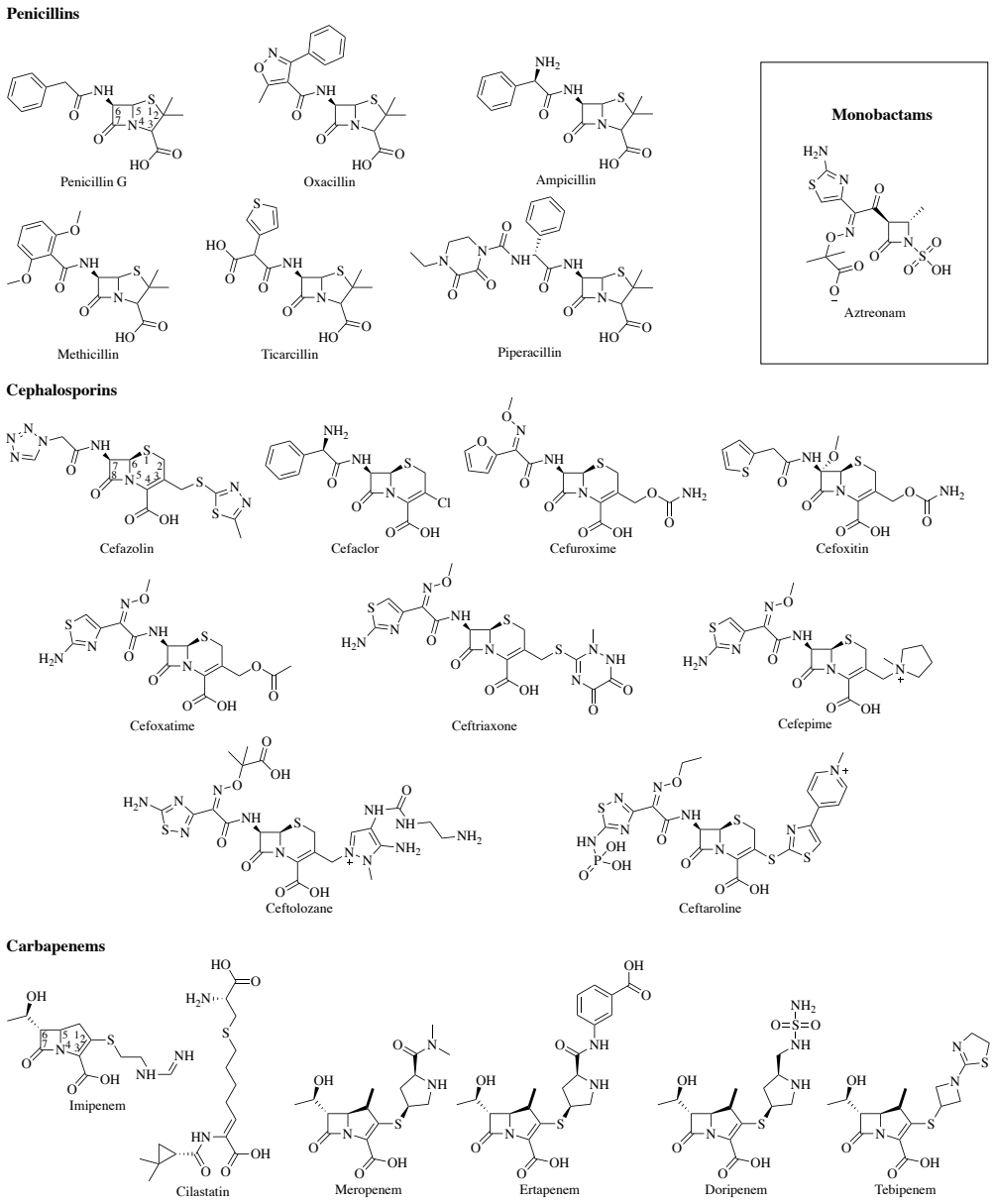

Figure 1-3. β-Lactam Antibiotics

streptococci (responsible for streptococcal pharyngitis, scarlet fever, and some skin infections, including necrotizing fasciitis).[63,64,73,145] The accidental discovery and production of 6-aminopenicillanic acid by Beecham Research Laboratories opened the door for semisynthetic penicillin analogs.[2,106,146,147] Penicillinase-resistant

penicillins debuted in 1960 with the approval of methicillin; oxacillin (1962), dicloxacillin (1968), nafcillin (1970), and cloxacillin (1974) followed.[148,149] Cloxacillin or dicloxacillin in combination with rifampin and mupirocin is moderately successful in treating MRSA carriers (50% recurrence).[63] The aminopenicillins, ampicillin and amoxicillin, were approved in 1963 and 1972 respectively and are still frequently used.[73,108] They are susceptible to penicillinases, but have increased Gram-negative and enterococci coverage.[63,64,73] Amoxicillin is especially well-absorbed orally and is used for outpatient conditions such as bronchitis, sinusitis, and urinary tract infections.[63,64,73,147] Ampicillin can be taken orally, but is more commonly used intravenously, often in combination with gentamicin, for severe infections including meningitis, endocarditis, pneumonia, pyelonephritis, skin-infections, intra-abdominal infections, and sepsis, and for empiric Gram-negative coverage.[63,64,73,108] The carboxypenicillins- ticarcillin (approved 1976) and carbenicillin (approved 1972, since discontinued), and ureidopenicillins- piperacillin and mezlocillin (both 1981) were developed for enhanced activity against Gram-negative rods, in particular *Pseudomonas aeruginosa*, hence their antipseudomonal descriptors.[63,64,73,108,149] They also have activity against anaerobes such as *Bacteroides fragilis*.[73] Ticarcillin and piperacillin are widely used, generally in formulation with β-lactamase inhibitors, though metronidazole or clindamycin is usually the preferred agent for anaerobes, and tobramycin for *Pseudomonas*.[63,64]

The first cephalosporin, cephalosporin C, was discovered in 1953 by Newton and Abraham after analyzing various extracts of an antibacterial-producing

mold isolated by Giuseppe Brotzu.[2,150,151] Although it was not as active as its sister compound cephalosporin N (later renamed penicillin N upon structural determination) or penicillin G, it sparked interest due to its improved stability to penicillinases.[2,150] Scientists at Eli Lilly were able to improve its antibacterial activity by hydrolyzing it to 7-amino-cephalosporinic acid and functionalizing position 7.[2,152,153] First-generation cephalosporins cephalothin and cephaloridine became commercially-available in 1964, followed by cephalexin (1965), cefazolin (1973), cefaclor (1979), and others.[2,108,151] First-generation cephalosporins have good coverage against Gram-positive methicillin-sensitive cocci, but are susceptible to Gram-negative penicillinases.[63,64,151] There are two subclasses of second-generation cephalosporins: cephems (with prototype cefuroxime approved in 1983) and cephamycins (cefoxitin, 1978).[73,108,151] They have moderate coverage against both Gram-negative bacilli and Gram-positive cocci.[73] The addition of a 7α-methoxy group in cephamycins was a surprising but welcome medicinal chemistry modification that conferred stability to β-lactamases, including extended spectrum β-lactamases (ESBLs).[2,108,151] Cefoxitin extended the spectrum of activity to include anaerobes.[2] Third-generation cephalosporins are active against Gram-negative pathogens (usually at the cost of Gram-positive activity).[73,108,151] This diverse groups includes N-acyl cephems (such as cefoperazone, approved 1982 and ceftibutin, 1995), oxyimino-cephems (such as cefotaxime, 1981; ceftriaxone, 1984; ceftazidime, 1985; cefixime, 1989; cefpodoxime, 1992; cefdinir, 1997), oxacephems (latamoxef, 1982), carbacephems, and isocephems.[73,108,151] The oxime group enhanced stability to β-lactamases, leading to the designation of

cefotaxime, ceftriaxone, and ceftazidime as expanded-spectrum cephalosporins, together with cefoperazone and fourth generation cefepime.[108] Oxacephems have improved activity (due to increased porin uptake and β-lactam-reactivity), but are more susceptible to β-lactamases, with the exception of latamoxef, which is stable to ESBLs.[108,151] Carbacephems have comparable activity but superior stability.[151] Fourth generation cephalosporins such as cefepime (approved 1996), cefclidine, and cefprozan) have antipseudomonal activity stemming from their quaternary ammonium moiety (also found in third generation cefpimizole and ceftazidime).[63,64,73,108,151] Their zwitterionic nature also promotes uptake through porins.[52,151] Fifth generation cephalosporins are catechol-containing cephems with have antipseudomonal activity that exploit the *tonB*-dependent iron transporters for improved cellular access; none have been approved thus far.[108,151] Sixth generation cephalosporins are narrow-spectrum agents and include antipseudomonal ceftolozane (2014), and anti-MRSA ceftaroline (2010) and ceftobiprole (2013).[63,64,108,151] Cephalosporins are widely used. First-generation cephalosporins are used orally for simple soft tissue infections, recurrent uncomplicated urinary tract infections, open fractures and dental prophylaxis. Intravenous cefazolin may be used for methicillin-sensitive *S. aureus* endocarditis and surgical prophylaxis.[63,64,70] Second-generation cephalosporins cefuroxime, cefoxitin, or cefotetan are also used for surgical prophylaxis, and the cephamycins can be used to provide anaerobic coverage.[63,64,70] Third generation cephalosporins are the mainstay treatment for Gram-negative infections.[58,65] Notable uses (amongst the many) include cefotaxime, ceftriaxone, or ceftazidime for empiric coverage for

septic shock of unknown origins, ceftriaxone for meningitis, ceftazidime or cefepime for nosocomial pneumonia, and ceftriaxone or cefixime for sexually-transmitted infections (gonorrhea or chancroid).[63,64,73] Ceftriaxone is also being investigated for its ability to modulate glutamate transporter-1, which is involved in neuroprotection, immunomodulation, and addiction.[106] Later generation cephalosporins are considered drugs of last resort and not used unless absolutely necessary.[65]

The first carbapenem, thienamycin, was isolated by Merck in 1976, but it was too unstable to be useful.[2,154] Addition of a N-formidoyl group to the 2-aminoethylsulfanyl substituent improved stability sufficiently to allow clinical introduction of imipenem in 1985, although it (and panipenem, approved 1993) requires coadministration with a dehydropeptidase I inhibitor (cilastatin or betamipron) to prevent rapid metabolism.[2,108,155] The addition of a C1 methyl group in meropenem (1995) overcame this problem, and long-acting ertapenem (2001) has a long enough half-life to permit once-daily dosing.[2,108,155,156] Carbapenems have broad-spectrum activity against both Gram-positive and Gram-negative species.[63,64,155] Imipenem and panipenem tend to be more effective against Gram-positive species, while meropenem, biapenem (2001), and ertapenem have more activity against Gram-negative (with the exceptions of *A baumanni* and *P. aeruginosa* for meropenem and ertapenem respectively).[108,155] Doripenem (2007) has both Gram-positive and Gram-negative coverage, and superior activity against *P. aeruginosa* and *A. baumannii*.[108,155] Tebipenem, the first oral carbapenem (approved 2009 in Japan) has just commenced clinical trials.[108,157,158] Carbapenems

are intrinsically resistant to most β-lactamases.[2,108,155,159] This is attributed to their ability to form a stable acyl-enzyme complex, where the pyrroline ring has tautomerized to a more stable configuration, the carbonyl is positioned outside the oxyanion hole, and the 6α-hydroxy substituent interferes with the hydrogen-bonding network necessary for deacylating attack.[155,159] However, they are usually reserved for severe infections that do not respond to first-line medications.[65,155]

Aztreonam (first reported in 1981 and approved in 1986) is the only approved monobactam.[2,62,141,160,161] It has activity against Gram-negative bacteria (*via* the 2-aminothiazolyl side chain also found in third generation cephalosporins), but not Gram-positive or anaerobes.[62–64,108,141] As it is the only β-lactam resistant to metallo-β-lactamases, it is held in reserve.[62,65,108]

The targets of these diverse antimicrobials are penicillin-binding proteins (PBPs), a heterogenous group of enzymes involved in the metabolism of peptidoglycan, a fundamental component of the bacterial cell wall.[73,139,155,162] PBPs include transpeptidases (catalyze the final step of peptidoglycan synthesis by forming a cross-bridge between the terminal D-aspartic acid of one glycan polymer and an amine acceptor on an adjacent strand), carboxypeptidases (hydrolyze D-Ala-D-Ala bonds to limit amount of substrate available for cross-linking), and endopeptidases (cleave crosslinks to allow peptidoglycan recycling).[84,85,89,139] They are roughly organized into class A, B, or C high-molecular-weight (often multifunctional proteins containing transpeptidase domains) or low-molecular-weight (usually carboxypeptidases).[84,85,89] All PBPs have a conserved active site

(α^2 and α/β domains connected by loop) featuring a serine residue for nucleophilic attack on the peptide carbonyl required for proteoglycan crosslinking or hydrolysis.[84,85,162] β-lactams mimic the terminal D-Ala-D-Ala substrate with an adjacent carboxylic acid (sulfonic acid in monobactams); however, when the serine residue attacks the carbonyl of the β-lactam, this forms a stable ester linkage, trapping the acylated enzyme in an inactive state.[139,162] The pattern of essential and supporting PBPs varies from species to species, with different PBPs having different affinities for the various β-lactam antimicrobials and inducing different morphological responses.[84,85,89,163–166] As a general rule, though, the bactericidal action of β-lactams is due to cell lysis following unchecked peptidoglycan degradation after inhibition of essential transpeptidases.[63,64,107,142,164]

In Gram-positive species, the main mechanism of resistance to β-lactams is target modification.[89] A classic example of this is the infamous methicillin-resistant *S. aureus* (MRSA). Here, resistance arises from the expression of an alternative, low-affinity PBP (PBP2a, encoded by *mecA*) in response to acylation of MecR transmembrane proteins by β-lactams.[62,78,79,89] PBP2a then takes over the transpeptidase activity, releasing the stalled acyl-enzymes.[89] In contrast, in Gram-negative species, resistance through drug-inactivation predominates.[89,142,167] The first β-lactamases were reported even before the clinical introduction of β-lactams.[168] Serine β-lactamases evolved from PBPs, and while they share the common fold, they are able to rapidly hydrolyze the ester linkage formed upon β-lactam ring-opening and release the catalytic serine.[84,85] Currently, there are over

1500 β-lactamases described, and more being added.[169] Traditionally β-lactamases have been classified according to their amino acid sequence (Ambler system), where Class A are penicillinases susceptible to β-lactamase inhibitors, Class B are metallo-β-lactamases, Class C are cephalosporinases (AmpC-type), and Class D are the oxacillinases (OXA).[142,170–172] Now, the Ambler system has largely been superseded by the Bush-Jacoby system, wherein β-lactamases are classified by functional characteristics such as substrates and inhibitors.[79,142,167] Under the Bush-Jacoby system, Classes A and D are combined into Group 2, while Class C is replaced by Group 1 and Class B by Group 3.[167] Groups 1 and 3 are serine β-lactamases (SBLs), while group 3 are metallo-β-lactamases (MBLs).

Group 1 (Class C) cephalosporinases were in fact the first β-lactamases described.[173] There are over 200 members of this group, including the AAC, ACT, CFE, CMY, DHA , FOX, LAT, MIR, and MOX families.[169] Though group 1 β-lactamases first came to light as a result of ampicillin-resistant isolates (thus the early AmpC moniker), cephalosporins are their preferential substrate, with turnover rates approaching the diffusion limit.[173,174] They are resistant to clavulanic acid, but may be inhibited by aztreonam.[79,142,167,173] There are some variants (CMY-10, CMY-19, CMY-37, and others) with extended-spectrum β-lactamase activity (extended-spectrum AmpC β-lactamases or ESACs, group 1e).[167] Group 1 β-lactamases are generally susceptible to carbapenems, with resistance due to high expression plus increased efflux and/or altered porins.[142,159,167,173] However, there are reports of Group 1 members with carbapenemase activity: CMY-10 in

Enterobacter aerogenes, and ADC-68 in *A. baumanni*.[159] The use of β-lactams, specifically aminopenicillins, clavulanic acid, and imipenem, has been shown to induce overexpression through AmpD de-repression.[142,167,173]

Group 2 is the largest group of β-lactamases, consisting of 12 subgroups. Subgroups 2a, 2b (except 2br and 2ber), 2c, 2e, and 2f are in Ambler Class A and inhibited by clavulanic acid; the 2d subgroups are in Ambler Class D and are not.[79,142,167] Group 2a are the original penicillinases that are inactive against cephalosporins, carbapenems, and aztreonam.[79,167] Group 2b β-lactamases hydrolyze penicillins and early cephalosporins.[79,142,167] Group 2be are extended-spectrum β-lactamases (ESBLs), which by definition hydrolyze the oxyiminocephalosporins (cefotaxime, ceftriaxone, ceftazidime, and other Group IIIB cephalosporins), as well as aztreonam.[108,151,175] Group 2c β-lactamases can hydrolyze the carboxypenicillins; Group 2ce have additional activity against cephalosporins.[79,142,167] Group 2e are cephalosporinases, distinguishable from Group 1 by their susceptibility to clavulanic acid and lack of affinity to aztreonam.[79,142,167] Group 2d are the OXA enzymes, which hydrolyze penicillins (with a preference for oxacillin and cloxacillin, hence their name).[99,167] They are always plasmid-mediated, and not usually susceptible to clavulanic acid.[99,167] Group 2de are extended-spectrum OXA enzymes: OXA-11,OXA-13, OXA-14, OXA-16, OXA-17, OXA-19, OXA-28; they are mostly derived from OXA-10 and found in *P. aeruginosa*.[99,167] Groups 2f and 2df are Class A and Class D carbapenemases respectively.[167] Constraints to their active sites (predominately through disulfide and hydrophobic bridges respectively) force carbapenem-enzyme

intermediates into the correct orientation for turnover.[159] Class A carbapenemases include SME, IMI, NMC-A, KPC, and GES enzymes and are inhibited by clavulanic acid.[100,159] SME, IMI, and NMC-A are mostly chromosomally-encoded, while KPC and GES are on plasmids.[100] Although all OXA enzymes can sufficiently deactivate carbapenems in poorly permeable species such as *A. baumannii*, only ten clades are considered true OXA carbapenemases: OXA-23, OXA-24/40, OXA-51, and OXA-58, OXA-143, OXA-211, OXA-213, OXA-214, OXA-229, OXA-235.[99,159,167] The first OXA carbapenemase, OXA-23, was found in Edinburgh in 1985, the same year imipenem was introduced.[99,100] OXA carbapenemases are found most commonly in Acinetobacter, all except the OXA-134, OXA-211, OXA-213, OXA-214, OXA-229, and OXA-235 have been mobilized on to plasmids.[99,159]

While Groups 1 and 2 (Classes A, C, and D) all share the conserved serine residue of their PBP ancestors, Group 3 (Class B) is not related, belonging instead to the metallohydrolase superfamily, and uses a metal ion (Zn^{2+}) to activate water molecules for nucleophilic attack.[104,159,176] The first transferable metallo-β-lactamase, imipenemase (IMP), was discovered in Japan in 1988.[103] Since then many more members have been reported.[100,176] There are three subclasses of metallo-β-lactamases: B1 (subgroup 3a) and B3 (3c) have two zinc ions and two water molecules (one bridging and one apical) in their active sites, whereas B2 (3b) has only a single zinc atom.[155,159,167,176] In subclasses B1 and B3, the first zinc (Zn1) acts as both a Lewis acid and a general base, guiding bridging water to attack the β-lactam ring and stabilizing the tetrahedral intermediate, while the second zinc

(Zn2) accepts the anionic pyrroline intermediate.[104,159] Subclass B2 has preferential activity against carbapenems relative to penicillins and cephalosporins, while Subclass B3 has poor carbapenem activity.[176] Subclass B1 is the most concerning, as it contains the broad-spectrum and plasmid-mobilized imipenemase (IMP), Verona imipenemase (VIM), and New Delhi metallo-β-lactamase (NDM) subfamilies, as well as others.[104,159,167,176] All MBLs hydrolyzes carbapenems, in addition to penicillins and cephalosporins, and are not inhibited by β-lactamases inhibitors such as clavulinate.[100,155,159,167,176] However, most are still susceptible to aztreonam and chelation of the metal cores destroys their activity.[159,167,176] Polymyxins may also be used, as MBLs are often encoded on plasmids containing resistance genes for aminoglycosides and fluroquinolones.[176]

1.3.2.1 New Delhi Metallo-β-Lactamase-1

The New Delhi metallo-β-lactamase (NDM) is a plasmid-mediated Class B1 metallo-β-lactamase with activity against all penicillins, cephalosporins, and carbapenems (Figure 1-4).[97,105,177] Furthermore it is often co-transmitted with resistance genes to aminoglycosides, chloramphenicol, macrolides, quinolones, and other β-lactamases.[97,177,178] First reported in 2008, it is now the third-most abundant carbapenemase, and has spread around world with outbreaks in 22 countries.[97,105] There are currently 24 variants, some of which have increased carbapenemase activity.[105]

NDM is unique amongst the β-lactams in that it is anchored to the outer membrane protein, which enhances its ability to withstand zinc deprivation.[105] It

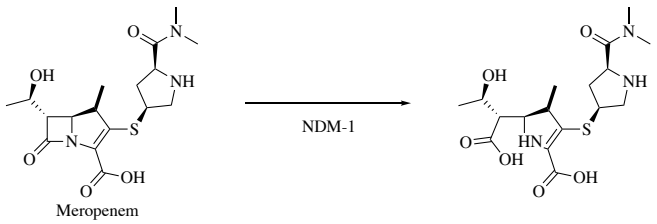

Figure 1-4. Mechanism of Carbapenem Hydrolysis by New Dehli Metallo-β-Lactamase-1

also benefits from a broad, shallow active site bordered by flexible loops that is able to accommodate and orient any carbapenem for hydrolysis.[177] There is still some ambiguity about the precise mechanism, but the general consensus is that the association of the carbapenem substrate replaces the bridging water atom from Zn2, activating it for nucleophilic attack on the β-lactam, which is now stabilized by coordination to both zinc centres.[177,179,180] The negative charge is distributed around the pyrroline ring until it is quenched at C3 by rate-limiting protonation from bulk solvent; the now-inactivated carbapenem is released, and water enters the active site to regenerate the enzyme.[177,179,180] Many groups are working on elucidating this mechanism in hopes it will lead to new effective antimicrobials or inhibitors.[159,177]

1.4 COMBINATION THERAPY

Combination therapy is the use of two or more agents to treat a single condition. It is found ubiquitously throughout clinical practice guidelines for conditions ranging from cancer and cardiovascular disease to diabetes and depression.[63,181–185] The international *Surviving Sepsis Campaign* in particular

specifically recommends use of multiple antimicrobials (typically at least a β-lactam and an aminoglycoside) for empiric coverage and synergistic effect, in addition to corticosteroids and vasopressors.[63,186] Coverage of multiple pathways and heterogeneous disease states, side effect attenuation, lower toxicity, clinical flexibility, and financial savings are other commonly-cited benefits.[183,186–188]

Combination therapy is an especially useful tool in the treatment of infectious disease, where, in addition to the benefits described above, it can be used to suppress the development of resistance and to counteract existing resistance pathways. For example, highly active anti-retroviral therapy (HAART) uses two nucleoside reverse-transcriptase inhibitors (NRTIs) plus either a non-nucleoside reverse-transcriptase inhibitor (NNRTI) or an integrase inhibitor (INSTI) to suppress viral load in HIV patients, thereby reducing development of resistant phenotypes, lowering risk of transmission, and slowing progression to AIDS.[63,73,189,190] Treatment for mutation-prone hepatitis C virus (HCV), responsible for chronic infection leading to end-stage liver disease, became curative upon addition of direct-acting antiviral agents (DAAs) telaprevir or boceprevir to the existing pegylated interferon and ribavirin regimen.[191] Current guidelines now use combinations of DAAs with or without interferon and ribavirin.[63,192] *Plasmodium falciparum*, the parasite commonly responsible for chloroquine-resistant malaria, is treated with artemisinin-based combination therapy (ACT), where a rapid-acting artemisinin derivative (usually artesunate) is partnered with longer-acting second agent (lumefantrine, amodiaquine, mefloquine, sulfadoxine-pyrimethamine, or piperaquine).[73,193] First-line treatment for *Mycoplasma tuberculosis* is treated by

quadruple therapy: isoniazid (INH), rifampin (RIF), pyrazinamide (PZA), and ethambutol (EMB), although resistance to this regimen is becoming more prominent.[63,106]

1.4.1 Antimicrobial Combination Therapy

Polypharmacy is an established practice in antimicrobial therapy. In addition to broad-spectrum coverage, such as required in tuberculosis and when the responsible organisms are not known, combinations of antibiotics are used to elicit synergistic effects.[194] Sulfamethoxazole (a sulfonamide class, the first approved class of antibiotic) and trimethoprim inhibit steps in the folate synthesis pathway; individually, both are bacteriostatic, but together they are bactericidal.[63,64,106,194] The streptogramins, dalfopristin/quinopristin and pristinamycin IA/IIA, similarly are only used together.[62,106] The binding of the streptogramin A facilitates the subsequent binding of the streptogramin B.[106] Oxacillin and vancomycin have a particularly interesting synergistic interaction; oxacillin induces expression of PBP2a, but PBP2a cannot accommodate the D-Ala-D-Lac peptidoglycan precursors used to evade vancomycin.[194] Antibiotics with different modes of action are also commonly co-administered. For example, peptidoglycan-targeting β-lactams are used to increase the intracellular concentrations of ribosomal-targeting aminoglycosides.[194] Colistin (polymyxin E) has been investigated for its effects on outer membrane permeability.[194] Additionally, some groups have taken this combinatorial approach a step further by physically linking two antimicrobial drugs

together to take advantage of synergistic interactions without the added complexity arising from administration of two separate drugs.[62]

For pan-resistant NDM infections, combination therapies are the only options. Regimens that showed some efficacy include dual therapy colistin and rifampin (or triple therapy with meropenem), colistin and aztreonam (with/without meropenem), colistin and fosfomycin, polymyxin B with aztreonam and amikacin, tigecycline and levofloxacin, and fosfomycin with meropenem and ertapenem.[105]

1.4.2 Adjuvant Therapy

The initial response to emerging bacterial resistance was to develop semisynthetic antibiotics with chemical groups that protected against β-lactamase hydrolysis.[2,148,194] However, with the rapid advent of new β-lactamases with activity against these "lactamase-resistant" antimicrobials, coupled with a decline in the discovery of new classes, the need for stewardship rose to prominence. The discovery of clavulanic acid, a β-lactam compound with only weak activity on its own that potentiates the activity of other antibacterial β-lactams,[195] turned attention towards the potential of adjuvants: compounds that enhance the activity of the primary agent but have little efficacy on their own.[196] Adjuvants can extend the life of already-approved drugs by counteracting resistance mechanisms, particularly enzyme-mediated ones such as β-lactamases, aminoglycoside-modifying enzymes, and ribosomal methyltransferases.[196] They also slow the development of resistance through enhancement of bactericidal activity, allowing lower doses to be given and for shorter intervals.[51,196,197] As they generally target nonessential pathways,

resistance to adjuvants develop at a much slower pace.[197,198] Adjuvants can also be used to modify the pharmacokinetic and pharmacodynamic properties of drugs. Dehydropeptidase I inhibitor cilastatin is administered alongside imipenem to prevent rapid metabolism, and lower doses may limit associated toxicity of some antibiotics.[51,108]

Class I adjuvants act on bacteria, and are broken down into two subclasses: IA, which inhibit active resistance mechanism (enzymatic modification, target alteration, and efflux upregulation), and IB, which inhibit passive mechanisms (efflux, membrane impermeability, and biofilms).[196] Class II adjuvants modulate the host's response.[196] Currently, all approved antibiotic adjuvants (the serine-β-lactamase inhibitors) belong to adjuvant class IA, and despite their success, no similar inhibitors have been approved for metallo-β-lactamases or resistance-conferring enzymes to other antibiotic classes.

1.4.2.1 Serine β-lactamase Inhibitors

The emergence of β-lactamases were described even before clinical introduction of β-lactam antibiotics.[168] In 1976, the first β-lactamase inhibitor-clavulanic acid, was reported, and was introduced to the clinic in 1981 (Figure 1-5).[147,195,199] Sulbactam and tazobactam followed in 1978 and 1984, respectively.[200,201] These inhibitors are based on the β-lactam scaffold, and work by a "suicide" mechanism.[147,148,199] They generally only have activity against Class A β-lactamases.[167] Clavulanic acid is usually combined with amoxicillin as orally-available Augmentin, but is occasionally used with ticarcillin (Timentin).[73,148]

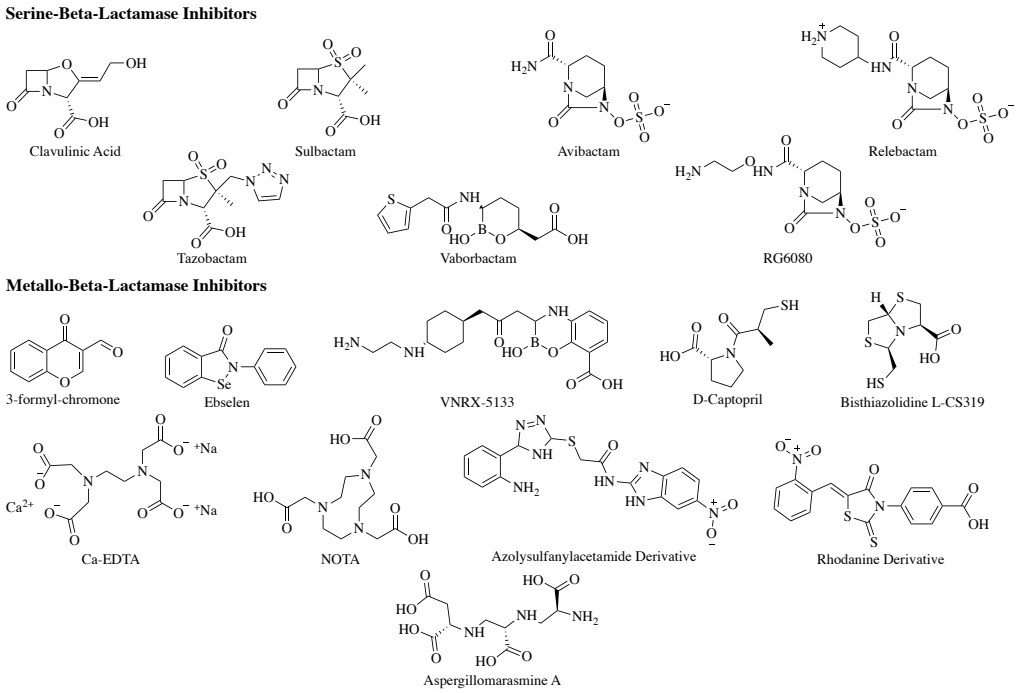

Figure 1-5. Inhibitors of β-Lactamases

Sulbactam is usually combined with ampicillin (Unasyn), and tazobactam with piperacillin (Zosyn) and ceftolozane (Zerbaxa).[73,148,196]

Avibactam, the first diazabicyclooctane inhibitor, was conditionally approved in 2015 as a combination with ceftazidime (Avycaz).[148,159,196] Avibactam has activity against Class A and C β-lactamases, including KPC carbapenemases.[148,159,202] Unlike the previous inhibitors, avibactam does not contain the β-lactam core and reversibly inhibits serine β-lactamases, allowing it to be given as a single dose (except against KPC-2, which causes fragmentation).[148,159] Other members in the pipeline include relebactam (in Phase 3 clinical trials) and RG6080, which may have some activity against OXA β-lactamases (preparing for Phase 2).[148,203]

Vaborbactam is another non-β-lactam inhibitor, which acts by mimicking the tetrahedral intermediates.[159,204] Approved in 2017, it has activity against Class A, C, and D β-lactamases.[159,204,205]

1.4.2.2. Metallo-β-Lactamase Inhibitors

Metallo-β-lactamases present several unique obstacles to inhibitor development. First of all, they have shallow, flexible active sites, with few conserved residues, rather than the narrow, deep sites of serine β-lactamases.[104,177] Hydrolysis is catalyzed by zinc ions rather than amino acid residues, so stable reaction intermediates are not formed.[104,176,177] Also, while there is very little sequence similarity between and even within (20% and 30% respectively) subclasses, there is sufficient similarity to human metalloenzymes to cause toxicity.[104,176,177]

No MBL inhibitors are currently approved. However, in recent years there has been flurry of work in this area, yielding over 500 reported MBL inhibitors from natural products, *de novo* synthesis, and *in silico* screening.[177] They can be roughly grouped into four categories: covalent, "copying", coordinating, and chelating.

There are a number of potential inhibitors that form covalent bonds with residues of the MBL active site. The first-generation cephalosporin cefaclor irreversibly acylates the conserved lysine residue in NDM-1 at supratherapeutic doses, and 3-formyl-chromone forms a Schiff base.[206,207] 3-formyl-chromone is noteworthy in that it shows selectivity for NDM over VIM.[206] Ebselen forms a

selenium-sulfide bond with Cys208 which results in loss of the zinc from the NDM-1 active site.[208] Nitroprusside and p-chloromercuricbenzoic acid (pCMB) also form covalent bonds with Cys208.[209]

Cyclic boronic acids, which act by "copying" the tetrahedral transition states of β-lactam hydrolysis, are some of the most promising broad-spectrum β-lactamase inhibitors.[210] Vaborbactam was approved in 2017 as a serine carbapenemase inhibitor, and cyclic boronic acids have since been shown to also inhibit metallo-β-lactamases NDM, VIM, IMP and BcII.[205,210] Venatorx is preparing to launch phase 3 clinical trial testing VNRX-5133 for efficacy in complicated urinary tract infections involving NDM, VIM, KPC, ESBL, and OXA carbapenemases.[203,211] Acyclic boronic acids have also been investigated as broad-spectrum β-lactamase inhibitors.[212] The bisthiazolidine and dipicolinic phosphonic acid derivatives (described below) also mimic the β-lactam ring and tetrahedral intermediates respectively.[104,177]

Coordinating inhibitors, which displace ligands from the zinc coordination complex without removing metal from the enzyme, are the most abundant.[104,177] D-captopril (an approved ACE inhibitor) showed early promise as an MBL inhibitor, using its thiol group to replace the bridging water molecule in NDM, VIM, IMP, SPM, BcII, CphA, ad BlaB carbapenemases.[213–215] This spawned a plethora of analogs.[177] One interesting family are the bisthiazolidine (BZT) inhibitors, which integrate the mercaptocarboxylic acid scaffold of D-captopril into a bicyclic system reminiscent of β-lactam antibiotics, rescuing their activity against bacterial strains harbouring NDM and other MBLs.[216] Thiorphan, tiopronin, dimercaprol, and

methisazone also showed ability to inhibit NDM, VIM, and IMP *via* zinc-coordinating thiol moieties, and isatin-β-thiosemicarbazone and spiro[indol]thiadiazole derivatives were optimized for activity against NDM-1.[104,177,217,218] Azolylsulfanylacetamides showed broad-spectrum inhibition of NDM, CcrA, Imis, and L1 enzymes *via* azole-coordination, with the exception of nitrobenzimidazole analogs which coordinate *via* their nitro substituents.[177] Interestingly, the full acetamide scaffold appears not to be necessary, as zinc can be coordinated by the thiol and triazole moieties.[219] Rhodanine derivatives similarly use nitro groups, and have been reported to inhibit all three classes of MBLs as well as SBLs.[220] Degradation products such as ML302F also coordinate zinc.[221] Dipicolinic acid itself chelates the zinc ion, but derivatives are able to inhibit VIM, NDM, and IMP enzymes through formation of stable zinc complexes with their carboxylic acids. 2-(4-Fluorobenzoyl)benzoic acid also forms complexes with VIM-2 through acid functionalities.[222]

Chelating inhibitors work by removing one or more zinc ions from the enzyme.[104] The best example of this is ethylenediamine-*N,N,N',N'*-tetracetic acid (EDTA), used in the lab to test for the presence of MBLs but generally too toxic for medicinal use.[104,177] However, the disodium salt (Ca-EDTA), which is approved to treat lead toxicity in Japan, was shown to restore carbapenem activity in NDM-1 *E. coli*.[223] 1,4,7-Triazacyclo- nonane-1,4,7-triacetic acid (NOTA) was also shown to inhibit NDM-1, as was its dithioic acid derivative.[177,224] Tris-picolylamine (TPA) and peptide-linked derivatives had activity against both VIM- and NDM-expressing *K. pneumonia* and *P. aeruginosa* strains, and disodium 2,3-diethylmaleate (DEM)

restored the activity of carbapenems and cephalosporins in VIM-, and to a smaller extent, NDM-containing *A. baumannii* and Enterobacteriaceae.[225,226]

Natural product Aspergillomarasmine A (AMA) also works by a chelating mechanism, through its four carboxylic acids and two backbone amines.[227,228] Previously investigated as an angiotensin-converting enzyme (ACE) and endothelin-converting enzyme (ECE) inhibitor, it was re-discovered through a whole-cell screen of potential MBL inhibitors.[227] AMA has activity against class B1 VIM, IMP, SPM, and most importantly, NDM lactamases.[104,227] *In vivo* activity was confirmed in mice infected with lethal doses of NDM-1-expressing *K. pneumonia*, and AMA has since been advanced to safety tests in rats and dogs.[227,229] There are four reported syntheses (using aziridine, acetonide-protected diols, and sulfamidate building blocks) that were used to assign the configuration (AMA is the *S,S,S* stereoisomer) and make a series of analogs to explore the structure-activity relationship.[230–234]

1.4.2.3 Aminoglycoside Modifying Enzyme Inhibitors

Copious examples of aminoglycoside kinase inhibitors, such as wortmannin, quercetin, 4-anilinoquinazoline, anthrapyrazolone, isoquinoline sulfonamide, and pyrazolopyrimidine derivatives, have been described in the literature (Figure 1-6).[235–239] An analog of acetylated gentamicin was shown to inhibit AAC(3) *in vitro*,[133] while chlorhexidine, pyrrolpyraziniums, and pyrrolidin-3-ols have been shown to inhibit various acetyltransferases.[240,241] Wortmannin, aranorosin, and isoquinoline sulfonamides inhibit the dual enzyme AAC(6')-

APH(2”).[236,238,242] β-thujaplicinol and various α-hydroxytropolone derivatives are the only scaffolds reported to inhibit ANTs.[243,244]

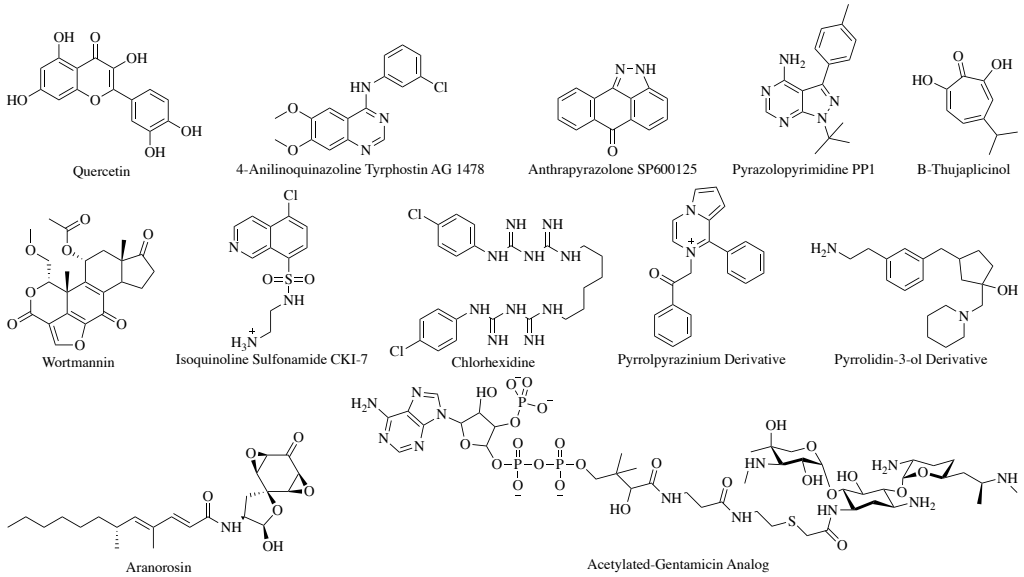

Figure 1-6. Inhibitors of Aminoglycoside-Modifying Enzymes

1.5 STATEMENT OF THESIS

Gram-negative bacteria cause serious infections, particularly in immune-compromised patients.[78,79] Our limited arsenal of antimicrobials effective against these pathogens is being rendered obsolete by resistance enzymes such as the aminoglycoside N-acetyltransferase-3 (AAC(3)), aminoglycoside O-nucleotidyltransferases-2” (ANT(2”)), and New Delhi metallo-β-lactamase-1 (NDM-1).[112] The objective of this thesis is to develop inhibitors to these enzymes that can be co-administered as adjuvant therapy with aminoglycosides and carbapenems in order to rescue their activity. Chapter 2 deals with the examination

of 3-benzylidene-2-indolinone inhibitors of AAC(3)-Ia. Chapter 3 describes the development of parallel synthetic methodology and subsequent SAR analysis of biphenyl isonicotinamide inhibitors of ANT(2")-Ia. Chapter 4 comprises a new synthetic approach designed to access position 6 of NDM-1 inhibitor AMA.

1.6 REFERENCES

(1) Carpenter, S.; Rigaud, M.; Barile, M.; Priest, T. J.; Perez, L.; Ferguson, J. B. An Interlinear Transliteration and English Translation of Portions of the Ebers Papyrus Possibly Having to Do with Diabetes Mellitus https://bxscience.edu/ourpages/auto/2008/11/10/43216077/egypt medicine.pdf (accessed Dec 24, 2018).

(2) Greenwood, D. *Antimicrobial Drugs: Chronicle of a Twentieth Century Medical Triumph*; Oxford University Press: Oxford, 2008.

(3) Hughes, J. P.; Rees, S.; Kalindjian, S. B.; Philpott, K. L. Principles of Early Drug Discovery. *Br. J. Pharmacol.* **2011**, *162* (6), 1239–1249.

(4) Mochly-Rosen, D.; Grimes, K. *A Practical Guide to Drug Development in Academia*; Mochly-Rosen, D., Grimes, K., Eds.; SpringerBriefs in Pharmaceutical Science & Drug Development; Springer International Publishing: Cham, 2014.

(5) Brodniewicz, T.; Grynkiewicz, G. Preclinical Drug Development. *Acta Pol. Pharm.* **2010**, *67* (6), 578–585.

(6) Lipinski, C. A.; Hopkins, A. Navigating Chemical Space for Biology and Medicine. *Nature* **2004**, *432* (November), 855–861.

(7) Dobson, C. M. Chemical Space and Biology. *Nature* **2004**, *432* (7019), 824–828.

(8) Pereira, D. A.; Williams, J. A. Origin and Evolution of High Throughput Screening. *Br. J. Pharmacol.* **2007**, *152* (1), 53–61.

(9) Dandapani, S.; Rosse, G.; Southall, N.; Salvino, J. M.; Thomas, C. J. Selecting, Acquiring, and Using Small Molecule Libraries for High-Throughput Screening. *Curr. Protoc. Chem. Biol.* **2012**, *4*, 177–191.

(10) Zhang, J.-H.; Chung, T. D. Y.; Oldenburg, K. R. A Simple Statistical

Parameter for Use in Evaluation and Validation of High Throughput Screening Assays. *J. Biomol. Screen.* **1999**, *4* (2), 67–73.

(11) Galloway, W. R. J. D.; Isidro-Llobet, A.; Spring, D. R. Diversity-Oriented Synthesis as a Tool for the Discovery of Novel Biologically Active Small Molecules. *Nat. Commun.* **2010**, *1* (6), 1–13.

(12) Tan, D. S. Diversity-Oriented Synthesis: Exploring the Intersections between Chemistry and Biology. *Nat. Chem. Biol.* **2005**, *1* (2), 74–84.

(13) Zhu, T.; Cao, S.; Su, P.-C.; Patel, R.; Shah, D.; Chokshi, H. B.; Szukala, R.; Johnson, M. E.; Hevener, K. E. Hit Identification and Optimization in Virtual Screening: Practical Recommendations Based on a Critical Literature Analysis. *J. Med. Chem.* **2013**, *56* (17), 6560–6572.

(14) Dove, A. Drug Screening--beyond the Bottleneck. *Nat. Biotechnol.* **1999**, *17* (9), 859–863.

(15) Wermuth, C. G. Search for New Lead Compounds: The Example of the Chemical and Pharmacological Dissection of Aminopyridazines. *J. Heterocycl. Chem.* **1998**, *35*, 1091–1100.

(16) Li, A. P. Screening for Human ADME/Tox Drug Properties in Drug Discovery. *Drug Discov. Today* **2001**, *6* (7), 357–366.

(17) Zhang, X.; Zhang, Y.; Ye, X.; Guo, X.; Zhang, T.; He, J. Overview of Phase IV Clinical Trials for Postmarket Drug Safety Surveillance: A Status Report from the ClinicalTrials.Gov Registry. *BMJ Open* **2016**, *6*, e010643.

(18) Schreiber, S. L. Target-Oriented and Diversity-Oriented Organic Synthesis in Drug Discovery. *Science* **2000**, *287* (5460), 1964–1969.

(19) Lam, K. S.; Salmon, S. E.; Hersh, E. M.; Hruby, V. J.; Kazmierski, W. M.; Knapp, R. J. A New Type of Synthetic Peptide Library for Identifying Ligand-Binding Activity. *Nature* **1991**, *354* (6348), 82–84.

(20) Merrifield, R. B. Solid Phase Peptide Synthesis. I. The Synthesis of a Tetrapeptide. *J. Am. Chem. Soc.* **1963**, *85* (14), 2149–2154.

(21) Geysen, H. M.; Rodda, S. J.; Mason, T. J. A Priori Delineation of a Peptide Which Mimics a Discontinuous Antigenic Determinant. *Mol. Immunol.* **1986**, *23* (7), 709–715.

(22) Rapoport, H.; Crowley, J. I. Cyclization Via Solid Phase Synthesis. Unidirectional Dieckmann Products from Solid Phase and Benzyl Triethylcarbinyl Pimelates. *J. Am. Chem. Soc.* **1970**, *92* (21), 6363–6365.

(23) Bunin, B. A.; Ellman, J. A. A General and Expedient Method for the Solid-Phase Synthesis of 1,4-Benzodiazepine Derivatives. *J. Am. Chem. Soc* **1992**, *114*, 10997–10998.

(24) Lipinski, C. A.; Lombardo, F.; Dominy, B. W.; Feeney, P. J. Experimental and Computational Approaches to Estimate Solubility and Permeability in Drug Discovery and Development Settings. *Adv. Drug Deliv. Rev.* **1997**, *23*, 3–25.

(25) Paterson, I.; Anderson, E. A. The Renaissance of Natural Products as Drug Candidates. *Science* **2005**, *310*, 451–453.

(26) Newman, D. J.; Cragg, G. M. Natural Products as Sources of New Drugs from 1981 to 2014. *J. Nat. Prod.* **2016**, *79* (3), 629–661.

(27) Newman, D. J.; Cragg, G. M.; Snader, K. M. Reviews Natural Products as Sources of New Drugs over the Period 1981-2002. *J. Nat. Prod.* **2003**, *66*, 1022–1037.

(28) Veber, D. F.; Johnson, S. R.; Cheng, H.-Y.; Smith, B. R.; Ward, K. W.; Kopple, K. D. Molecular Properties That Influence the Oral Bioavailability of Drug Candidates. *J. Med. Chem.* **2002**, *45*, 2615–2623.

(29) Teague, S.; Davis, A.; Leeson, P.; Oprea, T. The Design of Leadlike Combinatorial Libraries. *Angew. Chem. Int. Ed. Engl.* **1999**, *38* (24), 3743–3748.

(30) Wunberg, T.; Hendrix, M.; Hillisch, A.; Lobell, M.; Meier, H.; Schmeck, C.; Wild, H.; Hinzen, B. Improving the Hit-to-Lead Process: Data-Driven Assessment of Drug-like and Lead-like Screening Hits. *Drug Discov. Today* **2006**, *11* (3–4), 175–180.

(31) Evans, B. E.; Rittle, K. E.; Bock, M. G.; Dipardo, R. M.; Freidinger, R. M.; Whitter, W. L.; Lundell, G. F.; Veber, D. F.; Anderson, P. S.; Chang, R. S. L.; et al. Articles Methods for Drug Discovery: Development of Potent, Selective, Orally Effective Cholecystokinin Antagonistst. *J. Med. Chem* **1988**, *31*, 2235–2246.

(32) Welsch, M. E.; Snyder, S. A.; Stockwell, B. R. Privileged Scaffolds for Library Design and Drug Discovery. *Curr. Opin. Chem. Biol.* **2010**, *14*, 347–361.

(33) Wermuth, C. G. Selective Optimization of Side Activities: Another Way for Drug Discovery. *J. Med. Chem.* **2004**, *47* (6), 1303–1314.

(34) Stein, P. D.; Hunt, J. T.; Floyd, D. M.; Moreland, S.; J Dickinson, K. E.; Mitchell, C.; C-K Liu, E.; Webb, M. L.; Murugesan, N.; Dickey, J.; et al.

The Discovery of Sulfonamide Endothelin Antagonists and the Development of the Orally Active ETa Antagonist 5-(Dimethylamino)-IV-(3,4-Dimethyl-5- Isoxazolyl)-l-Naphthalenesu!Fonamide. *J. Med. Chem.* **1994**, *37* (3), 329–331.

(35) Pollinger, J.; Schierle, S.; Neumann, S.; Ohrndorf, J.; Kaiser, A.; Merk, D. Computer-assisted Selective Optimization of Side-activities - from Cinalukast to a PPARα Modulator. *ChemMedChem* **2019**, cmdc.201900286.

(36) Bebbington, M. W. P. Natural Product Analogues: Towards a Blueprint for Analogue-Focused Synthesis. *Chem. Soc. Rev.* **2017**, *46* (16), 5059–5109.

(37) Burke, M. D.; Schreiber, S. L.; Schreiber, S. L.; Burke, M. D. A Planning Strategy for Diversity-Oriented Synthesis. *Angew. Chem. Int. Ed* **2004**, *43*, 46–58.

(38) Rossiter, S. E.; Fletcher, M. H.; Wuest, W. M. Natural Products as Platforms To Overcome Antibiotic Resistance. *Chem. Rev.* **2017**, *117* (19), 12415–12474.

(39) Morrison, K. C.; Hergenrother, P. J. Natural Products as Starting Points for the Synthesis of Complex and Diverse Compounds. *Nat. Prod. Rep.* **2014**, *31* (1), 6–14.

(40) Patridge, E.; Gareiss, P.; Kinch, M. S.; Hoyer, D. An Analysis of FDA-Approved Drugs: Natural Products and Their Derivatives. *Drug Discov. Today* **2016**, *21* (2), 204–207.

(41) Njardarson, J. T.; Gaul, C.; Shan, D.; Huang, X.-Y.; Danishefsky, S. J. Discovery of Potent Cell Migration Inhibitors through Total Synthesis: Lessons from Structure-Activity Studies of (+)-Migrastatin. *J. Am. Chem. Soc.* **2004**, *126*, 1038–1040.

(42) Nören-Müller, A.; Reis-Corrêa, I.; Prinz, H.; Rosenbaum, C.; Saxena, K.; Schwalbe, H. J.; Vestweber, D.; Cagna, G.; Schunk, S.; Schwarz, O.; et al. Discovery of Protein Phosphatase Inhibitor Classes by Biology-Oriented Synthesis. *Proc. Natl. Acad. Sci. U. S. A.* **2006**, *103* (28), 10606–10611.

(43) Kaiser, M.; Wetzel, S.; Kumar, K.; Waldmann, H. Review Biology-Inspired Synthesis of Compound Libraries. *Cell. Mol. Life Sci.* **2008**, *65*, 1186–1201.

(44) Jencks, W. P. On the Attribution and Additivity of Binding Energies. *Proc. Natl. Acad. Sci. U. S. A.* **1981**, *78* (7), 4046–4050.

(45) Shuker, S. B.; Hajduk, P. J.; Meadows, R. P.; Fesik, S. W. Discovering High-Affinity Ligands for Proteins: SAR by NMR. *Science* **1996**, *274* (5292), 1531–1534.

(46) Erlanson, D. A.; Fesik, S. W.; Hubbard, R. E.; Jahnke, W.; Jhoti, H. Twenty Years on: The Impact of Fragments on Drug Discovery. *Nat. Rev. Drug Discov.* **2016**, *15* (9), 605–619.

(47) Erlanson, D. A.; Davis, B. J.; Jahnke, W. Perspective Fragment-Based Drug Discovery: Advancing Fragments in the Absence of Crystal Structures. *Cell Chem. Biol.* **2019**, *26*, 9–15.

(48) Wender, P. A.; Quiroz, R. V; Stevens, M. C. Function through Synthesis-Informed Design. *Acc. Chem. Res* **2015**, *48*, 752–760.

(49) Wender, P. A.; Miller, B. L. Synthesis at the Molecular Frontier. *Nature* **2009**, *460* (7252), 197–201.

(50) Wender, P. A.; Koehler, K. F.; Sharkey, N. A.; Dell'Aquila, M. L.; Blumberg, P. M. Analysis of the Phorbol Ester Pharmacophore on Protein Kinase C as a Guide to the Rational Design of New Classes of Analogs. *Proc. Natl. Acad. Sci. U. S. A.* **1986**, *83* (12), 4214–4218.

(51) Brown, E. D.; Wright, G. D. Antibacterial Drug Discovery in the Resistance Era. *Nature* **2016**, *529* (7586), 336–343.

(52) O'Shea, R.; Moser, H. E. Physicochemical Properties of Antibacterial Compounds: Implications for Drug Discovery. *J. Med. Chem.* **2008**, *51* (10), 2871–2878.

(53) Delcour, A. H. Outer Membrane Permeability and Antibiotic Resistance. *Biochim. Biophys. Acta* **2009**, *1794* (5), 808–816.

(54) Chopra, I.; Roberts, M. Tetracycline Antibiotics: Mode of Action, Applications, Molecular Biology, and Epidemiology of Bacterial Resistance. *Microbiol. Mol. Biol. Rev.* **2001**, *65* (2), 232–260.

(55) Hancock, R. E. W.; Bell, A. Antibiotic Uptake into Gram-Negative Bacteria. *Eur. J. Clin. Microbiol. Infect. Dis* **1988**, *7* (6), 713–720.

(56) Payne, D. J.; Miller, L. F.; Findlay, D.; Anderson, J.; Marks, L. Time for a Change: Addressing R&D and Commercialization Challenges for Antibacterials. *Philos. Trans. R. Soc. London B Biol. Sci.* **2015**, *370* (1670), 1–12.

(57) Silhavy, T. J.; Kahne, D.; Walker, S. The Bacterial Cell Envelope. *Cold Spring Harb. Perspect. Biol.* **2010**, *2* (5), a000414.

(58) Exner, M.; Bhattacharya, S.; Christiansen, B.; Gebel, J.; Goroncy-Bermes, P.; Hartemann, P.; Heeg, P.; Ilschner, C.; Kramer, A.; Larson, E.; et al. Antibiotic Resistance: What Is so Special about Multidrug-Resistant Gram-

Negative Bacteria? *GMS Hyg. Infect. Control* **2017**, *12*, Doc05.

(59) Alhariri, M.; Azghani, A.; Omri, A. Liposomal Antibiotics for the Treatment of Infectious Diseases. *Expert Opin. Drug Deliv.* **2013**, *10* (11), 1515–1532.

(60) Fernandes, P.; Martens, E. Antibiotics in Late Clinical Development. *Biochem. Pharmacol.* **2017**, *133*, 152–163.

(61) Schalk, I. J. Siderophore-Antibiotic Conjugates: Exploiting Iron Uptake to Deliver Drugs into Bacteria. *Clin. Microbiol. Infect.* **2018**, *24*, 801–802.

(62) Fair, R. J.; Tor, Y. Antibiotics and Bacterial Resistance in the 21st Century. *Perspect. Medicin. Chem.* **2014**, *6*, 25–64.

(63) *The Merck Manual of Diagnosis and Therapy*, 19th ed.; Porter, R. S., Kaplan, J. L., Albert, R. K., Bowman, M. A., Braunstein, G. D., Cohen, S., Emanuel, L., Fawcett, J., Frenkel, E. P., Hendrix, S. L., et al., Eds.; Merck Sharp & Dohme Corp., A Subsidary of Merck & Co, Inc.: Whitehouse Station, NJ, 2011.

(64) Schlecht, H. P.; Bruno, C. Overview of Antibacterial Drugs https://www.merckmanuals.com/en-ca/professional/infectious-diseases/bacteria-and-antibacterial-drugs/overview-of-antibacterial-drugs (accessed May 3, 2018).

(65) World Health Organization. *WHO Model List of Essential Medicines 20th List (March 2017)*; 2017.

(66) O'Neill, J. *Tackling Drug-Resistant Infections Globally: Final Report and Recommendations*; 2016.

(67) Conly, J.; Johnston, B. Where Are All the New Antibiotics? The New Antibiotic Paradox. *Can. J. Infect. Dis. Med. Microbiol. = J. Can. des Mal. Infect. la Microbiol. medicale* **2005**, *16* (3), 159–160.

(68) Butler, M. S.; Blaskovich, M. A.; Cooper, M. A. Antibiotics in the Clinical Pipeline at the End of 2015. *J. Antibiot. (Tokyo).* **2017**, *70* (1), 3–24.

(69) Fleming, A. On the Antibacterial Action of Cultures of a Penicillium, with Special Reference to Their Use in the Isolation of B. Influenzae. *Br. J. Exp. Pathol.* **1929**, *10* (3), 226–236.

(70) Enzler, M. J.; Berbari, E.; Osmon, D. R. Antimicrobial Prophylaxis in Adults. *Mayo Clin. Proc.* **2011**, *86* (7), 686–701.

(71) Howell, M. D.; Davis, A. M. Management of Sepsis and Septic Shock. *JAMA* **2017**, *317* (8), 847.

(72) Lipsky, B. A.; Berendt, A. R.; Cornia, P. B.; Pile, J. C.; Peters, E. J. G.; Armstrong, D. G.; Deery, H. G.; Embil, J. M.; Joseph, W. S.; Karchmer, A. W.; et al. 2012 Infectious Diseases Society of America Clinical Practice Guideline for the Diagnosis and Treatment of Diabetic Foot Infections A. *Clin. Infect. Dis.* **2012**, *54* (12), 132–173.

(73) Gladwin, M.; Trattler, B. *Clinical Microbiology Made Ridiculously Simple*, 3rd ed.; MedMaster, Inc: Miami, FL, 2002.

(74) Davies, J.; Davies, D. Origins and Evolution of Antibiotic Resistance. *Microbiol. Mol. Biol. Rev.* **2010**, *74* (3), 417–433.

(75) Peng, Z.; Jin, D.; Kim, H. B.; Stratton, C. W.; Wu, B.; Tang, Y.-W.; Sun, X. Update on Antimicrobial Resistance in Clostridium Difficile: Resistance Mechanisms and Antimicrobial Susceptibility Testing. *J. Clin. Microbiol.* **2017**, *55*, 1988–2008.

(76) Nguyen, T. V. A.; Anthony, R. M.; Bañuls, A.-L.; Nguyen, T. V. A.; Vu, D. H.; Alffenaar, J.-W. C. Bedaquiline Resistance: Its Emergence, Mechanism, and Prevention. *Clin. Infect. Dis.* **2018**, *66* (10), 1625–1630.

(77) WHO. *Global Action Plan on Antimicrobial Resistance*; Geneva, Switzerland, 2015.

(78) Pendleton, J. N.; Gorman, S. P.; Gilmore, B. F. Clinical Relevance of the ESKAPE Pathogens. *Expert Rev. Anti. Infect. Ther.* **2013**, *11* (3), 297–308.

(79) Santajit, S.; Indrawattana, N. Mechanisms of Antimicrobial Resistance in ESKAPE Pathogens. *Biomed Res. Int.* **2016**, *2016*, 1–8.

(80) Wright, G. D. Bacterial Resistance to Antibiotics: Enzymatic Degradation and Modification. *Adv. Drug Deliv. Rev.* **2005**, *57* (10), 1451–1470.

(81) Davies, J.; Davies, D. Origins and Evolution of Antibiotic Resistance. *Microbiol. Mol. Biol. Rev.* **2010**, *74* (3), 417–433.

(82) D'Costa, V. M.; King, C. E.; Kalan, L.; Morar, M.; Sung, W. W. L.; Schwarz, C.; Froese, D.; Zazula, G.; Calmels, F.; Debruyne, R.; et al. Antibiotic Resistance Is Ancient. *Nature* **2011**, *477* (7365), 457–461.

(83) Fernández, L.; Hancock, R. E. W. Adaptive and Mutational Resistance: Role of Porins and Efflux Pumps in Drug Resistance. *Clin. Microbiol. Rev.* **2012**, *25* (4), 661–681.

(84) Goffin, C.; Ghuysen, J. M. Multimodular Penicillin-Binding Proteins: An Enigmatic Family of Orthologs and Paralogs. *Microbiol. Mol. Biol. Rev.* **1998**, *62* (4), 1079–1093.

(85) Massova, I.; Mobashery, S. Kinship and Diversification of Bacterial Penicillin-Binding Proteins and β-Lactamases. *Antimicrob. Agents Chemother.* **1998**, *42* (1), 1–17.

(86) Blair, J. M. A.; Webber, M. A.; Baylay, A. J.; Ogbolu, D. O.; Piddock, L. J. V. Molecular Mechanisms of Antibiotic Resistance. *Nat. Rev. Microbiol.* **2015**, *13* (1), 42–51.

(87) Hall, C. W.; Mah, T.-F. Molecular Mechanisms of Biofilm-Based Antibiotic Resistance and Tolerance in Pathogenic Bacteria. *FEMS Microbiol. Rev.* **2017**, *41* (3), 276–301.

(88) Chambers, H. F. Methicillin Resistance in Staphylococci: Molecular and Biochemical Basis and Clinical Implications. *Clin. Microbiol. Rev.* **1997**, *10* (4), 781–791.

(89) Fisher, J. F.; Mobashery, S. β-Lactam Resistance Mechanisms: Gram-Positive Bacteria and Mycobacterium Tuberculosis. *Cold Spring Harb. Perspect. Med.* **2016**, *6* (5), a025221.

(90) Leclercq, R. Mechanisms of Resistance to Macrolides and Lincosamides: Nature of the Resistance Elements and Their Clinical Implications. *Clin. Infect. Dis.* **2002**, *34* (4), 482–492.

(91) Hidalgo, L.; Hopkins, K. L.; Gutierrez, B.; Ovejero, C. M.; Shukla, S.; Douthwaite, S.; Prasad, K. N.; Woodford, N.; Gonzalez-Zorn, B. Association of the Novel Aminoglycoside Resistance Determinant RmtF with NDM Carbapenemase in Enterobacteriaceae Isolated in India and the UK. *J. Antimicrob. Chemother.* **2013**, *68* (7), 1543–1550.

(92) Butler, M. S.; Hansford, K. A.; Blaskovich, M. A. T.; Halai, R.; Cooper, M. A. Glycopeptide Antibiotics: Back to the Future. *J. Antibiot. (Tokyo).* **2014**, *67* (9), 631–644.

(93) Aldred, K. J.; Kerns, R. J.; Osheroff, N. Mechanism of Quinolone Action and Resistance. *Biochemistry* **2014**, *53* (10), 1565–1574.

(94) Piddock, L. J. V. Clinically Relevant Chromosomally Encoded Multidrug Resistance Efflux Pumps in Bacteria. *Clin. Microbiol. Rev.* **2006**, *19* (2), 382–402.

(95) Rice, L. B. Federal Funding for the Study of Antimicrobial Resistance in Nosocomial Pathogens: No ESKAPE. *J. Infect. Dis.* **2008**, *197* (8), 1079–1081.

(96) Walsh, C.; Fisher, S.; Park, I.-S.; Prahalad, M.; Wu, Z. Bacterial Resistance to Vancomycin: Five Genes and One Missing Hydrogen Bond Tell the Story.

Chem. Biol. **1996**, *3*, 21–28.

(97) Yong, D.; Toleman, M. A.; Giske, C. G.; Cho, H. S.; Sundman, K.; Lee, K.; Walsh, T. R. Characterization of a New Metallo-Beta-Lactamase Gene, Bla(NDM-1), and a Novel Erythromycin Esterase Gene Carried on a Unique Genetic Structure in Klebsiella Pneumoniae Sequence Type 14 from India. *Antimicrob. Agents Chemother.* **2009**, *53* (12), 5046–5054.

(98) Yigit, H.; Queenan, A. M.; Anderson, G. J.; Domenech-Sanchez, A.; Biddle, J. W.; Steward, C. D.; Alberti, S.; Bush, K.; Tenover, F. C. Novel Carbapenem-Hydrolyzing Beta-Lactamase, KPC-1, from a Carbapenem-Resistant Strain of Klebsiella Pneumoniae. *Antimicrob. Agents Chemother.* **2001**, *45* (4), 1151–1161.

(99) Evans, B. A.; Amyes, S. G. B. OXA β-Lactamases. *Clin. Microbiol. Rev.* **2014**, *27* (2), 241–263.

(100) Queenan, A. M.; Bush, K. Carbapenemases: The Versatile Beta-Lactamases. *Clin. Microbiol. Rev.* **2007**, *20* (3), 440–458, table of contents.

(101) Ramírez-Estrada, S.; Borgatta, B.; Rello, J. Pseudomonas Aeruginosa Ventilator-Associated Pneumonia Management. *Infect. Drug Resist.* **2016**, *9*, 7–18.

(102) Hart, C. A.; Winstanley, C. Persistent and Aggressive Bacteria in the Lungs of Cystic Fibrosis Children. *Br. Med. Bull.* **2002**, *61* (1), 81–96.

(103) Watanabe, M.; Iyobe, S.; Inoue, M.; Mitsuhashi, S. Transferable Imipenem Resistance in Pseudomonas Aeruginosa. *Antimicrob. Agents Chemother.* **1991**, *35* (1), 147–151.

(104) Rotondo, C. M.; Wright, G. D. Inhibitors of Metallo-B-Lactamases. *Curr. Opin. Microbiol.* **2017**, *39*, 96–105.

(105) Wu, W.; Feng, Y.; Tang, G.; Qiao, F.; McNally, A.; Zong, Z. NDM Metallo-β-Lactamases and Their Bacterial Producers in Health Care Settings. *Clin. Microbiol. Rev.* **2019**, *32* (2), e00115-18.

(106) Aminov, R. History of Antimicrobial Drug Discovery: Major Classes and Health Impact. *Biochem. Pharmacol.* **2017**, *133*, 4–19.

(107) Tomasz, A. The Mechanism of the Irreversible Antimicrobial Effects of Penicillins: How the Beta-Lactam Antibiotics Kill and Lyse Bacteria. *Annu. Rev. Microbiol.* **1979**, *33* (1), 113–137.

(108) Bush, K.; Bradford, P. A. β-Lactams and β-Lactamase Inhibitors: An Overview. *Cold Spring Harb. Perspect. Med.* **2016**, *6* (8), a025247.

(109) Falagas, M. E.; Vouloumanou, E. K.; Samonis, G.; Vardakas, K. Z. Fosfomycin. *Clin. Microbiol. Rev.* **2016**, *29* (2), 321–347.

(110) Trimble, M. J.; Mlynárčik, P.; Kolář, M.; Hancock, R. E. W. Polymyxin: Alternative Mechanisms of Action and Resistance. *Cold Spring Harb. Perspect. Med.* **2016**, *6* (10), a025288.

(111) Taber, H. W.; Mueller, J. P.; Miller, P. F.; Arrow, A. S. Bacterial Uptake of Aminoglycoside Antibiotics. *Microbiol. Rev.* **1987**, *51* (4), 439–457.

(112) Ruppé, É.; Woerther, P.-L.; Barbier, F. Mechanisms of Antimicrobial Resistance in Gram-Negative Bacilli. *Ann. Intensive Care* **2015**, *5* (1), 21.

(113) Tenson, T.; Mankin, A. Antibiotics and the Ribosome. *Mol. Microbiol.* **2006**, *59* (6), 1664–1677.

(114) Gonzalez, U. S.; Spencer, J. P. Aminoglycosides: A Practical Review. *Am. Fam. Physician* **1998**, *58* (8), 1811–1820.

(115) Davis, B. D. Mechanism of Bactericidal Action of Aminoglycosides. *Microbiol. Rev.* **1987**, *51* (3), 341–350.

(116) Niccolai, D.; Tarsi, L.; Thomas, R. J. The Renewed Challenge of Antibacterial Chemotherapy. *Chem. Commun.* **1997**, No. 24, 2333–2342.

(117) Waksman, S. A.; Lechevalier, H. A. Neomycin, a New Antibiotic Active against Streptomycin-Resistant Bacteria, Including Tuberculosis Organisms. *Science* **1949**, *109* (2830), 305–307.

(118) Gardner, T. B.; Hill, D. R. Treatment of Giardiasis. *Clin. Microbiol. Rev.* **2001**, *14* (1), 114–128.

(119) Umezawa, H. Kanamycin: Its Discovery. *Ann. N. Y. Acad. Sci.* **1958**, *76* (2), 20–26.

(120) Weinstein, M. J.; Luedemann, G. M.; Oden, E. M.; Wagman, G. H.; Rosselet, J. P.; Marquez, J. A.; Coniglio, C. T.; Charney, W.; Herzog, H. L.; Black, J. Gentamicin, a New Antibiotic Complex from Micromonospora. *J. Med. Chem.* **1963**, *6* (4), 463–464.

(121) Reynolds, A. V; Hamilton-Miller, J. M. T.; Brumfitt, W. Newer Aminoglycosides-Amikacin and Tobramycin: An in-Vitro Comparison with Kanamycin and Gentamicin. *Br. Med. J.* **1974**, *28* (5934), 778–780.

(122) Kawaguchi, H.; Naito, T.; Nakagawa, S.; Fujisawa, K. I. BB-K 8, a New Semisynthetic Aminoglycoside Antibiotic. *J. Antibiot. (Tokyo)* **1972**, *25* (12), 695–708.

(123) Food and Drug Administration-Center for Drug Evaluation and Research. *Approved Drug Products with Therapeutic Equivalence Evaluations*, 38th ed.; U.S. Department of Health and Human Services, Ed.; 2018.

(124) U.S. Food and Drug Administration. *Drug Approval Package: ZEMDRI (Plazomicin)*; Silver Spring, 2018.

(125) Ramirez, M. S.; Tolmasky, M. E. Aminoglycoside Modifying Enzymes. *Drug Resist. Updat.* **2010**, *13*, 151–171.

(126) Labby, K. J.; Garneau-Tsodikova, S. Strategies to Overcome the Action of Aminoglycoside-Modifying Enzymes for Treating Resistant Bacterial Infections. *Future Med. Chem.* **2013**, *5* (11), 1285–1309.

(127) Maurin, M.; Raoult, D. Use of Aminoglycosides in Treatment of Infections Due to Intracellular Bacteria. *Antimicrob. Agents Chemother.* **2001**, *45* (11), 2977–2986.

(128) Li, L.; Zhou, R.; Geng, H.; Yue, L.; Ye, F.; Xie, Y.; Liu, J.; Kong, X.; Jiang, H.; Huang, J.; et al. Discovery of Two Aminoglycoside Antibiotics as Inhibitors Targeting the Menin–Mixed Lineage Leukaemia Interface. *Bioorg. Med. Chem. Lett.* **2014**, *24* (9), 2090–2093.

(129) Shaw, K. J.; Rather, P. N.; Hare, R. S.; Miller, G. H. Molecular Genetics of Aminoglycoside Resistance Genes and Familial Relationships of the Aminoglycoside-Modifying Enzymes. *Microbiol. Rev.* **1993**, *57* (1), 138–163.

(130) Shakya, T.; Wright, G. D. Nucleotide Selectivity of Antibiotic Kinases. *Antimicrob. Agents Chemother.* **2010**, *54* (5), 1909–1913.

(131) Brzezinska, M.; Benveniste, R.; Davies, J.; Daniels, P. J. L.; Weinstein, J. Gentamicin Resistance in Strains of Pseudomonas Aeruginosa Mediated by Enzymatic N-Acetylation of the Deoxystreptamine Moiety. *Biochemistry* **1972**, *11* (5), 761–766.

(132) Northrop, B. Kinetic Mechanisms of Gentamicin Acetyltransferase I . Antibiotic-Dependent Random Mechanisms. *J. Biol. Chem.* **1978**, *253* (17), 5902–5907.

(133) Williams, J. W.; Northrop, D. B. Synthesis of a Tight-Binding, Multisubstrate Analog Inhibitor of Gentamicin Acetyltransferase I. *J. Antibiot. (Tokyo).* **1979**, *32* (11), 1147–1154.

(134) Williams, J. W.; Northrop, D. B. Substrate Specificity and Structure-Activity Relationships of Gentamicin Acetyltransferase I. The Dependence of Antibiotic Resistance upon Substrate Vmax/Km Values. *J. Biol. Chem.*

1978, *253* (17), 5908–5914.

(135) Cox, G.; Stogios, P. J.; Savchenko, A.; Wright, G. D. Structural and Molecular Basis for Resistance to Aminoglycoside Antibiotics by the Adenylyltransferase ANT(2″)-Ia. *MBio* **2015**, *6* (1), e02180-14.

(136) Benveniste, R.; Davies, J. R-Factor Mediated Gentamicin Resistance: A New Enzyme Which Modifies Aminoglycoside Antibiotics. *FEBS Lett.* **1971**, *14* (5), 293–296.

(137) Gates, C. A.; Northrop, D. B. Alternative Substrate and Inhibition Kinetics of Aminoglycoside Nucleotidyltransferase 2''-I in Support of a Theorell-Chance Kinetic Mechanism. *Biochemistry* **1988**, *27* (10), 3826–3833.

(138) Shapiro, D. J.; Hicks, L. A.; Pavia, A. T.; Hersh, A. L. Antibiotic Prescribing for Adults in Ambulatory Care in the USA, 2007–09. *J. Antimicrob. Chemother.* **2014**, *69* (1), 234–240.

(139) Tipper, D. J.; Strominger, J. L. Mechanism of Action of Penicillins: A Proposal Based on Their Structural Similarity to Acyl-D-Alanyl-D-Alanine. *Proc. Natl. Acad. Sci. U. S. A.* **1965**, *54* (4), 1133–1141.

(140) Hashizume, T.; Ishino, F.; Nakagawa, J.; Tamaki, S.; Matsuhashi, M. Studies on the Mechanism of Action of Imipenem (N-Formimidoylthienamycin) in Vitro: Binding to the Penicillin-Binding Proteins (PBPs) in Escherichia Coli and Pseudomonas Aeruginosa, and Inhibition of Enzyme Activities Due to the PBPs in E. Coli. *J. Antibiot. (Tokyo)* **1984**, *37* (4), 394–400.

(141) Neu, H. C.; York, N. Aztreonam Activity, Pharmacology, and Clinical Uses. *Am. J. Med.* **1990**, *88* (suppl 3C), 2S-6S.

(142) Babic, M.; Hujer, A. M.; Bonomo, R. A. What's New in Antibiotic Resistance? Focus on Beta-Lactamases. *Drug Resist. Updat.* **2006**, *9* (3), 142–156.

(143) Abraham, E. P.; Chain, E.; Fletcher, C. M.; Gardner, A. D.; Heatley, N. G.; Jennings, M. A.; Florey, H. W. Further Observations on Penicillin. *Lancet* **1941**, *16*, 177–189.

(144) Grossman, C. M. The First Use of Penicillin in the United States. *Ann. Intern. Med.* **2008**, *149* (2), 135–136.

(145) Horn, D. L.; Zabriskie, J. B.; Cleary, P. P.; Ferretti, J. J.; Fischetti, V. A.; Gotschlich, E.; Kaplan, E. L.; Mccarty, M.; Opal, S. M.; Roberts, R. B.; et al. Why Have Group A Streptococci Remained Susceptible to Penicillin? Report on a Symposium*. *Clin. Infect. Dis.* **1998**, *26* (6), 1341–1345.

(146) Batchelor, F. R.; Doyle, F. P.; Nayler, J. H. C.; Rolinson, G. N. Synthesis of Penicillin: 6-Aminopenicillanic Acid in Penicillin Fermentations. *Nature* **1959**, *183* (4656), 257–258.

(147) Geddes, A. M.; Klugman, K. P.; Rolinson, G. N. Introduction: Historical Perspective and Development of Amoxicillin/Clavulanate. *Int. J. Antimicrob. Agents* **2007**, *30*, 109–112.

(148) Bush, K. A Resurgence of β-Lactamase Inhibitor Combinations Effective against Multidrug-Resistant Gram-Negative Pathogens. *Int. J. Antimicrob. Agents* **2015**, *46* (5), 483–493.

(149) Ursu, O.; Holmes, J.; Knockel, J.; Bologa, C. G.; Yang, J. J.; Mathias, S. L.; Nelson, S. J.; Oprea, T. I. DrugCentral: Online Drug Compendium. *Nucleic Acids Res.* **2017**, *45* (D1), D932–D939.

(150) Newton, G. G. F.; Abraham, E. P. Cephalosporin C, a New Antibiotic Containing Sulphur and D-α-Aminoadipic Acid. *Nature* **1955**, *175* (4456), 548–548.

(151) Bryskier, A.; Aszodi, J.; Chantot, J.-F. Parenteral Cephalosporin Classification. *Expert Opin. Investig. Drugs* **1994**, *3* (2), 145–171.

(152) Morin, R. B.; Jackson, B. G.; Flynn, E. H.; Roeske, R. W. Chemistry of Cephalosporin Antibiotics. I. 7-Aminocephalosporanic Acid from Cephalosporin C. *J. Am. Chem. Soc.* **1962**, *84* (17), 3400–3401.

(153) Chauvette, R. R.; Flynn, E. H.; Jackson, B. G.; Lavagnino, E. R.; Morin, R. B.; Mueller, R. A.; Pioch, R. P.; Roeske, R. W.; Ryan, C. W.; Spencer, J. L.; et al. Chemistry of Cephalosporin Antibiotics. II. Preparation of a New Class of Antibiotics and the Relation of Structure to Activity. *J. Am. Chem. Soc.* **1962**, *84* (17), 3401–3402.

(154) Kahan, J. S.; Kahan, F. M.; Goegelman, R.; Currie, S. A.; Jackson, M.; Stapley, E. O.; Miller, T. W.; Miller, A. K.; Hendlin, D.; Mochalest, S.; et al. Thienamycin, a New Beta-Lactam Antibiotic. I. Discovery, Taxonomy, Isolation and Physical Properties. *J. Antibiot.* **1979**, *32* (1), 1–12.

(155) Papp-Wallace, K. M.; Endimiani, A.; Taracila, M. A.; Bonomo, R. A. Carbapenems: Past, Present, and Future. *Antimicrob. Agents Chemother.* **2011**, *55* (11), 4943–4960.

(156) Shah, P. M.; Isaacs, R. D. Ertapenem, the First of a New Group of Carbapenems. *J. Antimicrob. Chemother.* **2003**, *52* (4), 538–542.

(157) Jain, A.; Utley, L.; Parr, T. R.; Zabawa, T.; Pucci, M. J. Tebipenem, the First Oral Carbapenem Antibiotic. *Expert Rev. Anti. Infect. Ther.* **2018**, *16* (7),

513–522.

(158) Spiro Therapeutics. Spero Therapeutics Announces FDA Acceptance of IND Application for SPR994 https://www.globenewswire.com/news-release/2019/02/04/1709692/0/en/Spero-Therapeutics-Announces-FDA-Acceptance-of-IND-Application-for-SPR994.html (accessed July 8, 2019).

(159) Tooke, C. L.; Hinchliffe, P.; Bragginton, E. C.; Colenso, C. K.; Hirvonen, V. H. A.; Takebayashi, Y.; Spencer, J. β-Lactamases and β-Lactamase Inhibitors in the 21st Century. *J. Mol. Biol.* **2019**, https://doi.org/10.1016/j.jmb.2019.04.002.

(160) Bush, K. Past and Present Perspectives on β-Lactamases. *Antimicrob. Agents Chemother.* **2018**, *62* (10), e01076-18.

(161) Sykes, R. B.; Cimarusti, C. M.; Bonner, D. P.; Bush, K.; Floyd, D. M.; Georgopapadakou, N. H.; Koster, W. H.; Liu, W. C.; Parker, W. L.; Principe, P. A.; et al. Monocyclic β-Lactam Antibiotics Produced by Bacteria. *Nature* **1981**, *291* (5815), 489–491.

(162) Rogers Yocum, R.; Rasmussen, J. R.; Strominger, J. L. The Mechanism of Action of Penicillin Penicillin Acylates the Active Site of Bacillus Stearothermophilus D-Alanine Carboxypeptidase. *J. Biol. Chem.* **1980**, *255* (9), 3977–3986.

(163) Gardner, A. D. Morphological Effects of Penicillin on Bacteria. *Nature* **1940**, *146* (3713), 837–838.

(164) Georgopapadakou, N. H.; Fung, A.; Liu, Y. Penicillin-Binding Proteins in Bacteria. *Antimicrob. Agents Chemother.* **1980**, *18* (1), 148–157.

(165) Curtis, N. A. C.; Orr, D.; Ross, G. W.; Boulton, M. G. Affinities of Penicillins and Cephalosporins for the Penicillin- Binding Proteins of Escherichia Coli K-12 and Their Antibacterial Activity. *Antimicrob. Agents Chemother.* **1979**, *16* (5), 533–539.

(166) Spratt, B. G. Distinct Penicillin Binding Proteins Involved in the Division, Elongation, and Shape of Escherichia Coli K12 (P-Lactam Antibiotics/Slab Gel Electrophoresis/Binding Protein Mutants). *Proc. Natl. Acad. Sci. U. S. A.* **1975**, *72* (8), 2999–3003.

(167) Bush, K.; Jacoby, G. A. Updated Functional Classification of Beta-Lactamases. *Antimicrob. Agents Chemother.* **2010**, *54* (3), 969–976.

(168) Abraham, E. P.; Chain, E. An Enzyme from Bacteria Able to Destroy Penicillin. *Nature* **1940**, *146* (3713), 837–837.

(169) Bush, K.; Palzkill, T.; Jacoby, G. ß-Lactamase Classification and Amino Acid Sequences for TEM, SHV and OXA Extended-Spectrum and Inhibitor Resistant Enzymes http://www.lahey.org/Studies/ (accessed Jul 18, 2018).

(170) Ambler, R. P. The Structure of Beta-Lactamases. *Philos. Trans. R. Soc. Lond. B. Biol. Sci.* **1980**, *289* (1036), 321–331.

(171) Jaurin, B.; Grundström, T. AmpC Cephalosporinase of Escherichia Coli K-12 Has a Different Evolutionary Origin from That of Beta-Lactamases of the Penicillinase Type. *Proc. Natl. Acad. Sci. U. S. A.* **1981**, *78* (8), 4897–4901.

(172) Ouellette, M.; Bissonnette, L.; Roy, P. H. Precise Insertion of Antibiotic Resistance Determinants into Tn21-like Transposons: Nucleotide Sequence of the OXA-1 Beta-Lactamase Gene. *Proc. Natl. Acad. Sci. U. S. A.* **1987**, *84* (21), 7378–7382.

(173) Jacoby, G. A. AmpC Beta-Lactamases. *Clin. Microbiol. Rev.* **2009**, *22* (1), 161–182.

(174) Eriksson-Grennberg, K. G.; Boman, H. G.; Jansson, J. A.; Thorén, S. Resistance of Escherichia Coli to Penicillins I. Genetic Study of Some Ampicillin-Resistant Mutants. *J. Bacteriol.* **1965**, *90* (1), 54–62.

(175) Bradford, P. A. Extended-Spectrum Beta-Lactamases in the 21st Century: Characterization, Epidemiology, and Detection of This Important Resistance Threat. *Clin. Microbiol. Rev.* **2001**, *14* (4), 933–951.

(176) Walsh, T. R.; Toleman, M. A.; Poirel, L.; Nordmann, P. Metallo-Beta-Lactamases: The Quiet before the Storm? *Clin. Microbiol. Rev.* **2005**, *18* (2), 306–325.

(177) Linciano, P.; Cendron, L.; Gianquinto, E.; Spyrakis, F.; Tondi, D. Ten Years with New Delhi Metallo-β-Lactamase-1 (NDM-1): From Structural Insights to Inhibitor Design. *ACS Infect. Dis.* **2019**, *5*, 9–34.

(178) Kumarasamy, K. K.; Toleman, M. A.; Walsh, T. R.; Bagaria, J.; Butt, F.; Balakrishnan, R.; Chaudhary, U.; Doumith, M.; Giske, C. G.; Irfan, S.; et al. Emergence of a New Antibiotic Resistance Mechanism in India, Pakistan, and the UK: A Molecular, Biological, and Epidemiological Study. *Lancet. Infect. Dis.* **2010**, *10* (9), 597–602.

(179) Feng, H.; Liu, X.; Wang, S.; Fleming, J.; Wang, D.-C.; Liu, W. The Mechanism of NDM-1-Catalyzed Carbapenem Hydrolysis Is Distinct from That of Penicillin or Cephalosporin Hydrolysis. *Nat. Commun.* **2017**, *8* (1), 2242.

(180) Lisa, M.-N.; Palacios, A. R.; Aitha, M.; González, M. M.; Moreno, D. M.;

Crowder, M. W.; Bonomo, R. A.; Spencer, J.; Tierney, D. L.; Llarrull, L. I.; et al. A General Reaction Mechanism for Carbapenem Hydrolysis by Mononuclear and Binuclear Metallo-β-Lactamases. *Nat. Commun.* **2017**, *8* (1), 538.

(181) Mokhtari, R. B.; Homayouni, T. S.; Baluch, N.; Morgatskaya, E.; Kumar, S.; Das, B.; Yeger, H.; Mokhtari, R. B.; Homayouni, T. S.; Baluch, N.; et al. Combination Therapy in Combating Cancer. *Oncotarget* **2017**, *8* (23), 38022–38043.

(182) Ezekowitz, J. A.; O'Meara, E.; McDonald, M. A.; Abrams, H.; Chan, M.; Ducharme, A.; Giannetti, N.; Grzeslo, A.; Hamilton, P. G.; Heckman, G. A.; et al. 2017 Comprehensive Update of the Canadian Cardiovascular Society Guidelines for the Management of Heart Failure. *Can. J. Cardiol.* **2017**, *33* (11), 1342–1433.

(183) Guerrero-García, C.; Rubio-Guerra, A. F. Combination Therapy in the Treatment of Hypertension. *Drugs Context* **2018**, *7*, 212531.

(184) American Diabetes Association. Approaches to Glycemic Treatment. *Diabetes Care* **2015**, *38* (Supplement 1), S41-48.

(185) Moret, C. Combination/Augmentation Strategies for Improving the Treatment of Depression. *Neuropsychiatr. Dis. Treat.* **2005**, *1* (4), 301–309.

(186) Rhodes, A.; Evans, L. E.; Alhazzani, W.; Levy, M. M.; Antonelli, M.; Ferrer, R.; Kumar, A.; Sevransky, J. E.; Sprung, C. L.; Nunnally, M. E.; et al. Surviving Sepsis Campaign. *Crit. Care Med.* **2017**, *45* (3), 486–552.

(187) European Medicines Agency Committee for Human Medicinal Products. *Committee for Human Medicinal Products (CHMP) Guideline on Clinical Development of Fixed Combination Medicinal Products*; 2017.

(188) Terrie, Y. C. Monitoring Combination Drug Therapy. *Pharmacy Times*. January 2010.

(189) WHO. *Consolidated Guidelines on the Use of Antiretroviral Drugs for Treating and Preventing Hiv Infection : Recommendations for a Public Health Approach.*; 2016.

(190) Lehman, D. A.; Chung, M. H.; Mabuka, J. M.; John-Stewart, G. C.; Kiarie, J.; Kinuthia, J.; Overbaugh, J. Lower Risk of Resistance after Short-Course HAART Compared with Zidovudine/Single-Dose Nevirapine Used for Prevention of HIV-1 Mother-to-Child Transmission. *J. Acquir. Immune Defic. Syndr.* **2009**, *51* (5), 522–529.

(191) Vachon, M.-L.; Dieterich, D. T. The Era of Direct-Acting Antivirals Has

Begun: The Beginning of the End for HCV? *Semin. Liver Dis.* **2011**, *31* (4), 399–409.

(192) AASLD-IDSA. HCV Guidance: Recommendations for Testing, Managing, and Treating Hepatitis C www.HCVGuidance.org (accessed Oct 7, 2018).

(193) WHO. *Guidelines for the Treatment of Malaria*; 2015.

(194) Kalan, L.; Wright, G. D. Antibiotic Adjuvants: Multicomponent Anti-Infective Strategies. *Expert Rev. Mol. Med.* **2011**, *13*, e5.

(195) Brown, A. G.; Butterworth, D.; Cole, M.; Hanscomb, G.; Hood, J. D.; Reading, C.; Rolinson, G. N. Naturally-Occurring Beta-Lactamase Inhibitors with Antibacterial Activity. *J. Antibiot. (Tokyo).* **1976**, *29* (6), 668–669.

(196) Wright, G. D. Antibiotic Adjuvants: Rescuing Antibiotics from Resistance. *Trends Microbiol.* **2016**, *24* (11), 862–871.

(197) Melander, R. J.; Melander, C. The Challenge of Overcoming Antibiotic Resistance: An Adjuvant Approach? *ACS Infect. Dis.* **2017**, *3* (8), 559–563.

(198) Rasko, D. A.; Sperandio, V. Anti-Virulence Strategies to Combat Bacteria-Mediated Disease. *Nat. Rev. Drug Discov.* **2010**, *9* (2), 117–128.

(199) Reading, C.; Cole, M. Clavulanic Acid: A Beta-Lactamase-Inhiting Beta-Lactam from Streptomyces Clavuligerus. *Antimicrob. Agents Chemother.* **1977**, *11* (5), 852–857.

(200) English, A. R.; Retsema, J. A.; Girard, A. E.; Lynch, J. E.; Barth, W. E. CP-45,899, a Beta-Lactamase Inhibitor That Extends the Antibacterial Spectrum of Beta-Lactams: Initial Bacteriological Characterization. *Antimicrob. Agents Chemother.* **1978**, *14* (3), 414–419.

(201) Aronoff, S. C.; Jacobs, M. R.; Johenning, S.; Yamabe, S. Comparative Activities of the Beta-Lactamase Inhibitors YTR 830, Sodium Clavulanate, and Sulbactam Combined with Amoxicillin or Ampicillin. *Antimicrob. Agents Chemother.* **1984**, *26* (4), 580–582.

(202) Bonnefoy, A.; Dupuis-Hamelin, C.; Steier, V.; Delachaume, C.; Seys, C.; Stachyra, T.; Fairley, M.; Guitton, M.; Lampilas, M.; Pharma, A. In Vitro Activity of AVE1330A, an Innovative Broad-Spectrum Non-B-Lactam B-Lactamase Inhibitor. *J. Antimicrob. Chemother.* **2004**, *54* (2), 410–417.

(203) U.S. National Institutes of Health. ClinicalTrials.gov https://clinicaltrials.gov/ (accessed Jul 10, 2019).

(204) Hecker, S. J.; Reddy, K. R.; Totrov, M.; Hirst, G. C.; Lomovskaya, O.; Griffith, D. C.; King, P.; Tsivkovski, R.; Sun, D.; Sabet, M.; et al. Discovery of a Cyclic Boronic Acid β-Lactamase Inhibitor (RPX7009) with Utility vs Class A Serine Carbapenemases. *J. Med. Chem.* **2015**, *58* (9), 3682–3692.

(205) US Food and Drug Administration. FDA Approves New antibacterial Drug https://www.fda.gov/news-events/press-announcements/fda-approves-new-antibacterial-drug (accessed Jul 10, 2019).

(206) Christopeit, T.; Albert, A.; Leiros, H.-K. S. Discovery of a Novel Covalent Non-β-Lactam Inhibitor of the Metallo-β-Lactamase NDM-1. *Bioorg. Med. Chem.* **2016**, *24* (13), 2947–2953.

(207) Thomas, P. W.; Cammarata, M.; Brodbelt, J. S.; Fast, W. Covalent Inhibition of New Delhi Metallo-β-Lactamase-1 (NDM-1) by Cefaclor. *ChemBioChem* **2014**, *15* (17), 2541–2548.

(208) Chiou, J.; Wan, S.; Chan, K.-F.; So, P.-K.; He, D.; Chan, E. W.-C.; Chan, T.-H.; Wong, K.; Tao, J.; Chen, S. Ebselen as a Potent Covalent Inhibitor of New Delhi Metallo-B-Lactamase (NDM-1). *Chem. Commun.* **2015**, *51* (46), 9543–9546.

(209) Thomas, P. W.; Spicer, T.; Cammarata, M.; Brodbelt, J. S.; Hodder, P.; Fast, W. An Altered Zinc-Binding Site Confers Resistance to a Covalent Inactivator of New Delhi Metallo-Beta-Lactamase-1 (NDM-1) Discovered by High-Throughput Screening. *Bioorg. Med. Chem.* **2013**, *21* (11), 3138–3146.

(210) Brem, J.; Cain, R.; Cahill, S.; Mcdonough, M. A.; Clifton, I. J.; Jiménez-Castellanos, J.-C.; Avison, M. B.; Spencer, J.; Fishwick, C. W. G.; Schofield, C. J. Structural Basis of Metallo-β-Lactamase, Serine-β-Lactamase and Penicillin-Binding Protein Inhibition by Cyclic Boronates. *Nat. Commun.* **2016**, *7*, 12406.

(211) VenatoRX Pharmaceuticals. Pipeline | VenatoRx Pharmaceuticals https://www.venatorx.com/pipeline/ (accessed Jul 11, 2019).

(212) Santucci, M.; Spyrakis, F.; Cross, S.; Quotadamo, A.; Farina, D.; Tondi, D.; De Luca, F.; Docquier, J.-D.; Prieto, A. I.; Ibacache, C.; et al. Computational and Biological Profile of Boronic Acids for the Detection of Bacterial Serine-and Metallo-β-Lactamases. *Sci. Rep.* **2017**, *7* (1), 17716.

(213) Heinz, U.; Bauer, R.; Wommer, S.; Meyer-Klaucke, W.; Papamichaels, C.; Bateson, J.; Adolph, H.-W. Coordination Geometries of Metal Ions in D- or L-Captopril-Inhibited Metallo-Beta-Lactamases. *J. Biol. Chem.* **2003**, *278* (23), 20659–20666.

(214) Guo, Y.; Wang, J.; Niu, G.; Shui, W.; Sun, Y.; Zhou, H.; Zhang, Y.; Yang, C.; Lou, Z.; Rao, Z. A Structural View of the Antibiotic Degradation Enzyme NDM-1 from a Superbug. *Protein Cell* **2011**, *2* (5), 384–394.

(215) Brem, J.; van Berkel, S. S.; Zollman, D.; Lee, S. Y.; Gileadi, O.; McHugh, P. J.; Walsh, T. R.; McDonough, M. A.; Schofield, C. J. Structural Basis of Metallo-β-Lactamase Inhibition by Captopril Stereoisomers. *Antimicrob. Agents Chemother.* **2016**, *60* (1), 142–150.

(216) González, M. M.; Kosmopoulou, M.; Mojica, M. F.; Castillo, V.; Hinchliffe, P.; Pettinati, I.; Brem, J.; Schofield, C. J.; Mahler, G.; Bonomo, R. A.; et al. Bisthiazolidines: A Substrate-Mimicking Scaffold as an Inhibitor of the NDM-1 Carbapenemase. *ACS Infect. Dis.* **2015**, *1* (11), 544–554.

(217) Song, G.-Q.; Wang, W.-M.; Li, Z.-S.; Wang, Y.; Wang, J.-G. First Identification of Isatin-β-Thiosemicarbazones as Novel Inhibitors of New Delhi Metallo-β-Lactamase-1: Chemical Synthesis, Biological Evaluation and Molecular Simulation. *Chinese Chem. Lett.* **2018**, *29* (6), 899–902.

(218) Falconer, S. B.; Reid-Yu, S. A.; King, A. M.; Gehrke, S. S.; Wang, W.; Britten, J. F.; Coombes, B. K.; Wright, G. D.; Brown, E. D. Zinc Chelation by a Small-Molecule Adjuvant Potentiates Meropenem Activity in Vivo against NDM-1-Producing Klebsiella Pneumoniae. *ACS Infect. Dis.* **2015**, *1* (11), 533–543.

(219) Spyrakis, F.; Celenza, G.; Marcoccia, F.; Santucci, M.; Cross, S.; Bellio, P.; Cendron, L.; Perilli, M.; Tondi, D. Structure-Based Virtual Screening for the Discovery of Novel Inhibitors of New Delhi Metallo-β-Lactamase-1. *ACS Med. Chem. Lett.* **2018**, *9* (1), 45–50.

(220) Xiang, Y.; Chen, C.; Wang, W.-M.; Xu, L.-W.; Yang, K.-W.; Oelschlaeger, P.; He, Y. Rhodanine as a Potent Scaffold for the Development of Broad-Spectrum Metallo-β-Lactamase Inhibitors. *ACS Med. Chem. Lett.* **2018**, *9* (4), 359–364.

(221) Brem, J.; van Berkel, S. S.; Aik, W.; Rydzik, A. M.; Avison, M. B.; Pettinati, I.; Umland, K.-D.; Kawamura, A.; Spencer, J.; Claridge, T. D. W.; et al. Rhodanine Hydrolysis Leads to Potent Thioenolate Mediated Metallo-β-Lactamase Inhibition. *Nat. Chem.* **2014**, *6* (12), 1084–1090.

(222) Christopeit, T.; Carlsen, T. J. O.; Helland, R.; Leiros, H.-K. S. Discovery of Novel Inhibitor Scaffolds against the Metallo-β-Lactamase VIM-2 by Surface Plasmon Resonance (SPR) Based Fragment Screening. *J. Med. Chem.* **2015**, *58* (21), 8671–8682.

(223) Yoshizumi, A.; Ishii, Y.; Livermore, D. M.; Woodford, N.; Kimura, S.; Saga, T.; Harada, S.; Keizo, Y.; Kazuhiro, T. Efficacies of Calcium-EDTA in

Combination with Imipenem in a Murine Model of Sepsis Caused by Escherichia Coli with NDM-1 β-Lactamase. *J. Infect. Chemother.* **2013**, *19* (5), 992–995.

(224) Somboro, A. M.; Tiwari, D.; Bester, L. A.; Parboosing, R.; Chonco, L.; Kruger, H. G.; Arvidsson, P. I.; Govender, T.; Naicker, T.; Essack, S. Y. NOTA: A Potent Metallo-β-Lactamase Inhibitor. *J. Antimicrob. Chemother.* **2015**, *70* (5), 1594–1596.

(225) Schnaars, C.; Kildahl-Andersen, G.; Prandina, A.; Popal, R.; Radix, S.; Le Borgne, M.; Gjøen, T.; Andresen, A. M. S.; Heikal, A.; Økstad, O. A.; et al. Synthesis and Preclinical Evaluation of TPA-Based Zinc Chelators as Metallo-β-Lactamase Inhibitors. *ACS Infect. Dis.* **2018**, *4* (9), 1407–1422.

(226) Livermore, D. M.; Mushtaq, S.; Morinaka, A.; Ida, T.; Maebashi, K.; Hope, R. Activity of Carbapenems with ME1071 (Disodium 2,3-Diethylmaleate) against Enterobacteriaceae and Acinetobacter Spp. with Carbapenemases, Including NDM Enzymes. *J. Antimicrob. Chemother.* **2013**, *68* (1), 153–158.

(227) King, A. M.; Reid-Yu, S. A.; Wang, W.; King, D. T.; De Pascale, G.; Strynadka, N. C.; Walsh, T. R.; Coombes, B. K.; Wright, G. D. Aspergillomarasmine A Overcomes Metallo-β-Lactamase Antibiotic Resistance. *Nature* **2014**, *510* (7506), 503–506.

(228) Bergstrom, A.; Katko, A.; Adkins, Z.; Hill, J.; Cheng, Z.; Burnett, M.; Yang, H.; Aitha, M.; Mehaffey, M. R.; Brodbelt, J. S.; *et al*. Probing the Interaction of Aspergillomarasmine A with Metallo-β-Lactamases NDM-1, VIM-2, and IMP-7. *ACS Infect. Dis.* **2018**, *4* (2), 135–145.

(229) Dolgin, E. Inner Workings: Combating Antibiotic Resistance from the Ground Up. *Proc. Natl. Acad. Sci. U. S. A.* **2016**, *113* (42), 11642–11643.

(230) Koteva, K.; King, A. M.; Capretta, A.; Wright, G. D. Total Synthesis and Activity of the Metallo-β-Lactamase Inhibitor Aspergillomarasmine A. *Angew. Chemie Int. Ed.* **2016**, *55* (6), 2210–2212.

(231) Liao, D.; Yang, S.; Wang, J.; Zhang, J.; Hong, B.; Wu, F.; Lei, X. Total Synthesis and Structural Reassignment of Aspergillomarasmine A. *Angew. Chemie Int. Ed.* **2016**, *55* (13), 4291–4295.

(232) Zhang, J.; Wang, S.; Wei, Q.; Guo, Q.; Bai, Y.; Yang, S.; Song, F.; Zhang, L.; Lei, X. Synthesis and Biological Evaluation of Aspergillomarasmine A Derivatives as Novel NDM-1 Inhibitor to Overcome Antibiotics Resistance. *Bioorg. Med. Chem.* **2017**, *25*, 5133–5141.

(233) Albu, S. A.; Koteva, K.; King, A. M.; Al-Karmi, S.; Wright, G. D.; Capretta, A. Total Synthesis of Aspergillomarasmine A and Related Compounds: A

Sulfamidate Approach Enables Exploration of Structure-Activity Relationships. *Angew. Chemie Int. Ed.* **2016**, *55* (42), 13259–13262.

(234) Zhang, J.; Wang, S.; Bai, Y.; Guo, Q.; Zhou, J.; Lei, X. Total Syntheses of Natural Metallophores Staphylopine and Aspergillomarasmine A. *J. Org. Chem.* **2017**, *82* (24), 13643–13648.

(235) Liu, Y.; Li, R.; Xiao, X.; Wang, Z. Molecules That Inhibit Bacterial Resistance Enzymes. *Molecules* **2019**, *24* (1), 43–65.

(236) Boehr, D. D.; Lane, W. S.; Wright, G. D. Active Site Labeling of the Gentamicin Resistance Enzyme AAC(6')-APH(2") by the Lipid Kinase Inhibitor Wortmannin. *Chem. Biol.* **2001**, *8* (8), 791–800.

(237) Shakya, T.; Stogios, P. J.; Waglechner, N.; Evdokimova, E.; Ejim, L.; Blanchard, J. E.; McArthur, A. G.; Savchenko, A.; Wright, G. D. A Small Molecule Discrimination Map of the Antibiotic Resistance Kinome. *Chem. Biol.* **2011**, *18* (12), 1591–1601.

(238) Daigle, D. M.; McKay, G. A.; Wright, G. D. Inhibition of Aminoglycoside Antibiotic Resistance Enzymes by Protein Kinase Inhibitors. *J. Biol. Chem.* **1997**, *272* (40), 24755–24758.

(239) Stogios, P. J.; Spanogiannopoulos, P.; Evdokimova, E.; Egorova, O.; Shakya, T.; Todorovic, N.; Capretta, A.; Wright, G. D.; Savchenko, A. Structure-Guided Optimization of Protein Kinase Inhibitors Reverses Aminoglycoside Antibiotic Resistance. *Biochem. J.* **2013**, *454* (2), 191–200.

(240) Green, K. D.; Chen, W.; Garneau-Tsodikova, S. Identification and Characterization of Inhibitors of the Aminoglycoside Resistance Acetyltransferase Eis from Mycobacterium Tuberculosis. *ChemMedChem* **2012**, *7* (1), 73–77.

(241) Chiem, K.; Jani, S.; Fuentes, B.; Lin, D. L.; Rasche, M. E.; Tolmasky, M. E. Identification of an Inhibitor of the Aminoglycoside 6′-N-Acetyltransferase Type Ib [AAC(6′)-Ib] by Glide Molecular Docking. *Medchemcomm* **2016**, *7* (1), 184–189.

(242) Suga, T.; Ishii, T.; Iwatsuki, M.; Yamamoto, T.; Nonaka, K.; Masuma, R.; Matsui, H.; Hanaki, H.; Ōmura, S.; Shiomi, K. Aranorosin Circumvents Arbekacin-Resistance in MRSA by Inhibiting the Bifunctional Enzyme AAC(6′)/APH(2″). *J. Antibiot. (Tokyo).* **2012**, *65* (10), 527–529.

(243) Hirsch, D. R.; Cox, G.; D'Erasmo, M. P.; Shakya, T.; Meck, C.; Mohd, N.; Wright, G. D.; Murelli, R. P. Inhibition of the ANT(2″)-Ia Resistance Enzyme and Rescue of Aminoglycoside Antibiotic Activity by Synthetic α-Hydroxytropolones. *Bioorg. Med. Chem. Lett.* **2014**, *24* (21), 4943–4947.

(244) Allen, N. E.; Alborn, W. E.; Hobbs, J. N.; Kirst, H. A. 7-Hydroxytropolone: An Inhibitor of Aminoglycoside-2"-O-Adenylyltransferase. *Antimicrob. Agents Chemother.* **1982**, *22* (5), 824–831.

2.0 Development and Structure-Activity Relationship Analysis of Substituted Indolinones as Aminoglycoside 3-*N*-Acetyltransferase AAC(3)-IA Inhibitors

2.1 Background

Bacterial resistance is a widespread and growing problem, with dire medical, social, and economic implications.[1] WHO has responded with the Global Action Plan on Antimicrobial Resistance, which focuses on, amongst other things, development of new technologies that counteract the development of resistance.[2]

Resistance can arise through a variety of mechanisms, including biofilm formation, target alteration or bypass, efflux pumps upregulation, porin loss, and drug inactivation.[3,4] With the tremendous challenges involved with bringing new antimicrobials to market,[5,6] researchers are studying these processes in hopes of finding a way to recycle the utility of old antibiotic classes. By targeting the enzymes involved in drug inactivation and discovering new inhibitors for these pathways, co-drugs or adjuvants can be developed and co-administered in order to circumvent antibiotic inactivation. This adjuvant approach was first used in 1970s with the addition of the β-lactamase inhibitor clavulanic acid to amoxicillin, but to date has not been successfully implemented in any other antibiotic class.[3,7,8]

Aminoglycosides and the enzymes involved in their inactivation are well-studied, and thus represent ideal candidates for this approach.[9–12] Aminoglycosides act on the 30S subunit of the ribosome, exerting their effects *via* mistranslation, membrane permeability and irreversible blockade of the initiation complex.[13] They are used primarily to treat Gram-negative infections, though they also have a role in the treatment of some Gram-positive and Mycobacterial infections.[10,14,15] Two aminoglycosides, gentamicin and amikacin, are designated as essential medicines by WHO.[16]

Resistance to aminoglycosides is mediated by aminoglycoside-modifying enzymes (AMEs). There are three main classes: aminoglycoside acetyltransferases (AACs), aminoglycoside nucleotidyltransferases (ANTs), and aminoglycoside phosphotransferases (APHs).[9,17] Aminoglycoside phosphotransferases and nucleotidyltransferases transfer phosphate and adenylphosphate groups respectively from ATP; acetyltransferases inactivate aminoglycosides by transferring acetyl groups from acetyl-CoA (Figure 2-1). While there are copious examples of APH and ANT inhibitors in the literature, there are comparatively fewer AAC inhibitors,[18,19,28–31,20–27] and only one reported *in vitro* inhibitor[32] for

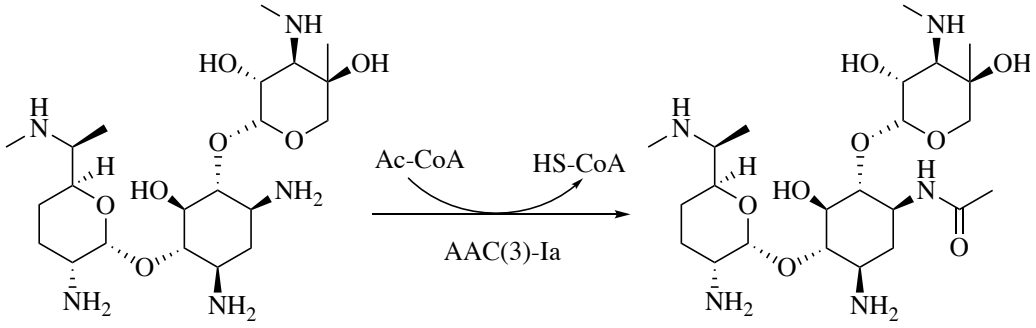

Figure 2-1. Mechanism of Gentamicin Inactivation by AAC(3)-*Ia*

AAC(3)-Ia, despite the fact that the enzyme is found in clinical isolates of three ESKAPE pathogens (*Acinetobacter baumannii*, *Klebsiella pneumonia*, and *Pseudomonas aeruginosa*).[17]

The chapter describes a high-throughput screening campaign aimed at discovering new small molecule inhibitors of AAC(3)-Ia and the identification of an indolinone family of heterocycles as a lead series. The chemistry that allows for the parallel synthesis of structurally related indolinones and the determination of a preliminary structure-activity relationship is also presented.

2.2 Screening and Target Identification

In vivo screening of AAC(3)-Ia was done using hyperpermeable, efflux-deficient *E. coli* BW25113 ΔbamB ΔtolC strains with pGDP4-*aac(3)-Ia* (Z' = 0.61) against two protein kinase libraries provided by GlaxoSmithKline.[33,34] These libraries were selected as it was hypothesized that the ability of kinase inhibitors to enter nucleotide-binding pockets of their target enzymes may allow them to similarly displace the purine-containing acetyl-CoA from the active site of AAC(3)-Ia.[35] Hyperpermeable *E. coli* was used to ensure compound penetration. It was noted that the hyperpermeable strains were sensitive to kanamycin despite the resistance gene, so gentamicin was used (MIC = 63 - 125 μg/mL). Of the 890 compounds screened, 21 showed selective inhibition (identified by percent growth difference of the resistant strain compared over the wildtype strain of ≥ 3 standard deviations from the mean).

In vitro testing with purified AAC(3)-Ia was performed using a coupled Ellman assay (Figure 2-2). An acetyl group is transferred from acetyl-CoA to gentamicin, freeing the thiol group of coenzyme A to attack 5,5'-dithiobis-(2-nitrobenzoic acid) (DTNB). A disulfide bond is formed, releasing 2-nitro-5-sulfanylbenzoic acid, which can be monitored by absorbance at 412 nm. This assay was used to verify *in vivo* hits (eight true hits, shown in Figure 2-3, panel A), and to screen the Bio Screen-Well kinase inhibitor library (80 compounds), yielding an additional six hits. Two were confirmed (Figure 2-3, panel B), and IC_{50} data determined. Of the confirmed hits from the three libraries, two compounds (**II-1** and **II-10**) shared a

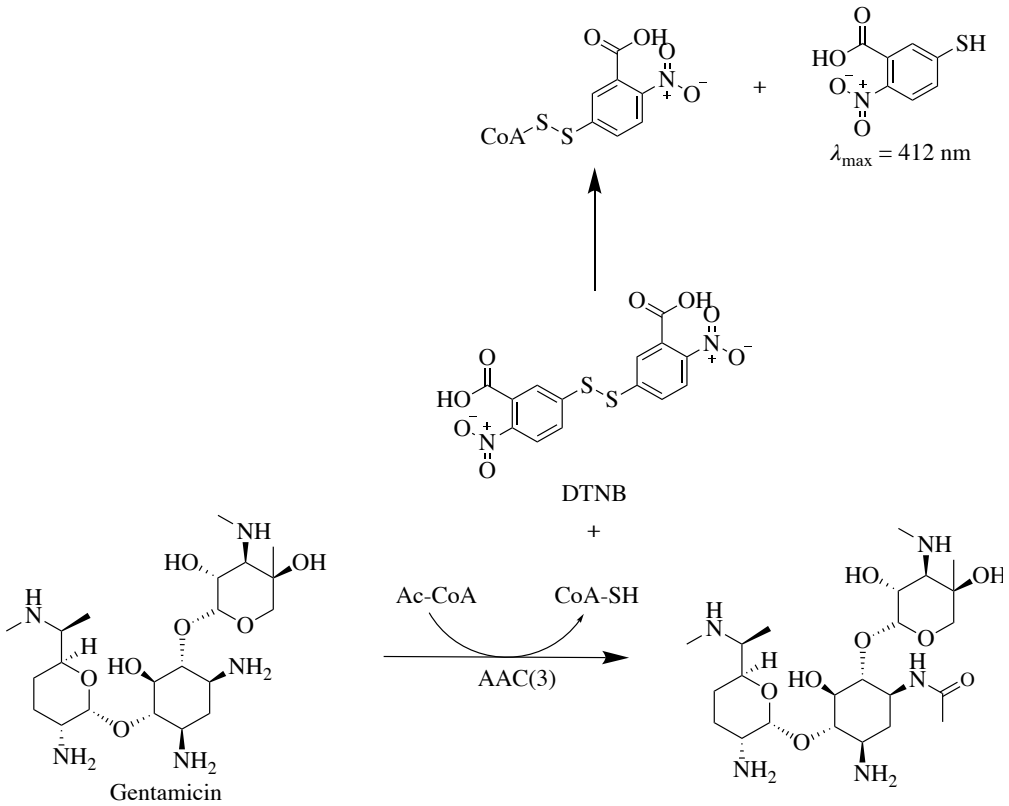

Figure 2-2. AAC(3)-Ia-Coupled Ellman Assay

common substituted 3-benzylidene-2-indolinone scaffold. This scaffold formed the basis for our subsequent library development.

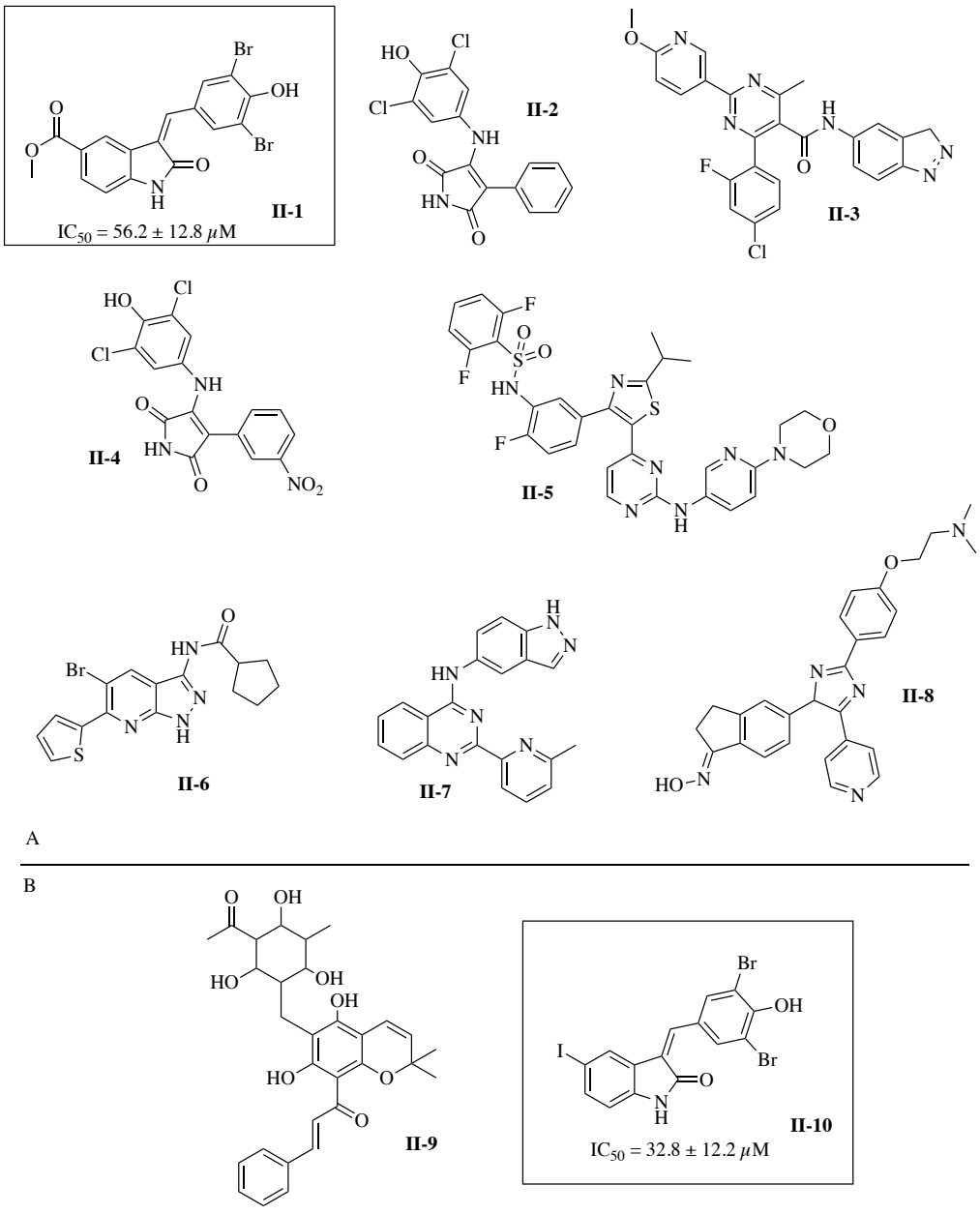

Figure 2-3. Confirmed Hits from GlaxoSmithKline (panel A) and Bio Screen-Well Kinase Inhibitor Libraries (panel B). Hits containing the 3-benzylidene-2-indolinone scaffold are boxed

2.3 INDOLINONE LIBRARY SYNTHESIS

In an effort to determine the structure-activity interactions of the 3-benzylidine-2-indolinone family with AAC(3)-Ia and to provide compounds with better overall pharmacokinetic properties, a synthetic method was developed that would allow for the parallel synthesis of a family of related indolin-2-one derivatives substituted at the 3- and 5-positions (Figure 2-4).

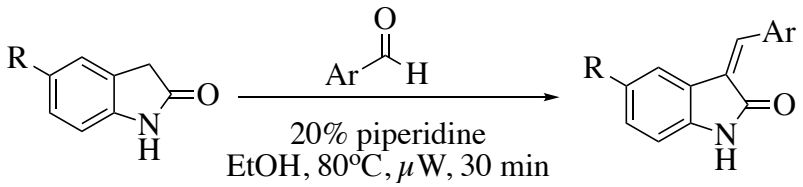

Figure 2-4. Synthetic Scheme for Parallel Synthesis of AAC(3)-Ia Inhibitor Library

While the preparation of these heterocycles has been described previously in the literature, the approaches suffer from long reaction times and/or harsh conditions.[36–38] The most promising of the protocols involves the Knoevenagel condensation of indolin-2-one and an aromatic aldehyde in the presence of 20% piperidine refluxed in ethanol (mechanism shown in Figure 2-5).[36] When these conditions were replicated with microwave irradiation in place of conventional heating, reaction times were reduced to 30 min. Use of an ammonium acetate:acetic acid buffer further improved this reaction, as studies have shown that acidic environments promote imine formation, with optimal formation at pH 4.5.[39]

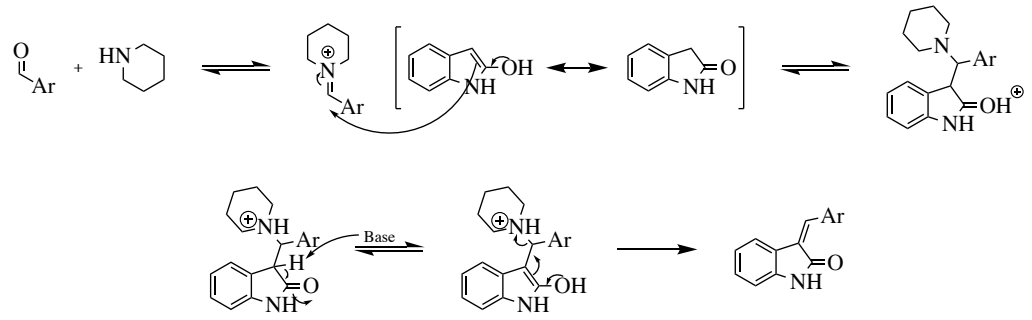

Figure 2-5. Mechanism of Imine-Promoted Knoevenagel Aldol Condensation

Using this methodology, a small 3-benzylidine-2-indolinone library was prepared and screened for inhibitory activity (Figure 2-6). Original hit **II-1** was re-synthesized, as was a close analog of hit **II-10** (with a bromine instead of an iodine). Analogs with a carboxylic acid, hydroxyl, or hydrogen were also made to further explore the effect of substituents at position 5 (**II-18**, **II-21**, and **II-29**). The essentiality of the 3,5-dibromo-4-hydroxyphenyl pharmacophore was also investigated, with analogs where one or more of the substituents on the benzyl ring was missing (for example **II-14**, **II-16**, **II-30**, **II-32**, and **II-34**) or substituted (**II-13**, **II-33**, **II-35**, **II-36**, and **II-37**), or the phenyl group was replaced by a furan (**II-12**) or pyridine ring (**II-31**). It should also be noted that most of the compounds were formed as a mixture of the (*E*)- and (*Z*)-isomers, typically with the (*Z*)-isomer predominating. However, in almost all of the compounds with a carboxylic acid at position 5 the (*E*)-isomer predominated.

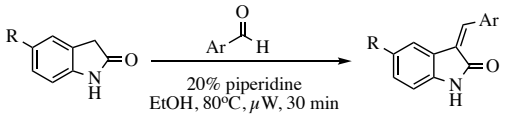

		Yield (%)	Z:E			Yield (%)	Z:E
II-1[a]	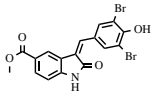	61	2:1	**II-24**[d]	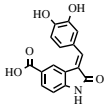	66	3:5
II-11[a]	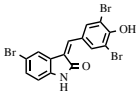	65	4:1	**II-25**[d]	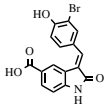	36	1:7
II-12	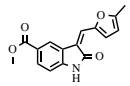	77	>20:1	**II-26**[d]	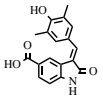	44	1:2
II-13	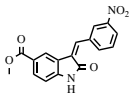	91	3:2	**II-27**[d]	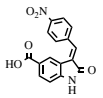	37	3:5
II-14	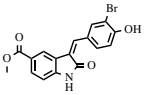	77	3:1	**II-28**[d]	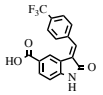	58	1:4
II-15		69	>20:1	**II-29**[e]	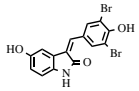	87	14:1
II-16	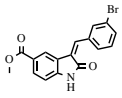	93	3:2	**II-30**	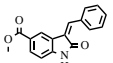	71	7:3
II-17	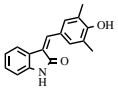	75	3:1	**II-31**	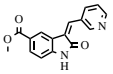	94	1:1
II-18[b]	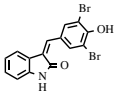	56	2:1	**II-32**[f]	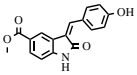	88	>20:1
II-19[c]	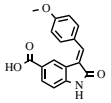	20	2:5	**II-33**	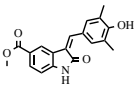	95	2:1
II-20[c]	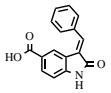	25	1:3	**II-34**	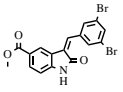	82	10:9
II-21[d]	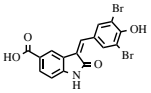	13	5:4	**II-35**[g]	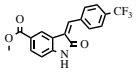	77	3:2
II-22[d]	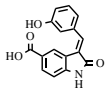	41	1:3	**II-36**	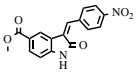	90	10:9
II-23[d]	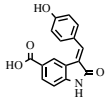	23	1:3	**II-37**[h]	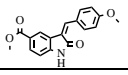	84	>20:1

[a]Reaction time = 6 h. [b]72 h reflux. [c]Reaction time = 1.5 h. [d]0.44 M NH_4OAc in 3:1 EtOH:HOAc solution (pH 4.5). [e]0.55 M NH_4OAc:HOAc in EtOH (titrated to pH 4.5). [f]Reaction time = 20 min. [g]Reaction time = 1 h. [h]MeOH.

Figure 2-6. Indolinone Library with Reaction Conditions and Isomeric Ratios

2.4 Structure-Activity Relationship Analysis

Preliminary testing with the AAC(3)-Ia-coupled Ellman assay used in screening verification revealed several problems that needed to be addressed before a complete SAR analysis could proceed. It became apparent that the initial hit **II-1** degrades in DMSO thus complicating analysis. In addition, the poor solubility of the library in DMSO made acquiring meaningful IC_{50} data impossible, as many of the compounds initially screened precipitated out of solution even at very low concentrations, and thus could not be properly tested for SAR.

It was initially thought that hydrolysis of the methyl ester at position 5 would provide a quick and facile way to improve the solubility of the indolinone library and allow for more accurate inhibition studies. However, searching the literature yielded no examples of hydrolysis of 5-carbomethoxy-2-indoline olefins. Attempts at hydrolysis of the esters formed under standard conditions with multiple reagents resulted in degradation of the heterocyclic system (Table 2-1), so a small

Table 2-1. Methyl Ester Hydrolysis Conditions Tested

Methyl Ester		
II-1	NaOH (aq)	i. MeOH, 65°C, 1h ii. DOWEX exchange resin
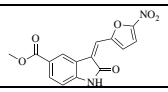	NaOH (aq)	i. MeOH, 65°C, 1h ii. DOWEX exchange resin
II-34	LiOH	i. 10:1 MeOH:H_2O, RT, 19 h ii. DOWEX exchange resin
II-34	NaOH (aq)	i. MeOH, 50°C, 24 h
II-1	LiOH	10:1 MeOH:H_2O, RT, 24h
II-1	LiOH	i. 10:1 MeOH: H_2O, 50°C, 48 h ii. DOWEX exchange resin
II-1	Me_3SnOH	i anh DCE, 85°C, 2h ii. 5% HCl wash

number of carboxylic acid-analogs were made using the developed methodology in Figure 2-4. Unfortunately, the presence of a carboxylic acid at position 5 reversed the geometric isomer ratio in almost all cases. Isomeric resolution by differential crystallization and by preparative HPLC was attempted without success, so SAR analysis was done with the understanding that the mixture composition would be a confounding factor.

An additional issue with the AAC(3)-Ia-coupled Ellman assay was also discovered. Many of the compounds (particularly those with bromobenzyl substituents) had high absorbance at 412 nm, generating high background signal. A fluorescence-based assay was therefore sought. The original plan was to simply to replace Ellman's reagent with fluorescent indicator BODIPY FL L-cysteine,[40] but this was unsuccessful. Thankfully, a commercially-available fluorescent thiol quantitation kit from Sigma Aldrich[41] was found, allowing analysis to proceed.

Freshly-purified AAC(3)-Ia was used for SAR analysis. As previously reported affinity purification procedures were not reproducible,[42] a new protocol was developed, using freeze-thaw cycles for cell lysis and cobalt beads to pull out His-tagged protein.

A total of 28 compounds were screened for activity against AAC(3)-Ia at 200 μM using this assay. IC_{50} values were determined for compounds showing at least 50% inhibition (Figure 2-7). These results show that the 3,5-dibromo-4-hydroxybenzyl pharmacophore present in both of the initial hits is the ideal moiety for inhibitory activity (IC_{50} = 4.3 ± 1.4 μM). The benzylidene functionality is essential- replacement of the benzyl with a furanyl or pyridinyl functionality results

in immediate loss of activity. The 3-bromine substituent is essential as well, while loss of the 3-hydroxyl groups can be tolerated to some degree, as shown by **II-14**, **II-16**, and **II-34**. Substitution at the 5-position of the 3-benzylidine-2-indolinone scaffold (**II-29**, **II-11**, and **II-18**) is also accommodated fairly well, though the methyl ester functionality of the **II-1** has the greatest activity. A notable exception to this trend is carboxylic acid-analog **II-21**, which does not display inhibitory activity.

These results were followed up with checkerboard assays to test for synergy between the compounds and gentamicin. Synergy is when the activity of combination is greater than the activity of the two independent drugs; this would be expected if the AAC(3)-Ia inactivation of gentamicin was inhibited. Increasing concentrations of one compound (in this case gentamicin) were added along one axis and increasing concentrations of the other compound (in this case the AAC(3)-Ia inhibitors) were added along the other, and synergy was assessed through calculation of the Fractional Inhibitory Concentration (FIC, Equation 2-1):

$$FIC = \frac{MIC_{A\ in\ combination}}{MIC_A} + \frac{MIC_{B\ in\ combination}}{MIC_B} \quad (2\text{-}1)$$

A FIC $\leq$ 0.5 indicates a synergistic interaction while a FIC $\geq$ 2 is considered antagonistic. Values in between are indeterminant. Unfortunately, none of the compounds tested showed synergy, though two of them, **II-1** and **II-11** had some intrinsic activity against *E. coli* BW25113 ΔbamB ΔtolC pGDP4-*aac(3)-Ia* strains with MICs of 8-16 μg/mL and 4 μg/mL respectively (Figures 2-9 and 2-10).

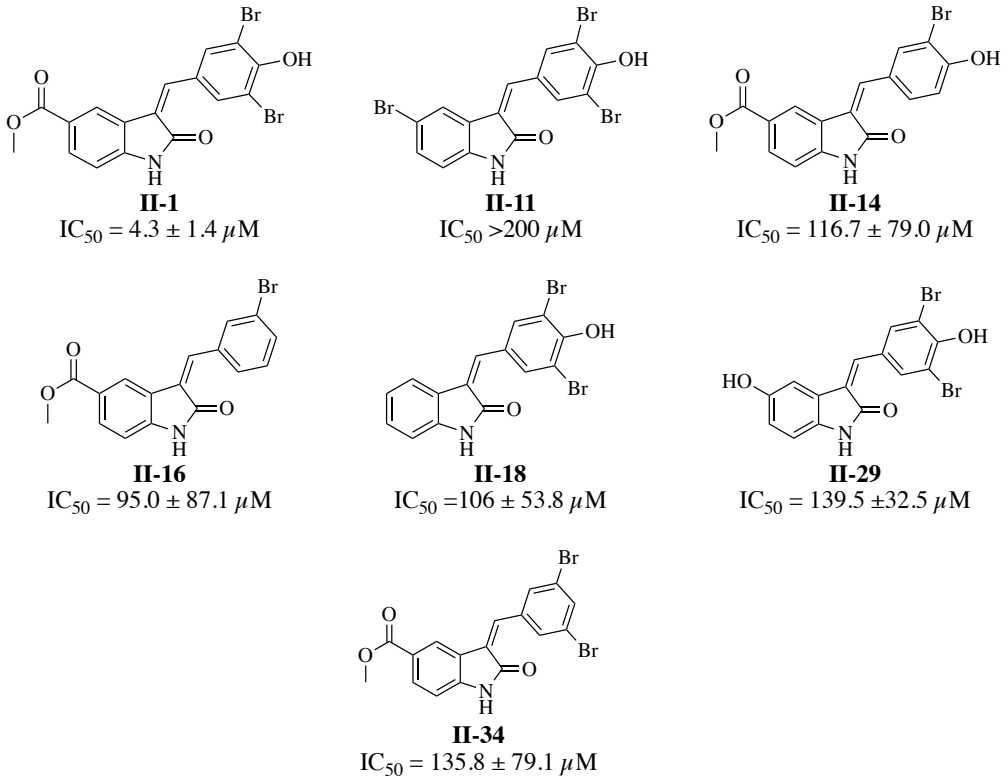

Figure 2-7. AAC(3)-Ia Inhibitors with IC_{50} Values

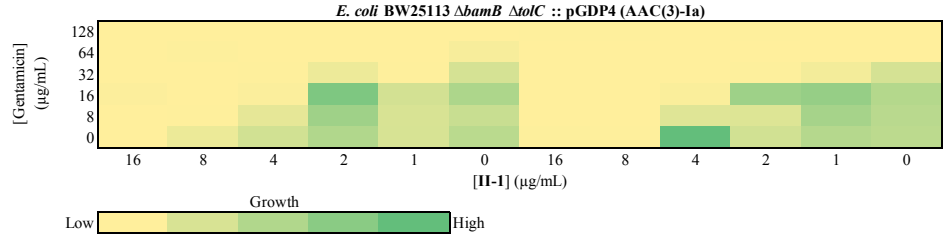

Figure 2-8. Checkerboard Assay for Interaction of **II-1** and Gentamicin in *E. coli* BW25113 Δ*tolC*Δ*bamB* pGDP4:*aac(3)-Ia*. $FIC \leq 0.5$ is considered synergistic, $FIC \geq 2$ is antagonistic, and $0.5 < FIC < 2$ is indeterminant/additive

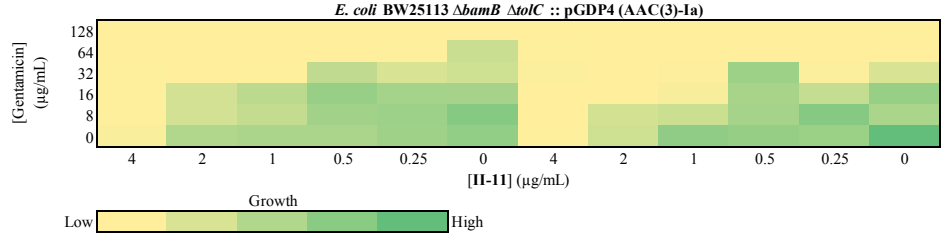

Figure 2-9. Checkerboard Assay for Interaction of **II-11** and Gentamicin in *E. coli* BW25113 Δ*tolC*Δ*bamB* pGDP4:*aac(3)-Ia*. $FIC \leq 0.5$ is considered synergistic, $FIC \geq 2$ is antagonistic, and $0.5 < FIC < 2$ is indeterminant/additive

2.5 Implications and Future Work

A collection of kinase inhibitors was screened against AAC(3)-Ia using both cell- and enzyme-based assays. Two of the hits possessed a 3-benzylidene-2-indolinone core, which formed the scaffold for subsequent library assembling and SAR analysis. It was determined the most potent inhibitor is the initial hit **II-1** (IC_{50} = 4.3 ± 1.4 μM), and that modifications to either the 3,5-dibromo-4-hydroxybenzylidine pharmacophore at position 3 or the methyl ester at position 5 had a detrimental effect on activity. The ineffectiveness of **II-1** in the cell-based assay may indicate that these compounds are not able to penetrate even the hyper-permeable *E. coli* strain.

Future directions include SAR to explore the effect of substitutions at other locations on the indolinone core to improve solubility and potency and to develop methods to control or resolve geometric isomers.

2.6 EXPERIMENTAL

2.6.1 SYNTHESIS

Materials and Instrumentation

Microwave reactions were performed in 2.0 – 5.0 mL microwave vials, sealed under ambient atmosphere, and loaded to a CEM Discover SP-D 80 Microwave Reactor (100 W, < 100 psi). Heated non-microwave reactions were performed in a temperature-controlled oil bath. TLC was performed on F-254 (0.25 mm) precoated silica gel (Merck) and visualized under UV, aqueous $KMnO_4$, or aqueous ninhydrin stain. Flash column chromatography purifications were performed using a normal phase Teledyne Isco CombiFlash® Rf 200 with standard RediSep RF 12 g silica columns.

Compounds were characterized by ^{1}H NMR, ^{13}C NMR, DEPT Q, NOESY, ESI-MS, and HRMS. NMR spectra were obtained from a Bruker AvanceIII 700 (700 MHz). Chemical shifts are reported as ppm, coupling constants in Hz, and peaks were calibrated to the solvent residual peak ($CDCl_3$ = 7.26 (^{1}H), 77.16 (^{13}C), DMSO-d_6 = 2.50 (^{1}H), 39.51 (^{13}C)). Mass spectrometry was conducted with a Bruker Maxis 4G/TOF in either positive or negative ion mode with direct infusion.

General Procedure for Microwave-Assisted Aldol Condensation

To a clean microwave vial charged with a stir bar was added the oxindole (1.0 equiv.), aldehyde (1.2 equiv.), piperidine (0.2 equiv.), and absolute ethanol (to achieve a concentration of 0.25 M) as the solvent. The vial was then sealed with a microwave cap and irradiated for thirty minutes at 79 °C. After cooling to room

temperature, the contents of the vial were purified by flash column chromatography or filtration to yield the corresponding title compound.

For experimental and characterization of (*Z*)-methyl 3-(3,5-dibromo-4-hydroxybenzylidene)-2-oxoindoline-5-carboxylate (**II-1**), (*Z*)-5-bromo-3-(3,5-dibromo-4-hydroxybenzylidene)indolin-2-one (**II-11**), (*Z*)-methyl 3-((5-methylfuran-2-yl)methylene)-2-oxoindoline-5-carboxylate (**II-12**), (*Z*)-methyl 3-(3-nitrobenzylidene)-2-oxoindoline-5-carboxylate (**II-13**), (*Z*)-methyl 3-(4-bromo-3-hydroxybenzylidene)-2-oxoindoline-5-carboxylate (**II-14**), (*Z*)-3-(5-methylfuran-2-yl)methylene)indolin-2-one (**II-15**), (*Z*)-methyl 3-(3-bromobenzylidene)-2-oxoindoline-5-carboxylate (**II-16**), (*Z*)-3-(4-hydroxy-3,5-dimethylbenzylidene)indolin-2-one (**II-17**), (*Z*)-3-(3,5-dibromo-4-hydroxybenzylidene)indolin-2-one (**II-18**), (*Z*)-3-(3,5-dibromo-4-hydroxybenzylidene)-5-hydroxyindolin-2-one (**II-29**), (*Z*)-methyl 3-(3,5-dibromo-4-hydroxybenzylidene)-2-oxoindoline-5-carboxylate (**II-30**), (*Z*)-methyl 2-oxo-3-(pyridin-3-ylmethylene)indoline-5-carboxylate (**II-31**), (*Z*)-methyl 3-(4-hydroxybenzylidene)-2-oxoindoline-5-carboxylate (**II-32**), (*Z*)-methyl 3-(4-hydroxy-3,5-dimethylbenzylidene)-2-oxoindoline-5-carboxylate (**II-33**), (*Z*)-methyl 3-(3,5-dibromobenzylidene)-2-oxoindoline-5-carboxylate (**II-34**), (*Z*)-methyl 2-oxo-3-[4-(trifluoromethyl)benzylidene]indoline-5-carboxylate (**II-35**), and (*Z*)-methyl 3-(4-nitrobenzylidene)-2-oxoindoline-5-carboxylate (**II-36**), please see Leckett 2016.[43]

(*E*)-3-(4-methoxybenzylidene)-5-carboxyindolin-2-one (II-19)

5-carboxyoxindole (24.2 mg, 0.14 mmol) and 4-methoxybenzaldehyde (18.5 μL, 0.17 mmol) were added to ethanol (3 mL) in a microwave tube charged with a stir bar as per general procedure. Piperidine (3 μL, 0.03 mmol) was added and the tube was sealed and microwaved for 90 minutes. After cooling to room temperature, the solution was concentrated under reduced pressure and purified by column chromatography (5% methanol in dichloromethane) to provide the title compound as a yellow powder in a mixture with the *Z* isomer (8 mg, 20%). ^{1}H NMR (700 MHz; DMSO-d_6) for the *E* isomer: δ12.64 (bs, 1H), 10.93 (s, 1H), 8.27 (s, 1H), , 7.85 (dd, J = 8.2 Hz, ^{4}J = 1.4 Hz, 1H), 7.74 (d, J= 8.6 Hz, 2H), 7.67 (s, 1H), 7.11 (d, J = 8.7 Hz, 2H), 6.95 (d, J = 8.2 Hz, 1H), 3.86 (s, 3H). ^{13}C NMR (176 MHz; DMSO-d_6) for the *E* isomer: δ169.24 (C), 167.18 (C), 161.55 (C), 160.88 (C), 146.22 (C), 137.39 (CH), 131.74 (CH), 131.62 (CH), 126.38 (C), 124.81 (C), 123.07 (CH), 121.10 (C), 114.35 (CH), 109.70 (CH), 55.51 (CH_3). ^{1}H NMR (700 MHz; DMSO-d_6) for the *Z* isomer: δ10.94 (s, 1H), 8.54 (d, J = 8.8 Hz, 2H), 8.27 (s, 1H), 7.96 (s, 1H), 7.82 (dd, J = 8.1 Hz, ^{4}J = 1.5 Hz, 1H), 7.05 (d, J = 8.9 Hz, 2H), 6.90 (d, J = 8.1 Hz, 1H), 3.85 (s, 3H). ^{13}C NMR (176 MHz; DMSO-d_6) for the *Z* isomer: δ167.71 (C), 167.55 (C), 143.77 (C), 138.52 (CH), 134.84 (CH), 131.19 (CH), 126.97 (C), 125.39 (C), 122.88 (C), 120.52 (CH), 113.87 (CH), 108.88 (CH), 48.64 (CH_3). HRMS (ESI) for $C_{17}H_{13}NO_4$: Calculated $[M+H]^+$: 296.0918 and $[M+Na]^+$: 318.0737. Found $[M+H]^+$: 296.0913 and $[M+Na]^+$: 318.0731.

(*E*)-3-benzylidene-5-carboxyindolin-2-one (II-20)

5-carboxyoxindole (25.0 mg, 0.14 mmol) and benzaldehyde (17 μL, 0.17 mmol) were added to ethanol (2 mL) in a microwave tube charged with a stir bar as per general procedure. Piperidine (3 μL, 0.03 mmol) was added and the tube was sealed and microwaved for 90 minutes. After cooling to room temperature, the solution was concentrated under reduced pressure and purified by column chromatography (5% methanol in dichloromethane) to provide the title compound as a yellow powder in a mixture with the *Z* isomer (9.4 mg, 25%). ^{1}H NMR (700 MHz; DMSO-d_6) for the *E* isomer: δ12.65 (bs, 1H), 10.98 (bs, 1H), 8.18 (s, 1H), 7.86 (d, J =8.2 Hz, 1H), 7.74 (m, 3H), 7.54 (m, 3H), 6.96 (d, J = 7.0 Hz, 1H). ^{13}C NMR (176 MHz; DMSO-d_6) for the *E* isomer: δ168.83 (C), 167.30 (C), 137.03 (CH), 134.13 (C), 133.84 (C), 132.00 (CH), 130.01 (CH), 129.31 (CH), 128.75 (CH), 126.87 (C), 123.35 (CH), 120.71 (C), 109.72 (CH). ^{1}H NMR (700 MHz; DMSO-d_6) for the *Z* isomer: δ10.98 (bs, 1H), 8.43 (m, 2H), 8.33 (s, 1H), 8.02 (s, 1H), 7.86 (d, J =8.2 Hz, 1H), 7.48 (m, 3H), 6.90 (d, 7.8 Hz, 1H). ^{13}C NMR (176 MHz; DMSO-d_6) for the *Z* isomer: δ167.00 (C), 146.48 (C), 144.23 (C), 138.38 (CH), 132.12 (CH), 130.85 (CH), 130.67 (CH), 128.17 (CH), 125.72 (C), 124.81 (C), 121.03 (CH), 108.95 (CH). HRMS (ESI) for $C_{16}H_{11}NO_3$: Calculated $[M+H]^+$: 266.0812 and $[M+Na]^+$: 288.0631. Found $[M+H]^+$: 266.0810 and $[M+Na]^+$: 288.0629.

(*Z*)-3-(3,5-dibromo-4-hydroxybenzylidene)-5-carboxyindolin-2-one (II-21)

5-carboxyoxindole (46.0 mg, 0.26 mmol) and 3,5-dibromo-4-hydroxybenzaldehyde (98.5 mg, 0.35 mmol) were added to a 0.44 M ammonium acetate in 3:1 ethanol:acetic acid solution (pH 4.5) (3 mL) in a microwave tube

charged with a stir bar as per general procedure. Piperidine (3 μL, 0.03 mmol) was added and the tube was sealed and microwaved for 30 minutes. After cooling to room temperature, ether was added to precipitate the product, which was filtered by gravity and washed with methanol to yield the title compound as a yellow powder in a mixture with the *E* isomer (14.8 mg, 13%). ^{1}H NMR (700 MHz; DMSO-d_6) for the *Z* isomer: δ12.66 (bs, 2H), 11.03 (s, 1H), 8.87 (s, 2H), 8.30 (s, 1H), 7.93 (s, 1H), 7.85 (dd, J = 8.1 Hz, ^{4}J = 1.5 Hz, 1H), 6.94 (d, J = 8.1 Hz, 1H). ^{13}C NMR (176 MHz; DMSO-d_6) for the *Z* isomer: δ167.60 (C), 167.35 (C), 136.49 (CH), 135.71 (CH), 130.62 (CH), 125.02 (C), 123.69 (C), 123.57 (C), 120.90 (CH), 120.71 (C), 111.96 (C), 111.23 (C), 109.09 (CH). ^{1}H NMR (700 MHz; DMSO-d_6) for the *E* isomer: δ10.99 (s, 1H), 10.70 (bs, 2H), 8.21 (s, 1H), 7.97 (s, 2H), 7.88 (dd, J = 8.2 Hz, ^{4}J = 1.5 Hz, 1H), 7.58 (s, 1H), 6.97 (d, J = 8.2 Hz, 1H). ^{13}C NMR (176 MHz; DMSO-d_6) for the *E* isomer: δ168.77 (C), 166.85 (C), 146.67 (C), 144.12 (C), 134.53 (CH), 133.48 (CH), 132.02 (CH), 123.16 (CH), 109.92 (CH). HRMS (ESI) for $C_{16}H_9Br_2NO_4$: Calculated $[M+H]^+$: 437.8971 and $[M+Na]^+$: 461.8770. Found $[M+H]^+$: 437.1927 and $[M+Na]^+$: 461.8748.

(*E*)-3-(3-hydroxybenzylidene)-5-carboxyindolin-2-one (II-22)

5-carboxyoxindole (30.5 mg, 0.17 mmol) and 3-hydroxybenzaldehyde (34.7 mg, 0.28 mmol) were added to a 0.44 M ammonium acetate in 3:1 ethanol:acetic acid solution (pH 4.5) (3 mL) in a microwave tube charged with a stir bar as per general procedure. Piperidine (3 μL, 0.03 mmol) was added and the tube was sealed and microwaved for 30 minutes. After cooling to room temperature, the solution was concentrated under reduced pressure and purified by column chromatography

(3.6% acetic acid 6.4% methanol in dichloromethane) to provide the title compound in a mixture with the *Z* isomer (19.8 mg, 41%). ^{1}H NMR (700 MHz; DMSO-d_6) for the *E* isomer: δ10.97 (s, 1H), 9.78 (bs, 1H), 8.23 (s, 1H), 7.86 (dd, J = 8.1 Hz, ^{4}J = 1.5 Hz, 1H), 7.63 (s, 1H), 7.34 (t, 7.8 Hz, 1H), 7.13 (d, 7.5 Hz, 1H), 7.09 (s, 1H), 6.96 (d, J = 8.2 Hz, 1H), 6.90 (dd, J = 7.9 Hz, ^{4}J = 2.3 Hz, 1H). ^{13}C NMR (176 MHz; DMSO-d_6) for the *E* isomer: δ169.12 (C), 167.57 (C), 157.81 (C), 157.14 (C), 137.61 (CH), 135.51 (C), 135.22 (C), 132.15 (CH), 130.09 (CH), 126.84 (C), 123.91 (CH), 120.96 (C), 120.19 (CH), 117.30 (CH), 115.90 (CH), 109.91 (CH). ^{1}H NMR (700 MHz; DMSO-d_6) for the *Z* isomer: δ10.97 (s, 1H), 9.59 (s, 1H), 8.31 (s, 1H), 7.97 (s, 1H), 7.91 (s, 1H), 7.86 (dd, J = 8.4 Hz, ^{4}J = 1.5 Hz, 1H), 7.79 (d, J = 7.7 Hz, 1H), 7.27 (t, J = 7.9 Hz, 1H), 6.90 (m, 2H). ^{13}C NMR (176 MHz; DMSO-d_6) for the *Z* isomer: δ167.30 (C), 139.01 (CH), 130.99 (CH), 129.31 (CH), 123.91 (CH), 121.27 (CH), 118.67 (CH), 118.29 (CH), 109.12 (CH). HRMS (ESI) for $C_{16}H_{11}NO_4$: Calculated $[M+H]^+$: 282.0761 and $[M+Na]^+$: 304.0580. Found $[M+H]^+$: 282.0759 and $[M+Na]^+$: 304.0576.

(*E*)-3-(4-hydroxybenzylidene)-5-carboxyindolin-2-one (II-23)

5-carboxyoxindole (25.5 mg, 0.14 mmol) and 4-hydroxybenzaldehyde (21.6 mg, 0.18 mmol) were added to a 0.44 M ammonium acetate in 3:1 ethanol:acetic acid solution (pH 4.5) (3 mL) in a microwave tube charged with a stir bar as per general procedure. Piperidine (3 µL, 0.03 mmol) was added and the tube was sealed and microwaved for 30 minutes. After cooling to room temperature, the solution was concentrated under reduced pressure and purified by column chromatography (3.6% acetic acid 6.4% methanol in dichloromethane) to provide the title compound

in a mixture with the *Z* isomer (9.3 mg, 23%). ^{1}H NMR (700 MHz; DMSO-d_6) for the *E* isomer: δ10.91 (s, 1H), 10.24 (s, 1H), 8.33 (s, 1H), 7.85 (dd, J = 8.1 Hz, ^{4}J = 1.5 Hz, 1H), 7.65 (d, J = 8.6 Hz, 2H), 7.63 (s, 1H), 6.94 (d, J = 8.3 Hz, 1H), 6.92 (d, J = 8.6 Hz, 2H). ^{13}C NMR (176 MHz; DMSO-d_6) for the *E* isomer: δ169.29 (C), 167.68 (C), 159.57 (C), 131.95 (CH), 131.28 (CH), 125.53 (C), 125.49 (C), 124.69 (C), 123.85 (C), 122.94 (CH), 121.14 (C), 120.18 (CH), 115.61 (CH), 109.48 (CH). ^{1}H NMR (700 MHz; DMSO-d_6) for the *Z* isomer: δ10.89 (s, 1H), 10.31 (s, 1H), 8.47 (d, J = 8.8 Hz, 2H), 8.26 (s, 1H), 7.86 (s, 1H), 7.81 (dd, J = 8.1 Hz, ^{4}J = 1.6 Hz, 1H), 6.89 (d, J = 7.9 Hz, 1H), 6.86 (d, J = 8.8 Hz, 2H). ^{13}C NMR (176 MHz; DMSO-d_6) for the *Z* isomer: δ167.50 (C), 167.12 (C), 164.46 (C), 138.94 (CH), 137.86 (CH), 135.18 (CH), 129.80 (CH), 121.70 (C), 115.21 (CH), 108.67 (CH). HRMS (ESI) for $C_{16}H_{11}NO_4$: Calculated $[M+H]^+$: 282.0761. Found $[M+H]^+$: 282.0759.

(*E*)-3-(3,4-dihydroxybenzylidene)-5-carboxyindolin-2-one (II-24)

5-carboxyoxindole (29.9 mg, 0.17 mmol) and 3,4-dihydroxybenzaldehyde (24.0 mg, 0.17 mmol) were added to a 0.44 M ammonium acetate in 3:1 ethanol:acetic acid solution (pH 4.5) (3 mL) in a microwave tube charged with a stir bar as per general procedure. Piperidine (3 µL, 0.03 mmol) was added and the tube was sealed and microwaved for 30 minutes. After cooling to room temperature, the solution was concentrated under reduced pressure and purified by column chromatography (3.6% acetic acid 6.4% methanol in dichloromethane) to provide the title compound in a mixture with the *Z* isomer (32.9 mg, 66%). ^{1}H NMR (700 MHz; DMSO-d_6) for the *E* isomer: δ10.89 (bs, 1H), 8.41 (s, 1H), 7.85 (dd, J = 8.3 Hz, ^{4}J = 1.3 Hz,

1H), 7.81 (s, 1H), 7.56 (s, 1H), 7.19 (d, ^{4}J = 1.4 Hz, 1H), 7.12 (dd, J = 8.9 Hz, ^{4}J = 1.6 Hz, 1H), 6.95 (d, J = 8.0 Hz, 1H), 6.89 (d, J = 8.1 Hz, 1H). ^{13}C NMR (176 MHz; DMSO-d_6) for the *E* isomer: δ169.42 (C), 167.65 (C), 148.11 (C), 145.46 (C), 138.36 (CH), 131.22 (CH), 125.63 (C), 125.12 (C), 123.53 (C), 123.15 (CH), 122.50 (CH), 121.23 (C), 116.92 (CH), 115.68 (CH), 109.50 (CH), 48.56 (C). ^{1}H NMR (700 MHz; DMSO-d_6) for the *Z* isomer: δ8.28 (d, ^{4}J = 1.4 Hz, 1H), 8.26 (d, ^{4}J = 1.3 Hz, 1H), 7.81 (m, 1H), 6.89 (d, J = 8.1 Hz, 1H), 6.83 (d, J = 8.0 Hz, 1H). ^{13}C NMR (176 MHz; DMSO-d_6) for the *Z* isomer: δ167.49 (C), 167.13 (C), 149.44 (C), 146.07 (C), 144.64 (C), 143.51 (C), 139.64 (CH), 129.67 (CH), 127.08 (CH), 125.97 (C), 121.32 (C), 120.12 (CH), 119.61 (CH), 115.14 (CH), 108.62 (CH), 43.75 (C). HRMS (ESI) for $C_{16}H_{11}NO_5$: Calculated $[M+H]^+$: 298.0710. Found $[M+H]^+$: 298.0707.

(*E*)-3-(3-bromo-4-hydroxybenzylidene)-5-carboxyindolin-2-one (II-25)

5-carboxyoxindole (25.0 mg, 0.14 mmol) and 3-bromo-4-hydroxybenzaldehyde (36.6 mg, 0.18 mmol) were added to a 0.44 M ammonium acetate in 3:1 ethanol:acetic acid solution (pH 4.5) (3 mL) in a microwave tube charged with a stir bar as per general procedure. Piperidine (3 μL, 0.03 mmol) was added and the tube was sealed and microwaved for 30 minutes. After cooling to room temperature, the precipitate was filtered by gravity and washed with methanol to yield the title compound as a yellow powder in a mixture with the *Z* isomer (18.3 mg, 36%). ^{1}H NMR (700 MHz; DMSO-d_6) for the *E* isomer: δ12.62 (bs, 1H), 11.03 (bs, 1H), 10.95 (s, 1H), 8.27 (s, 1H), 7.94 (d, ^{4}J = 2.0 Hz, 1H), 7.86 (dd, J = 8.1 Hz, ^{4}J = 1.6 Hz, 1H), 7.64 (dd, J = 8.4 Hz, ^{4}J = 1.9 Hz, 1H), 7.60 (s, 1H), 7.09

(d, J = 8.4 Hz, 1H), 6.96 (d, J = 8.1 Hz, 1H). ^{13}C NMR (176 MHz; DMSO-d_6) for the *E* isomer: δ169.00 (C), 166.98 (C), 146.43 (C), 136.25 (CH), 134.55 (CH), 131.69 (CH), 130.63 (CH), 126.39 (C), 125.16 (C), 123.46 (C), 123.08 (C), 123.05 (CH), 120.95 (C), 116.27 (CH), 109.76 (CH), 108.92 (CH). ^{1}H NMR (700 MHz; DMSO-d_6) for the *Z* isomer: δ11.27 (s, 1H), 10.97 (s, 1H), 9.74 (d, J = ^{4}1.5 Hz, 1H), 8.99 (d, ^{4}J = 2.3 Hz, 1H), 8.33 (dd, J = 8.6 Hz, ^{4}J = 2.1 Hz, 1H), 8.29 (d, ^{4}J = 1.7 Hz, 1H), 7.91 (s, 1H), 7.84 (dd, J = 8.2 Hz, ^{4}J = 1.6Hz, 1H), 7.04 (d, J = 8.5 Hz, 1H), 6.91 (d, J = 8.1 Hz, 1H). ^{13}C NMR (176 MHz; DMSO-d_6) for the *Z* isomer: δ167.66 (C), 167.41 (C), 156.73 (C), 155.96 (C), 143.89 (C), 137.39 (CH), 137.25 (CH), 134.19 (CH), 130.26 (CH), 127.02 (C), 125.26 (C), 123.55 (C), 120.61 (CH), 115.87 (CH), 109.64 (C), 109.20 (C). HRMS (ESI) for $C_{16}H_{10}BrNO_4$: Calculated $[M+H]^+$: 359.9866 and $[M+Na]^+$: 381.9685. Found $[M+H]^+$: 359.9858 and $[M+Na]^+$: 381.9676.

(*E*)-3-(3,5-dimethyl-4-hydroxybenzylidene)-5-carboxyindolin-2-one (II-26)

5-carboxyoxindole (25.6 mg, 0.14 mmol) and 3,5-dimethyl-4-hydroxybenzaldehyde (27.5, 0.18 mmol) were added to a 0.44 M ammonium acetate in 3:1 ethanol:acetic acid solution (pH 4.5) (3 mL) in a microwave tube charged with a stir bar as per general procedure. Piperidine (3 µL, 0.03 mmol) was added and the tube was sealed and microwaved for 30 minutes. After cooling to room temperature, the precipitate was filtered by gravity and washed with methanol to yield the title compound as a yellow powder in a mixture with the *Z* isomer (19.6 mg, 44%). ^{1}H NMR (700 MHz; DMSO-d_6) for the *E* isomer: δ12.60 (bs, 1H), 10.89 (s, 1H), 9.07 (bs, 1H), 8.25 (s, 1H), 7.84 (dd, J = 8.2 Hz, ^{4}J = 1.6 Hz, 1H),

7.58 (s, 1H), 7.42 (s, 2H), 6.95 (d, J = 8.2 Hz, 1H), 2.23 (s, 6H). ^{13}C NMR (176 MHz; DMSO-d_6) for the *E* isomer: δ169.28 (C), 167.05(C), 155.65 (C), 146.05 (C), 138.16(CH), 133.88 (CH), 131.13 (CH), 130.59 (CH), 124.67 (C), 124.54 (C), 123.71 (C), 123.64 (C), 121.25 (C), 109.50 (CH), 16.36 (CH_3). ^{1}H NMR (700 MHz; DMSO-d_6) for the *Z* isomer: δ10.86 (s, 1H), 9.07 (bs, 1H), 8.45 (s, 2H), 8.25 (s, 1H), 7.81 (m, 2H), 6.90 (d, J = 8.1 Hz, 1H), 2.22 (s, 6H). ^{13}C NMR (176 MHz; DMSO-d_6) for the *Z* isomer: δ167.59(C), 167.46(C), 156.75 (C), 143.52 (C), 139.30(CH), 129.67 (CH), 125.64 (C), 125.50 (C), 123.37 (C), 123.12 (CH), 121.44 (C), 120.06 (CH), 108.66 (CH), 16.66 (CH_3). HRMS (ESI) for $C_{18}H_{15}NO_4$: Calculated $[M+H]^+$: 310.1074. Found $[M+H]^+$: 310.1065.

(*E*)-3-(4-nitrobenzylidene)-5-carboxyindolin-2-one (II-27)

5-carboxyoxindole (25.6 mg, 0.14 mmol) and 4-nitrobenzaldehyde (26.5 mg, 0.18 mmol) were added to a 0.44 M ammonium acetate in 3:1 ethanol:acetic acid solution (pH 4.5) (3 mL) in a microwave tube charged with a stir bar as per general procedure. Piperidine (3 μL, 0.03 mmol) was added and the tube was sealed and microwaved for 30 minutes. After cooling to room temperature, the precipitate was filtered by gravity and washed with methanol to yield the title compound as an orange powder in a mixture with the *Z* isomer (17.3 mg, 37%). ^{1}H NMR (700 MHz; DMSO-d_6) for the *E* isomer: δ10.99 (bs, 1H), 8.38 (d, J = 8.6 Hz, 2H), 8.01 (m, 2H), 7.89 (m, 1H), 7.75 (s, 1H), 6.97 (d, J = 8.1 Hz, 1H). ^{13}C NMR (176 MHz; DMSO-d_6) for the *E* isomer: δ168. 41 (C), 167.05 (C), 147.60 (C), 147.54 (C), 141.19 (C), 140.08 (C), 132.69 (CH), 130.57 (CH), 129.36 (C), 123.81 (CH), 123.67 (CH), 121.90 (CH), 120.07 (C), 109.92 (CH). ^{1}H NMR (700 MHz; DMSO-

d_6) for the *Z* isomer: δ10.99 (bs, 1H), 8.56 (d, J = 8.8 Hz, 2H), 8.38 (s, 1H), 8.31 (d, J = 8.9 Hz, 2H), 8.15 (s, 1H), 8.01 (s, 1H), 7.89 (m, 1H), 6.92 (d, J = 8.1 Hz, 1H). ^{13}C NMR (176 MHz; DMSO-d_6) for the *Z* isomer: δ167.27 (C), 166.89 (C), 146.72 (C), 144.78 (C), 134.91 (CH), 133.95 (CH), 132.66 (CH), 131.87 (CH), 129.16 (C), 124.12 (C), 123.13 (CH), 109.24 (CH). HRMS (ESI) for $C_{16}H_{10}N_2O_5$: Calculated $[M+H]^+$: 311.0663 and $[M+Na]^+$: 333.0482. Found $[M+H]^+$: 311.0653 and $[M+Na]^+$: 333.0471.

(*E*)-3-[4-(trifluoromethyl)benzylidene]-5-carboxyindolin-2-one (II-28)

5-carboxyoxindole (27.9 mg, 0.15 mmol) and 4-(trifluoromethyl)benzaldehyde (24 µL, 0.18 mmol) were added to a 0.44 M ammonium acetate in 3:1 ethanol:acetic acid solution (pH 4.5) (3 mL) in a microwave tube charged with a stir bar as per general procedure. Piperidine (3 µL, 0.03 mmol) was added and the tube was sealed and microwaved for 30 minutes. After cooling to room temperature, the solution was concentrated under reduced pressure and purified by column chromatography (1.8% acetic acid 3.2% methanol in dichloromethane) to provide the title compound as a powder in a mixture with the *Z* isomer (29.3 mg, 58%). ^{1}H NMR (700 MHz; DMSO-d_6) for the *E* isomer: δ11.07 (s, 1H), 8.01 (d, ^{4}J = 1.1 Hz, 1H), 7.93 (m, 4H), 7.89 (dd, J = 8.1 Hz, ^{4}J = 1.4 Hz, 1H), 7.77 (s, 1H), 6.99 (d, J = 8.2 Hz, 1H). ^{13}C NMR (176 MHz; DMSO-d_6) for the *E* isomer: δ168.50 (C), 167.76 (C), 138.53 (C), 136.06 (CH), 135.01 (CH), 132.50 (CH), 129.97 (CH), 128.58 (C), 125.62 (C), 124.92 (CH), 123.50 (CH), 121.64 (CH), 120.34 (C), 109.97 (CH), 70.66 (C), 19.18 (C). ^{1}H NMR (700 MHz; DMSO-d_6) for the *Z* isomer: δ11.07 (s, 1H), 8.53 (d, J = 8.2 Hz, 2H), 8.37 (d, ^{4}J = 1.1 Hz, 1H), 8.12 (s, 1H), 7.89 (dd, J = 8.1 Hz, ^{4}J = 1.4

Hz, 1H), 7.84 (d, J = 8.3 Hz, 2H), 6.94 (d, J = 8.1 Hz, 1H). ^{13}C NMR (176 MHz; DMSO-d_6) for the *Z* isomer: δ167.22 (C), 167.11 (C), 146.84 (C), 144.79 (C), 137.62 (C), 132.20 (CH), 131.57 (CH), 128.00 (C), 125.60 (C), 124.90 (CH), 124.33 (C), 109.23 (CH), 70.25 (C), 18.09 (C). HRMS (ESI) for $C_{17}H_{10}F_3NO_3$: Calculated $[M-H]^-$: 332.0529. Found $[M-H]^-$: 332.0535.

(Z)-Methyl 3-(4-methoxybenzylidene)-2-oxoindoline-5-carboxylate (II-37)

Methyl oxindole-5-carboxylate (0.144 g, 0.754 mmol) and 4-methoxybenzaldehyde (110 µL, 0.905 mmol) were added to methanol (3 mL) in a microwave tube charged with a stir bar as per general procedure. Piperidine (0.0148 mL, 0.150 mmol) was then added and the tube was sealed and microwaved for 30 min to provide the title compound (195.5 mg, 84%). ^{1}H NMR (700 MHz; DMSO-d_6): δ10.99 (s, 1H), 8.30 (s, 1H), 7.87 (dd, J = 8.2 Hz, ^{4}J = 1.5 Hz, 1H), 7.74 (d, J = 8.7 Hz, 2H), 7.69 (s, 1H), 7.12 (d, J = 8.7 Hz, 2H), 6.98 (d, J = 8.2 Hz, 1H), 3.87 (s, 3H), 3.78 (s, 3H). ^{13}C NMR (176 MHz; DMSO-d_6): δ169.13 (C), 166.03 (C), 160.98 (C), 146.72 (C), 137.77 (CH), 131.77 (CH), 131.42 (CH), 126.28 (C), 124.54 (C), 122.84 (CH), 122.28 (C), 121.31 (C), 114.34 (CH), 109.89 (CH), 55.53 (CH_3), 51.99 (CH_3). HRMS (ESI) for $C_{18}H_{15}NO_4$: Calculated $[M+H]^+$: 310.1074 and $[M+Na]^+$: 332.0893. Found $[M+H]^+$: 310.1089 and $[M+Na]^+$: 332.0917.

2.6.2 Biological Testing

Escherichia coli BW25113 Δ*bamB* Δ*tolC* Screening Constructs and Screening Conditions

For screening constructs and conditions, please see Azad 2016.[42]

Purification of Aminoglycoside 3-*N*- Acetyltransferase AAC(3)-Ia

Unless stated otherwise, materials were purchased from Sigma (Oakville, Ontario). A 10 mL overnight LB culture of BL21 (DE3) pLysS *E. coli* harbouring pET28a-*aac(3)-Ia* (supplemented with 50 μg/mL kanamycin) was used to inoculate 2 x 250 mL LB broth supplemented with 50 μg/mL kanamycin. Cells were grown at 30°C for 2-3 h, then induced with 1 mM IPTG and grown for another 3 h. Cells were harvested (6000 rpm for 15 min at 15°C) and washed with 60 mL of saline. Cells were collected by centrifugation at 4200 rpm for 30 min at 15°C and stored at -20°C for future use. Thawed pellets were resuspended in ice cold lysis buffer (50 mM HEPES, 150 mM NaCl, 1 mM PMSF, 0.1 mg/mL DNase, 1 mM 2-mercaptoethanol) and lysed by 5 freeze-thaw cycles. Lysate was centrifuged for 10 minutes at 4°C and the supernatant was added to Talon Superflow cobalt resin. Samples were incubated at room temperature for 30 minutes on the rotator, pelleted, and washed (50 mM HEPES, 300 mM NaCl, 10 mM imidazole) and eluted with 50 mM HEPES, 300 mM NaCl, 500 mM imidazole. Fractions containing AAC(3)-Ia were identified on 15% sodium dodecyl sulfate polyacrylamide gel electrophoresis (SDS-PAGE) gel (a band of ~18.6 kDa corresponded to AAC(3)-Ia), pooled, and dialyzed to remove imidazole to yield 670 mg of protein. Protein concentrations were estimated by absorbance at 280 nm. Samples were aliquoted and stored in 15% glycerol at -80°C.

Monitoring AAC(3)-Ia Activity *in vitro* (Ellman Assay)

AAC(3)-Ia activity was monitored spectrophotometrically by measuring production of 2-nitro-5-thiobenzoate (TNB^{2-}, extinction coefficient = 14, 150 M^{-}

$^{1}cm^{-1}$) resulting from the cleavage of 5,5'- dithiobis-(2-nitrobenzoic acid) (DTNB) by free coenzyme A sulfhydryl groups released upon acetyl transfer.[44] AAC(3)-Ia activity was monitored spectrophotometrically for 10 min at 25°C at 412 nm using a TECAN M1000 plate reader in a 96-well format. Reactions were initiated with gentamicin sulfate following 10 min incubation time at room temperature. Final concentrations of 3 mM DTNB and 0.1 M HEPES (pH 8) were used.

Monitoring AAC(3)-Ia Activity *in vitro* (Sigma-Aldrich® Fluorometric Thiol Quantification Assay)

AAC(3)-Ia activity was monitored fluorometrically via the thiol quantification kit from Sigma-Aldrich (λ_{ex} = 490 nm, λ_{em} = 535 nm).[41] Inhibitors (in 1-2% DMSO), AAC(3)-Ia (final concentration ~0.1 mg/mL), and acetyl-CoA (final concentration 50 μM) were incubated in kit buffer for 10 minutes at room temperature. Thiol reagent® was added and the reaction was immediately initiated with gentamicin (final concentration 250 μM) and monitored for 15 min at room temperature using a TECAN M100 plate reader in 96-well format. GraphPad Prism was used to plot IC_{50} data.

Checkerboard Assays

Checkerboard assays were performed in 96-well plates using *Escherichia coli* BW25113 Δ*bamB* Δ*tolC* with pGDP4-*aac(3)-Ia*. Colonies taken from an overnight LB plate containing 100 μg/mL ampicillin were suspended in saline at an OD_{600} of 0.1, and diluted for a final concentration of 1/500 in Mueller-Hinton broth (Thermo Fisher Scientific, Nepean, ON) per well. One well with no antibiotic or

compound served as a positive growth control on each plate. MICs were performed according to the National Committee of Laboratory Safety and Standards (NCLSS) guidelines prior to testing and used to determine the concentration range needed. Decreasing concentrations of gentamicin were combined with decreasing concentrations of compound. Plates were incubated at 37°C for 24 h. Cell viability was monitored by OD (λ = 600 nm). FIC was calculated using Equation 2-1:

$$FIC = \frac{MIC_{A\ in\ combination}}{MIC_A} + \frac{MIC_{B\ in\ combination}}{MIC_B} \quad (2\text{-}1)$$

where FIC $\leq$ 0.5 is considered synergistic, 0.5 < FIC < 2.0 is neutral, and FIC $\geq$ 2.0 is antagonistic.

2.7 REFERENCES

(1) O'Neill, J. *Tackling Drug-Resistant Infections Globally: Final Report and Recommendations*; 2016.

(2) WHO. *Global Action Plan on Antimicrobial Resistance*; Geneva, Switzerland, 2015.

(3) Wright, G. D. Antibiotic Adjuvants: Rescuing Antibiotics from Resistance. *Trends Microbiol.* **2016**, *24* (11), 862–871.

(4) Santajit, S.; Indrawattana, N. Mechanisms of Antimicrobial Resistance in ESKAPE Pathogens. *Biomed Res. Int.* **2016**, *2016*, 1–8.

(5) Brown, E. D.; Wright, G. D. Antibacterial Drug Discovery in the Resistance Era. *Nature* **2016**, *529* (7586), 336–343.

(6) Payne, D. J.; Miller, L. F.; Findlay, D.; Anderson, J.; Marks, L. Time for a Change: Addressing R&D and Commercialization Challenges for Antibacterials. *Philos. Trans. R. Soc. London B Biol. Sci.* **2015**, *370* (1670), 1–12.

(7) Reading, C.; Cole, M. Clavulanic Acid: A Beta-Lactamase-Inhiting Beta-Lactam from Streptomyces Clavuligerus. *Antimicrob. Agents Chemother.* **1977**, *11* (5), 852–857.

(8) Geddes, A. M.; Klugman, K. P.; Rolinson, G. N. Introduction: Historical Perspective and Development of Amoxicillin/Clavulanate. *Int. J. Antimicrob. Agents* **2007**, *30*, 109–112.

(9) Shaw, K. J.; Rather, P. N.; Hare, R. S.; Miller, G. H. Molecular Genetics of Aminoglycoside Resistance Genes and Familial Relationships of the Aminoglycoside-Modifying Enzymes. *Microbiol. Rev.* **1993**, *57* (1), 138–163.

(10) Gonzalez, U. S.; Spencer, J. P. Aminoglycosides: A Practical Review. *Am. Fam. Physician* **1998**, *58* (8), 1811–1820.

(11) Wright, G. D.; Thompson, P. R. Aminoglycoside Phosphotransferases: Proteins, Structure, and Mechanism. *Front. Biosci.* **1999**, *4*, 9–21.

(12) Labby, K. J.; Garneau-Tsodikova, S. Strategies to Overcome the Action of Aminoglycoside-Modifying Enzymes for Treating Resistant Bacterial Infections. *Future Med. Chem.* **2013**, *5* (11), 1285–1309.

(13) Davis, B. D. Mechanism of Bactericidal Action of Aminoglycosides. *Microbiol. Rev.* **1987**, *51* (3), 341–350.

(14) Reeves, A. Z.; Campbell, P. J.; Sultana, R.; Malik, S.; Murray, M.; Plikaytis, B. B.; Shinnick, T. M.; Posey, J. E. Aminoglycoside Cross-Resistance in Mycobacterium Tuberculosis Due to Mutations in the 5' Untranslated Region of WhiB7. *Antimicrob. Agents Chemother.* **2013**, *57* (4), 1857–1865.

(15) Le, T.; Bayer, A. S.; Bayer, A. S. Combination Antibiotic Therapy for Infective Endocarditis. *Clin. Infect. Dis.* **2003**, *36* (5), 615–621.

(16) World Health Organization. *WHO Model List of Essential Medicines 20th List WHO Model List of Essential Medicines (March 2017) Explanatory Notes*; 2017.

(17) Ramirez, M. S.; Tolmasky, M. E. Aminoglycoside Modifying Enzymes. *Drug Resist. Updat.* **2010**, *13*, 151–171.

(18) Daigle, D. M.; McKay, G. A.; Wright, G. D. Inhibition of Aminoglycoside Antibiotic Resistance Enzymes by Protein Kinase Inhibitors. *J. Biol. Chem.* **1997**, *272* (40), 24755–24758.

(19) Boehr, D. D.; Lane, W. S.; Wright, G. D. Active Site Labeling of the Gentamicin Resistance Enzyme AAC(6')-APH(2") by the Lipid Kinase Inhibitor Wortmannin. *Chem. Biol.* **2001**, *8* (8), 791–800.

(20) Boehr, D. D.; Draker, K.; Koteva, K.; Bains, M.; Hancock, R. E.; Wright, G. D. Broad-Spectrum Peptide Inhibitors of Aminoglycoside Antibiotic

Resistance Enzymes. *Chem. Biol.* **2003**, *10* (2), 189–196.

(21) Green, K. D.; Chen, W.; Garneau-Tsodikova, S. Identification and Characterization of Inhibitors of the Aminoglycoside Resistance Acetyltransferase Eis from Mycobacterium Tuberculosis. *ChemMedChem* **2012**, *7* (1), 73–77.

(22) Lin, D. L.; Tran, T.; Adams, C.; Alam, J. Y.; Herron, S. R.; Tolmasky, M. E. Inhibitors of the Aminoglycoside 6'-N-Acetyltransferase Type Ib [AAC(6')-Ib] Identified by in Silico Molecular Docking. *Bioorg. Med. Chem. Lett.* **2013**, *23* (20), 5694–5698.

(23) Li, Y.; Green, K. D.; Johnson, B. R.; Garneau-Tsodikova, S. Inhibition of Aminoglycoside Acetyltransferase Resistance Enzymes by Metal Salts. *Antimicrob. Agents Chemother.* **2015**, *59* (7), 4148–4156.

(24) Prabu, A.; Hassan, S.; Prabuseenivasan; Shainaba, A. S.; Hanna, L. E.; Kumar, V. Andrographolide: A Potent Antituberculosis Compound That Targets Aminoglycoside 2′-N-Acetyltransferase in Mycobacterium Tuberculosis. *J. Mol. Graph. Model.* **2015**, *61*, 133–140.

(25) Garzan, A.; Willby, M. J.; Green, K. D.; Gajadeera, C. S.; Hou, C.; Tsodikov, O. V; Posey, J. E.; Garneau-Tsodikova, S. Sulfonamide-Based Inhibitors of Aminoglycoside Acetyltransferase Eis Abolish Resistance to Kanamycin in Mycobacterium Tuberculosis. *J. Med. Chem.* **2016**, *59* (23), 10619–10628.

(26) Garzan, A.; Willby, M. J.; Green, K. D.; Tsodikov, O. V; Posey, J. E.; Garneau-Tsodikova, S. Discovery and Optimization of Two Eis Inhibitor Families as Kanamycin Adjuvants against Drug-Resistant M. Tuberculosis. *ACS Med. Chem. Lett.* **2016**, *7* (12), 1219–1221.

(27) Willby, M. J.; Green, K. D.; Gajadeera, C. S.; Hou, C.; Tsodikov, O. V; Posey, J. E.; Garneau-Tsodikova, S. Potent Inhibitors of Acetyltransferase Eis Overcome Kanamycin Resistance in Mycobacterium Tuberculosis. *ACS Chem. Biol.* **2016**, *11* (6), 1639–1646.

(28) Garzan, A.; Willby, M. J.; Ngo, H. X.; Gajadeera, C. S.; Green, K. D.; Holbrook, S. Y. L.; Hou, C.; Posey, J. E.; Tsodikov, O. V; Garneau-Tsodikova, S. Combating Enhanced Intracellular Survival (Eis)-Mediated Kanamycin Resistance of Mycobacterium Tuberculosis by Novel Pyrrolo[1,5-a]Pyrazine-Based Eis Inhibitors. *ACS Infect. Dis.* **2017**, *3* (4), 302–309.

(29) Tran, T.; Chiem, K.; Jani, S.; Arivett, B. A.; Lin, D.; Lad, R.; Jimenez, V.; Farone, M. B.; Debevec, G.; Santos, R.; et al. Identification of a Small Molecule Inhibitor of the Aminoglycoside 6'-N-Acetyltransferase Type Ib [AAC(6')-Ib] Using Mixture-Based Combinatorial Libraries. *Int. J.*

Antimicrob. Agents **2018**, *51* (5), 752–761.

(30) Zárate, S. G.; De la Cruz Claure, M. L.; Benito-Arenas, R.; Revuelta, J.; Santana, A. G.; Bastida, A. Overcoming Aminoglycoside Enzymatic Resistance: Design of Novel Antibiotics and Inhibitors. *Molecules* **2018**, *23* (2), 284.

(31) Ngo, H. X.; Green, K. D.; Gajadeera, C. S.; Willby, M. J.; Holbrook, S. Y. L.; Hou, C.; Garzan, A.; Mayhoub, A. S.; Posey, J. E.; Tsodikov, O. V; et al. Potent 1,2,4-Triazino[5,6 b]Indole-3-Thioether Inhibitors of the Kanamycin Resistance Enzyme Eis from Mycobacterium Tuberculosis. *ACS Infect. Dis.* **2018**, *4* (6), 1030–1040.

(32) Williams, J. W.; Northrop, D. B. Synthesis of a Tight-Binding, Multisubstrate Analog Inhibitor of Gentamicin Acetyltransferase I. *J. Antibiot. (Tokyo).* **1979**, *32* (11), 1147–1154.

(33) Elkins, J. M.; Fedele, V.; Szklarz, M.; Abdul Azeez, K. R.; Salah, E.; Mikolajczyk, J.; Romanov, S.; Sepetov, N.; Huang, X.-P.; Roth, B. L.; et al. Comprehensive Characterization of the Published Kinase Inhibitor Set. *Nat. Biotechnol.* **2016**, *34* (1), 95–103.

(34) Drewry, D.; Willson, T.; Zuercher, W. Seeding Collaborations to Advance Kinase Science with the GSK Published Kinase Inhibitor Set (PKIS). *Curr. Top. Med. Chem.* **2014**, *14* (3), 340–342.

(35) Burk, D. L.; Berghuis, A. M. Protein Kinase Inhibitors and Antibiotic Resistance. *Pharmacol. Ther.* **2002**, *93* (2–3), 283–292.

(36) Ribeiro, C. J. A.; Amaral, J. D.; Rodrigues, C. M. P.; Moreira, R.; Santos, M. M. M. Synthesis and Evaluation of Spiroisoxazoline Oxindoles as Anticancer Agents. *Bioorg. Med. Chem.* **2014**, *22* (1), 577–584.

(37) Villemin, D.; Martin, B. Potassium Fluoride on Alumina: Dry Synthesis of 3- Arylidene-1,3-Dihydro-Indol-2-One under Microwave Irradiation. *Synth. Commun.* **1998**, *28* (17), 3201–3208.

(38) Suthar, S. K.; Bansal, S.; Alam, M. M.; Jaiswal, V.; Tiwari, A.; Chaudhary, A.; Alex, A. T.; Joseph, A. Design, Synthesis, and Biological Evaluation of Oxindole Derivatives as Antidepressive Agents. *Bioorg. Med. Chem. Lett.* **2015**, *25* (22), 5281–5285.

(39) Erkkilä, A.; Majander, I.; Pihko, P. M. Iminium Catalysis. *Chem. Rev.* **2001**, *107* (12), 5416–5470.

(40) Monton, M. R. N.; Lebert, J. M.; Little, J. R. L.; Nair, J. J.; McNulty, J.; Brennan, J. D. A Sol-Gel-Derived Acetylcholinesterase Microarray for

Nanovolume Small-Molecule Screening. *Anal. Chem.* **2010**, *82* (22), 9365–9373.

(41) *Sigma-Aldrich® Fluorometric Thiol Quantitation Kit*.

(42) Azad, M. A. Reversing Antibiotic Resistance with Inhibitors of Bacterial Acetyltransferases, McMaster University, 2016.

(43) Leckett, K. Development and Application of Synthetic Methods for the Production of Small Molecule Libraries, McMaster University, 2016.

(44) Ellman, G. L.; Courtney, K. D.; Andres, V.; Featherstone, R. M. A New and Rapid Colorimetric Determination of Acetylcholinesterase Activity. *Biochem. Pharmacol.* **1961**, *7* (2), 88–95.

2.8 SUPPLEMENTARY DATA

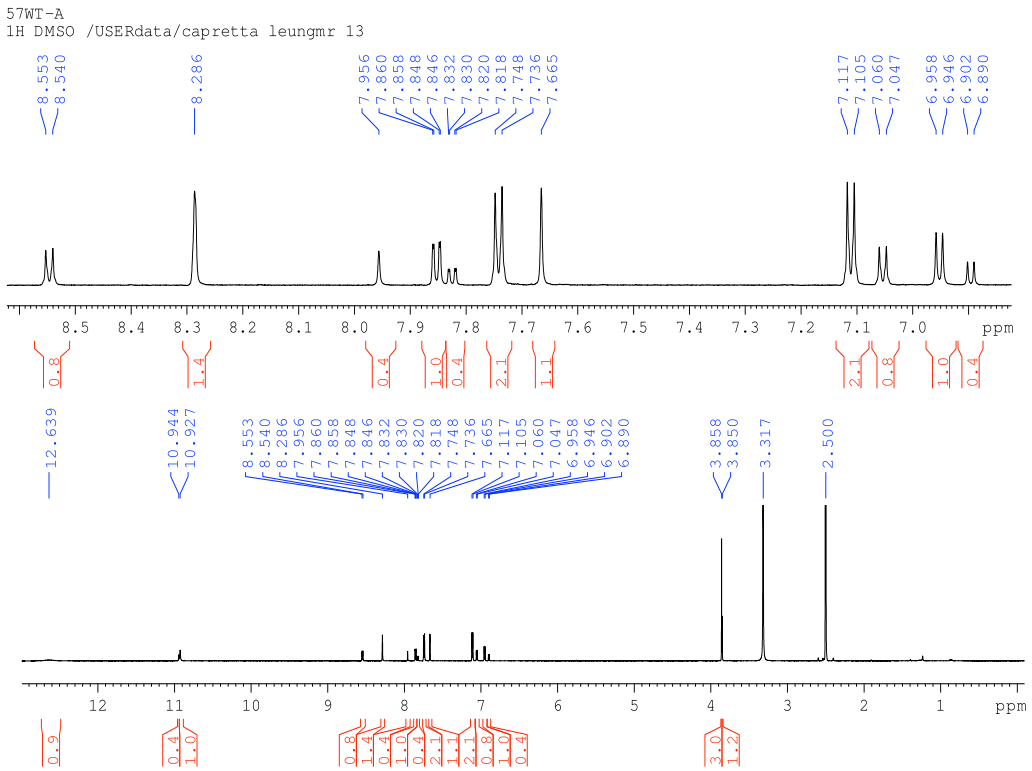

Figure S2-1. ^{1}H NMR of 3-(4-Methoxybenzylidene)-5-Carboxyindolin-2-one (**II-19**)

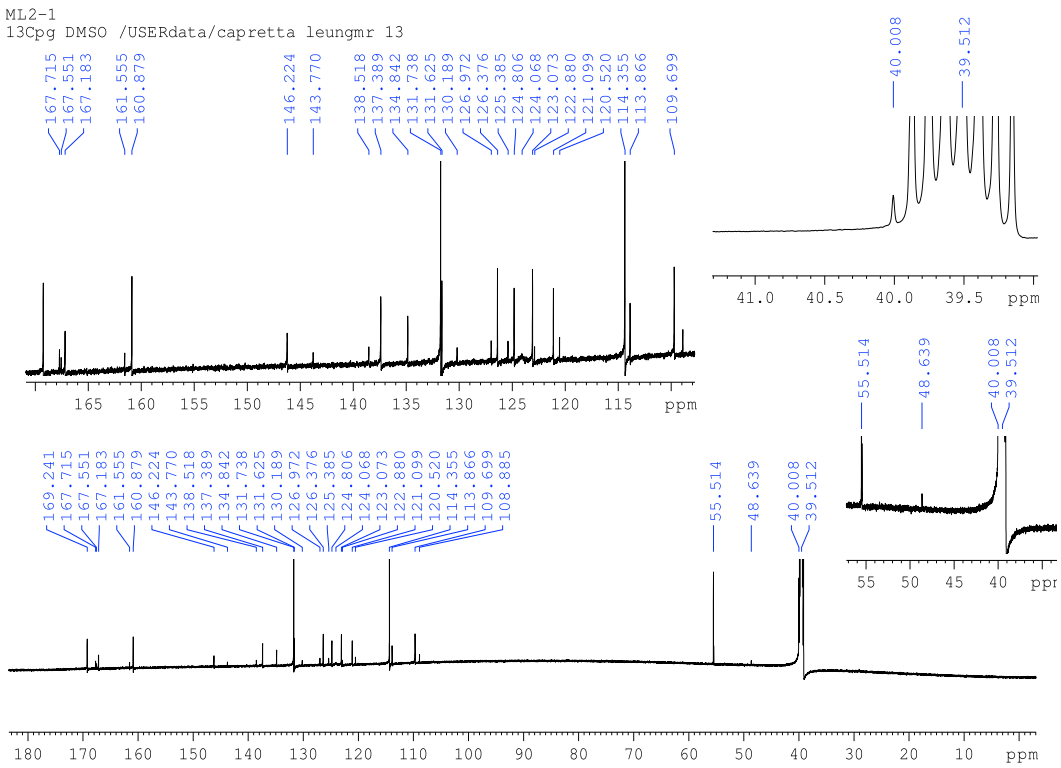

Figure S2-2. ^{13}C NMR of 3-(4-Methoxybenzylidene)-5-Carboxyindolin-2-one (**II-19**)

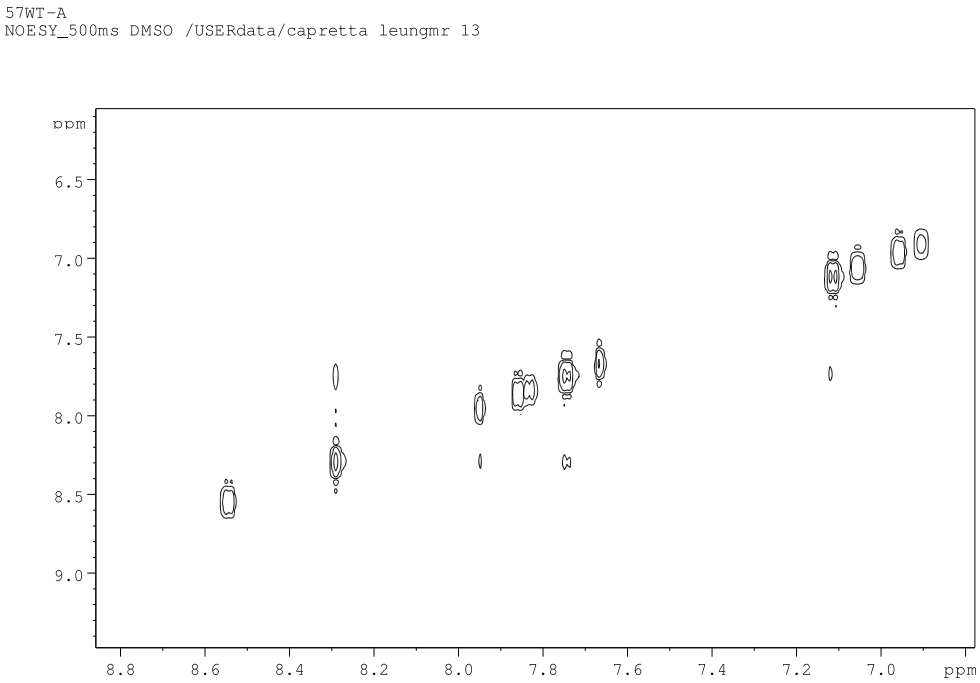

Figure S2-3. NOE of 3-(4-Methoxybenzylidene)-5-Carboxyindolin-2-one (**II-19**)

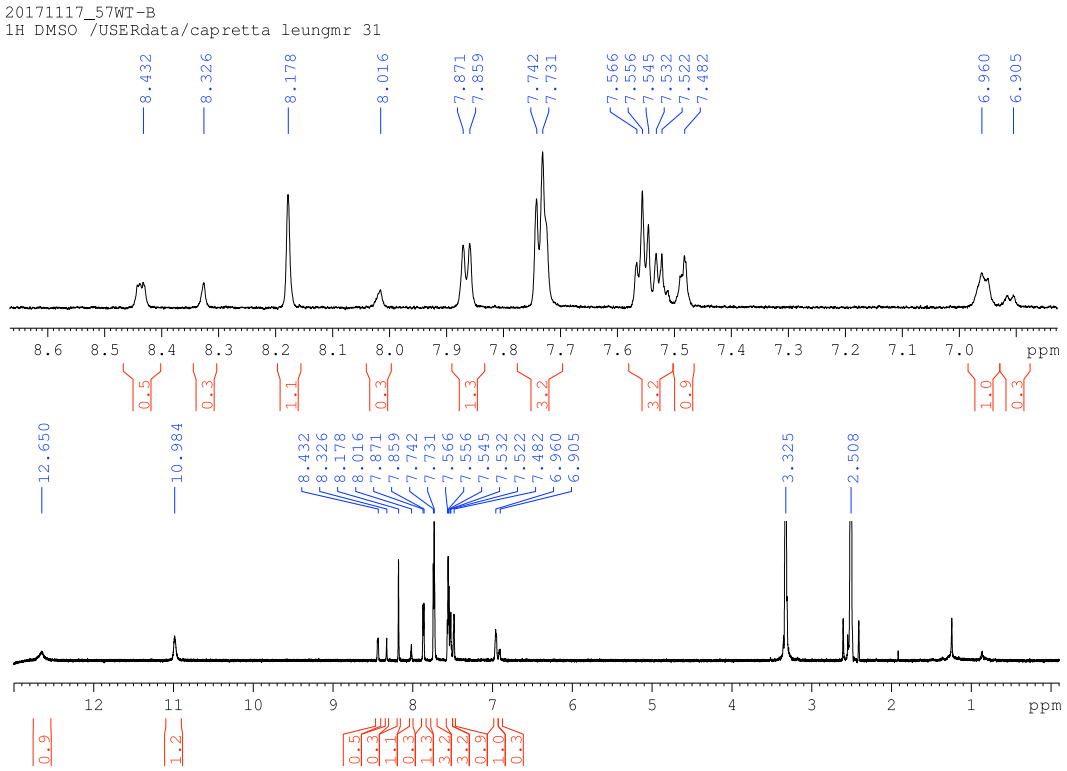

Figure S2-4. ^{1}H NMR of 3-Benzylidene-5-Carboxyindolin-2-one (**II-20**)

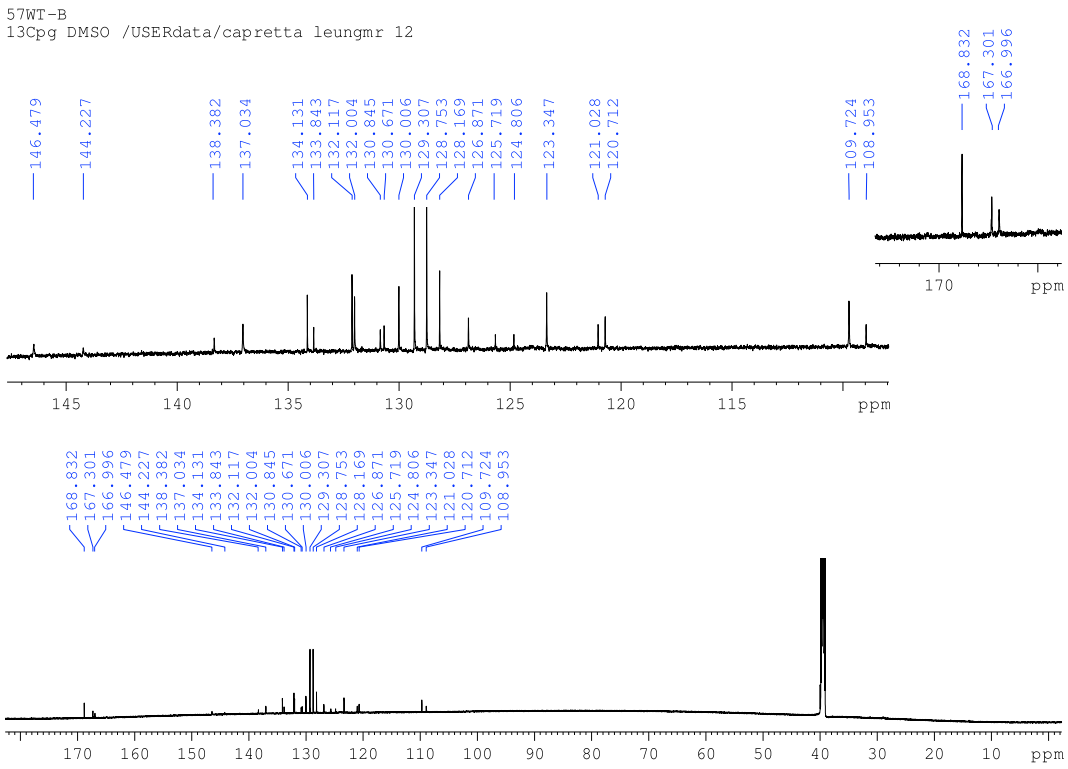

Figure S2-5. ^{13}C NMR of 3-Benzylidene-5-Carboxyindolin-2-one (**II-20**)

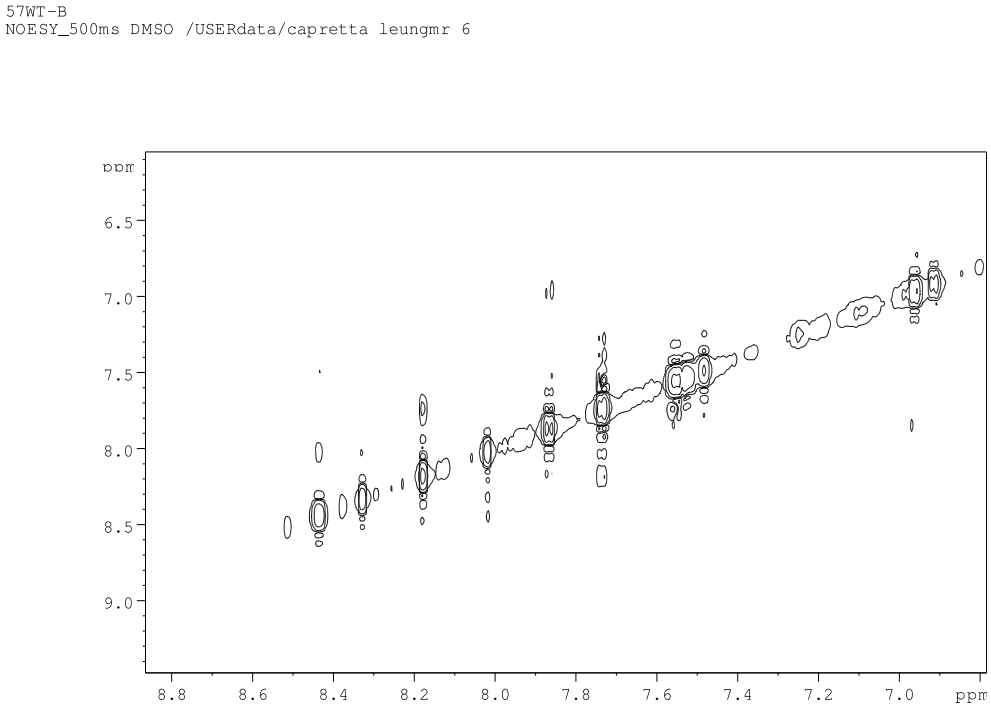

Figure S2-6. NOE of 3-Benzylidene-5-Carboxyindolin-2-one (**II-20**)

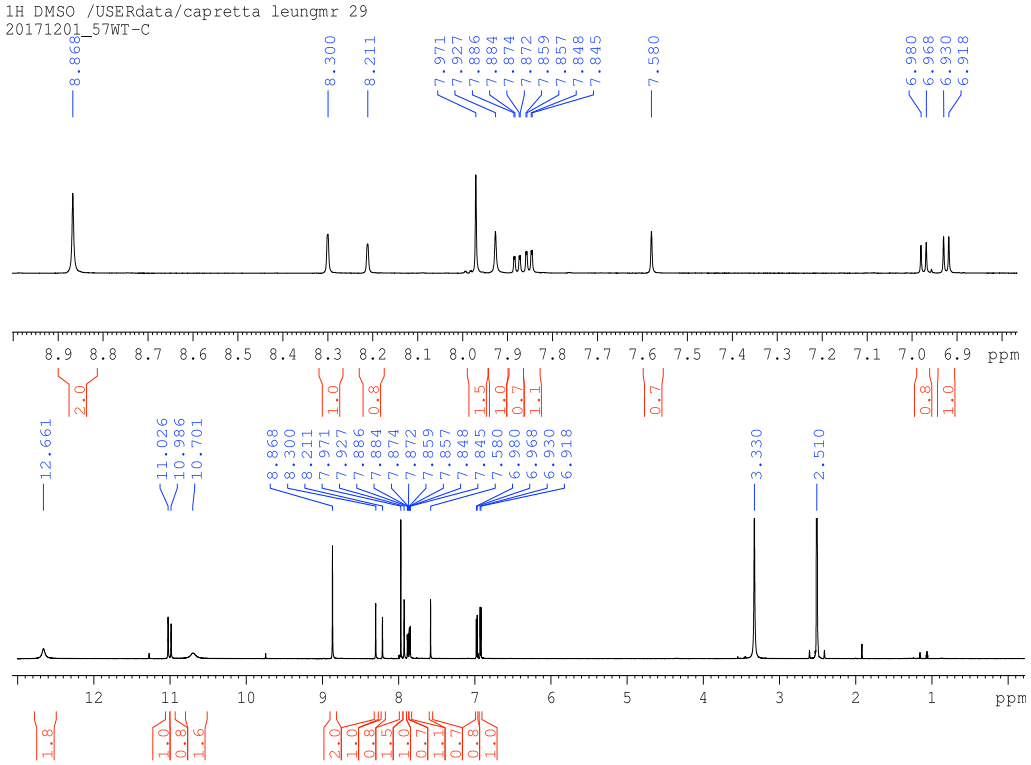

Figure S2-7. ^{1}H NMR of 3-(3,5-Dibromo-4-Hydroxybenzylidene)-5-Carboxyindolin-2-one (**II-21**)

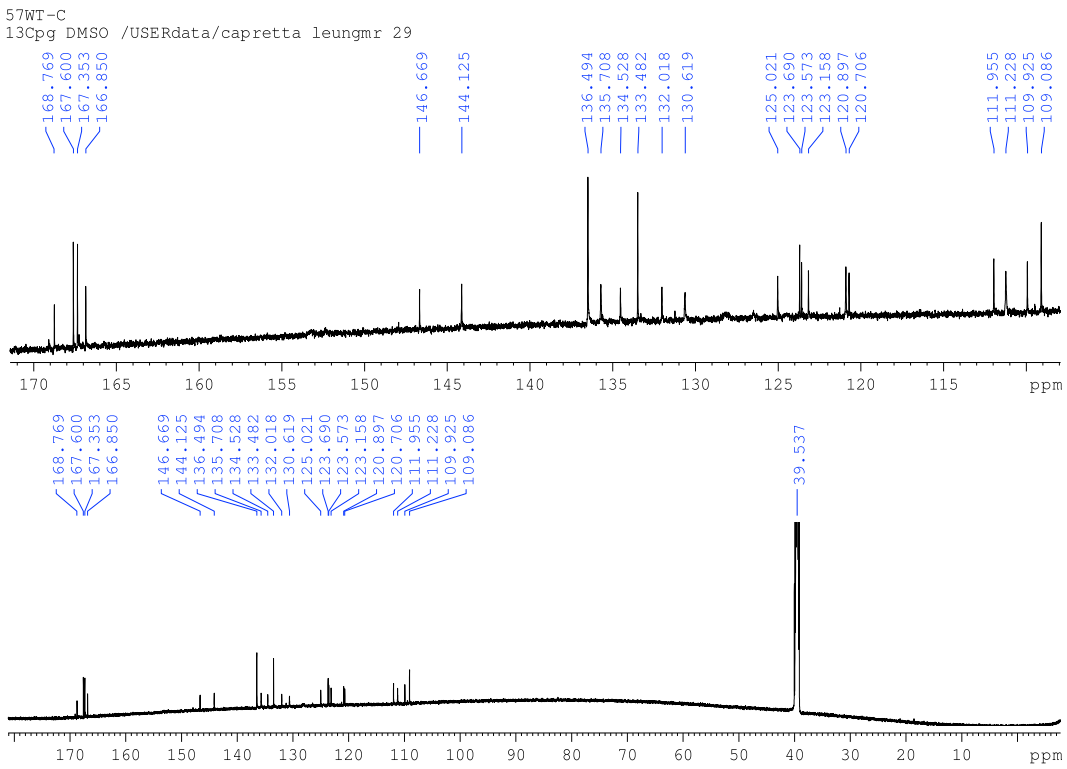

Figure S2-8. ^{13}C NMR of 3-(3,5-Dibromo-4-Hydroxybenzylidene)-5-Carboxyindolin-2-one (**II-21**)

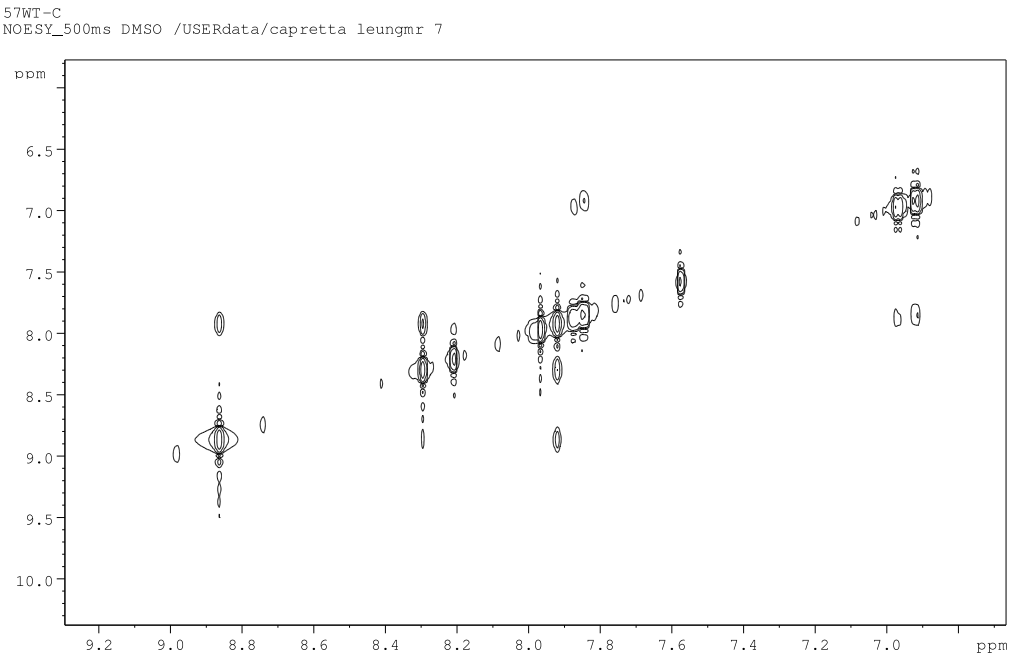

Figure S2-9. NOE of 3-(3,5-Dibromo-4-Hydroxybenzylidene)-5-Carboxyindolin-2-one (**II-21**)

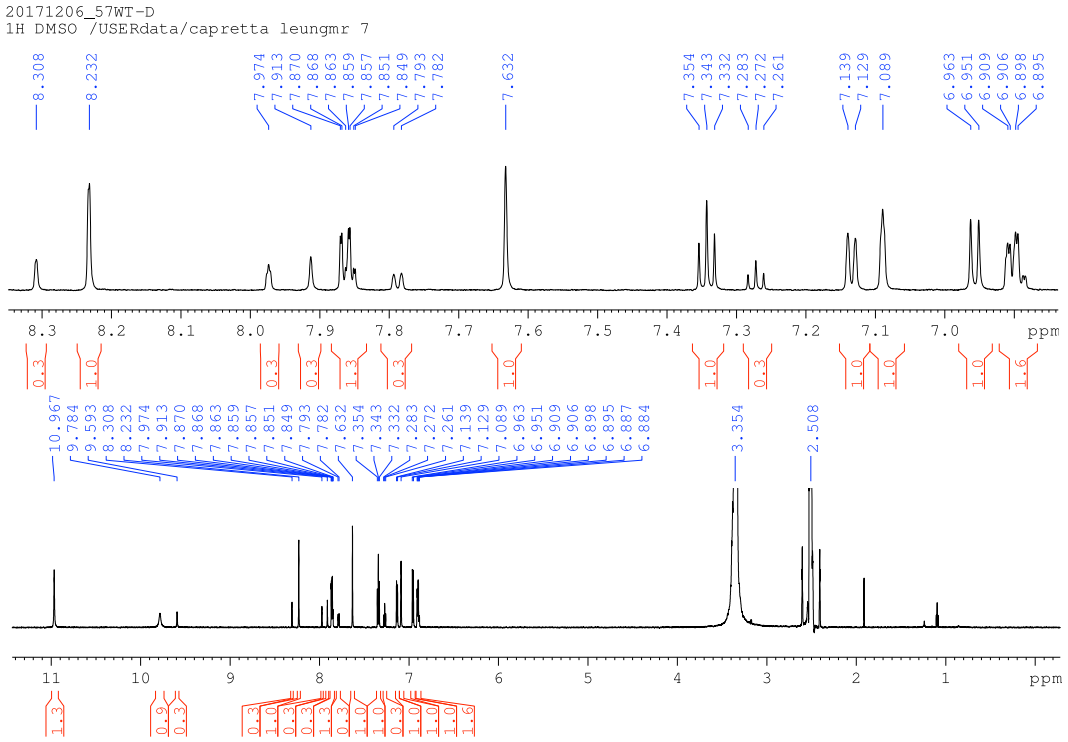

Figure S2-10. ^{1}H NMR of 3-(3-Hydroxybenzylidene)-5-Carboxyindolin-2-one (**II-22**)

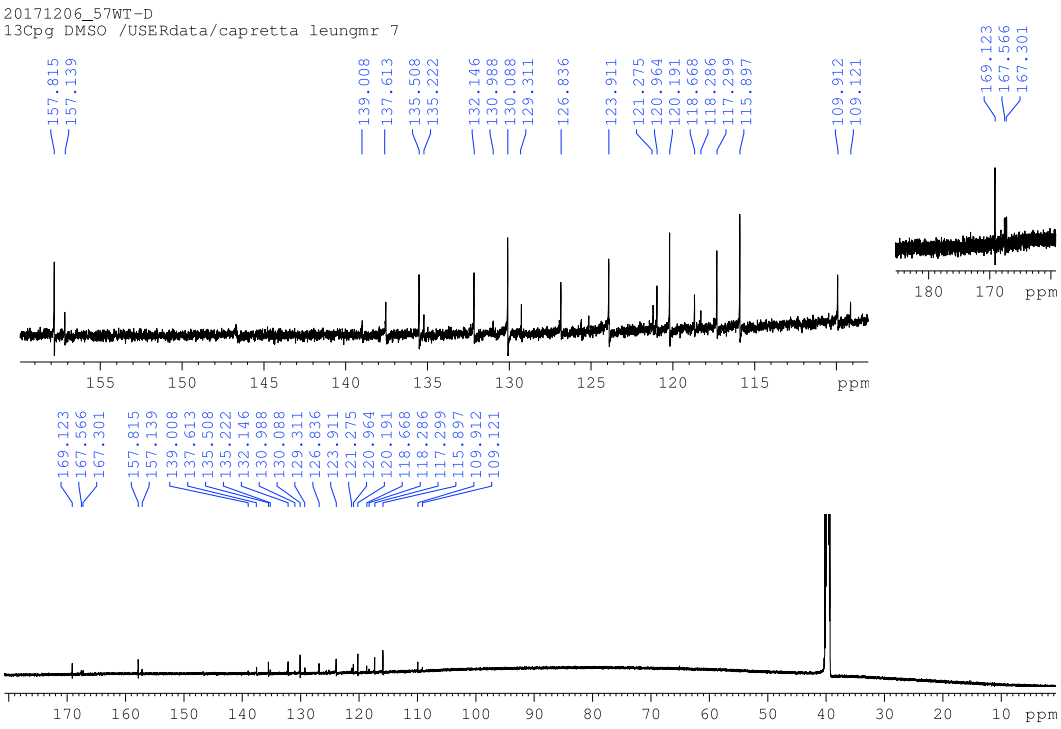

Figure S2-11. ^{13}C NMR of 3-(3-Hydroxybenzylidene)-5-Carboxyindolin-2-one (**II-22**)

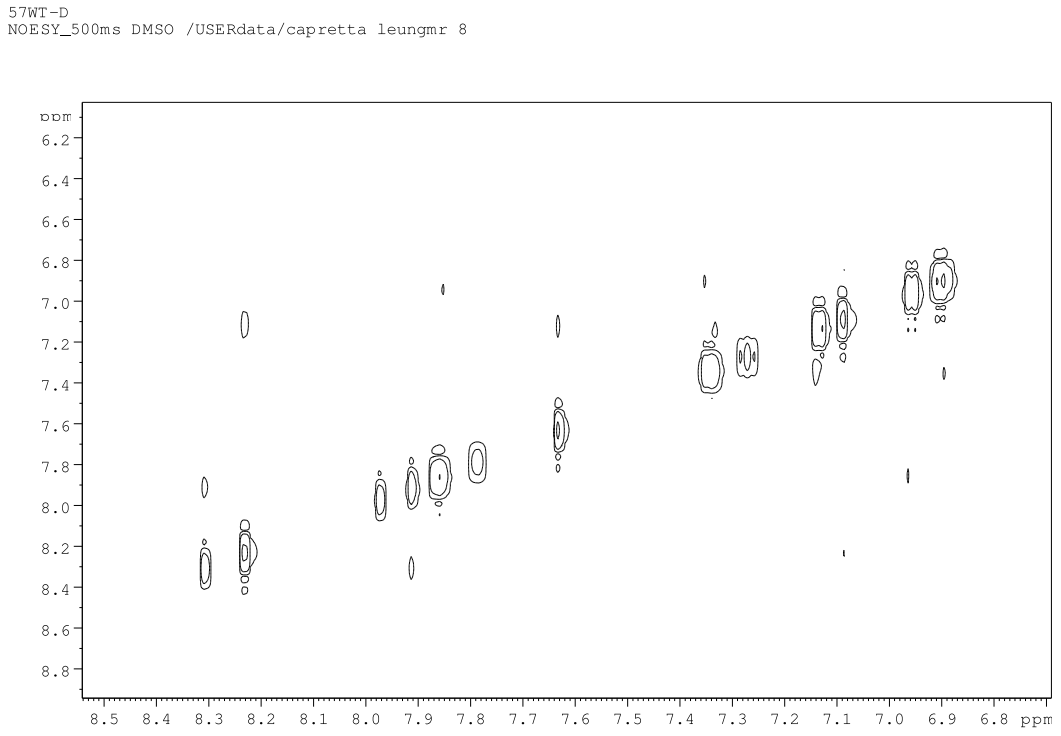

Figure S2-12. NOE of 3-(3-Hydroxybenzylidene)-5-Carboxyindolin-2-one (**II-22**)

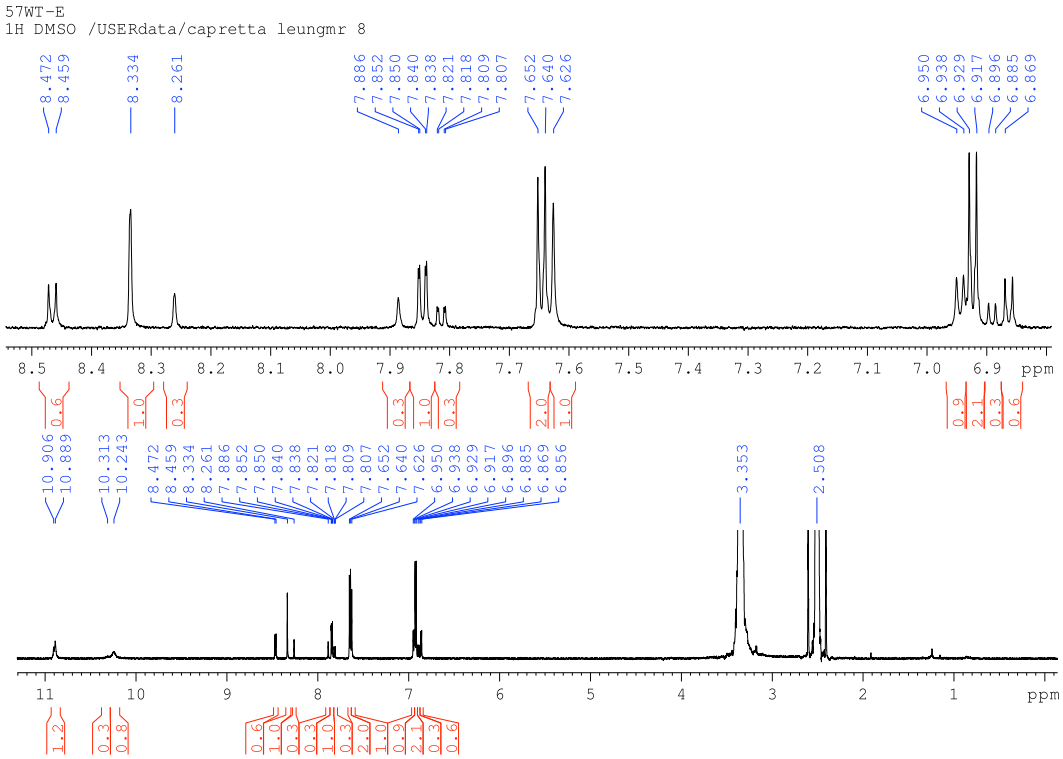

Figure S2-13. ^{1}H NMR of 3-(4-Hydroxybenzylidene)-5-Carboxyindolin-2-one (**II-23**)

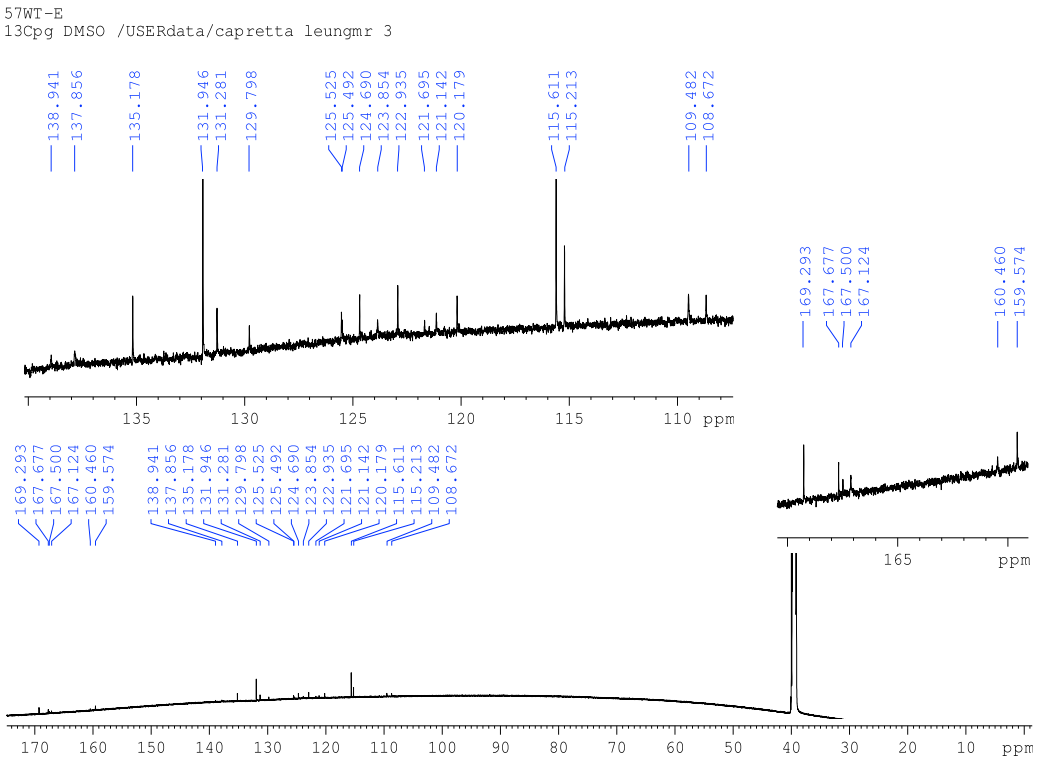

Figure S2-14. ^{13}C NMR of 3-(4-Hydroxybenzylidene)-5-Carboxyindolin-2-one (**II-23**)

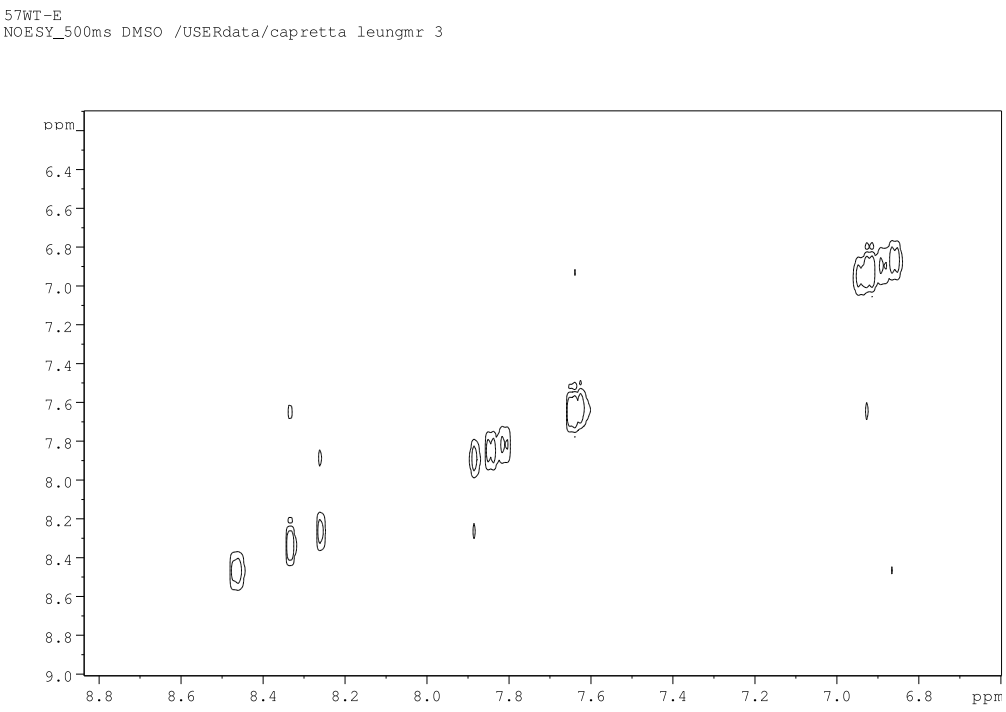

Figure S2-15. NOE of 3-(4-Hydroxybenzylidene)-5-Carboxyindolin-2-one (**II-23**)

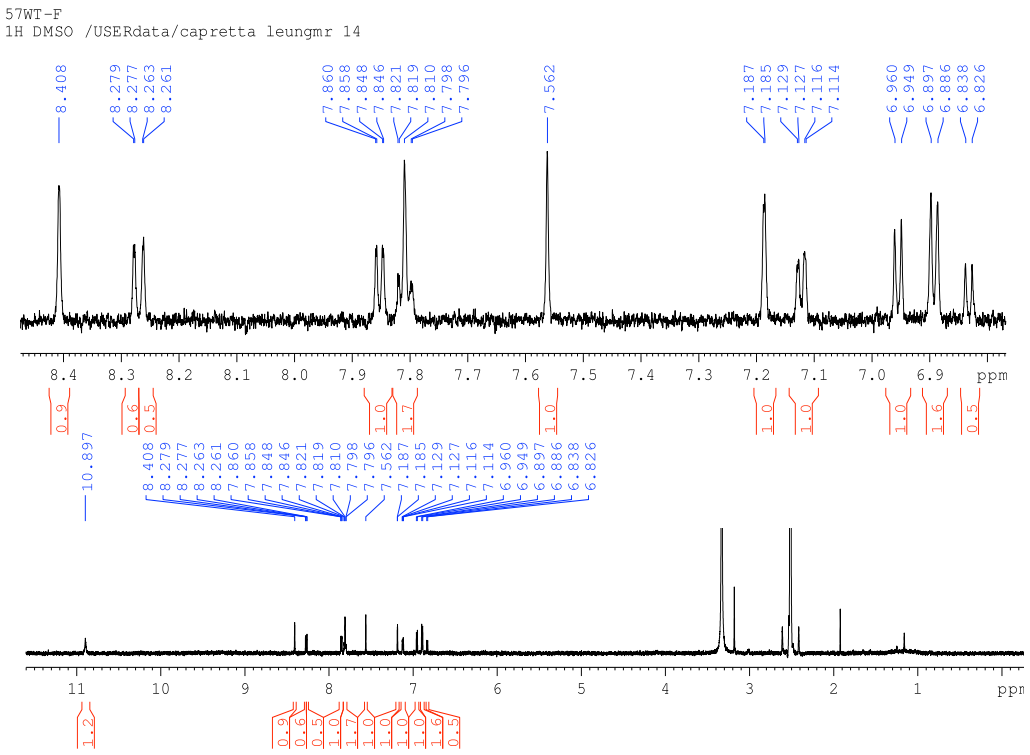

Figure S2-16. ^{1}H NMR of 3-(3,4-Dihydroxybenzylidene)-5-Carboxyindolin-2-one (**II-24**)

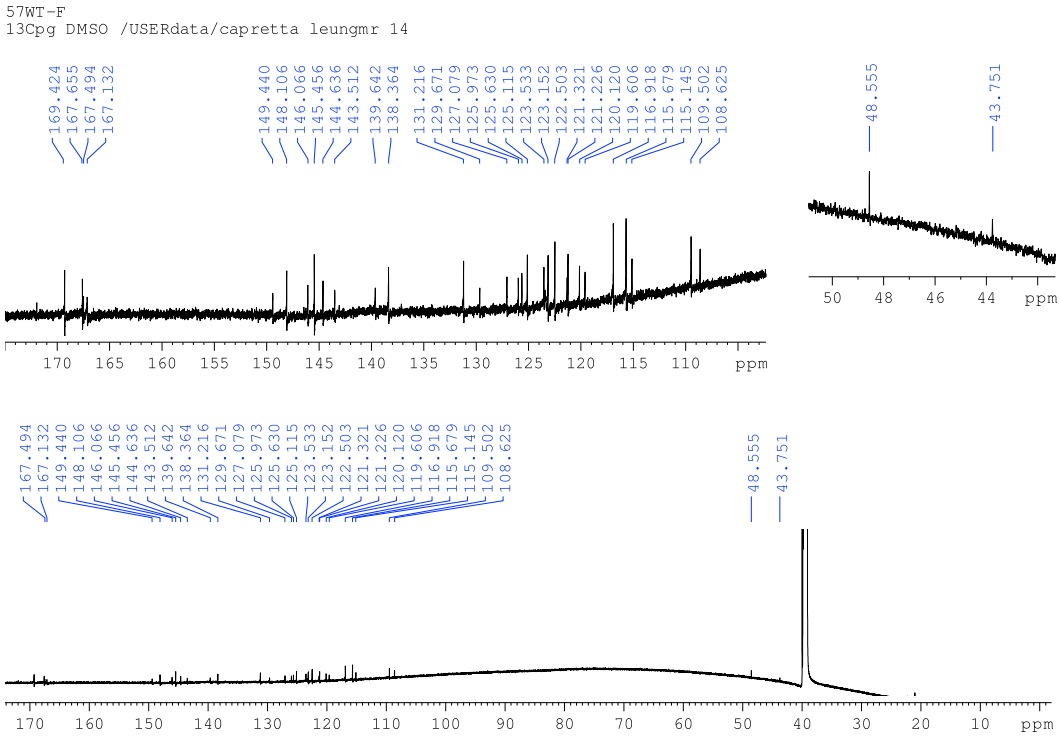

Figure S2-17. ^{13}C NMR of 3-(3,4-Dihydroxybenzylidene)-5-Carboxyindolin-2-one (**II-24**)

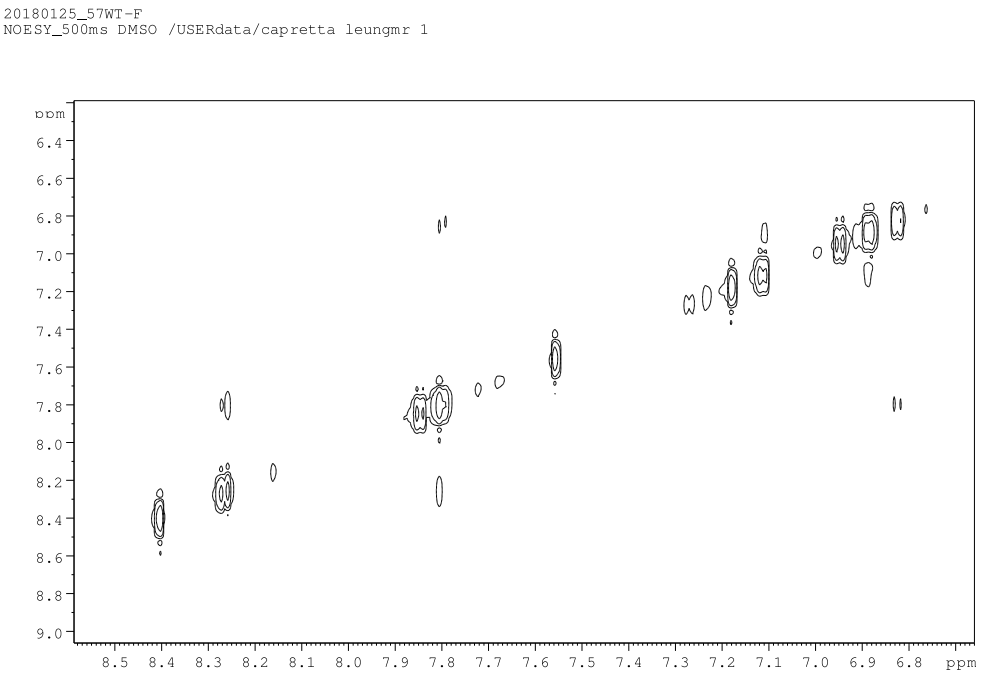

Figure S2-18. NOE of 3-(3,4-Dihydroxybenzylidene)-5-Carboxyindolin-2-one (**II-24**)

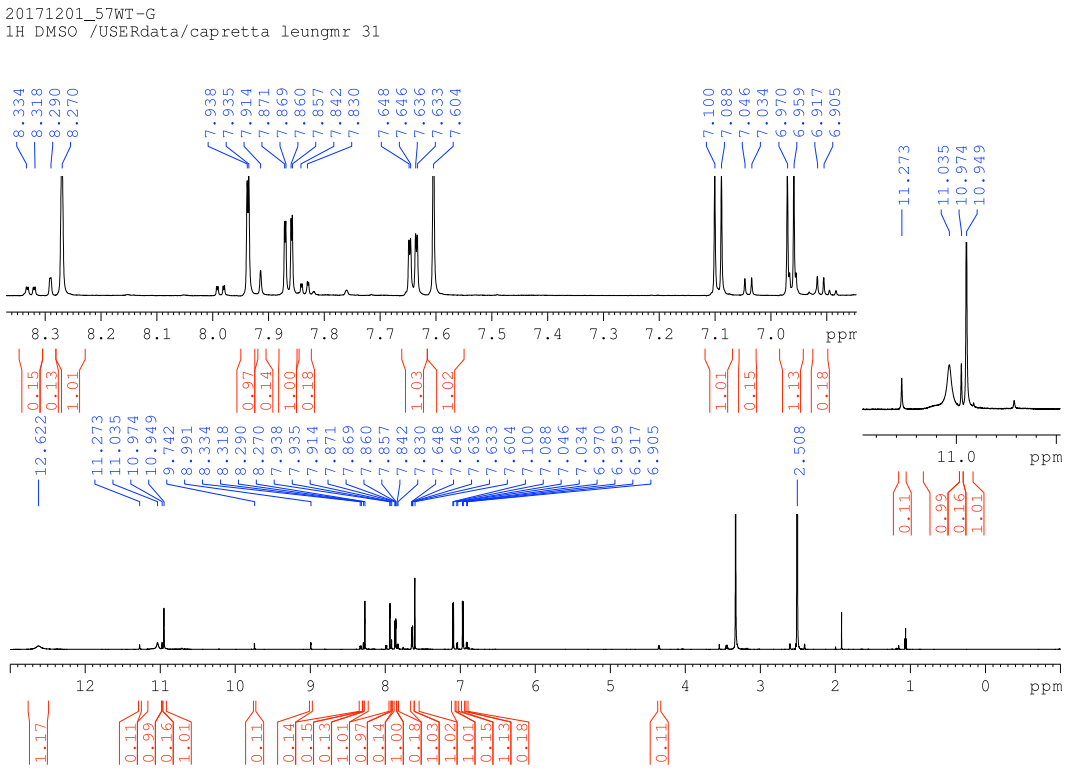

Figure S2-19. ^{1}H NMR of 3-(3-Bromo-4-Hydroxybenzylidene)-5-Carboxyindolin-2-one (**II-25**)

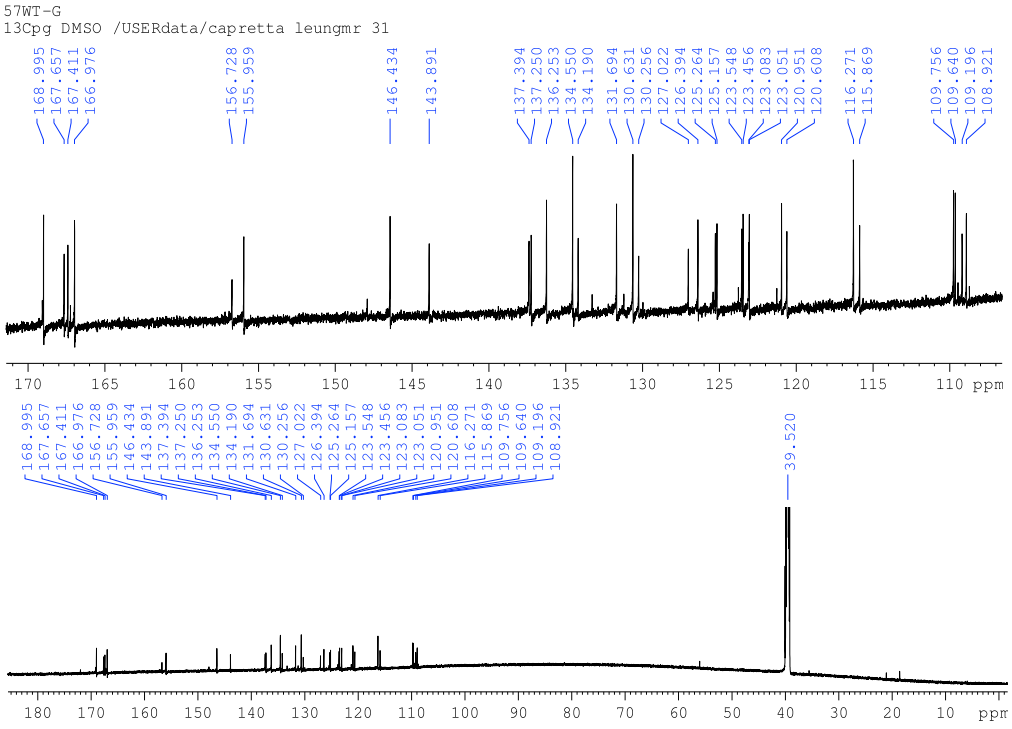

Figure S2-20. ^{13}C NMR of 3-(3-Bromo-4-Hydroxybenzylidene)-5-Carboxyindolin-2-one (**II-25**)

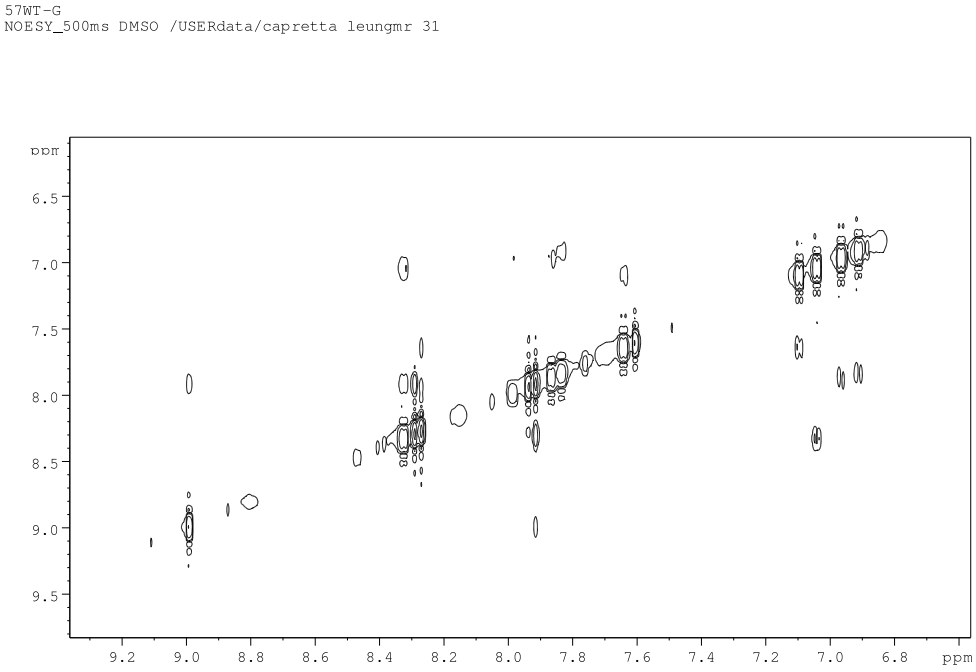

Figure S2-21. NOE of 3-(3-Bromo-4-Hydroxybenzylidene)-5-Carboxyindolin-2-one (**II-25**)

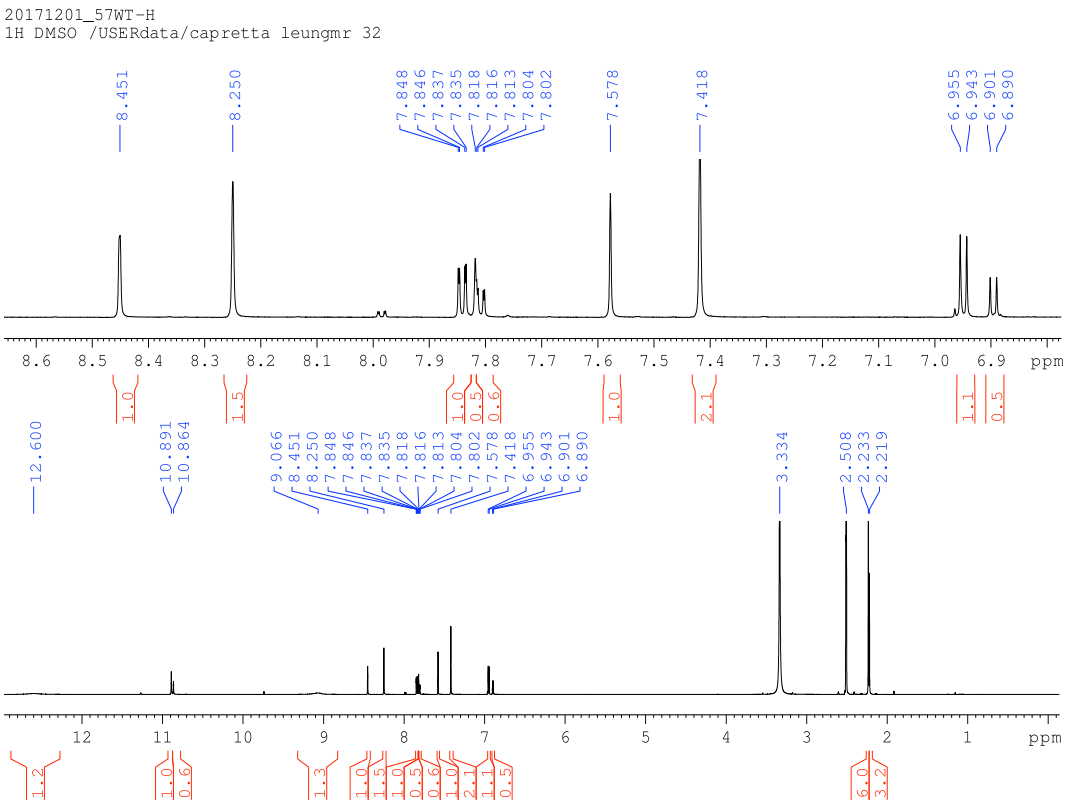

Figure S2-22. ^{1}H NMR of 3-(3,5-Dimethyl-4-Hydroxybenzylidene)-5-Carboxyindolin-2-one (**II-26**)

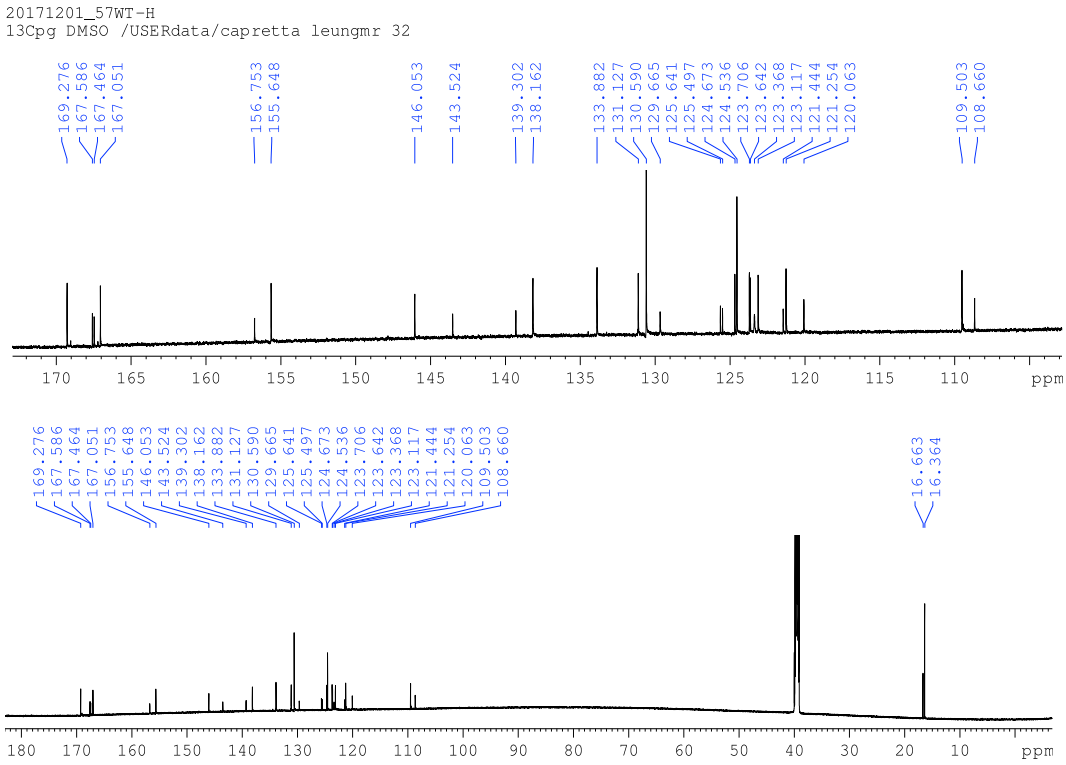

Figure S2-23. ^{13}C NMR of 3-(3,5-Dimethyl-4-Hydroxybenzylidene)-5-Carboxyindolin-2-one (**II-26**)

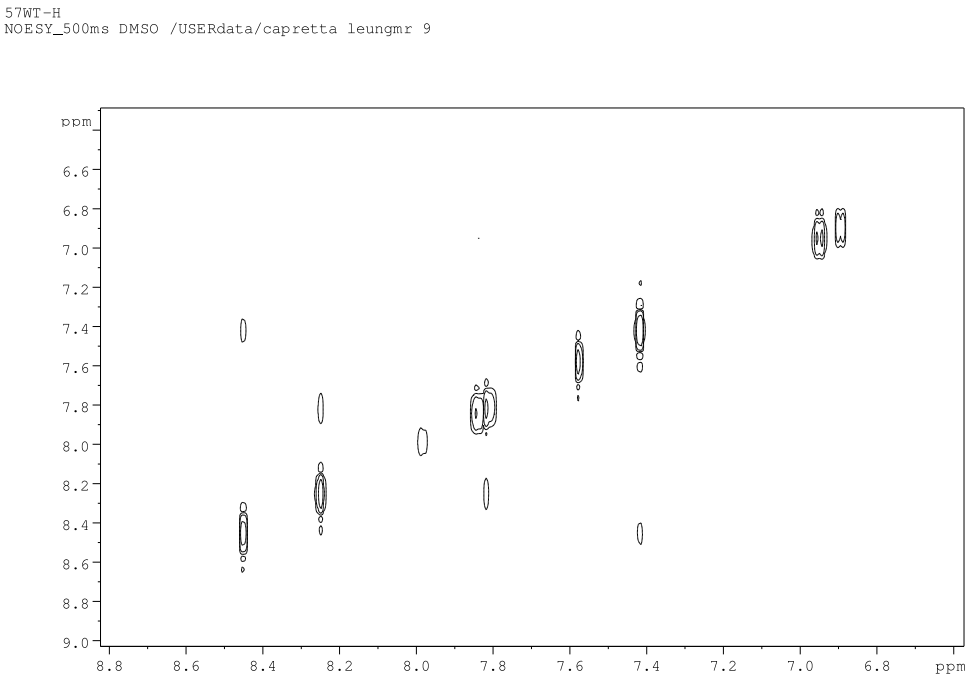

Figure S2-24. NOE of 3-(3,5-Dimethyl-4-Hydroxybenzylidene)-5-Carboxyindolin-2-one (**II-26**)

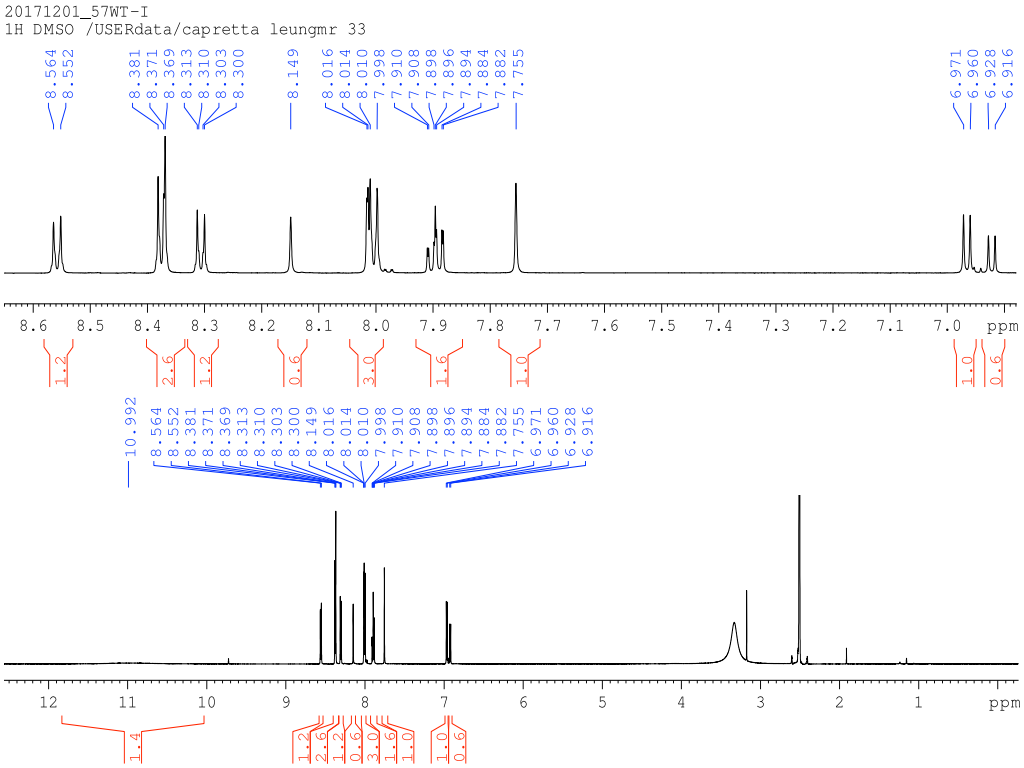

Figure S2-25. ^{1}H NMR of 3-(4-Nitrobenzylidene)-5-Carboxyindolin-2-one (**II-27**)

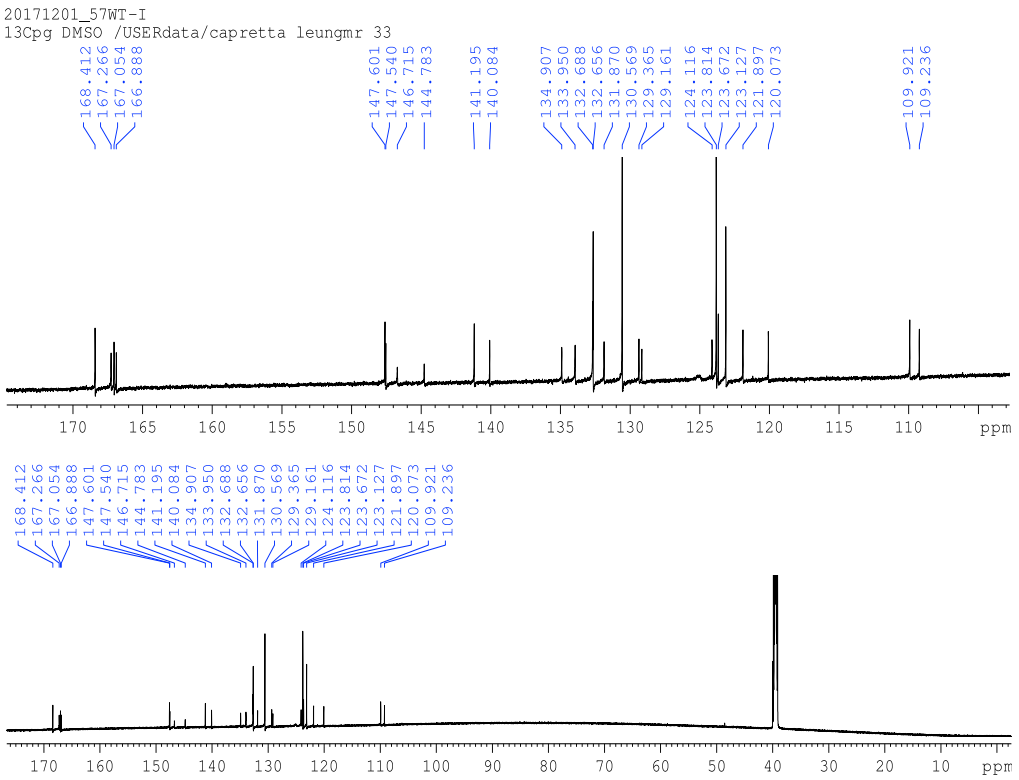

Figure S2-26. ^{13}C NMR of 3-(4-Nitrobenzylidene)-5-Carboxyindolin-2-one (**II-27**)

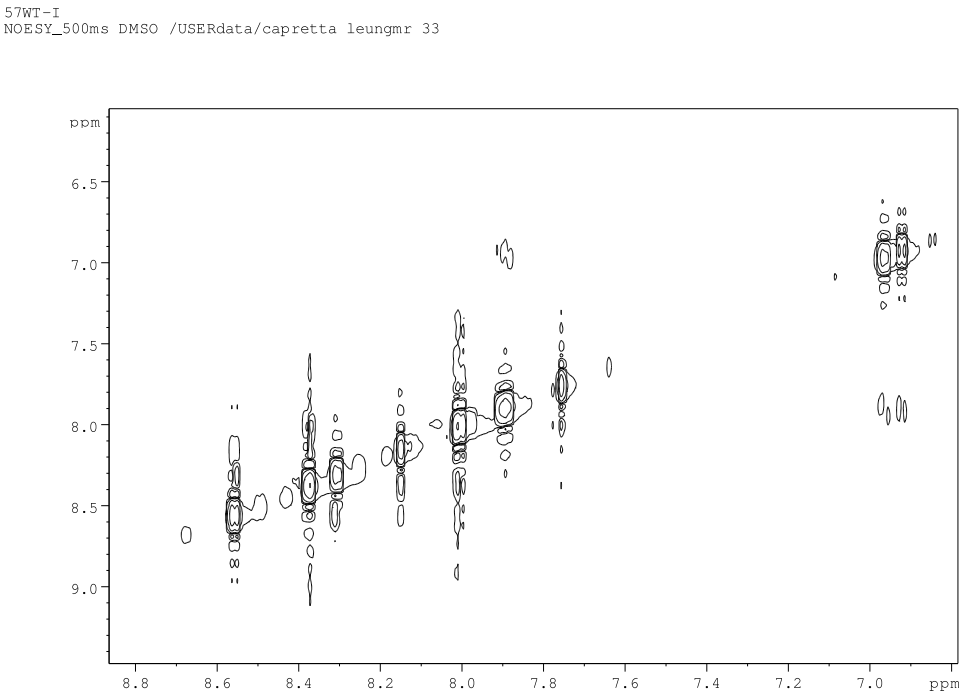

Figure S2-27. NOE of 3-(4-Nitrobenzylidene)-5-Carboxyindolin-2-one (**II-27**)

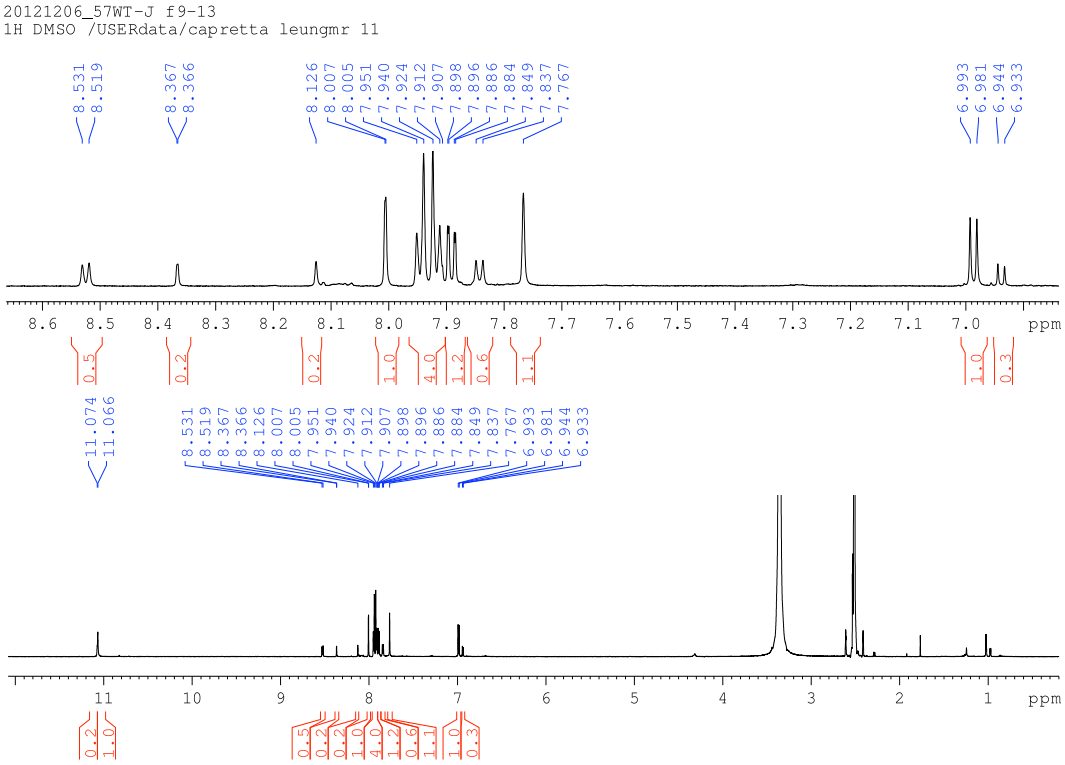

Figure S2-28. ^{1}H NMR of 3-[4-(Trifluoromethyl)benzylidene]-5-Carboxyindolin-2-one (**II-28**)

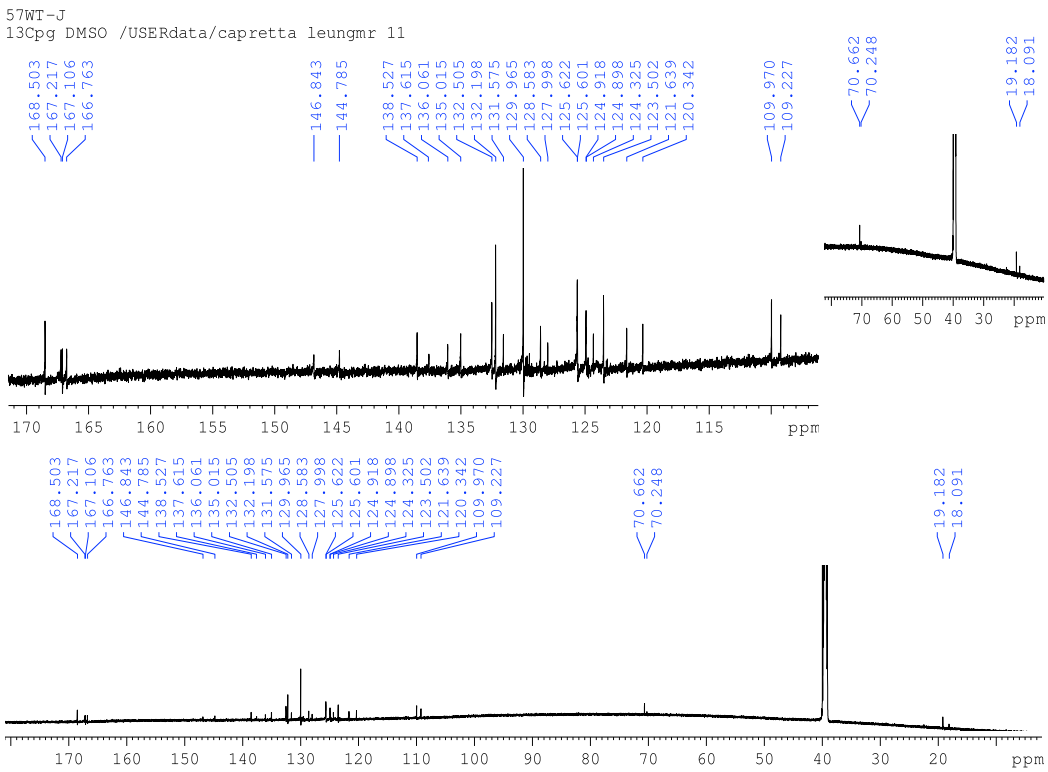

Figure S2-29. ^{13}C NMR of 3-[4-(Trifluoromethyl)benzylidene]-5-Carboxyindolin-2-one (**II-28**)

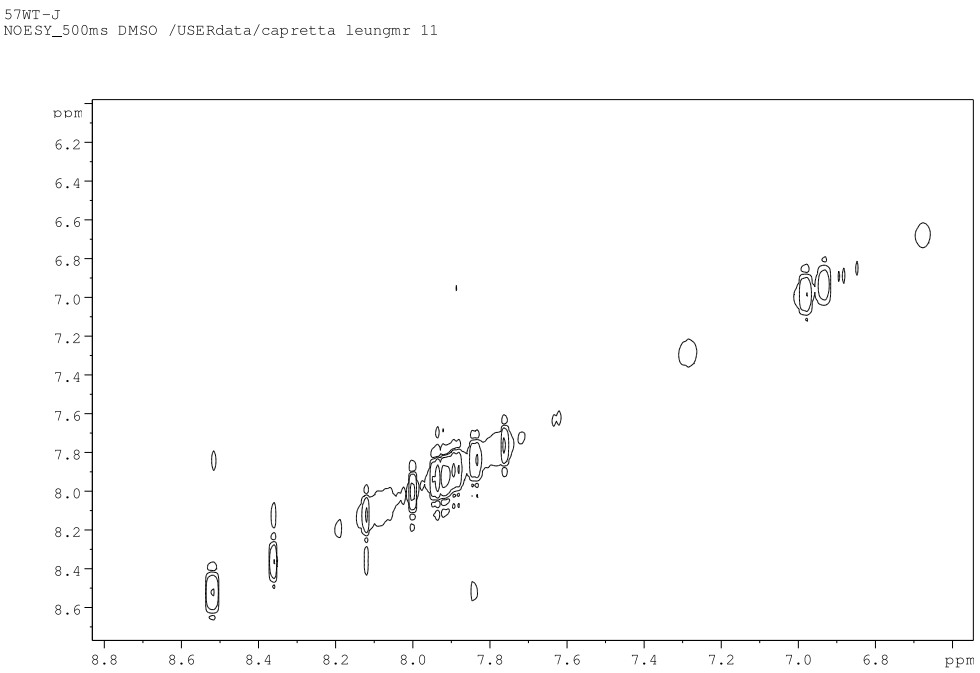

Figure S2-30. NOE of 3-[4-(Trifluoromethyl)benzylidene]-5-Carboxyindolin-2-one (**II-28**)

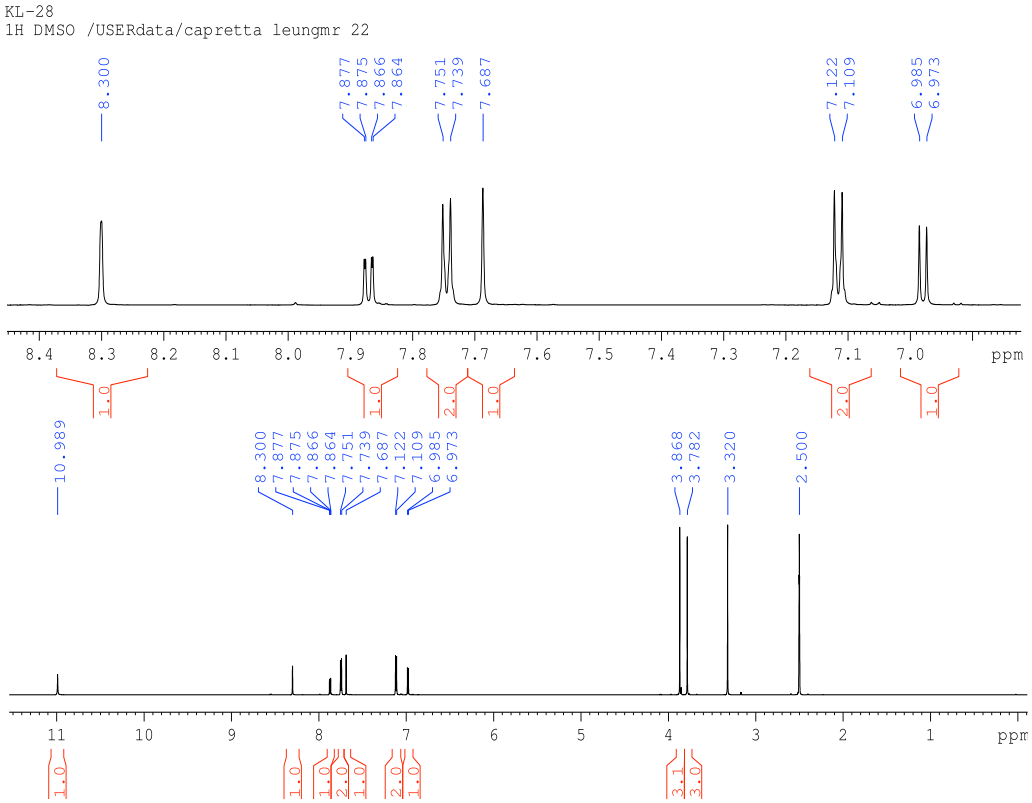

Figure S2-31. ^{1}H NMR of Methyl 3-(4-Methoxybenzylidene)-2-Oxoindoline-5-Carboxylate (**II-37**)

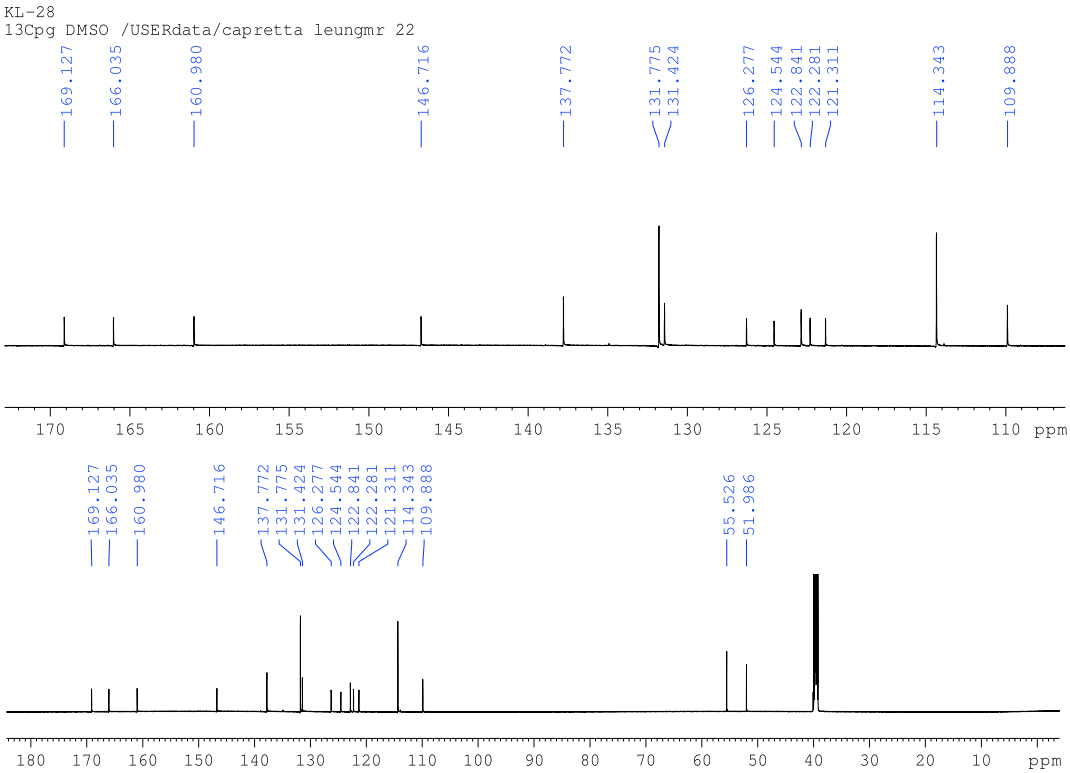

Figure S2-32. ^{13}C NMR of Methyl 3-(4-Methoxybenzylidene)-2-Oxoindoline-5-Carboxylate (**II-37**)

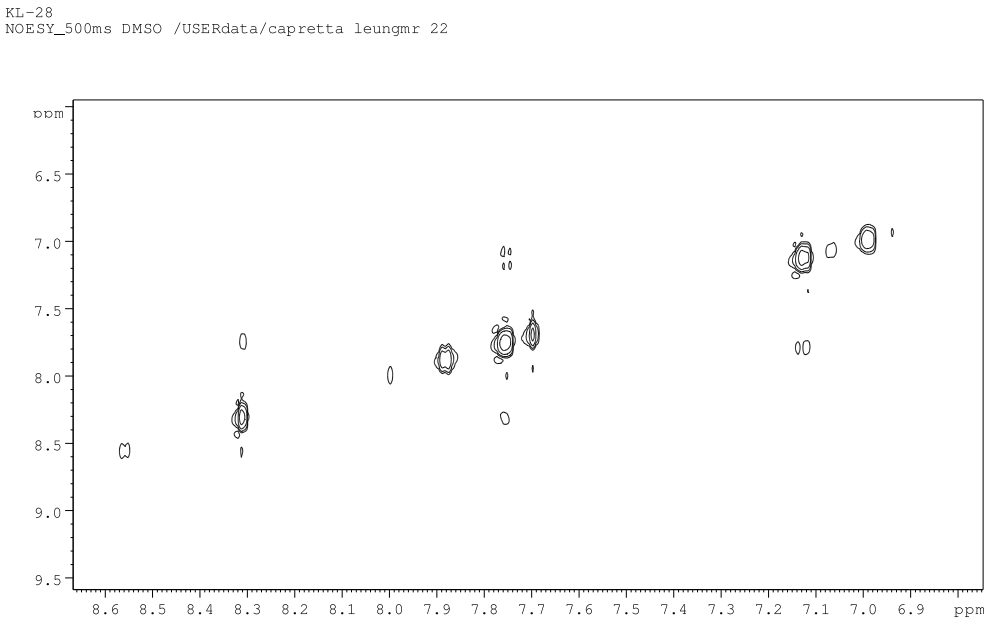

Figure S2-33. NOE of Methyl 3-(4-Methoxybenzylidene)-2-Oxoindoline-5-Carboxylate (**II-37**)

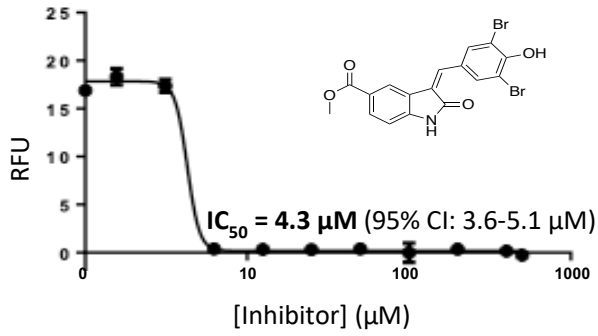

Figure S2-34. AAC(3)-Ia/**1** Concentration-Response Curve

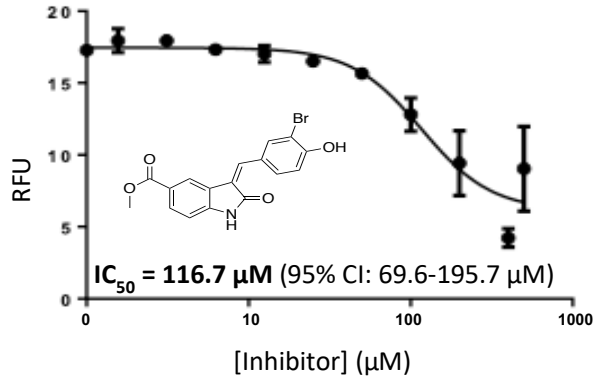

Figure S2-35. AAC(3)-Ia/**14** Concentration-Response Curve

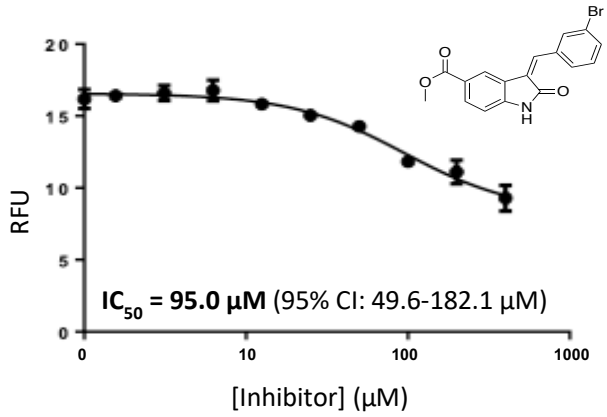

Figure S2-36. AAC(3)-Ia/**16** Concentration-Response Curve

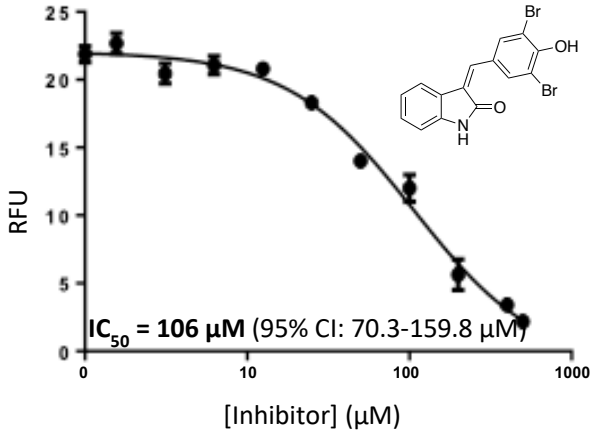

Figure S2-37. AAC(3)-Ia/**18** Concentration-Response Curve

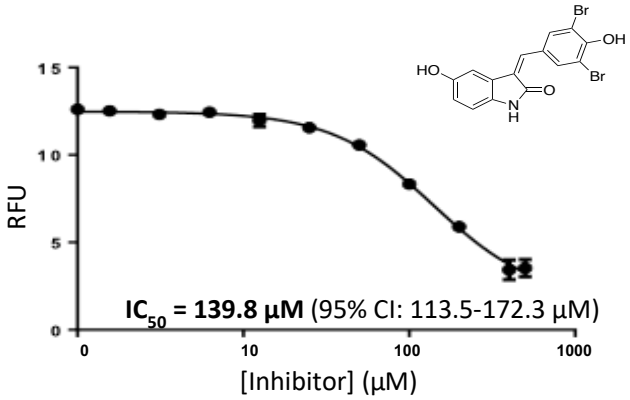

Figure S2-38. AAC(3)-Ia/**29** Concentration-Response Curve

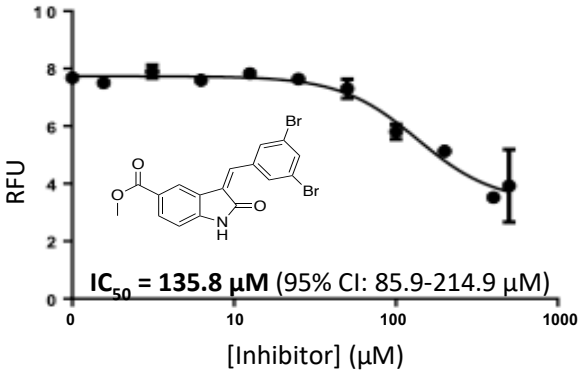

Figure S2-39. AAC(3)-Ia/**34** Concentration-Response Curve

3.0 Development and Structure-Activity Relationship Analysis of Biphenyl Isonicotinamides as Aminoglycoside 2”-O-Nucleotidyltransferase ANT(2”)-Ia Inhibitors

3.1 Background

Antibiotic resistance is a growing threat with severe social, political, and economic ramifications.[1,2] However, development of new antimicrobials has become an increasingly challenging area for the pharmaceutical sector, with scientific roadblocks, complex regulatory landscapes, and diminished investment returns.[3] As a result, strategies that minimize the inherent risk associated with drug campaigns have become very attractive, and efforts are being made to repurpose current compounds rather than reinventing the wheel.

The selective optimization of side activities (SOSA) method involves screening focused libraries of existing pharmaceuticals for “side effects” that confer activity against a new target; medicinal chemistry techniques are then used to optimize that desired activity and decrease activity against the previous target.[4] Since these compounds have been previously investigated as drug candidates, some data on human safety and pharmacologic properties already exists, streamlining the approval process and decreasing the likelihood that late-stage leads will have to be thrown out for toxicity issues.[4,5]

Another method that has been become increasingly popular in antibacterial circles is the use of adjuvants: compounds with minimal inherent antimicrobial activity themselves that enhance or restore the activity of other antibiotic drugs.[6] For example, β-lactamase inhibitors such as clavulinate have been used since 1981 to prevent inactivation of penicillin antibiotics from serine β-lactamases.[7,8] In addition to extending the life of already-approved drugs, as adjuvants generally do not target essential pathways, resistance to them develops at a much slower rate.[5,6,9,10]

Aminoglycosides are a class of antibiotics used to treat serious Gram-negative infections.[11–13] Resistance most commonly arises through actions of aminoglycoside-modifying enzymes (AMEs), which catalyze the addition of a chemical adduct, thereby blocking access to its binding side.[14] Aminoglycoside 2”-*O*-nucleotidyltransferase ANT (2”), is one such enzyme, transferring an adenine-phosphate group from ANT to the 2”-hydroxyl (Figure 3-1).[15] It is hypothesized

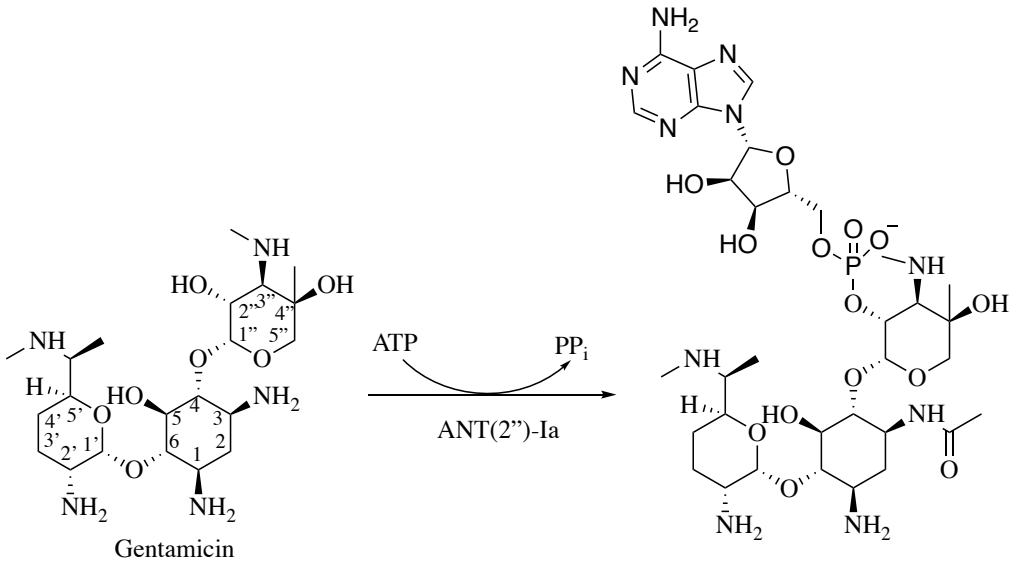

Figure 3-1. Mechanism of Gentamicin Inactivation by ANT(2”)-Ia

that inhibiting ANT (2") will suppress resistance, restoring the efficacy of this drug class.

Previous *in vivo* screening of two protein kinase libraries[16,17] provided by GlaxoKlineSmith identified two compounds (compounds **III-1** and **III-2**, Figure 3-2) with a N-[(1,1-biphenyl)-3-yl]-pyridine-4-carboxamide core as inhibitors of ANT (2")-Ia.[18] These compounds were initially investigated as p38 MAP kinase inhibitors for rheumatoid arthritis, but are thought to similarly inhibit other nucleotide-binding enzymes through the ATP-binding pocket.[18–26]

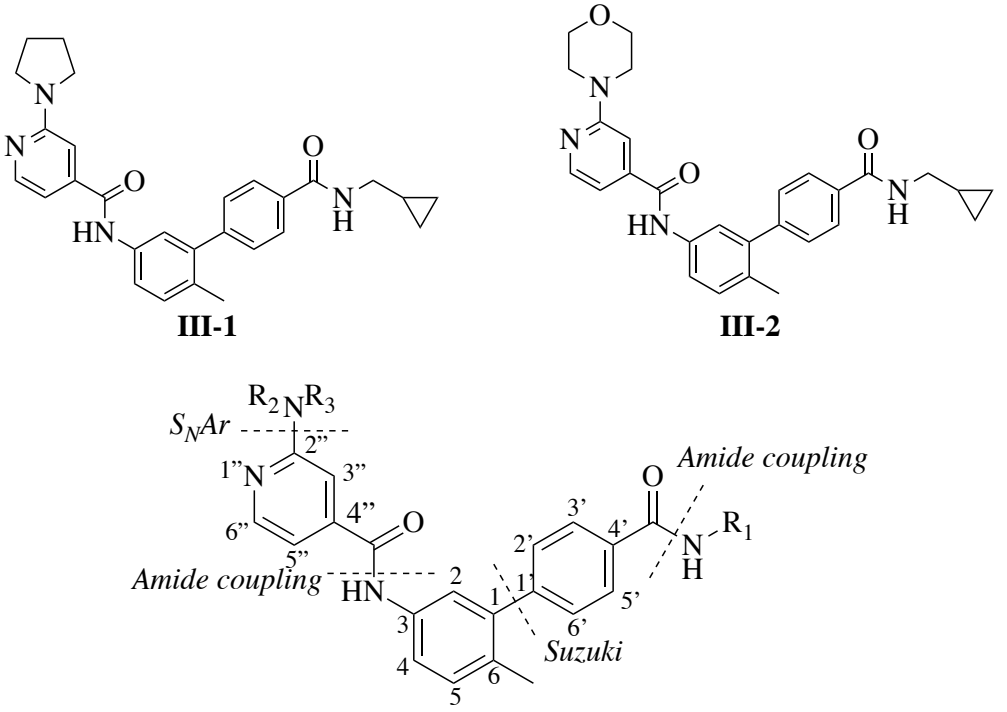

Figure 3-2. Hits from Cell-Based ANT(2")-Ia Screen with the Common Biphenyl Isonicotinamide Scaffold. Retrosynthetic deconstruction is shown

This chapter describes the development of streamlined parallel synthetic approach that allows for functionalization of the biphenyl isonicotinamide scaffold and preliminary structure-activity relationship against ANT(2")-Ia.

3.2 PARALLEL SYNTHESIS METHODOLOGY

The two hits from the ANT(2")-Ia cell-based screen both contain a 6-methyl-(1,1')-biphenyl core, decorated on the Eastern side (position 4') with a methylcyclopropylamide, and coupled on the Western side to isonicotinic acid (4-pyridine-carboxylic acid) through an amide linkage. Variation is introduced at position 2" through a nucleophilic aromatic substitution (S_NAr). Our initial synthetic strategy (Figure 3-3) focused on building a core biphenyl isonicotinamde scaffold, which could be functionalized on either end. The 5'-amino-2'-methyl-[1,1'-biphenyl]-4-carboxylic core would be formed by a Suzuki coupling, followed by an acyl chloride coupling to install the isonicotinamide (pyridine-4-carboxamide) moiety. Lewis acid-catalyzed transacylation with various amines would allow variation to be introduced at the Eastern end, and a nucleophilic aromatic substitution would do likewise on the Western side.

Suzuki reactions are palladium-catalyzed cross-coupling reactions between organohalides and boronic acids. The mechanism is shown in Figure 3-4. The first step is oxidative addition, where the Pd(0) catalyst with its coordinated ligands donate electron density into the σ* molecular orbital of the aryl halide. The carbon-halide bond is cleaved and the catalyst is oxidized to Pd(II). Electron-withdrawing

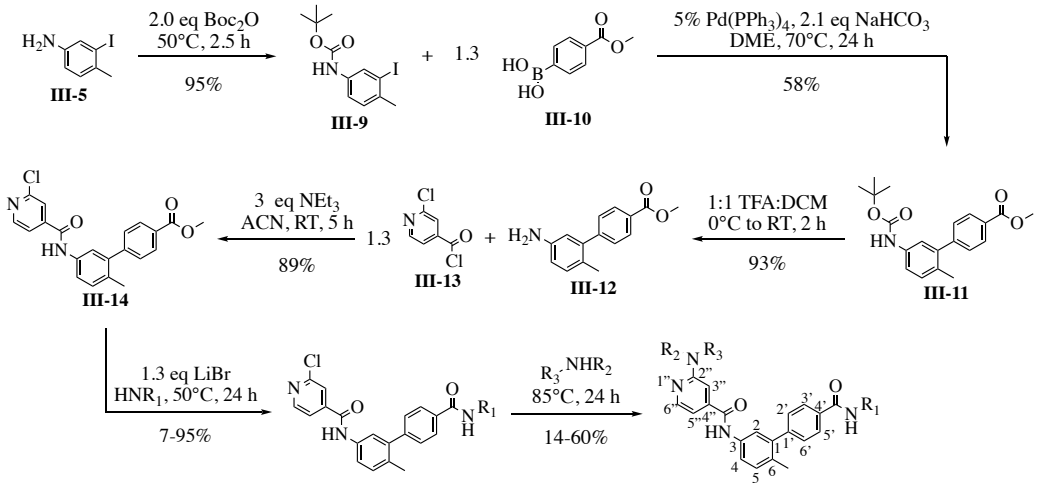

Figure 3-3. Initial Parallel Synthetic Route

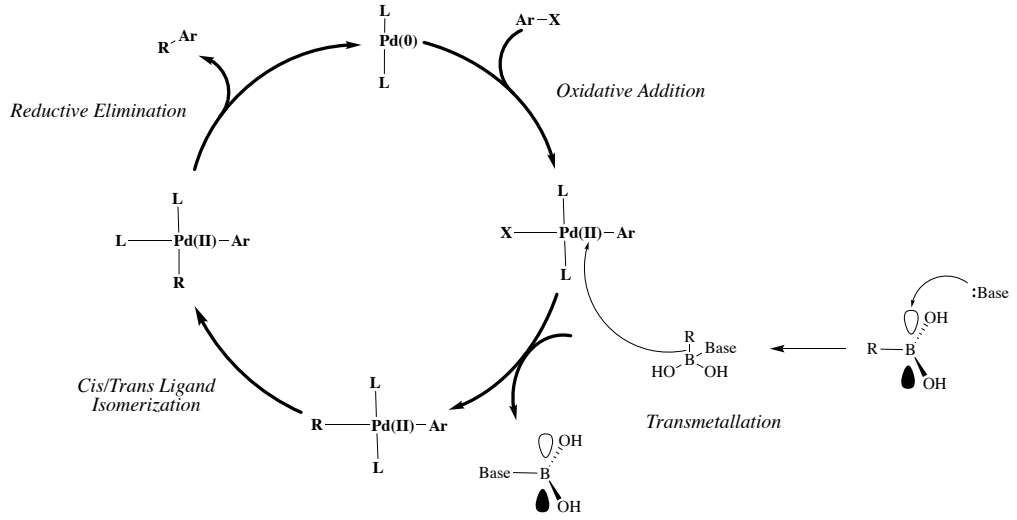

Figure 3-4. Suzuki Mechanism

groups on the aryl halide aid in this step by destabilizing the σ bond and therefore lowering the energy of the σ* orbital. Next, the boronic acid is activated by base, which donates electrons into boron's empty p orbital to complete its octet. Boron is a group 3 metal, stable with six electrons; it therefore ejects the "R" group in the

above scheme, which displaces the halide from palladium during transmetallation. Electron-donating groups will increase this process. There is rearrangement of ligands around the palladium core, then the coupled product is released and the catalyst returns to its Pd(0) state. Boronic esters can also be used, and are more stable to oxygen due to electron density from their alkyl chains, but therefore less reactive.[27]

There were two possible sets of commercially-available coupling partners that could be used for the purposes of this synthesis: 5-amino-2-methylphenylboronic acid pinacol ester (**III-3**) and 4-iodobenzoic acid (**III-4**), or 3-iodo-4-methylaniline (**III-5**) and 4-carboxyphenylboronic acid (**III-6**) (Figure 3-5). It was expected that 5-amino-2-methylphenylboronic acid pinacol ester and 4-iodobenzoic acid would work better, as amino groups are electron-donating and carboxylic acids are withdrawing. However, upon extensive optimization of reaction conditions (Table 3-1), it was found that the iodoaniline and 4-carboxyphenylboronic acid pairing was in fact superior. Various ligands were also

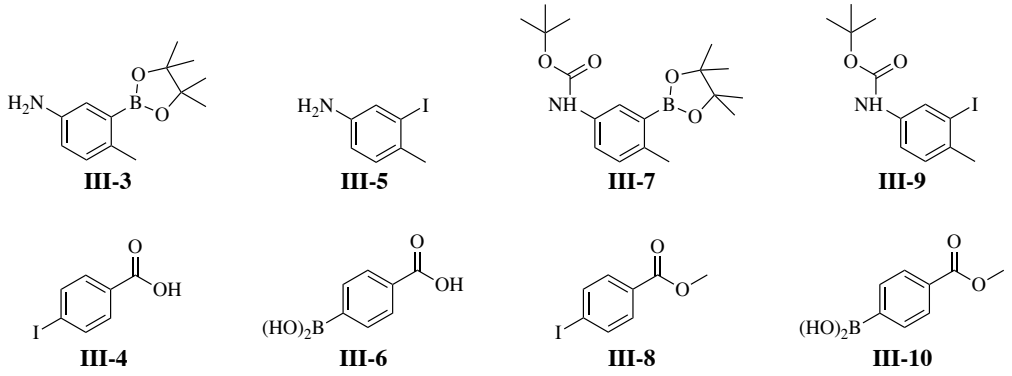

Figure 3-5. Possible Suzuki Coupling Partners

sampled, including Buchwald ligand ^{t}BuXPhos and 2,4-dimethoxyphenyl phosphaadamantane (PAPh(OMe)$_2$, Figure 3-6) but results were not superior to those obtained with the standard triphenylphosphine (PPh_3) ligand. Poisoning of the catalyst was also a concern due to heteroatom functional groups present on the coupling partners. Thus, the amine was protected with a *tert*-butoxycarbonyl (Boc) group (compound **III-9**) and coupled with commercially-available 4-methoxyphenylboronic acid (**III-10**) using tetrakistriphenylphosphine palladium (0) as the catalyst and sodium bicarbonate as the base to yield methyl 5'-{[(*tert*-butoxy)carbonyl]amino}-2'-methyl-1,1'-biphenyl-4-carboxylate (**III-11**).[28] The Boc protecting group was removed with trifluoroacetic acid, and the resulting amine **III-12** reacted with commercially-available chloropyridinyl-4-carbonyl chloride (**III-13**) to form the amide (**III-14**) in a protocol modified from Angell *et al*.[22,24,25]

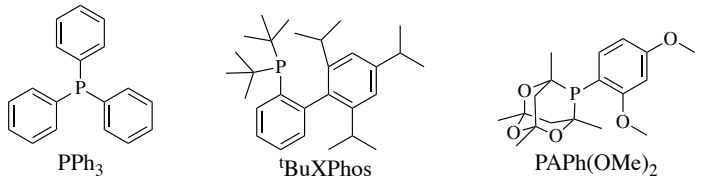

Figure 3-6. Suzuki Ligand Structures

The isonicotinamide biphenyl scaffold **III-14** has two functionalities susceptible to amine attack: an acyl chloride-like imine on the Western end and a methyl ester-protected carboxylic acid on the Eastern, and so careful consideration reaction order and conditions were needed to control product formation. While work could simultaneously proceed on both ends of the molecule, it was soon apparent that the Eastern carbonyl was much more reactive than the Western imine, and so this amide bond was formed first.

Table 3-1. Suzuki Coupling Conditions Screened

Halo-alkane	Boronic acid	Catalyst	Base	Solvent	Reaction Conditions	Yield (%)	Ref.
III-5	**III-6**	10% $Pd(OAc)_2$, 20% tBuXPhos	K_3PO_4	2:1 EtOH:H_2O	100°C, 24 h	10	29
III-4	**III-7**	10% $Pd(OAc)_2$, 20% tBuXPhos	K_3PO_4	2:1 EtOH:H_2O	100°C, 24 h	6	29
III-9	**III-6**	10% $Pd(OAc)_2$, 20% tBuXPhos	K_3PO_4	2:1 EtOH:H_2O	100°C, 24 h	28	29
III-4	**III-7**	10% $Pd(OAc)_2$, 20% tBuXPhos	K_3PO_4	2:1 EtOH:H_2O	100°C, 24 h	20	29
III-8	**III-7**	10% $Pd(OAc)_2$, 20% tBuXPhos	K_3PO_4	2:1 EtOH:H_2O	100°C, 24 h	18	29
III-5	**III-10**	10% $Pd(OAc)_2$, 20% tBuXPhos	K_3PO_4	2:1 EtOH:H_2O	100°C, 24 h	9	29
III-9	**III-10**	1% Pd_2dba_3, 2% $PAPh(OMe)_2$	Cs_2CO_3	Toluene	70°C, 24 h	35	30
III-9	**III-10**	1% $Pd[PAPh(OMe)_2]_2$	Cs_2CO_3	Toluene	70°C, 24 h	46	31
III-9	**III-10**	2 x 1% $Pd[PAPh(OMe)_2]_2$	Cs_2CO_3	Toluene	70°C, 24 h	16	31
III-9	**III-10**	2 x {0.5% Pd_2dba_3, 1% $PAPh(OMe)_2$}	Cs_2CO_3	Toluene	70°C, 24 h	33	30
III-9	**III-10**	1% Pd_2dba_3, 2% $PAPh(OMe)_2$	Cs_2CO_3	Toluene	70°C, 30 min μW	19	30
III-9	**III-10**	1% $Pd[PAPh(OMe)_2]_2$	Cs_2CO_3	Toluene	70°C, 30 min μW	7	31
III-9	**III-10**	1% $Pd[PAPh(OMe)_2]_2$	Cs_2CO_3	Toluene	100°C, 24 h	36	31
III-9	**III-10**	5% $Pd(PPh_3)_4$	$NaHCO_3$	5:1 DME:H_2O	70°C, 24 h	58	28
III-9	**III-10**	10% $Pd[PAPh(OMe)_2]_2$	Cs_2CO_3	Toluene	70°C, 24 h	27	31

The Eastern amide bond was readily installed using a variety of methods: the amide could be formed directly from the methyl ester *via* lithium bromide-catalyzed transacylation (modified from Abaee *et al*.[32], Figure 3-3), or from the deprotected carboxylic acid *via* thionyl chloride activation or coupling agents. The lithium bromide-catalyzed transacylation had the benefit of being a single-step reaction, but was limited to inexpensive, readily-available, and liquid amines, and

removal of excess amine afterwards was difficult. Furthermore, this method was not well-adapted for parallel synthesis as it was discovered that the nucleophilic aromatic substitution (S_NAr) on the Western side of the molecule was prevented by a methyl ester. Thus, it was decided to cleave the methyl ester and couple the resulting carboxylic acid.

Cleavage of the methyl ester proceeded rapidly under based-catalyzed conditions, usually reaching completion in under an hour (Figure 3-7A).[21,25] 5'-(2-Chloropyridine-4-amido)-2'-methyl-[1,1'-biphenyl]-4-carboxylic acid (**III-15**) had improved phase separation relative to the Boc-protected biphenyl (**III-16**), but the amide bond was susceptible to cleavage with longer reaction times. Serendipitously, it was noted that the unprotected 5'-amino-2'-methyl-[1,1'-biphenyl]-4-carboxylic acid (**III-17**) precipitated upon neutralization, allowing for isolation of pure product following vacuum filtration without need for further workup. Furthermore, the two deprotection steps could be performed consecutively, obviating the neutralization and extraction steps following the Boc cleavage, to give the desired product in 89% yield for two steps (Figure 3-7B).

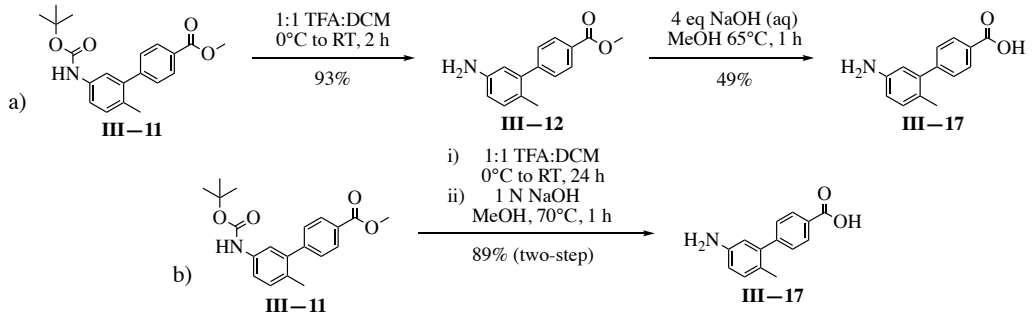

Figure 3-7. Formation of 5'-Amino-2'-Methyl-[1,1'-Biphenyl]-4-Carboxylic Acid (**III-17**) *via* a) sequential and b) one-pot TFA-catalyzed Boc and base-catalyzed methyl ester deprotections

Thus **III-17** became the new core scaffold, as it could be easily produced in gram quantities.

Following methyl ester hydrolysis, various coupling agents were investigated for use in forming the amide bond. The HATU/HBTU combination used by Angell *et al*.[25] (Figure 3-8) worked well, but purification was problematic for some compounds, particularly **III-18** and **III-19**. Thionyl chloride and dimethylformamide could be used to activate the carboxylic acid to an acid chloride through *in situ* formation of a Vilsmeier salt (Figure 3-9), thereby circumventing the purification issues in troublesome compounds, but toxicity and water-susceptibility made this method unwieldy.[20] Attempts to use the Vilsmeier salt as a substitute chlorinating agent were unsuccessful. EDC was finally identified as a

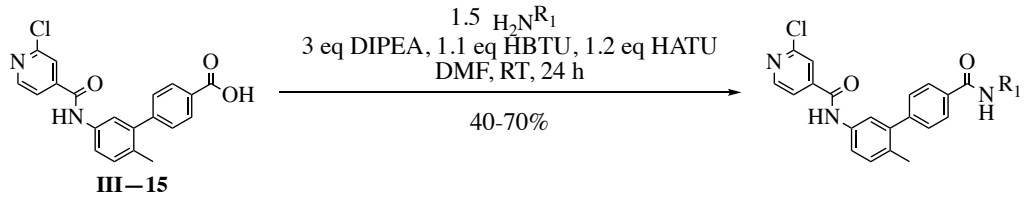

Figure 3-8. HATU/HBTU Coupling Combination from Angell *et al*.[25]

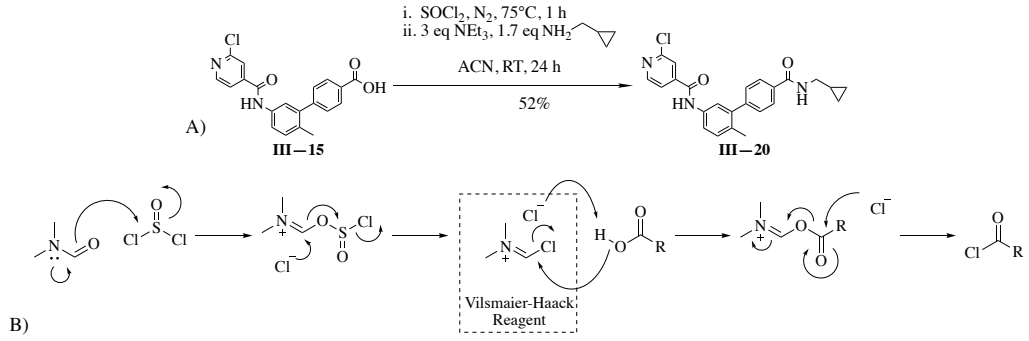

Figure 3-9. A) Sample Amide Coupling *via* Thionyl Chloride Activation and B) Reaction Mechanism with *In Situ* Vilsmeier-Haack Reagent Formation

suitable coupling agent, striking a balance between activity and ease of purification (Figure 3-10).

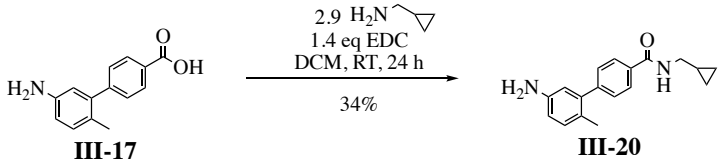

Figure 3-10. Sample Amide Coupling Using EDC

As previously mentioned, the 2-chloropyridine on the Western end was much more stable to substitution. This was surprising, as the chloro-imine functionality was expected to have reactivity similar to an acid chloride. However, yields were poor, even with the extremely harsh conditions required (microwave reflux in neat amine for several hours), and removal of excess amine was difficult. Several key compounds could not be synthesized, including initial hit **III-2** and any compounds containing the methyl ester functionality (for example **III-21** and **III-22**). While pyrrolide-containing **III-1** and its analog **III-23** could be obtained, such substantial product loss and the requirement for individualized purification protocols at the final step of a multistep synthesis was not viable for library generation. Consequently, the synthetic protocol was revised to that shown in Figure 3-11, where the limiting S_NAr step is moved to a separate arm of the synthesis. This change also allowed for coupling with commercially-available aromatic acids, thereby greatly increasing the amount of variation generated.

Nucleophilic aromatic substitution on 2-chloropyridine-4-carboxylic acid (**III-24**) proceeded rapidly in N-propylamine, typically not requiring further purification. The 2-morpholin-4-yl-pyridine-4-carboxylic acid (**III-25**) required for **III-2** was more challenging. The reaction was pushed to completion after 6 h

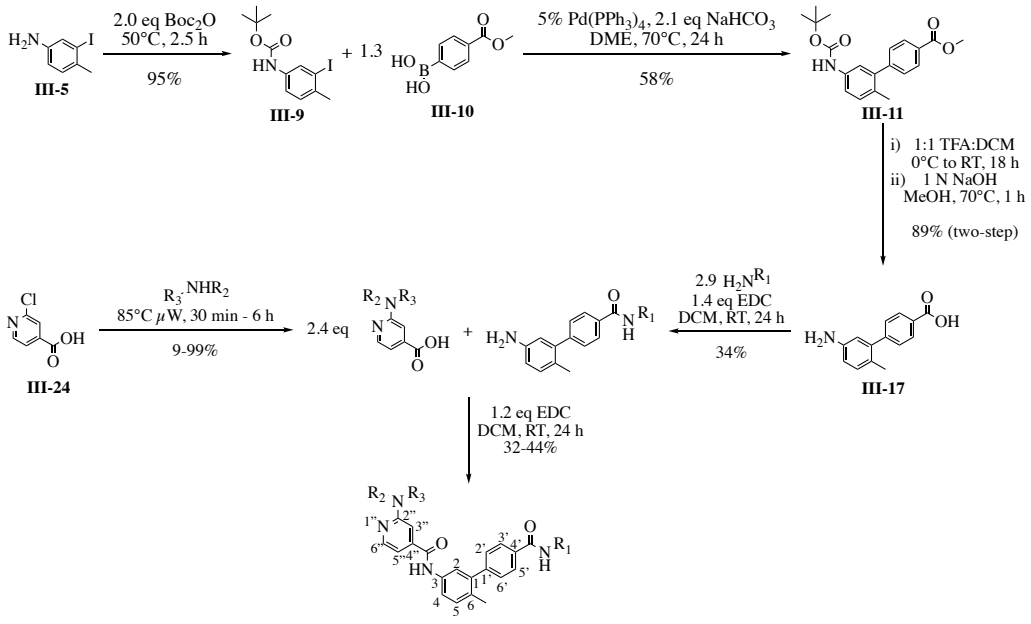

Figure 3-11. Revised Parallel Synthesis Strategy

in the microwave, but removal of morpholine was problematic. The product was too polar for extraction and automated column chromatography system purification was not sufficient. A review of the literature suggested that refluxing ethyl acetate would dissolve morpholine and allow product collection by filtration.[33] When this method was tried, however, it was discovered that the filtered crystals were in fact the morpholine salt and the filtrate contained the desired product. These conditions were reproduced by adding saturated ammonium chloride to the crude reaction mixture, lyophilizing it to an off-white powder, and refluxing it in ethyl acetate. The filtrate could then be purified by an automated column chromatography system to yield the pure product (Figure 3-12).

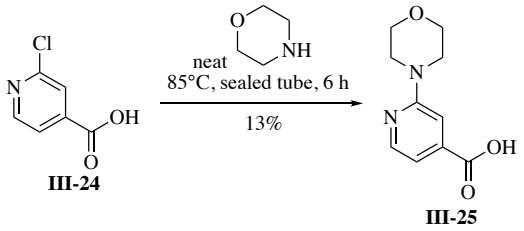

Figure 3-12. S_NAr Reaction of Isonicotinic Acid in Morpholine

The resulting substituted isonicotinic acid could then be coupled to the 5'-amino-2'-methyl-[1,1'-biphenyl]-4-carboxylic acid scaffold. Various coupling conditions were screened (HATU, PyBop, Vilsmaier salt, thionyl chloride, and EDC), and EDC was selected for its coupling effectiveness and ease of purification.

With this synthetic methodology in hand, a small library of 19 compounds was assembled (Figure 3-13), including re-syntheses of initial hits **III-1** and **III-2** and various analogs with which to investigate structure-activity relationships. Compounds **III-18** and **III-29** are analogs of the initial hits with a chlorine or hydrogen atom respectively at position 2" instead of a S_NAr substituent. Compound **III-23** is an analog of initial hit **III-1** with a carboxylic acid in place of the methylcyclopropamide. Compounds **III-21**, **III-29**, and **III-30** can be directly compared to further investigate the effect of the Eastern substituent, as can **III-14**, **III-15**, **III-18**, **III-19**, **III-27**, and **III-28**. Compound **III-22** is similar to **III-21**, but with phenyl instead of pyridine ring, testing the effect of the aromatic heterocycle. Compounds **III-12**, **III-17**, and **III-20** similarly test the essentiality of the isonicotinamide, paring down the Western end to the core biphenyl motif, and can be compared against each other to determine the effect of the Eastern substituent.

3.3 Structure-Activity Relationship Analysis

The inhibitor library was screened for activity against *E. coli* BW25113 Δ*tolC* Δ*bamB* pGDP4:*ant(2")-Ia* (Figure 3-14). Compounds were tested at a final

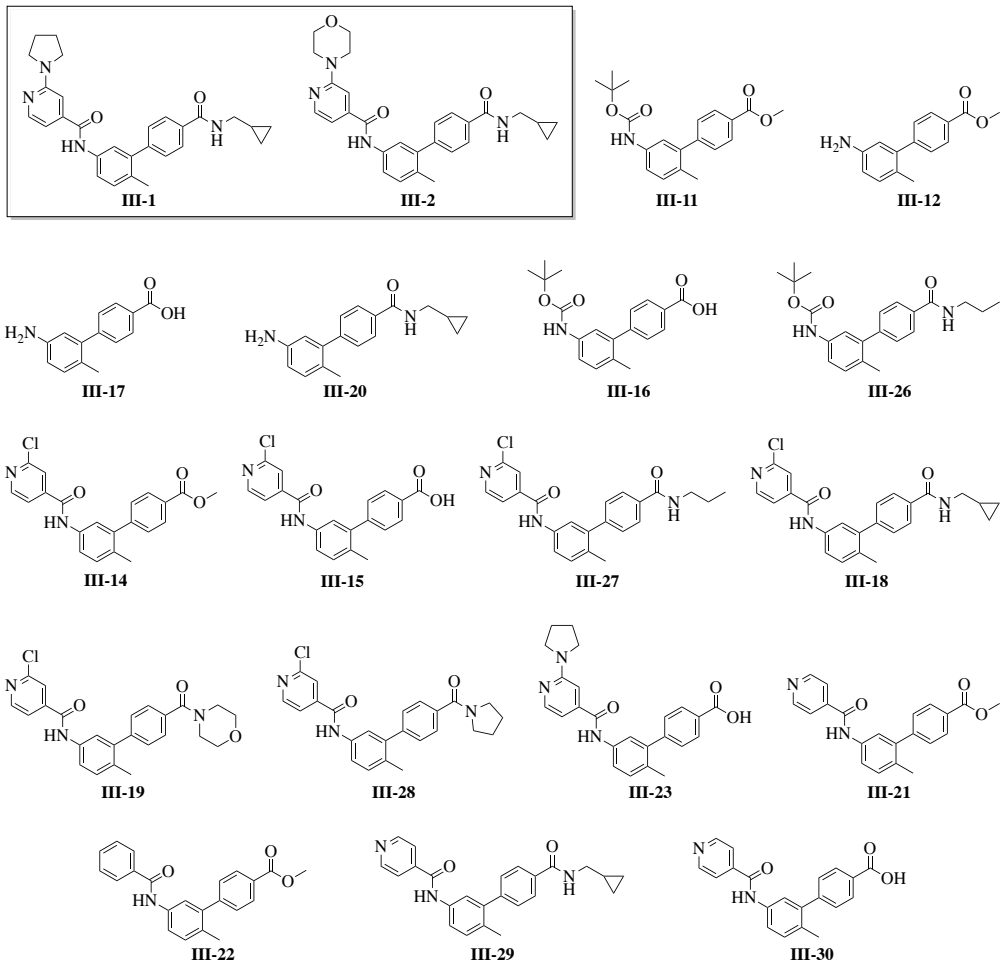

Figure 3-13. ANT(2")-Ia Inhibitor Library. Initial hits are boxed

concentration of 50 μM in the presence of a sub-inhibitory concentration of gentamicin (¼ MIC = 4 μg/mL), and growth was measured by absorbance at 600 nm after 18 h incubation at 37°C. β-Thujaplicinol was used as a positive control.[34] Percent growth was calculated using matched parent-strain controls, and compounds with the highest relative inhibition were followed up with specificity and dose-dependency studies. Re-synthesis of **III-1** showed about 25% inhibition. Re-synthesis of **III-2** did not show inhibition against the resistant strain, though

previous results have noted variable response. Several compounds showed improved activity against ANT (2") at 50 μM, most notably **III-16** (66%), **III-14** (87%), **III-21** (100%), **III-22** (55%), and **III-30** (95%). Compound **III-29** showed inhibition similar to the initial hit **III-1**. These results indicate that the N-cyclopropylmethylamide is not essential for activity, and indeed has a detrimental effect. The methyl ester and carboxylic acid show similar activity at this position. On the Western end, substitution at 2" position has a similarly nonessential/negative effect. A chlorine atom (**III-14**) is tolerated, perhaps because of *in situ* removal. The isonicotinamide moiety appears to have the greatest activity; any modification results in a loss of activity, particularly when the hydrophobic functionality is removed.

Compound	% Inhibition
B-thuj	101%
III-1	25%
III-11	36%
III-12	15%
III-14	87%
III-15	38%
III-16	66%
III-17	8%
III-18	26%
III-19	7%
III-2	5%
III-20	13%
III-21	100%
III-22	55%
III-23	21%
III-26	36%
III-27	4%
III-28	16%
III-29	26%
III-30	95%

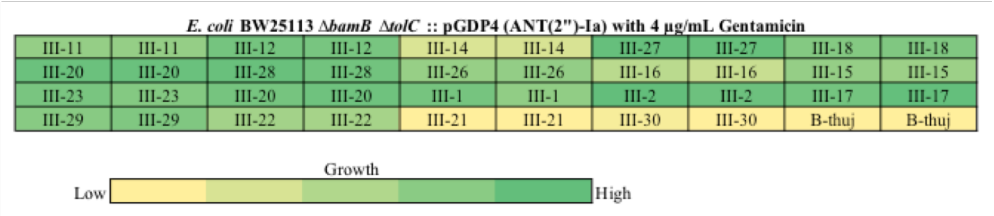

Figure 3-14. *E. coli* BW25113 Δ*tolC*Δ*bamB* pGDP:*ant(2")-Ia* Screening Results

The majority of the compounds in the inhibitor library showed equivalent or greater nonspecific inhibition of the parent strain *E. coli* BW25113 Δ*tolC* Δ*bamB* in the absence of gentamicin (Figure 3-15). Compound **III-21** showed complete inhibition at 50 μM, as did β-thujaplicinol. Interestingly, **III-30** showed only

partial inhibition (56%), indicating some selectivity. Follow-up MICs were performed on **III-1**, **III-16**, **III-14**, **III-18**, **III-21**, and **III-30** to test for any intrinsic antibiotic activity. Compounds **III-16** and **III-21** had MICs of 128 and 16 µg/mL respectively. Compounds **III-18**, **III-1**, and **III-30** showed dose-dependence, but did not show complete inhibition of cell growth at 128 µg/mL. Compounds **III-14** also showed dose-dependence, but to a maximum of 85% inhibition at 8 µg/mL.

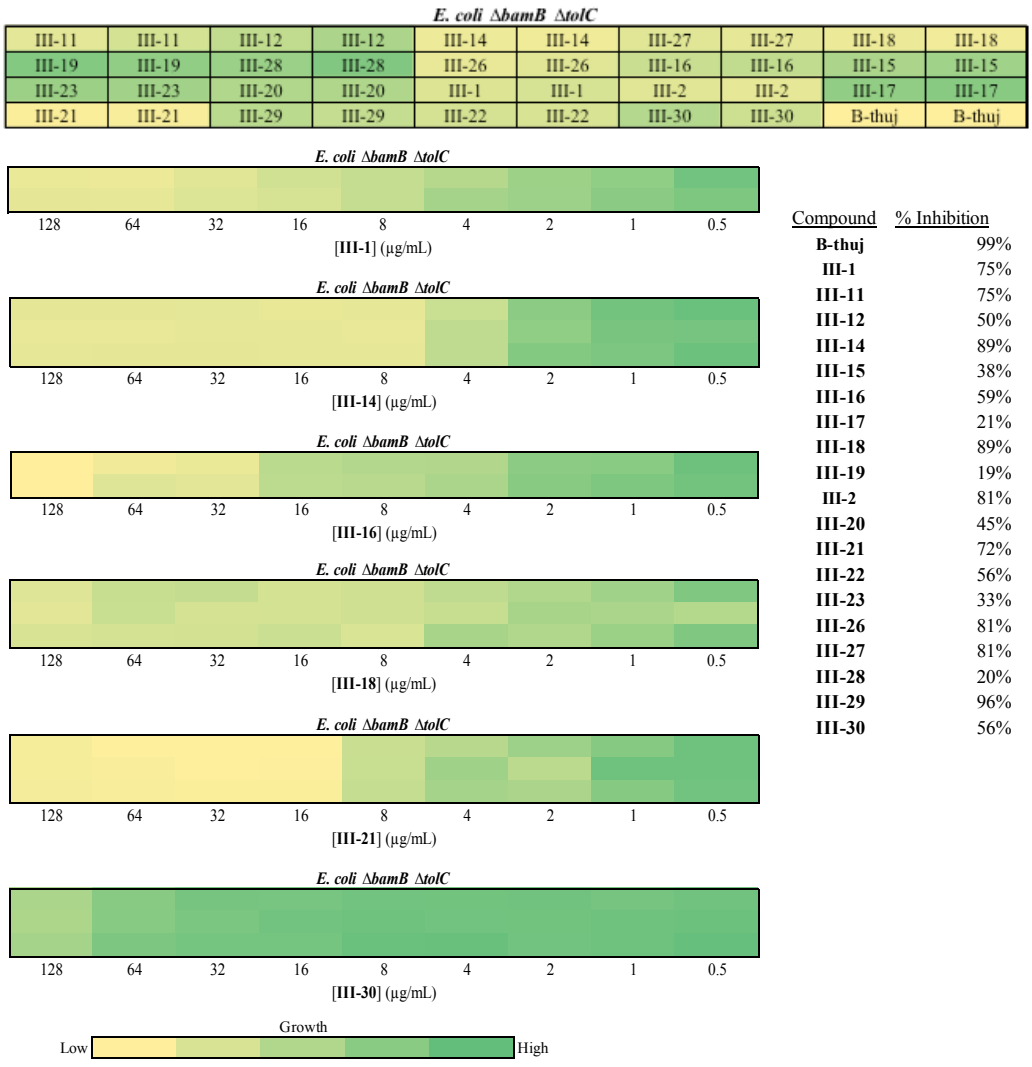

Figure 3-15. *E. coli* BW25113 Δ*tolC*Δ*bamB* Screening Results and MICs

Compound **III-21** demonstrated dose-dependent inhibition of *E. coli* BW25113 Δ*tolC* Δ*bamB* pGDP4:*ant(2")-Ia* with an MIC of 16 µg/mL (Figure 3-16). Checkerboard assays using combinations of varying concentrations of gentamicin and inhibitor were run to assess synergy. Compound **III-21** showed only additive effects with gentamicin (FIC = 1, Figure 3-17), providing further evidence of a nonspecific method of inhibition. Interestingly, Compound **III-30**, which differed from **III-21** only in the methyl ester protecting group, had minimal intrinsic activity of its own (MIC ≥128 µg/mL, Figure 3-16), but showed synergy with gentamicin (FIC = 0.4, Figure 3-18). This indicates that the methyl ester contributes to nonspecific inhibition and does not actually target ANT (2")-Ia. It may be that this nonspecific inhibition masks the effect of **III-21** on its own, as the synergistic effect

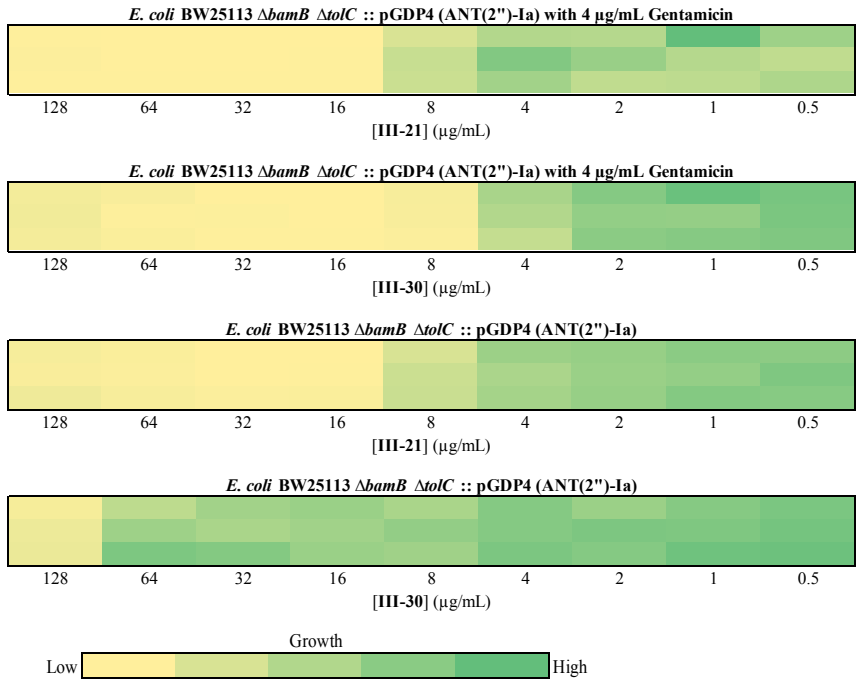

Figure 3-16. Dose-Dependency and MIC Determinations for **III-21** and **III-30** in *E. coli* BW25113 Δ*tolC*Δ*bamB* pGDP:*ant(2")-Ia*

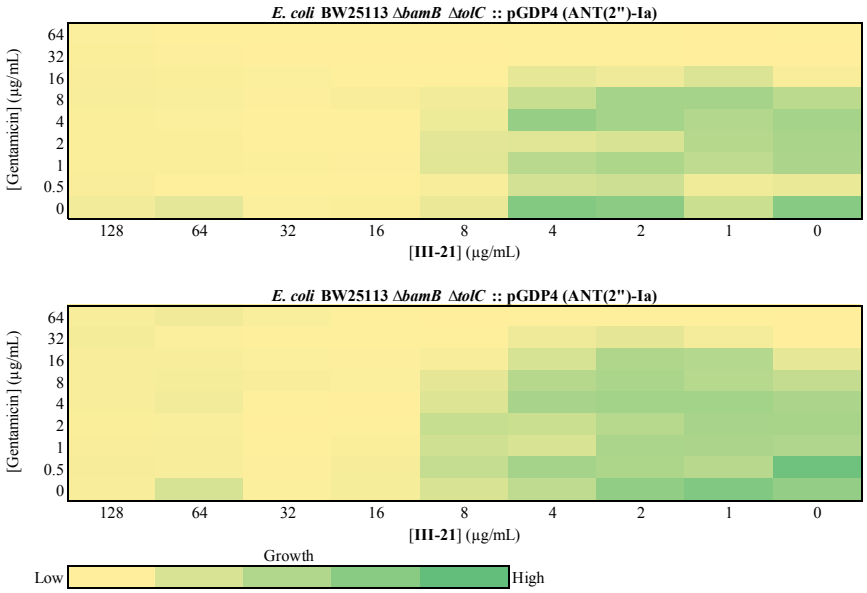

Figure 3-17. Checkerboard Assays for Interaction of **III-21** and Gentamicin in *E. coli* BW25113 Δ*tolC*Δ*bamB* pGDP:*ant(2")-Ia*. *FIC* ≤ 0.5 is considered synergistic, *FIC* > 2 is antagonistic, and 0.5 < *FIC* < 0.2 is indeterminant/additive

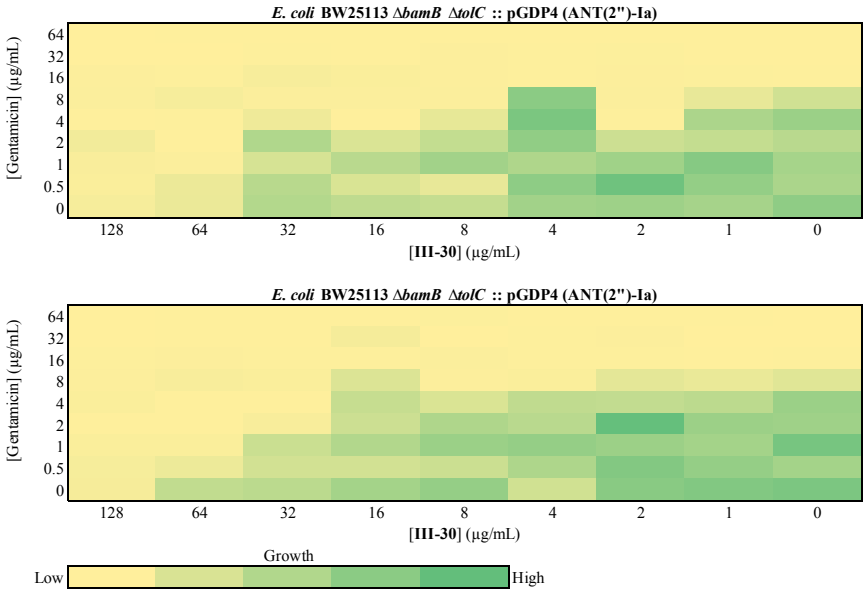

Figure 3-18. Checkerboard Assays for Interaction of **III-30** and Gentamicin in *E. coli* BW25113 Δ*tolC*Δ*bamB* pGDP:*ant(2")-Ia*. *FIC* ≤ 0.5 is considered

of **III-30** appears at a concentration of 16-32 μg/mL.

The library was also screened at 100 μM, 200 μM, and 500 μM against purified ANT(2")-Ia coupled to the EnzCkek® pyrophosphatase assay (Figure 3-19) as previously described.[34,35] β-Thujaplicinol was tested alongside as a positive control.[34] Solubility issues were noted at 500 μM for many of the compounds. Surprisingly, the almost all compounds, including **III-30**, showed no inhibition. Compound **III-22** was the notable exception, showing 59% inhibition at 500 μM; however, this is suspected to be due to an excess of precipitate as the compound was not fully soluble even at 100 μM with heat and showed only 14% at both 100 μM and 200 μM. Furthermore, biphenyls are known in the literature to cause false positives through aggregation.[36] These results reinforce the notion that any cellular growth inhibition was the result of nonspecific interaction. It is unknown why **III-30** did not inhibit the purified enzyme as it demonstrated some selectivity and synergy with cells. The enzyme assay chosen may not be the best selection as it has a narrow response window (the maximum signal was only 0.2 AU above the background absorbance) and significant problems with solubility at the concentrations used for screening.

3.4 Implications and Future Work

A parallel synthetic methodology was developed for synthesizing various N-[(1,1-biphenyl)-3-yl]-pyridine-4-carboxamide analogs. It was anchored by a core scaffold of 5'-amino-2'-methyl-[1,1'-biphenyl]-4-carboxylic acid, which

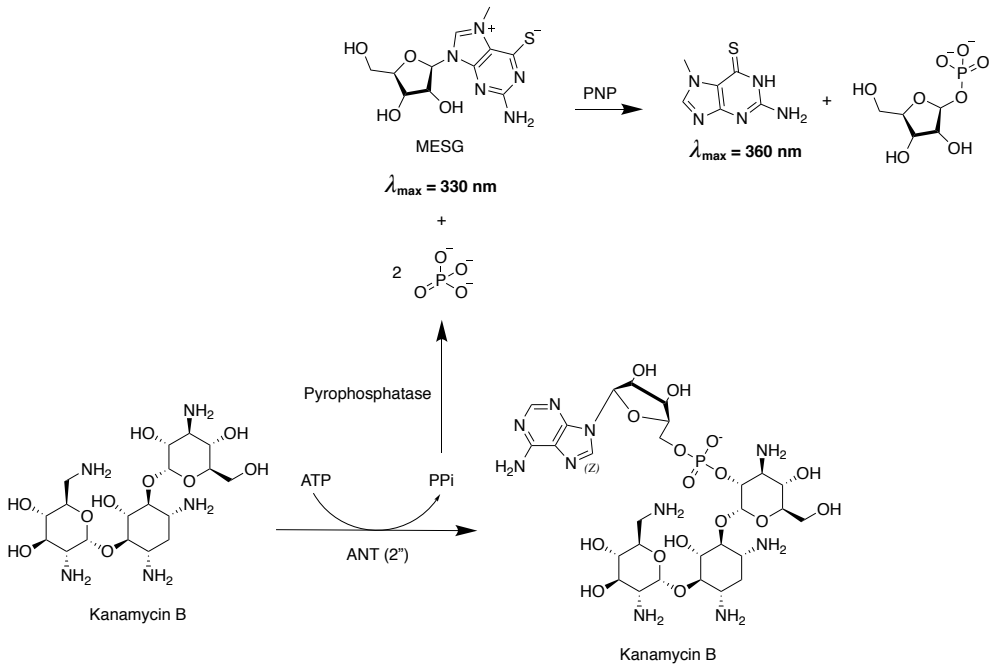

Figure 3-19. Pyrophosphatase-Coupled ANT(2")-Ia Assay[35]

could be produced in gram quantities, and then coupled on either end to introduce amide and substituted isonicotinamide functionalities. A small library of compounds was produced and tested for inhibitory activity against ANT (2")-Ia in live-cell and enzyme assays. SAR analysis revealed that substitution at position 2" of the isonicotinamide moiety had a detrimental effect on activity, as did amide functionalities at position 4' of the biphenyl. Compound **III-30** was the most promising compound of this series, selectively rescuing gentamicin activity in cells harbouring *ant(2")-Ia*. However, these results were not translatable to assays with purified ANT(2")-Ia, possibly due to obscuration from poor compound solubility coupled with the narrow detection window of the assay. Future work includes

optimizing the enzyme assay and further SAR exploring the effect of substituents on the biphenyl and pyridine rings.

3.5 EXPERIMENTAL

3.5.1 SYNTHESIS

Materials and Instrumentation

Microwave reactions were performed in 2.0 – 5.0 mL microwave vials, sealed under ambient atmosphere, and loaded to a CEM Discover SP-D 80 Microwave Reactor (100 W, < 100 psi). Heated non-microwave reactions were performed in a temperature-controlled oil bath. TLC was performed on F-254 (0.25 mm) precoated silica gel (Merck) or F-254 (0.2 mm) precoated RP-18 (C18) modified silica gel (MilliporeSigma) and visualized under UV. Ninhydrin, bromocresol green, or anisaldehyde stains were used as needed. Flash column chromatography purifications were performed using a normal phase Teledyne Isco Combiflash® Rf 200 with standard RediSep RF silica columns (4 g to 24 g).

Compounds were characterized by ^{1}H NMR, ^{13}C NMR, DEPT Q, and HRMS. NMR spectra were obtained from a Bruker AvanceIII 700 (700 MHz). Chemical shifts are reported as ppm, coupling constants in Hz, and peaks were calibrated to the solvent residual peak ($CDCl_3$ = 7.26 (^{1}H), 77.16 (^{13}C) or MeOD = 3.31 (^{1}H), 49.00 (^{13}C)). Mass spectrometry was conducted with a Bruker Maxis 4G/TOF in either positive or negative ion mode with direct infusion.

***tert*-Butyl-N-(3-iodo-4-methylphenyl)carbamate (III-9)**: 3-iodo-4-methylaniline (**III-5**) (1047.9 mg, 4.48 mmol) and di-*tert*-butyl dicarbonate (2165.9 mg, 9.92 mmol) were stirred at 50°C for 2.5 h. The resulting dark brown reaction mixture was purified by automated column chromatography system (10% ethyl ether in hexanes, R_f = 0.32) to yield *tert*-butyl-N-(3-iodo-4-methylphenyl)carbamate as an off-white powder (674.2 mg, 95%). ^{1}H NMR (700 MHz; $CDCl_3$) δ 7.88 (s, 1H), 7.21 (dd, J = 9.4 Hz, 1H), 7.11 (d, J = 8.1 Hz, 1H), 6.35 (s, 1H), 2.37 (s, 3H), 1.51 (s, 9H)). ^{13}C NMR (176 MHz; $CDCl_3$) δ 152.62 (C), 137.01 (C), 136.01 (C), 129.60 (CH), 128.66 (CH), 118.56 (CH), 100.89 (C), 80.91 (C), 28.45 (CH_3), 27.33 (CH_3). HRMS (ESI) for $C_{12}H_{16}INO_2$: Calculated $[M+Na]^+$ 356.0118. Found $[M+Na]^+$ 356.0116.

Methyl 5'-{[(*tert*-butoxy)carbonyl]amino}-2'-methyl-[1,1'-biphenyl]-4-carboxylate (III-11): *tert*-Butyl-N-(3-iodo-4-methylphenyl)carbamate (**III-9**) (255.5 mg, 0.77 mmol), 4-methoxyphenylboronic acid (**III-10**) (172.5 mg, 0.95 mmol), and $Pd(PPh_3)_4$ (46.6 mg, 0.04 mmol) were dissolved in 12.5 mL of 1,2-dimethyoxyethane and flushed with nitrogen for 5 min. Sodium bicarbonate (146.9mg, 2.91 mmol) was added and the system purged for 2 min.[28] The solution was refluxed at 70°C for 24 h then purified by solid-loading automated column chromatography system to yield methyl 5'-(*tert*-butoxycarbonylamino)-2'-methyl-1,1'-biphenyl-4-carboxylate as an off-white powder (151.4 mg, 58%). ^{1}H NMR (600 MHz; $CDCl_3$) δ 8.06 (d, J = 8.5 Hz, 2H), 7.38 (d, J = 7.8 Hz, 2H), 7.28 (s, 1H), 7.25 (d, 9.9 Hz, 1H), 7.18 (d, J = 8.5 Hz, 1H), 6.48 (s, broad, 1H), 3.94 (s, 3H), 2.16 (s, 3H), 1.51 (s, 3H). ^{13}C NMR (151 MHz;

$CDCl_3$) δ 167.18 (C), 152.95 (C), 146.58 (C), 141.53 (C), 136.35 (C), 131.12 (CH), 129.96 (C), 129.56 (CH), 129.35 (CH), 128.80 (C), 119.90 (CH), 118.26 (CH), 80.64 (C), 52.26 (CH_3), 28.47 (CH_3), 19.77 (CH_3). HRMS (ESI) for $C_{20}H_{23}NO_4$: Calculated $[M+Na]^+$ 364.1519. Found $[M+H]^+$ 364.1516.

Methyl 5'-amino-2'-methyl-[1,1'-biphenyl]-4-carboxylate (III-12): Methyl 5'-{[(*tert*-butoxy)carbonyl]amino}-2'-methyl-1,1'-biphenyl-4-carboxylate (**III-11**) (221.1 mg, 0.65 mmol) was dissolved in 8 mL of dichloromethane and chilled to 0°C. 8 mL of chilled trifluoroacetic acid was added dropwise, and the reaction mixture was stirred at room temperature for two hours. The reaction mixture was neutralized with sodium hydroxide, extracted into ethyl acetate, washed with brine, dried with magnesium sulfate, and concentrated yield methyl 5'-amino-2'-methyl-1,1'-biphenyl-4-carboxylate as a pale yellow residue (144.2 mg, 93%). ^{1}H NMR (700 MHz; $CDCl_3$) δ 8.07 (d, J = 8.5 Hz, 2H), 7.38 (d, J = 9.9 Hz, 2H), 7.06 (d, 8.1 Hz, 1H), 6.64 (dd, J = 8.0 Hz, ^{4}J = 2.6 Hz, 1H), 6.58 (d, ^{4}J = 2.5 Hz, 1H), 3.94 (s, 3H), 3.60 (s, 2 H, broad), 2.14 (s, 3H). ^{13}C NMR (176 MHz; $CDCl_3$) δ 167.17 (C), 147.10 (C), 144.34 (C), 141.60 (C), 131.41 (CH), 129.40 (CH), 129.21 (CH), 128.58 (C), 125.06 (C), 116.44 (CH), 114.90 (CH), 52.17 (CH_3), 19.43 (CH_3). HRMS (ESI) for $C_{15}H_{15}NO_2$: Calculated $[M+H]^+$ 242.1176. Found $[M+H]^+$ 242.1175.

5'-Amino-2'-methyl-[1,1'-biphenyl]-4-carboxylic acid (III-17): Methyl 5'-{[(*tert*-butoxy)carbonyl]amino}-2'-methyl-1,1'-biphenyl-4-carboxylate (**III-11**) (453.2 mg, 1.33 mmol) was dissolved in 9 mL of dichloromethane and cooled to

0°C. 9 mL of trifluoroacetic acid at 0°C was added dropwise and the reaction stirred at room temperature overnight. The reaction mixture was evaporated and re-dissolved in 4 mL of methanol. Sodium hydroxide (1N, 12 mL) was added and the reaction refluxed at 70°C for 1 h. The product was neutralized with hydrochloric acid (1N, 6 mL) and the white powder collected by vacuum filtration and washed with water (268.1 mg, 89%).

Compound **III-17** could also be made from methyl 5'-amino-2'-methyl-1,1'-biphenyl-4-carboxylate (**III-12**). Compound **III-12** (43.0 mg, 0.18 mmol) was dissolved in 1 mL of methanol. Sodium hydroxide (350 µL, 1.0 M) was added, and the reaction was refluxed for 30 min. The reaction mixture was evaporated, redissolved in water and neutralized with hydrochloric acid, and the resulting tan powder filtered and washed with water (16.3 mg, 40%). ^{1}H NMR (700 MHz; MeOD) δ 8.06 (d, J = 8.1 Hz, 2H), 7.40 (d, J = 8.1 Hz, 2H), 7.06 (d, J = 8.1 Hz, 1H), 6.73 (dd, J = 8.1 Hz, ^{4}J = 2.3 Hz, 1H), 6.67 (d, J = 2.2 Hz, 1H), 2.13 (s, 3H). ^{13}C NMR (176 MHz; MeOD) δ 169.84 (C), 148.62 (C), 145.21 (C),142.84 (C), 132.23 (CH), 130.57 (CH), 130.34 (C), 130.24 (CH), 126.56 (C), 118.38 (CH), 117.05 (CH), 19.57 (CH_3). HRMS (ESI) for $C_{14}H_{13}NO_2$: Calculated $[M+H]^+$ 228.1020. Found $[M+H]^+$ 228.1023.

5'-Amino-N-(cyclopropylmethyl)-2'-methyl-[1,1'-biphenyl]-4-carboxamide (III-20): 5'-amino-2'-methyl-[1,1'-biphenyl]-4-carboxylic acid (**III-17**) (268.1 mg, 1.18 mmol) and EDC (306.3 mg, 1.60 mmol) were dissolved in 20 mL of dichloromethane. Methylcyclopropylamine (480 µL, 5.5 mmol) was added, and the reaction was capped and stirred at room temperature overnight. 250 mL of

water was added, and the crude product was extracted into ethyl acetate (2 x 25 mL), washed with water (25 mL) and brine (25 mL), dried with magnesium sulfate, and purified by automated column chromatography system to yield 5'-amino-N-(cyclopropylmethyl)-2'-methyl-[1,1'-biphenyl]-4-carboxamide as a colourless oil (65.6 mg, 20%). ^{1}H NMR (600 MHz; $CDCl_3$) δ 7.81 (d, J = 8.0 Hz, 2H), 7.37 (d, J = 8.0 Hz, 2H), 7.06 (d, J = 8.0 Hz, 1H), 6.66 (dd, J = 8.1 Hz, ^{4}J = 2.3 Hz, 1 H), 6.59 (d, ^{4}J = 2.2 Hz, 1H), 6.27 (s, 1H, broad), 3.80 (s, 2H, broad), 3.35 (t, J = 6.2 Hz, 2H), 2.13 (s, 3H), 1.09 (m, 1H), 0.57 (dt, J = 5.2 Hz, J = 6.6 Hz, 2H), 0.29 (dt, J = 5.0 Hz, J = 5.0 Hz, 2H). ^{13}C NMR (151 MHz; $CDCl_3$) δ 167.47 (C), 145.53 (C), 144.01 (C), 141.76 (C), 133.24 (C), 131.45 (CH), 129.42 (CH), 126.80 (CH), 125.46 (C), 116.72 (CH), 115.02 (CH), 45.11 (CH_2), 19.51 (CH_3), 10.92 (CH), 3.64 (CH_2). HRMS (ESI) for $C_{18}H_{20}NO_2$: Calculated $[M+H]^+$ 281.1648. Found $[M+H]^+$ 281.1663.

5'-{[(*tert*-Butoxy)carbonyl]amino}-2'-methyl-[1,1'-biphenyl]-4-carboxylic acid (III-16): Methyl 5'-{[(*tert*-butoxy)carbonyl]amino}-2'-methyl-1,1'-biphenyl-4-carboxylate (**III-11**) (101.1 mg, 0.30 mmol) was dissolved in 2 mL of methanol. Sodium hydroxide (280 µL of 2.5 M) was added, and the reaction was refluxed for 1 h. The reaction mixture was evaporated, redissolved in ethyl acetate/water and neutralized with hydrochloric acid, then extracted twice into ethyl acetate, washed with water and brine, and dried with magnesium sulfate to produce 5'-{[(*tert*-butoxy)carbonyl]amino}-2'-methyl-[1,1'-biphenyl]-4-carboxylic acid as a white powder (28.1 mg, 29%). ^{1}H NMR (700 MHz; MeOD-d_4) δ 8.07 (d, J = 8.3 Hz, 2H), 7.41 (d, J = 8.3 Hz, 2H), 7.31 (d, J = 10.2 Hz, 1H), 7.28 (s, 1H), 7.18 (d, J =

8.3 Hz, 1H), 2.18 (s, 3H), 1.50 (s, 9H). ^{13}C NMR (176 MHz; MeOD-d_4) δ 169.96 (C), 155.44 (C), 148.04 (C), 142.54 (C), 138.40 (C), 131.80 (CH), 130.63 (CH), 130.40 (C), 130.29 (CH), 120.92 (CH), 119.44 (CH), 80.84 (C), 28.73 (CH_3), 19.81 (CH_3). HRMS (ESI) for $C_{19}H_{21}NO_4$: Calculated $[M+Na]^+$ 350.1363. Found $[M+Na]^+$ 350.1361.

***tert*-Butyl N-{6-methyl-4'-(propylcarbamoyl)-[1,1'-biphenyl]-3-yl}carbamate (III-26)**: Methyl 5'-{[(*tert*-butoxy)carbonyl]amino}-2'-methyl-1,1'-biphenyl-4-carboxylate (**III-11**) (45.2 mg, 0.13 mmol) and lithium bromide (8.4 mg, 0.10 mmol) was dissolved 2 mL of N-propylamine, stirred at 50°C overnight, evaporated, and purified by automated column chromatography system to yield *tert*-butyl N-[6-methyl-4'-(propylcarbamoyl)-[1,1'-biphenyl]-3-yl)carbamate as a colourless oil (32.3 mg, 66%). ^{1}H NMR (700 MHz; $CDCl_3$) δ 7.79 (d, J = 8.0 Hz, 2H), 7.36 (d, J = 8.6 Hz, 2H), 7.25 (m, 2H), 7.18 (d, J = 9.2 Hz, 1H), 6.51 (s, 1H), 6.21 (t, broad, 1H), 3.45 (q, J = 6.6 Hz, 2H), 2.18 (s, 3H), 1.66 (sex, J = 7.5 Hz, 2H), 1.50 (s, 9H), 1.01 (t, J = 8.0 Hz, 3H). ^{13}C NMR (176 MHz; $CDCl_3$) δ 167.56 (C), 152.93 (C), 145.00 (C), 141.51 (C), 136.28 (C), 133.41 (C), 131.10 (CH), 129.92 (C), 129.47 (CH), 126.83 (CH), 199.90 (CH), 118.16 (CH), 80.61 (CH), 41.86 (CH_2), 28.47 (CH_3), 23.13 (CH_2), 19.75 (CH_3), 11.59 (CH_3). HRMS (ESI) for $C_{22}H_{28}N_2O_3$: Calculated $[M+H]^+$ 369.2173, $[M+Na]^+$ 391.1992. Found $[M+H]^+$ 369.2156 $[M+Na]^+$ 391.1983.

Methyl 5'-(2-chloropyridine-4-amido)-2'-methyl-[1,1'-biphenyl]-4-carboxylate (III-14): Methyl 5'-amino-2'-methyl-[1,1'-biphenyl]-4-carboxylate

(**III-12**) (132.0 mg, 0.55 mmol) was dissolved in 5 mL of acetonitrile. Triethylamine (250 μL, 1.79 mmol) was added and the reaction mixture cooled to 0°C. 2-chloropyridine-4-carbonyl chloride (90 μL, 0.73 mmol) was dissolved in 5 mL of acetonitrile and added dropwise. The reaction was stirred at room temperature for 5 h, evaporated, and purified by automated column chromatography system (gradient to 10% ethyl acetate in hexanes) to yield methyl 5'-(2-chloropyridine-4-amido)-2'-methyl-[1,1'-biphenyl]-4-carboxylate (185.0 mg, 89%). ^{1}H NMR (700 MHz; $CDCl_3$) δ 8.48 (d, J = 4.8 Hz, 1H), 8.43 (s, broad, 1H), 8.04 (d, J = 8.3 Hz, 2H), 7.75 (s, 1H), 7.64 (d, 4.9 Hz, 1H), 7.61 (dd, J = 8.3 Hz, ^{4}J = 2.0 Hz, 1H), 7.43 (d, ^{4}J = 1.7 Hz, 1H), 7.34 (d, J = 8.3 Hz, 2H), 7.25 (d, J = 8.6 Hz, 1H), 3.91 (s, 3H), 2.22 (s, 1H). ^{13}C NMR (176 MHz; $CDCl_3$) δ 167.30 (C), 162.69 (C), 152.66 (C), 150.69 (CH), 146.02 (C), 145.15 (C), 141.64 (C), 135.00 (C), 132.64 (C), 131.38 (CH), 129.63 (CH), 129.25 (CH), 128.86 (C), 122.23 (CH), 121.79 (CH), 120.25 (CH), 119.98 (CH), 52.36 (CH_3), 19.98 (CH_3). HRMS (ESI) for $C_{21}H_{17}ClN_2O_3$: Calculated $[M+Na]^+$ 403.0825. Found $[M+Na]^+$ 403.0828.

5'-(2-Chloropyridine-4-amido)-2'-methyl-[1,1'-biphenyl]-4-carboxylic acid (III-15): Methyl 5'-(2-chloropyridine-4-amido)-2'-methyl-[1,1'-biphenyl]-4-carboxylate (**III-14**) (376.0 mg, 0.99 mmol) was dissolved in 11 mL of methanol. Sodium hydroxide (4 mL, 1 N) was added, and the reaction was refluxed for 1 h. The reaction mixture was evaporated to a bright green residue, redissolved in ethyl acetate/water, and brought to pH 7 with hydrochloric acid. Brine was added to precipitate the desired product as a white powder, and 5'-(2-chloropyridine-4-

amido)-2'-methyl-[1,1'-biphenyl]-4-carboxylic acid was collected by filtration (176.6 mg, 49%). ^{1}H NMR (700 MHz; MeOD) δ 8.54 (d, J = 5.1 Hz, 1H), 8.01, (d, J = 8.1 Hz, 2H), 7.93 (s, 1H), 7.83 (dd, J = 5.1 Hz, ^{4}J = 1.4 Hz, 1H), 7.69 (dd, J = 8.3 Hz, ^{4}J = 2.2 Hz, 1H), 7.52 (d, ^{4}J = 2.2 Hz, 1H), 7.34 (d, J = 8.1 Hz, 2H), 7.30 (d, J = 8.3 Hz, 1H), 2.25 (s, 3H). ^{13}C NMR (176 MHz; MeOD) δ 175.25 (C), 164.89 (C), 153.15 (C), 151.53 (CH), 147.38 (C), 144.84 (C), 143.57 (C), 137.96 (C), 137.09 (C), 133.38 (C), 131.84 (CH), 130.28 (CH), 129.59 (CH), 123.76 (CH), 123.29 (CH), 121.98 (CH), 121.30 (CH), 20.14 (CH_3). HRMS (ESI) for $C_{20}H_{15}ClN_2O_3$: Calculated $[M-H]^-$ 365.0693. Found $[M-H]^-$ 365.0699.

2-Chloro-N-{6-methyl-4'-(propylcarbamoyl)-[1,1'-biphenyl]-3-yl}pyridine-4-carboxamide (III-27): Methyl 5'-(2-chloropyridine-4-amido)-2'-methyl-[1,1'-biphenyl]-4-carboxylate (**III-14**) (25 mg, 0.66 mmol) and lithium bromide (7.5 mg, 0.086 mmol) were dissolved 1.5 mL of N-propylamine, heated at 50°C overnight, evaporated, and purified by automated column chromatography system to yield 2-chloro-N-[6-methyl-4'-(propylcarbamoyl)-[1,1'-biphenyl]-3-yl]pyridine-4-carboxamide as a yellow oil (25.7 mg, 95%). ^{1}H NMR (600 MHz; $CDCl_3$) δ 9.35 (s, 1H), 8.45 (d, J = 5.0 Hz, 1H), 7.88 (s, 1H), 7.78 (dd, J = 8.1, ^{4}J = 1.9 Hz, 1H), 7.75 (d, J = 5.2 Hz, 1H), 7.68 (d, J = 8.2 Hz, 2H), 7.34 (d, ^{4}J = 1.7 Hz, 1H), 7.23 (m, 3H), 6.42 (t, J = 5.9 Hz, 1H), 3.32 (q, J = 6.8 Hz, 2H), 2.18 (s, 3H), 1.80 (s, 1H), 1.58 (sex, J = 7.3 Hz, 2H), 0.91 (t, J = 7.3, 3H). ^{13}C NMR (176 MHz; $CDCl_3$) δ 167.68 (C), 162.67 (C), 152.59 (C), 150.61 (CH), 145.23 (C), 144.60 (C), 141.41 (C), 135.37 (C), 133.25 (C), 132.35 (C), 131.27 (CH), 129.40 (CH), 126.83 (CH), 122.46 (CH),121.87 (CH), 120.34 (CH), 120.13 (CH), 42.00 (CH_2), 22.98 (CH_3),

19.96 (CH_3), 11.56 (CH_3). HRMS (ESI) for $C_{23}H_{22}ClN_3O_2$: Calculated $[M+Na]^+$ 430.1298. Found $[M+Na]^+$ 430.1299.

2-Chloro-N-{4'-[(cyclopropylmethyl)carbamoyl]-6-methyl-[1,1'-biphenyl]-3-yl}pyridine-4-carboxamide (III-18): 5'-(2-Chloropyridine-4-amido)-2'-methyl-[1,1'-biphenyl]-4-carboxylic acid (**III-15**) (29.4 mg, 0.08 mmol) was dissolved in 1 mL of thionyl chloride and refluxed under nitrogen for 1 h. The mixture was coevaporated with 1:1 toluene:dichloromethane to form a yellow powder that was dissolved in 2 mL of acetonitrile. Triethylamine (29 µL, 0.21 mmol) and methylcyclopropylamine (10 µL, 0.12 mmol) were added, and the reaction stirred at room temperature overnight, evaporated, and purified by automated column chromatography system (16.4 mg, 52%). ^{1}H NMR (700 MHz; $CDCl_3$) δ 9.20 (s, 1H), 8.49 (d, ^4J = 5.0 Hz, 1H), 7.88 (s, 1H), 7.80 (dd, J =8.0 Hz, ^4J = 1.1 Hz, 1H), 7.76 (d, J = 4.6 Hz, 1H), 7.73 (d, J = 8.1 Hz, 2H), 7.37 (s, 1H), 7.27 (m, 3H), 6.42 (t, J = 5.0 Hz, 1H), 3.22 (t, J = 6.2 Hz, 2H), 2.21 (s, 3H), 1.01 (m, 1H), 0.54 (m, 2H), 0.23 (m, 2H). ^{13}C NMR (176 MHz; $CDCl_3$) δ 167.63 (C), 162.88 (C), 152.52 (C), 150.54 (CH), 145.34 (C), 144.72 (C), 141.34 (C), 135.55 (C), 133.08 (C), 132.30 (C), 131.30 (CH), 129.41 (CH), 126.90 (CH), 122.54 (CH), 121.93 (CH), 120.50 (CH), 120.33 (CH), 45.22 (CH_2), 20.01 (CH_3), 10.73 (CH), 3.66 (CH_2). HRMS (ESI) for $C_{24}H_{22}ClN_3O_2$: Calculated $[M+H]^+$ 420.1473. Found $[M+H]^+$ 420.1477. Calculated $[M+Na]^+$ 442.1293. Found $[M+Na]^+$ 442.1299.

2-Chloro-N-{6-methyl-4'-(morpholine-4-carbonyl)-[1,1'-biphenyl]-3-yl}pyridine-4-carboxamide (III-19): 5'-(2-Chloropyridine-4-amido)-2'-methyl-

[1,1'-biphenyl]-4-carboxylic acid (**III-15**) (27.8 mg, 0.08 mmol), HATU (40.9 mg, 0.11 mmol), and HBTU (29.8 mg, 0.08 mmol) were dissolved 1 mL of dimethylformamide. DIPEA (36 µL, 0.21 mmol) and morpholine (10 µL, 0.11 mmol) were added and the reaction was stirred at room temperature for two days. Crude product was extracted into ethyl acetate, washed with water and brine, dried over magnesium sulfate, and partially purified by automated column chromatography system (crude yield 13.7 mg, 42%). ^{1}H NMR (700 MHz; $CDCl_3$) δ 8.52 (d, J = 5.1 Hz, 1H), 8.41 (s, 1H), 7.78 (s, 1H), 7.66 (d, J = 4.6 Hz, 1H), 7.56 (d, J= 8.1 Hz, 1H), 7.50 (s, 1H), 7.42 (d, J = 8.5 Hz, 2H), 7.34 (d, J = 8.1 Hz, 2H), 7.28 (d, J = 8.3 Hz, 1H), 3.51-3.77 (m, 8H), 2.24 (s, 3H). ^{13}C NMR (176 MHz; $CDCl_3$) δ 170.51 (C), 162.55 (C), 152.68 (C), 150.74 (CH), 145.22 (C), 143.17 (C), 141.66 (C), 135.17 (C), 134.00 (C), 132.60 (C), 131.31 (CH), 129.47 (CH), 127.15 (CH), 122.25 (CH), 121.98 (CH), 120.08 (CH), 120.04 (CH), 67.03 (CH_2), 38.75 (CH_2), 20.09 (CH_3). HRMS (ESI) for $C_{24}H_{22}ClN_3O_3$: Calculated $[M+H]^+$ 436.1422. Found $[M+H]^+$ 436.1143.

2-Chloro-N-{6-methyl-4'-(pyrrolidine-1-carbonyl)-[1,1'-biphenyl]-3-yl}pyridine-4-carboxamide (III-28): 5'-(2-Chloropyridine-4-amido)-2'-methyl-[1,1'-biphenyl]-4-carboxylic acid (**III-15**) (25.0 mg, 0.07 mmol), HATU (36.9 mg, 0.10 mmol), and HBTU (31.3 mg, 0.08 mmol) were dissolved 1 mL of dimethylformamide. DIPEA (36 µL, 0.21 mmol) and pyrrolidine (10 µL, 0.11 mmol) were added and the reaction was stirred at room temperature for two days. Crude product was extracted into ethyl acetate, washed with water and brine, dried over magnesium sulfate, and purified by automated column chromatography

system (4.0 mg, 14%). ^{1}H NMR (700 MHz; $CDCl_3$) δ 8.54 (s, J = 5.1 Hz, 1H), 8.48 (s, 1H), 7.83 (s, 1H), 7.70 (d, J = 4.4 Hz, 1H), 7.67 (dd, J = 6.7 Hz, ^{4}J = 1.5 Hz, 1H), 7.52 (d, J = 8.1 Hz, 2H), 7.43 (s, 1H), 7.31 (d, J = 8.1 Hz, 2H), 7.29 (d, J = 8.3 Hz, 1H), 3.62 (t, J = 7.0 Hz, 2H), 3.49 (t, J = 7.6 Hz, 2H), 2.25 (s, 3H), 1.97 (quint, J = 6.8 Hz, 2H), 1.91 (quint, J = 6.5 Hz, 2H). ^{13}C NMR (176 MHz; $CDCl_3$) δ 169.74 (C), 162.50 (C), 152.74 (C), 150.76 (CH), 145.28 (C), 142.96 (C), 141.89 (C), 135.88 (C), 135.11 (C), 132.68 (C), 131.32 (CH), 129.14 (CH), 127.18 (CH), 122.28 (CH), 121.95 (CH), 120.03 (CH), 120.03 (CH), 49.87 (CH_2), 46.46 (CH_2), 26.56 (CH_2), 24.59 (CH_2), 20.09 (CH_3). HRMS (ESI) for $C_{24}H_{22}ClN_3O_2$: Calculated $[M+Na]^+$ 442.1293. Found $[M+Na]^+$ 442.1294.

2'-Methyl-5'-[(2-pyrrolidin-1-yl)pyridine-amido]-1,1'-biphenyl-4-carboxylic acid (III-23): 5'-(2-Chloropyridine-4-amido)-2'-methyl-[1,1'-biphenyl]-4-carboxylic acid (**III-15**) (27.4 mg, 0.07 mmol) was dissolved in 0.5 mL of pyrrolidine and stirred at 85°C for 1 d. Reaction mixture was evaporated, extracted into ethyl acetate. The evaporated reaction mixture was dissolved in ethyl acetate, washed with saturated ammonium chloride and brine, dried with magnesium sulfate, and purified by automated column chromatography system (4.3 mg, 14%). ^{1}H NMR (700 MHz; MeOD) δ 8.13 (dd, J = 5.4 Hz, ^{4}J = 0.53 Hz, 1H), 8.09 (d, J = 8.3 Hz, 2H), 7.65 (dd, J = 8.2 Hz, ^{4}J = 2.3 Hz, 1H), 7.58 (d, J = 2.2 Hz, 1H), 7.46 (d, J = 8.3 Hz, 2H), 7.31 (d, J = 8.3 Hz, 1H), 6.98 (dd, J = 5.4 Hz, ^{4}J = 1.4 Hz, 1H), 6.95 (s, broad, 1H), 3.50 (t, J = 6.7 Hz, 4H), 2.25 (s, 3H), 2.06 (m, 4H). ^{13}C NMR (176 MHz; MeOD) δ 167.51 (C), 158.66 (C), 148.97 (CH), 147.62 (C), 145.25 (C), 142.69 (C), 137.41 (C), 132.92 (C), 131.93 (CH), 130.70 (CH), 130.53 (C), 130.29

(CH), 130.21 (C), 123.30 (CH), 121.77 (CH), 109.57 (CH), 106.64 (CH), 48.03 (CH_2), 26.44 (CH_2), 20.01 (CH_3). HRMS (ESI) for $C_{24}H_{23}N_3O_3$: Calculated $[M-H]^-$ 400.1661. Found $[M-H]^-$400.1672.

N-{4'-[(cyclopropylmethyl)carbamoyl]-6-methyl-[1,1'-biphenyl]-3-yl}-2-(pyrrolidin-1-yl)pyridine-4-carboxamide (III-1): 2-Chloro-N-{4'-[(cyclopropylmethyl)carbamoyl]-6-methyl-[1,1'-biphenyl]-3-yl}pyridine-4-carboxamide (**III-18**) (15.7 mg, 0.04 mmol) was dissolved in 0.5 mL of pyrrolidine at stirred at 85°C for 18 h. Reaction mixture was evaporated, extracted into ethyl acetate, washed with water and brine, and dried over magnesium sulfate. Crude product was re-dissolved in methanol and brought to pH 8 with aqueous sodium bicarbonate to remove pyrrolidinium chloride salt prior to purification by automated column chromatography system (7.2 mg, 42%). ^{1}H NMR (700 MHz; $CDCl_3$) δ8.24 (d, J = 5.2 Hz, 1H), 8.07 (s, 1H, broad), 7.81 (d, J = 8.1 Hz, 2H), 7.62 (dd, J = 8.6 Hz, 1H), 7.50 (s, 1H), 7.39 (d, J = 8.1 Hz, 2H), 7.28 (d, 8.3 Hz, 1H), 6.85 (s, 1H), 6.81 (d, J = 5.0 Hz, 1H), 6.30 (t, 1H), 3.51 (s, 4H), 3.33 (t, J = 6.2 Hz, 2H), 2.24 (s, 3H), 2.03 (m, 4H), 1.08 (m, 1H), 0.57 (m, 2H), 0.29 (m, 2H). ^{13}C NMR (176 MHz; $CDCl_3$) δ167.40 (C), 165.03 (C),144.71 (CH), 143.28 (C),141.61 (C),135.66 (C),133.50 (C),131.98 (C),131.26 (CH), 129.47 (CH), 127.94 (C),127.12 (C),126.93 (CH), 121.62 (CH), 119.91 (CH), 107.34 (CH), 104.99 (CH), 47.06 (CH_2), 45.15 (CH_2), 25.66 (CH_2), 20.02 (CH_3), 10.82 (CH), 3.66 (CH_2). HRMS (ESI) for $C_{28}H_{30}N_4O_2$: Calculated $[M+H]^+$455.2442. Found $[M+H]^+$.455.2441.

Methyl 2'-methyl-5'-(pyridine-4-amido)-[1,1'-biphenyl]-4-carboxylate (III-21): Methyl 5'-amino-2'-methyl-[1,1'-biphenyl]-4-carboxylate (**III-14**) (23 mg, 0.10 mmol), isonicotinic acid (33 mg, 0.27 mmol), and EDC (27 mg, 0.14 mmol) were dissolved in 2.5 mL off dichloromethane and stirred overnight. The reaction mixture was extracted into ethyl acetate, washed with water and brine, dried over magnesium sulfate, and purified by automated column chromatography system (9.0 mg, 29%). ^{1}H NMR (700 MHz; MeOD) δ 8.72 (d, J = 6.0 Hz, 2H), 8.09 (d, J = 8.2 Hz, 2H), 7.88 (dd, J = 4.6 Hz, ^{4}J = 1.5 Hz, 2H), 7.65 (dd, J = 8.2 Hz, ^{4}J = 2.2 Hz, 1H), 7.61 (d, ^{4}J = 2.1 Hz, 1H), 7.47 (d, J = 8.2 Hz, 2H), 7.32 (d, J = 8.3 Hz, 1H), 3.94 (s, 3H), 2.25 (s, 3H). ^{13}C NMR (176 MHz; MeOD) δ 168.41 (C), 166.25 (C), 151.01 (CH), 147.97 (C), 144.51 (C), 142.59 (C), 137.37 (C), 133.08 (C), 132.03 (C), 130.51 (CH), 130.45 (CH), 130.10 (CH), 123.17 (CH), 123.14 (CH), 121.74 (CH), 52.68 (CH_3), 20.02 (CH_3). HRMS (ESI) for $C_{21}H_{18}N_2O_3$: Calculated $[M+H]^+$ 347.1390. Found $[M+H]^+$ 347.1414. Calculated $[M+Na]^+$ 369.1210. Found $[M+Na]^+$ 369.1258.

Methyl 5'-benzamido-2'-methyl-[1,1'-biphenyl]-4-carboxylate (III-22): Methyl 5'-amino-2'-methyl-[1,1'-biphenyl]-4-carboxylate (**III-14**) (27.0 mg, 0.11 mmol), 1-ethyl-3-(3-dimethylaminopropyl)carbodiimide hydrochloride (28.4 mg, 0.15 mmol), and benzoic acid (34.4 mg, 0.28 mmol) was dissolved in 2 mL of dichloromethane and stirred overnight. The orange liquid was extracted into ethyl acetate, then washed with brine and dried with magnesium sulfate. The organic phase was then purified by normal phase, solid-loading automated column chromatography system (25% hexanes:ethyl acetate) to yield methyl 5'-benzamido-

2'-methyl-[1,1'-biphenyl]-4-carboxylate. (13.5 mg, 35%).^{1}H NMR (600 MHz; $CDCl_3$) δ 8.07 (d, J = 8.1 Hz, 2H), 7.93 (bs, 1H), 7.87 (d, J = 7.6 Hz, 2H), 7.60 (d, J = 6.9 Hz, 1H), 7.54 (t, J = 7.4 Hz, 1H), 7.51 (s, 1H), 7.47 (t, J = 7.7 Hz, 2H), 7.40 (d, J = 8.1 Hz, 2H), 7.27 (d, J = 9.1 Hz, 1H), 3.94 (s, 3H), 2.24 (s, 3H). ^{13}C NMR (151 MHz; $CDCl_3$) δ 167.19 (C), 165.88 (C), 146.34 (C), 141.57 (C), 135.94 (C), 135.02 (C), 133.77 (C), 131.99 (CH), 131.64 (C), 131.26 (CH), 129.59 (CH), 129.36 (CH), 128.92 (CH), 127.14 (CH), 121.52 (CH), 119.96 (CH), 52.29 (CH_3), 19.98 (CH_3). HRMS (ESI) for $C_{22}H_{19}NO_3$: Calculated $[M+H]^+$ 346.1438. Found $[M+H]^+$ 346.1441. Calculated $[M+Na]^+$ 368.1257. Found $[M+Na]^+$ 368.1265.

N-{4'-[(cyclopropylmethyl)carbamoyl]-6-methyl-[1,1'-biphenyl]-3-yl}pyridine-4-carboxamide (III-29): 5'-amino-N-(cyclopropylmethyl)-2'-methyl-[1,1'-biphenyl]-4-carboxamide (**III-20**) (23.9 mg, 0.09 mmol), isonicotinic acid (29.9 mg, 0.24 mmol), and EDC (22.0 mg, 0.11 mmol) were dissolved in 2 mL of dichloromethane and stirred at room temperature overnight. The reaction was quenched with water, and the product was extracted into ethyl acetate, washed with water and brine, dried over magnesium sulfate, and purified by automated column chromatography system (10.5 mg, 32%). ^{1}H NMR (700 MHz; $CDCl_3$) δ 8.77 (bs, 2H), 8.41 (s, 1H), 7.79 (m, 4H), 7.70 (d, J =7.4 Hz, 1H), 7.46 (s, 1H), 7.36 (d, J= 8.1 Hz, 2H), 7.29 (d, J = 8.3 Hz, 1H), 6.31 (t, J = 4.6 Hz), 3.28 (dd, J = 5.6 Hz, J = 6.8 Hz, 2H), 2.23 (s, 3H), 1.05 (m, 1H), 0.56 (dt, J = 6.1 Hz, J = 6.4 Hz, 2H), 0.26 (dt, J = 4.9 Hz, J = 5.0 Hz, 2H). ^{13}C NMR (176 MHz; $CDCl_3$) δ 167.46 (C), 163.88 (C), 150.67 (CH), 144.68 (C), 142.33 (C), 141.61 (C), 135.48 (C), 133.43 (C), 132.33 (C), 131.36 (CH), 129.48 (CH), 126.95 (CH), 121.75 (CH), 121.25 (CH),

120.15 (CH), 45.20 (CH_2), 20.05 (CH_3), 10.85 (CH), 3.68 (CH_2). HRMS (ESI) for $C_{24}H_{23}N_3O_2$: Calculated $[M+H]^+$ 386.1863. Found $[M+H]^+$ 386.1880.

2-(Morpholin-4-yl)pyridine-4-carboxylic acid (III-25): 2-chloropyridine-4-carboxylic acid (**III-24**) (314.0 mg, 2.00 mmol) was dissolved in 4 mL of morpholine and heated in a sealed tube (85°C) for 6 hours. A salt was formed by protonating excess morpholine with 10 mL of saturated ammonium chloride. The salt was refluxed in ethyl acetate at 80°C for 2 hours, then filtered, and the filtrate purified by automated column chromatography system to yield a 1:1 ratio of the two rotomers (54.2 mg, 13%). ^{1}H NMR (600 MHz; MeOD) * denotes rotomer. δ 8.49 (d, J = 5.0 Hz, 1H), *8.22 (d, J = 5.1 Hz, 1H), 7.89 (s, 1H), 7.83 (dd, J= 5.0 Hz, ^{4}J =0.9 Hz, 1H), *7.33 (s, 1H), *7.18 (dd, J = 5.2 Hz, ^{4}J = 0.9 Hz, 1H), 3.80 (t, J = 4.9 Hz, 4H), 3.53 (t, J = 4.9 Hz, 4 H). ^{1}H NMR (151 MHz; MeOD) * denotes rotomer. δ 168.94 (C), 167.68 (C), 161.47 (C), 153.03 (C), 151.43 (CH), *149.15 (CH), 145.41 (C), 142.18 (C), 125.28 (CH), 123.46 (CH), *113.90 (CH), *108.52 (CH), 67.72 (CH_2), 46.88 (CH_2). HRMS (ESI) for $C_{10}H_{12}N_2O_3$: Calculated $[M+H]^+$ 209.0921. Found $[M+H]^+$ 209.0924.

N-{4'-[(cyclopropylmethyl)carbamoyl]-6-methyl-[1,1'-biphenyl]-3-yl}-2-(morpholin-4-yl)pyridine-4-carboxamide (III-2): To 2-(morpholin-4-yl)pyridine-4-carboxylic acid (44.2 mg, 0.21 mmol) and EDC (27.0 mg, 0.14 mmol) was added 5'-amino-N-(cyclopropylmethyl)-2'-methyl-[1,1'-biphenyl]-4-carboxamide (**III-20**) (17.5 mg, 0.06 mmol) dissolved in 3 mL of dichloromethane. The reaction was stirred overnight and quenched with water. The product was

extracted into ethyl acetate, washed with water and brine, dried over magnesium sulfate, and purified by automated column chromatography system (1.4 mg, 4 %). ^{1}H NMR (700 MHz; $CDCl_3$) δ 8.31 (d, J = 5.0 Hz, 1H), (7.83, d, J = 8.3 Hz, 3H), 7.60 (d, J = 7.77 Hz, 1H), 7.47 (s, 1H), 7.40 (d, J = 8.1 Hz, 2H), 7.30 (d, J = 8.3 Hz, 1H), 7.13 (s, 1H), 6.92 (d, J = 4.8 Hz), 6.25 (s, 1H), 3.82 (t, J = 4.9 Hz, 4H), 3.59 (t, J = 4.9 Hz, 4H), 3.35 (dd, J = 7.0 Hz, J = 5.5 Hz, 2H), 2.24 (s, 3H), 1.10 (m, 1H), 0.58 (dt, J = 6.7 Hz, J = 5.3 Hz, 2H), 0.30 (dt, J = 4.8 Hz, J = 5.0 Hz, 2H). ^{13}C NMR (176 MHz; $CDCl_3$) δ 167.33 (C), 160.34 (C), 149.15 (CH), 144.86 (C), 144.62 (C), 143.84 (C), 141.74 (C), 135.40 (C), 133.60 (C), 132.27 (C), 131.35 (CH), 129.49 (CH), 126.97 (CH), 121.60 (CH), 119.89 (CH), 109.60 (CH), 105.12 (CH), 66.83 (CH_2), 45.56 (CH_2), 45.18 (CH_2), 20.06 (CH_3), 10.91 (CH), 3.68 (CH_2). HRMS (ESI) for $C_{28}H_{30}N_4O_3$: Calculated $[M+H]^+$ 471.2391. Found $[M+H]^+$ 471.2399.

2'-Methyl-5'-(pyridine-4-amido)-[1,1'-biphenyl]-4-carboxylic acid (III-30): Isonicotinic acid (34.5 mg, 0.28 mmol) and EDC (27.8 mg, 0.15 mmol) were stirred at room temperature for 1 hour. 5'-Amino-2'-methyl-[1,1'-biphenyl]-4-carboxylic acid (**III-17**) (26.7 mg, 0.12 mmol) was then added and stirred at room temperature for 48 h. Ammonium chloride (~6-7 mL) was added to the colourless liquid and the product was extracted into ethyl acetate, washed with brine, dried with magnesium sulfate., and purified by solid-loading automated column chromatography system to yield a white powder (10.0 mg, 26%). ^{1}H NMR (700 MHz; MeOD) δ 8.74 (d, J = 5.3 Hz, 2H), 8.10 (d, J = 8.2 Hz, 2H), 7.89 (d, J = 5.3 Hz, 2H), 7.66 (dd, J = 8.7 Hz, ^{4}J = 2.0 Hz, 1H), 7.61 (d, ^{4}J = 2.0 Hz, 1H), 7.47 (d, J = 8.2 Hz, 2H), 7.33 (d, J

= 8.3 Hz, 1 H), 2.26 (s, 3H). ^{13}C NMR (176 MHz; MeOD) δ 169. 90 (C), 166.25 (C), 151.01 (CH), 147.67 (C), 144.54 (C), 142.75 (C), 137.34 (C), 133.17 (C), 131.99 (CH), 130.94 (C), 130.73 (CH), 130.32 (CH), 123.20 (CH), 123.14 (CH), 121.69 (CH), 20.02 (CH_3). HRMS (ESI) for $C_{20}H_{16}N_2O_3$: Calculated $[M+H]^+$ 333.1234. Found $[M+H]^+$ 333.1327. Calculated $[M+Na]^+$ 355.1053. Found $[M+Na]^+$ 355.1148. Calculated $[M-H]^-$ 331.1088. Found $[M-H]^-$ 331.1346.

3.5.2 Biological Testing

Escherichia coli BW25113 Δ*bamB* Δ*tolC* Screening Constructs and Screening Conditions

For screening constructs and conditions, please see Cox 2017.[18]

Overexpression and Purification of ANT(2")-Ia

For ANT(2")-Ia purification conditions, please see Cox 2015.[15]

Testing *In Vivo* Activity of Inhibitors

Inhibitors were first screened at ¼ of the MIC for gentamicin (4 μg/mL) in *E. coli* BW25113 Δ*tolC*Δ*bamB* pGDP:*ant(2")-Ia* as described Cox 2017.[18] 1 μL of 5 mM compound solutions in DMSO were added to wells of 96-well U-bottom plates. Compounds were screened in duplicate. β-Thujaplicinol was included in every plate as an inhibition control. DMSO was used as a growth control. Overnight cultures were diluted 1:1000 in MHB II. 99 μL of diluted cell culture and gentamicin (¼ MIC) were added to each well for a final compound concentration of 50 μM. Plates were incubated at 37°C with aeration for 18 h. Cell growth was monitored by OD (λ = 600 nm). The parental strain *E. coli* BW25113

Δ*tolC*Δ*bamB* was subjected to identical conditions to account for background absorbance. OD_{600} of each well was compared to growth controls to determine percent inhibition of growth.

Dose-dependency studies and minimum inhibitory concentrations (MICs) were assessed in diluted overnight cultures of in *E. coli* BW25113 Δ*tolC*Δ*bamB* pGDP:*ant(2")-Ia* as described above. ¼ MIC gentamicin was added to the diluted culture for dose-dependency studies. No gentamicin was used in MIC tests. Compounds were tested in duplicate at concentrations of 0.5 to 128 μg/mL.

Inhibitors were also screened against parental *E. coli* BW25113 Δ*tolC*Δ*bamB* for nonspecific inhibition. 1 μL of 5 mM compound solutions in DMSO were added to wells of 96-well U-bottom plates in duplicate. Overnight cultures were diluted 1:1000 in MHB II, and 99 μL of diluted cell culture were added to each well for a final compound concentration of 50 μM. OD_{600} was read following 18 h incubation at 37°C with aeration and compared to growth controls. Some compounds were selected for follow-up MIC determination in the parental strain, as described above.

Checkerboard Assays

1 μL of increasing gentamicin (0.5 to 64 μg/mL) and inhibitor concentrations (1 to 64 μg/mL) were added to wells of a U-bottom 96-well plate. Overnight cultures of *E. coli* BW25113 Δ*bamB* Δ*tolC* with pGDP4-*ant(2")-Ia* were diluted 1:1000 in MHB II, and 98 μL added to each well for a final volume of 100 μL. Plates were incubated at 37°C with aeration for 18 h. Cell growth was

monitored by OD (λ = 600 nm). FIC was calculated according to the equation:

$$FIC = \frac{MIC_{A\ in\ combination}}{MIC_A} + \frac{MIC_{B\ in\ combination}}{MIC_B}$$

where FIC ≤ 0.5 is considered synergistic, 0.5 < FIC < 2.0 is neutral, and FIC ≥ 2.0 is antagonistic.

Monitoring ANT(2")-Ia Activity *In Vitro*

The EnzChek® pyrophosphate assay was used to monitor inhibition of ANT(2")-Ia according to manufacturer's guidelines.[35] Assays were performed in duplicate in flat bottom 96-well plates. Final concentrations of ANT(2")-Ia and ATP were 50 μg/mL and 50 μM respectively. Inhibitors (max 1% v/v DMSO) were dissolved in buffer and heated to improve solubility. The reaction mixture was incubated at room temperature for 10 min before initiation with gentamicin (final concentration 40 μM), and monitored at 360 nm for 15 min at room temperature using a TECAN M100 plate reader in 96-well format. GraphPad Prism was used to plot IC_{50} data.

3.6 REFERENCES

(1) O'Neill, J. *Tackling Drug-Resistant Infections Globally: Final Report and Recommendations*; 2016.

(2) WHO. *Global Action Plan on Antimicrobial Resistance*; Geneva, Switzerland, 2015.

(3) Payne, D. J.; Miller, L. F.; Findlay, D.; Anderson, J.; Marks, L. Time for a Change: Addressing R&D and Commercialization Challenges for Antibacterials. *Philos. Trans. R. Soc. London B Biol. Sci.* **2015**, *370* (1670), 1–12.

(4) Wermuth, C. G. Selective Optimization of Side Activities: Another Way for Drug Discovery. *J. Med. Chem.* **2004**, *47* (6), 1303–1314.

(5) Brown, E. D.; Wright, G. D. Antibacterial Drug Discovery in the Resistance Era. *Nature* **2016**, *529* (7586), 336–343.

(6) Wright, G. D. Antibiotic Adjuvants: Rescuing Antibiotics from Resistance. *Trends Microbiol.* **2016**, *24* (11), 862–871.

(7) Geddes, A. M.; Klugman, K. P.; Rolinson, G. N. Introduction: Historical Perspective and Development of Amoxicillin/Clavulanate. *Int. J. Antimicrob. Agents* **2007**, *30*, 109–112.

(8) Reading, C.; Cole, M. Clavulanic Acid: A Beta-Lactamase-Inhiting Beta-Lactam from Streptomyces Clavuligerus. *Antimicrob. Agents Chemother.* **1977**, *11* (5), 852–857.

(9) Melander, R. J.; Melander, C. The Challenge of Overcoming Antibiotic Resistance: An Adjuvant Approach? *ACS Infect. Dis.* **2017**, *3* (8), 559–563.

(10) Rasko, D. A.; Sperandio, V. Anti-Virulence Strategies to Combat Bacteria-Mediated Disease. *Nat. Rev. Drug Discov.* **2010**, *9* (2), 117–128.

(11) *The Merck Manual of Diagnosis and Therapy*, 19th ed.; Porter, R. S., Kaplan, J. L., Albert, R. K., Bowman, M. A., Braunstein, G. D., Cohen, S., Emanuel, L., Fawcett, J., Frenkel, E. P., Hendrix, S. L., et al., Eds.; Merck Sharp & Dohme Corp., A Subsidary of Merck & Co, Inc.: Whitehouse Station, NJ, 2011.

(12) Schlecht, H. P.; Bruno, C. Overview of Antibacterial Drugs https://www.merckmanuals.com/en-ca/professional/infectious-diseases/bacteria-and-antibacterial-drugs/overview-of-antibacterial-drugs (accessed May 3, 2018).

(13) Gonzalez, U. S.; Spencer, J. P. Aminoglycosides: A Practical Review. *Am. Fam. Physician* **1998**, *58* (8), 1811–1820.

(14) Shaw, K. J.; Rather, P. N.; Hare, R. S.; Miller, G. H. Molecular Genetics of Aminoglycoside Resistance Genes and Familial Relationships of the Aminoglycoside-Modifying Enzymes. *Microbiol. Rev.* **1993**, *57* (1), 138–163.

(15) Cox, G.; Stogios, P. J.; Savchenko, A.; Wright, G. D. Structural and Molecular Basis for Resistance to Aminoglycoside Antibiotics by the Adenylyltransferase ANT(2″)-Ia. *MBio* **2015**, *6* (1), e02180-14.

(16) Drewry, D.; Willson, T.; Zuercher, W. Seeding Collaborations to Advance

Kinase Science with the GSK Published Kinase Inhibitor Set (PKIS). *Curr. Top. Med. Chem.* **2014**, *14* (3), 340–342.

(17) Elkins, J. M.; Fedele, V.; Szklarz, M.; Abdul Azeez, K. R.; Salah, E.; Mikolajczyk, J.; Romanov, S.; Sepetov, N.; Huang, X.-P.; Roth, B. L.; et al. Comprehensive Characterization of the Published Kinase Inhibitor Set. *Nat. Biotechnol.* **2016**, *34* (1), 95–103.

(18) Cox, G.; Sieron, A.; King, A. M.; De Pascale, G.; Pawlowski, A. C.; Koteva, K.; Wright, G. D. A Common Platform for Antibiotic Dereplication and Adjuvant Discovery. *Cell Chem. Biol.* **2017**, *24* (1), 98–109.

(19) Angell, R. M. (GlaxoSmithKline); Bamborough, P.; Cleasby, A.; Cockerill, S. G.; Jones, K. L.; Mooney, C. J.; Somers, D. O.; Walker, A. L. Biphenyl Amide P38 Kinase Inhibitors 1: Discovery and Binding Mode. *Bioorg. Med. Chem. Lett.* **2008**, *18* (1), 318–323.

(20) Angell, R. M.; Angell, T. D.; Bamborough, P.; Brown, D.; Brown, M.; Buckton, J. B.; Cockerill, G. S.; Edwards, C. D.; Jones, K. L.; Longstaff, T.; et al. Biphenyl Amide P38 Kinase Inhibitors 2: Optimisation and SAR. *Bioorg. Med. Chem. Lett.* **2008**, *18* (1), 324–328.

(21) Angell, R. M.; Aston, N. M.; Bamborough, P.; Buckton, J. B.; Cockerill, S.; DeBoeck, S. J.; Edwards, C. D.; Holmes, D. S.; Jones, K. L.; Laine, D. I.; et al. Biphenyl Amide P38 Kinase Inhibitors 3: Improvement of Cellular and in Vivo Activity. *Bioorg. Med. Chem. Lett.* **2008**, *18* (15), 4428–4432.

(22) Angell, R. M.; Angell, T. D.; Bamborough, P.; Bamford, M. J.; Chung, C.; Cockerill, S. G.; Flack, S. S.; Jones, K. L.; Laine, D. I.; Longstaff, T.; et al. Biphenyl Amide P38 Kinase Inhibitors 4: DFG-In and DFG-Out Binding Modes. *Bioorg. Med. Chem. Lett.* **2008**, *18* (15), 4433–4437.

(23) Angell, R. M.; Aston, N. M.; Bamborough, P.; Bamford, M. J.; Cockerill, G. S.; Flack, S. S.; Laine, D. I.; Walker, A. L. Biphenyl-Derivatives as P38-Kinase Inhibitors. WO 03/033457 A1, 2003.

(24) Angell, R. M.; Aston, N. M.; Bamborough, P.; Bamford, M. J.; Cockerill, G. S.; Flack, S. S.; Laine, D. I.; Walker, A. L. Biphenylcarboxylic Amide Derivatives as P38 Kinase Inhibitors. WO 03/033483 A1, 2003.

(25) Angell, R. M.; Aston, N. M.; Bamborough, P.; Bamford, M. J.; Cockerill, G. S.; Flack, S. S.; Laine, D. I.; Merrick, S. J.; Smith, K. J.; Walker, A. L.. 5'-Acylamino-1,1'-Biphenyl-4-Carboxamide Derivatives and Their Uses as P38 Kinase Inhibitors. WO 03/032971 A1, 2003.

(26) Burk, D. L.; Berghuis, A. M. Protein Kinase Inhibitors and Antibiotic Resistance. *Pharmacol. Ther.* **2002**, *93* (2–3), 283–292.

(27) Lennox, A. J. J.; Lloyd-Jones, G. C. Selection of Boron Reagents for Suzuki-Miyaura Coupling. *Chem. Soc. Rev.* **2014**, *43* (1), 412–443.

(28) Kilic-Kurt, Z.; Bakar, F.; Olgen, S. Synthesis, Biological, and Computational Evaluation of Novel 1,3,5-Substituted Indolin-2-One Derivatives as Inhibitors of Src Tyrosine Kinase. *Arch. Pharm. (Weinheim).* **2015**, *348* (10), 715–729.

(29) Al-Karmi, S. A. Molecular Imaging Agents for Cathepsin B, McMaster University, 2016.

(30) Adjabeng, G.; Brenstrum, T.; Wilson, J.; Frampton, C.; Robertson, A.; Hillhouse, J.; McNulty, J.; Capretta, A. Novel Class of Tertiary Phosphine Ligands Based on a Phospha-Adamantane Framework and Use in the Suzuki Cross-Coupling Reactions of Aryl Halides under Mild Conditions. *Org. Lett.* **2003**, *5* (6), 953–955.

(31) Leckett, K. Development and Application of Synthetic Methods for the Production of Small Molecule Libraries, McMaster University, 2016.

(32) Abaee, M. S.; Akbarzadeh, E.; Sharifi, R.; Mojtahedi, M. M. Environmentally Friendly Transesterification and Transacylation Reactions under LiBr Catalysis. *Monatshefte fur Chemie* **2010**, *141* (7), 757–761.

(33) Kishikawa, Kuniyuki;Yamada, Yusuke; Kusaka, Hiroko; Mori, Kiyotoshi; Nakasato, Y. Isoquinoline Derivative. 2008026704, 2008.

(34) Hirsch, D. R.; Cox, G.; D'Erasmo, M. P.; Shakya, T.; Meck, C.; Mohd, N.; Wright, G. D.; Murelli, R. P. Inhibition of the ANT(2″)-Ia Resistance Enzyme and Rescue of Aminoglycoside Antibiotic Activity by Synthetic α-Hydroxytropolones. *Bioorg. Med. Chem. Lett.* **2014**, *24* (21), 4943–4947.

(35) *EnzChek® Pyrophosphate Assay Kit (E-6645)*.

(36) Müller, G. Medicinal Chemistry of Target Family-Directed Masterkeys. *Drug Discov. Today* **2003**, *8* (15), 681–691.

3.7 SUPPLEMENTARY DATA

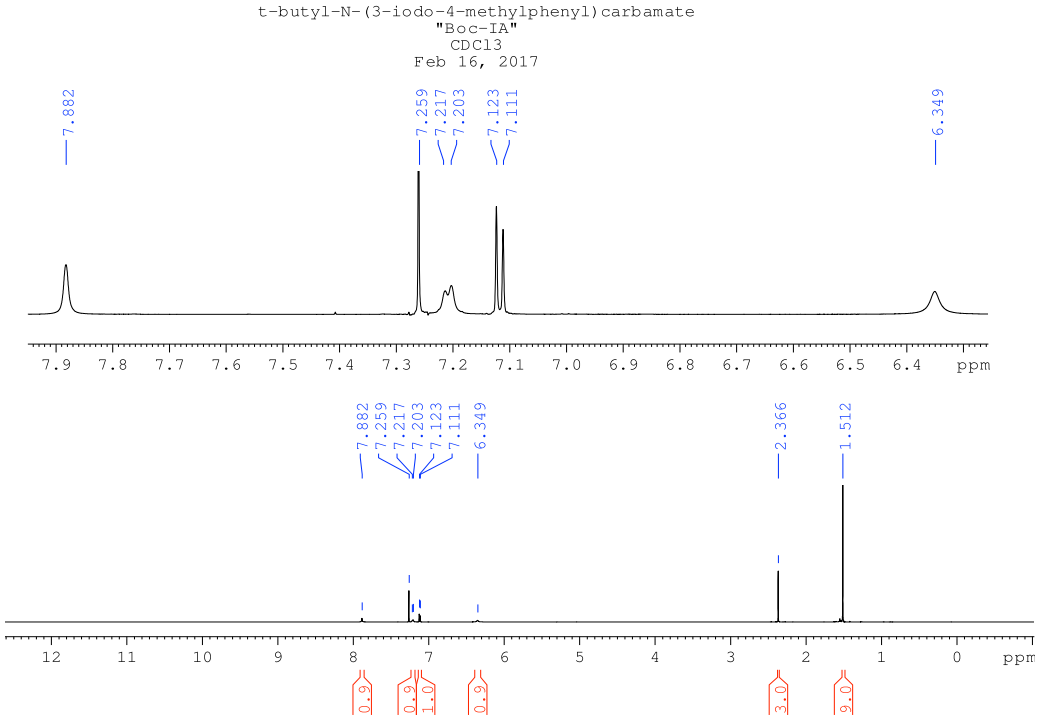

Figure S3-1. ^{1}H NMR of *tert*-Butyl-N-(3-Iodo-4-Methylphenyl)carbamate (**III-9**)

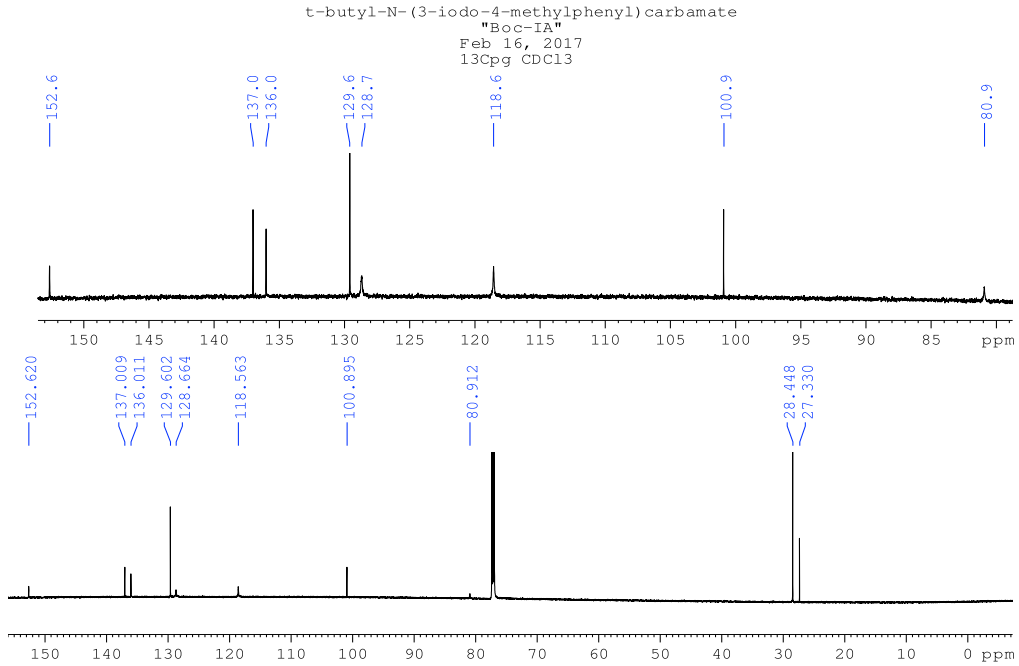

Figure S3-2. ^{13}C NMR of *tert*-Butyl-N-(3-Iodo-4-Methylphenyl)carbamate (**III-9**)

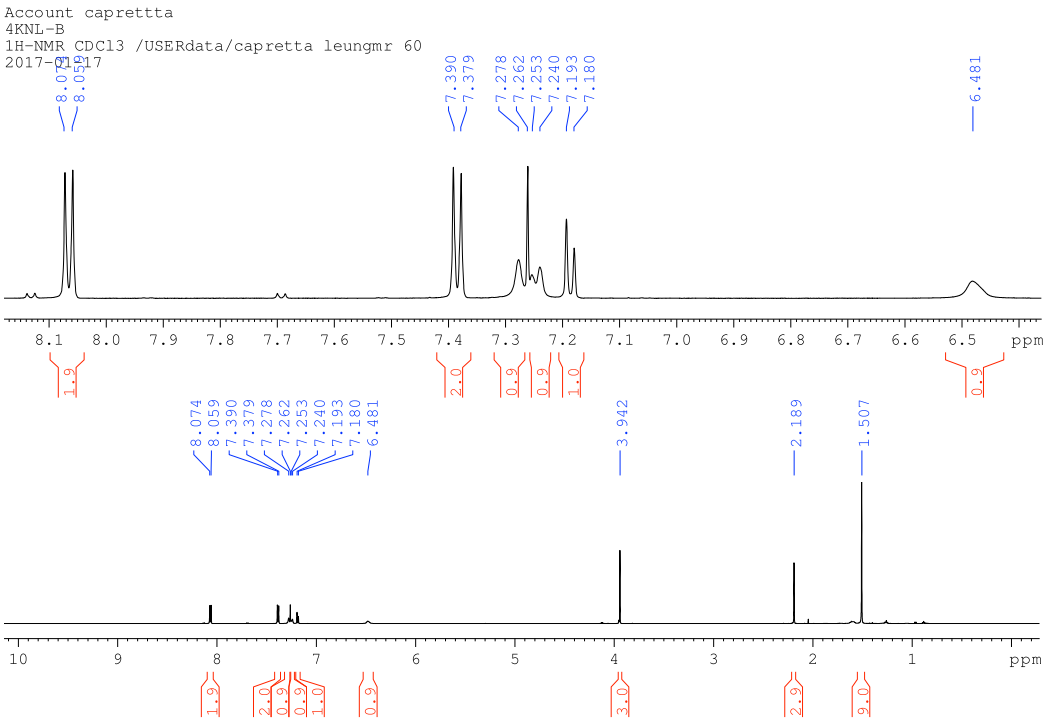

Figure S3-3. ^{1}H NMR of Methyl 5'-{[(*tert*-Butoxy)carbonyl]amino}-2'-Methyl-[1,1'-Biphenyl]-4-Carboxylate (**III-11**)

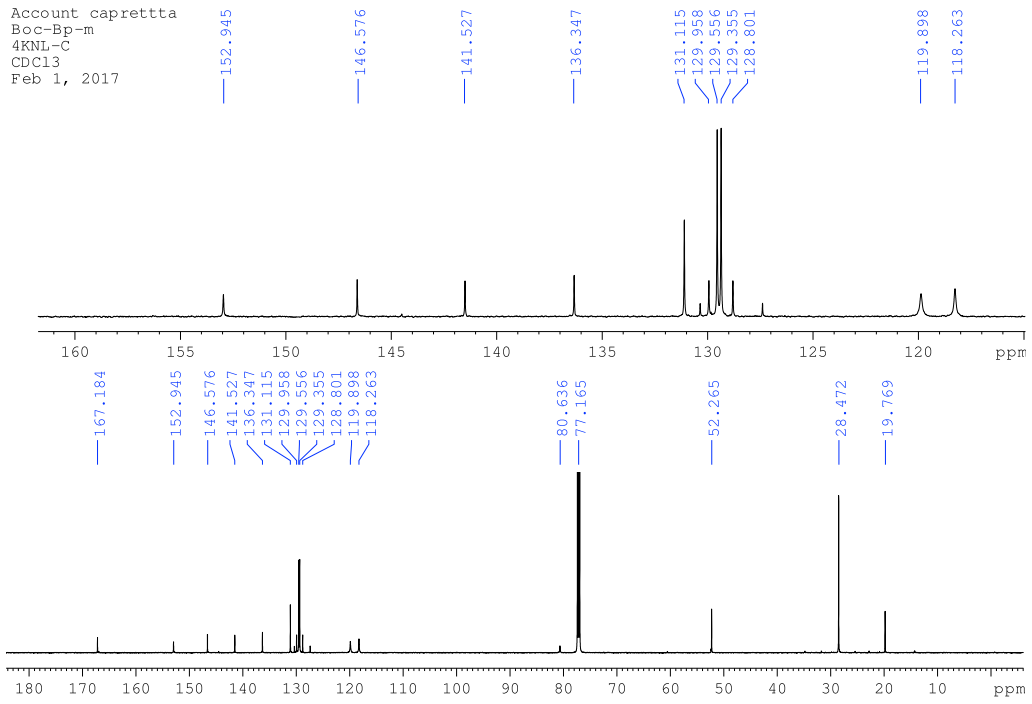

Figure S3-4. ^{13}C NMR of Methyl 5'-{[(*tert*-Butoxy)carbonyl]amino}-2'-Methyl-[1,1'-Biphenyl]-4-Carboxylate (**III-11**)

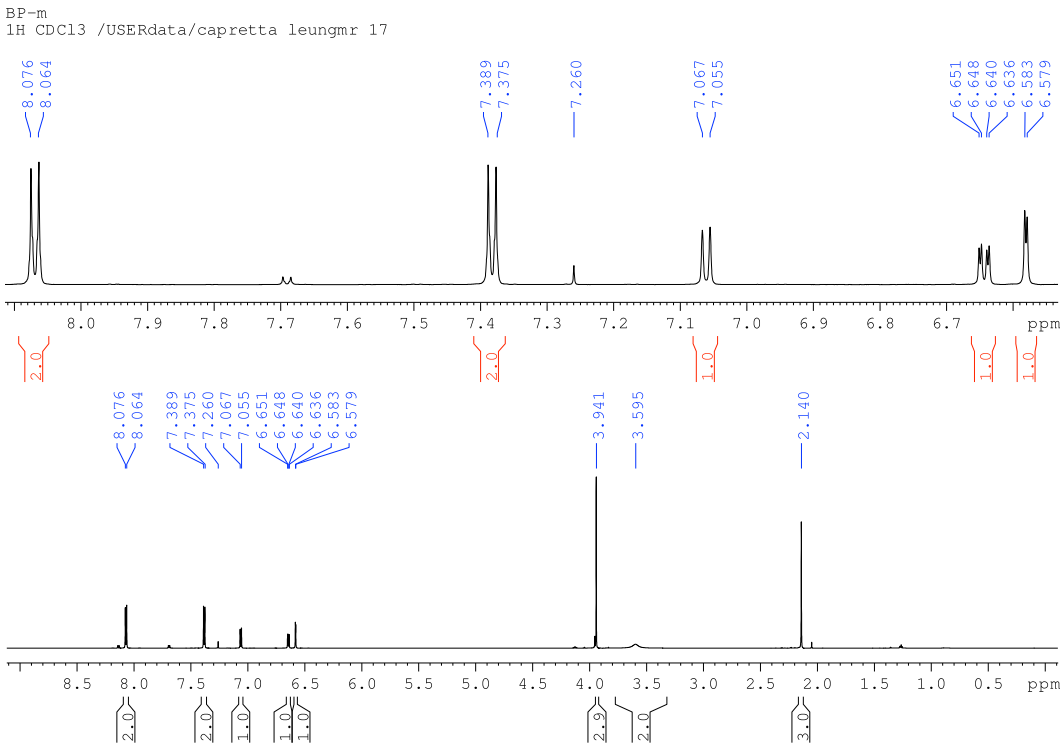

Figure S3-5. ^{1}H NMR of Methyl 5'-Amino-2'-Methyl-[1,1'-Biphenyl]-4-Carboxylate (**III-12**)

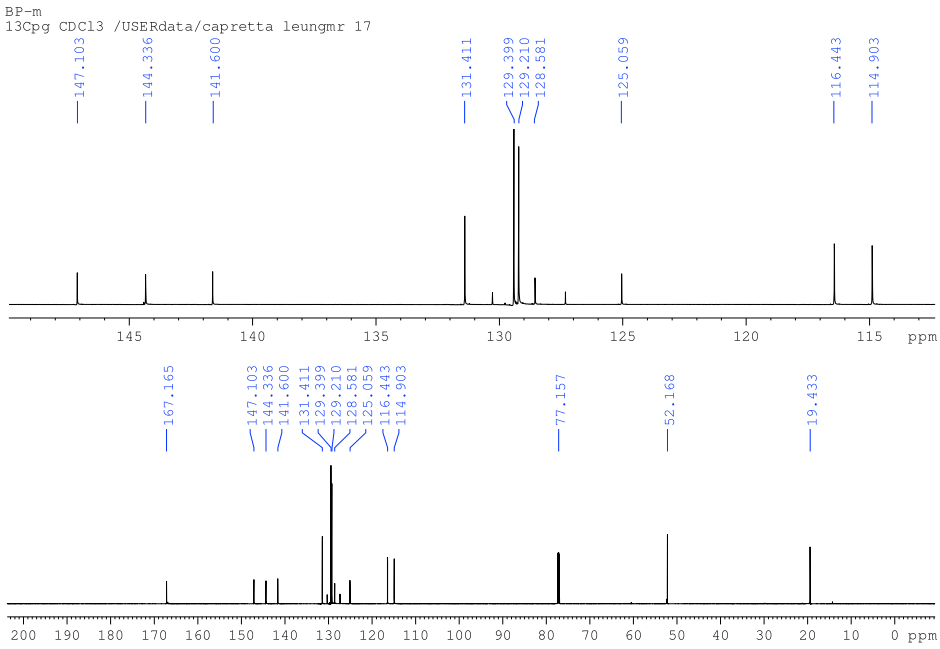

Figure S3-6. ^{13}C NMR of Methyl 5'-Amino-2'-Methyl-[1,1'-Biphenyl]-4-Carboxylate (**III-12**)

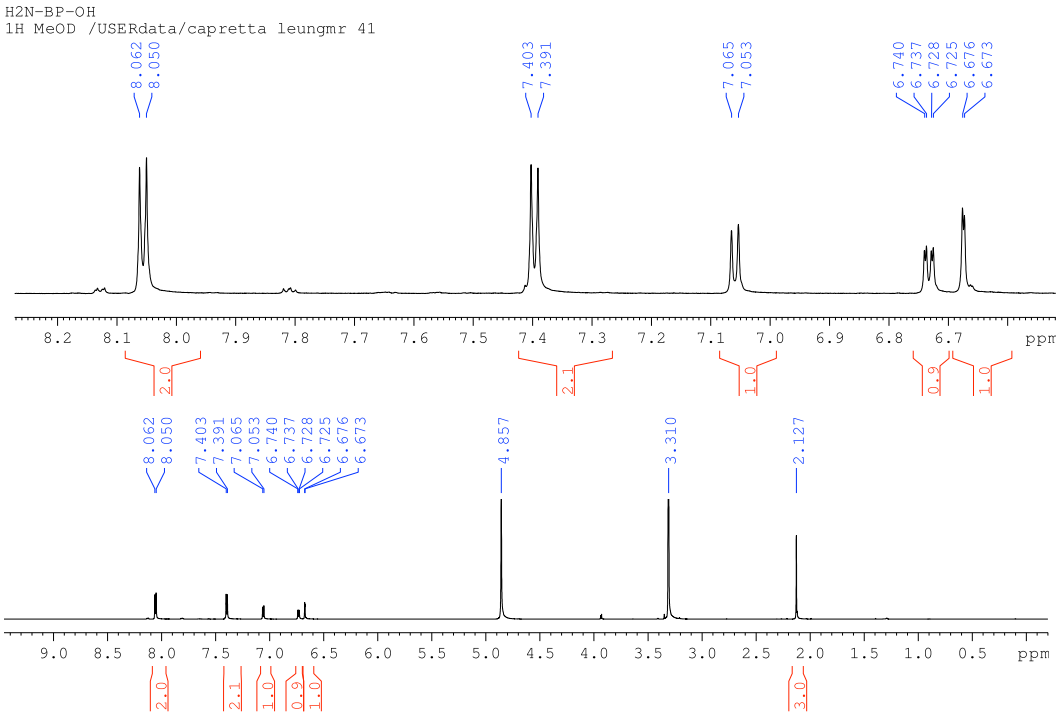

Figure S3-7. ^{1}H NMR of 5'-Amino-2'-Methyl-[1,1'-Biphenyl]-4-Carboxylic Acid (**III-17**)

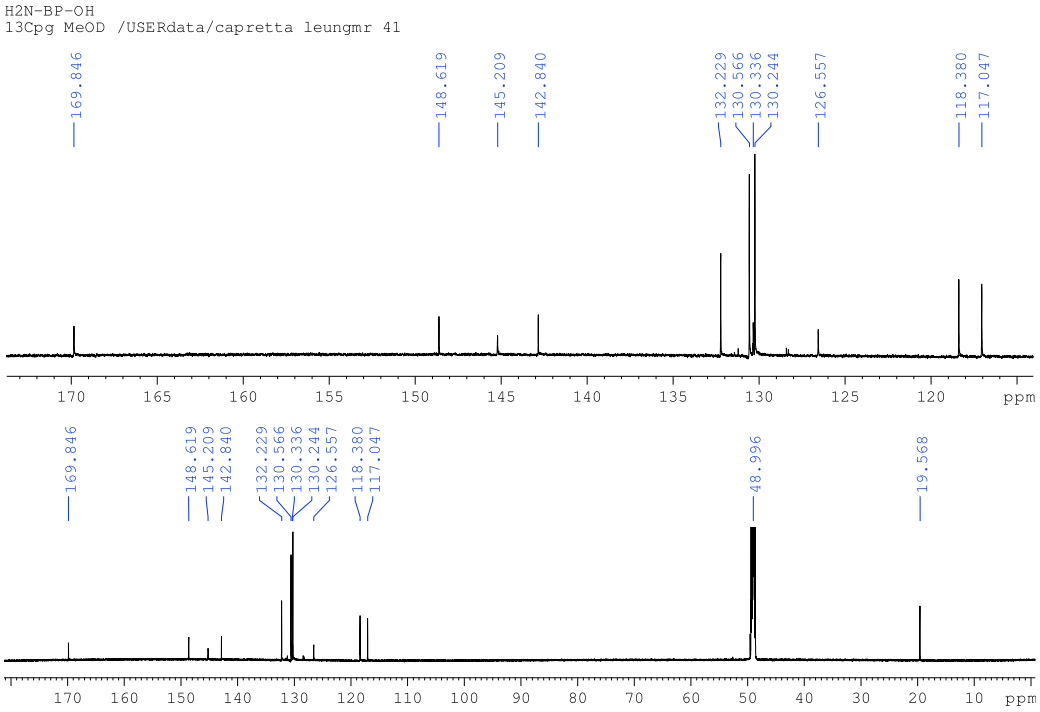

Figure S3-8. ^{13}C NMR of 5'-Amino-2'-Methyl-[1,1'-Biphenyl]-4-Carboxylic Acid (**III-17**)

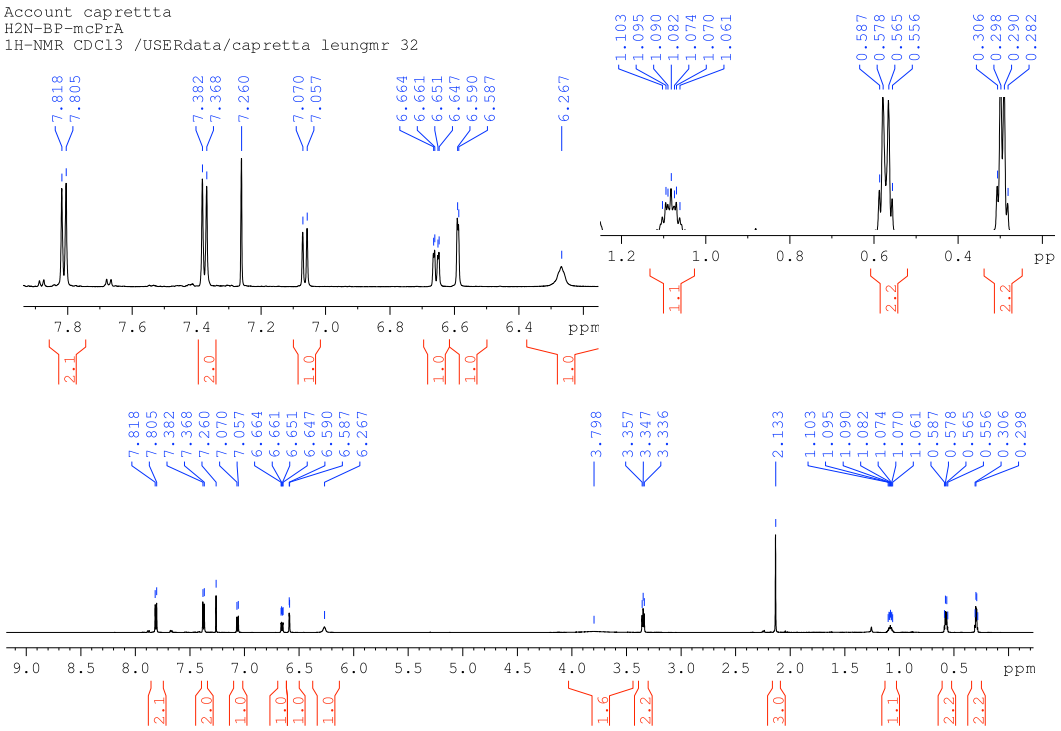

Figure S3-9. ^{1}H NMR of 5'-Amino-N-(Cyclopropylmethyl)-2'-Methyl-[1,1'-Biphenyl]-4-Carboxamide (**III-20**)

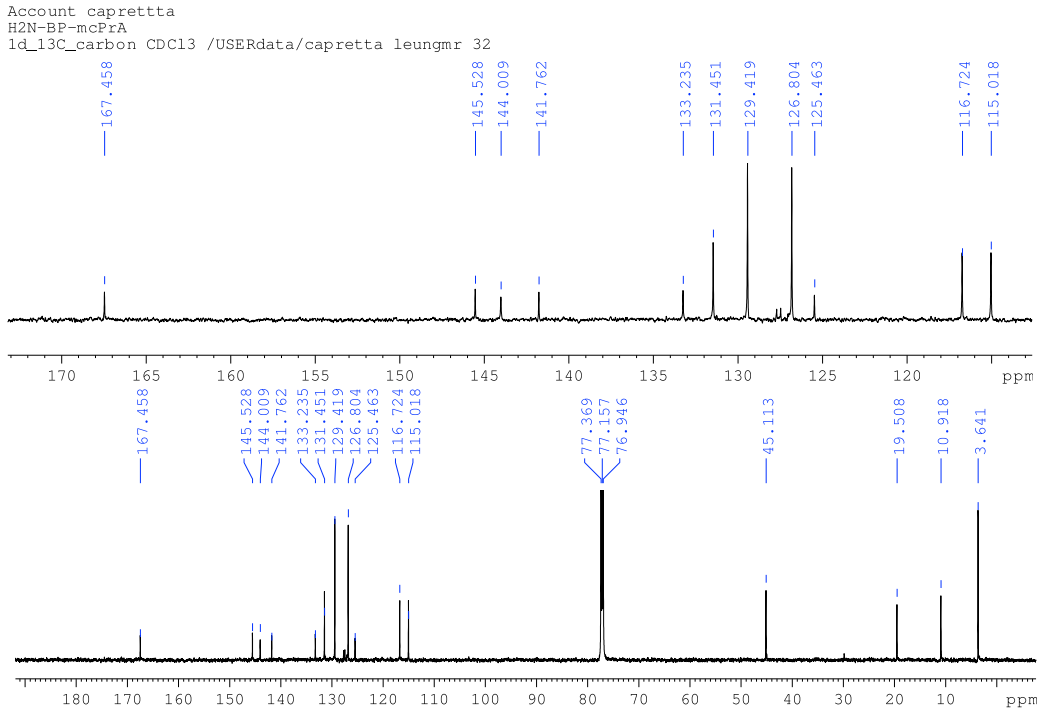

Figure S3-10. ^{13}C NMR of 5'-Amino-N-(Cyclopropylmethyl)-2'-Methyl-[1,1'-Biphenyl]-4-Carboxamide (**III-20**)

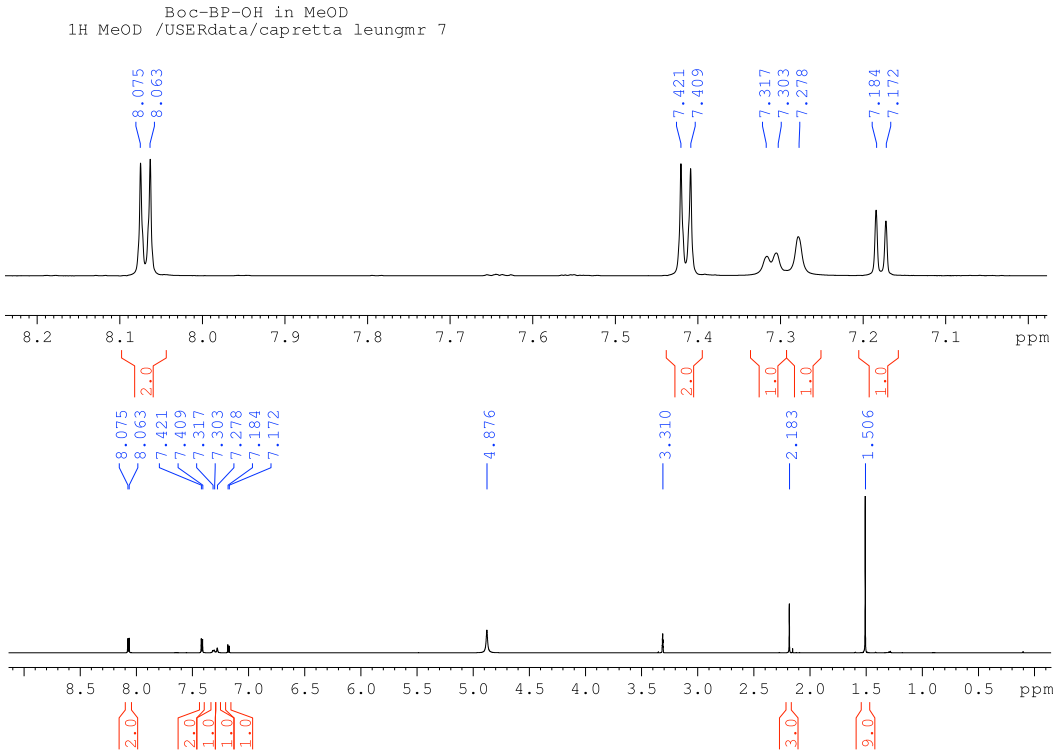

Figure S3-11. ^{1}H NMR of 5'-{[(*tert*-Butoxy)carbonyl]amino}-2'-Methyl-[1,1'-Biphenyl]-4-Carboxylic Acid (**III-16**)

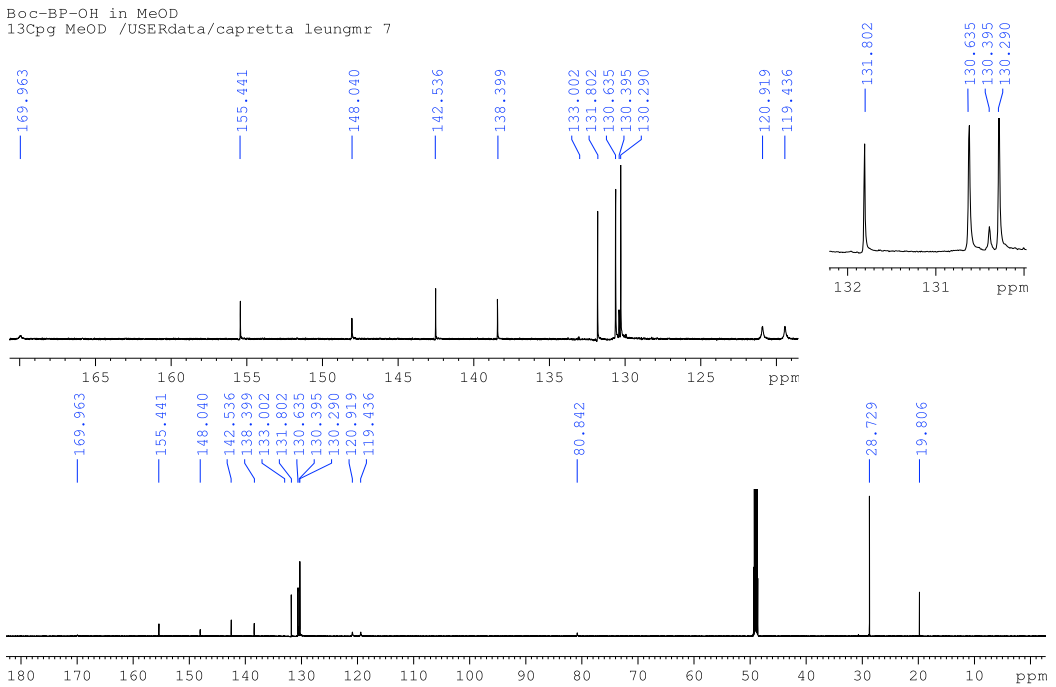

Figure S3-12. ^{13}C NMR of 5'-{[(*tert*-Butoxy)carbonyl]amino}-2'-Methyl-[1,1'-Biphenyl]-4-Carboxylic Acid (**III-16**)

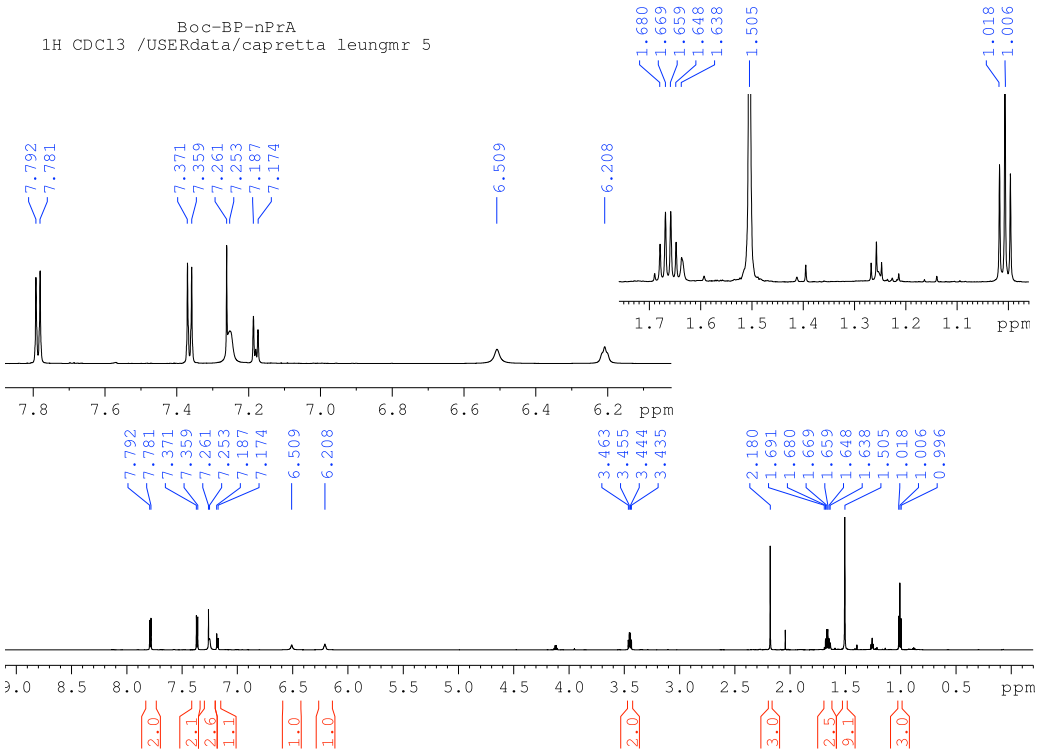

Figure S3-13. ^{1}H NMR of *tert*-Butyl N-{6-Methyl-4'-(Propylcarbamoyl)-[1,1'-Biphenyl]-3-yl}carbamate (**III-26**)

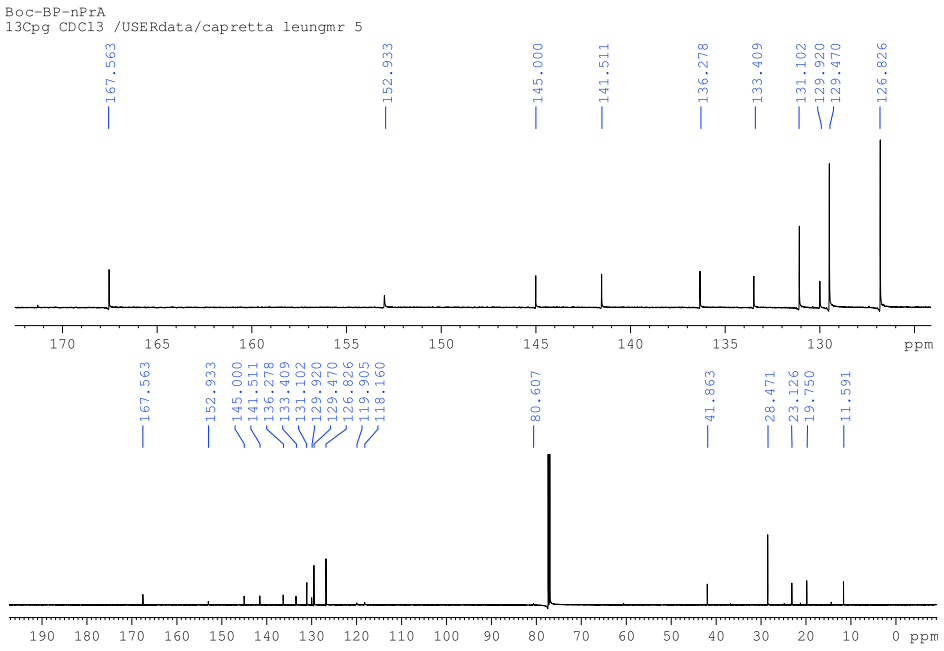

Figure S3-14. ^{13}C NMR of *tert*-Butyl N-{6-Methyl-4'-(Propylcarbamoyl)-[1,1'-Biphenyl]-3-yl}carbamate (**III-26**)

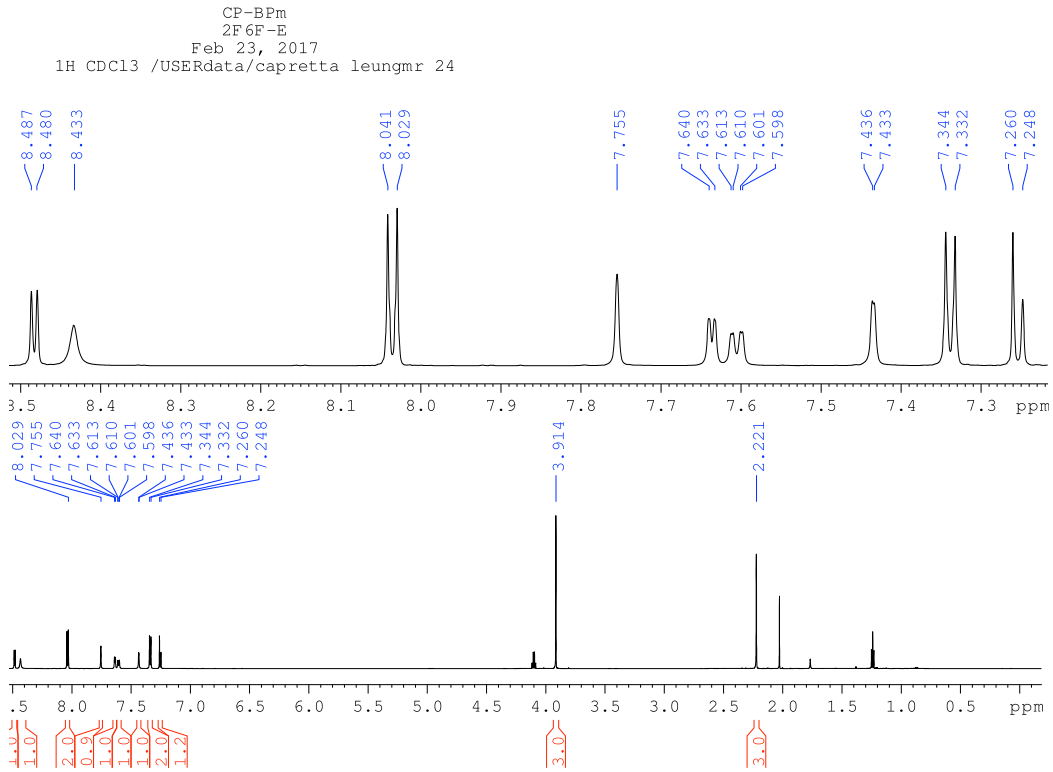

Figure S3-15. ^{1}H NMR of Methyl 5'-(2-Chloropyridine-4-Amido)-2'-Methyl-[1,1'-Biphenyl]-4-Carboxylate (**III-14**)

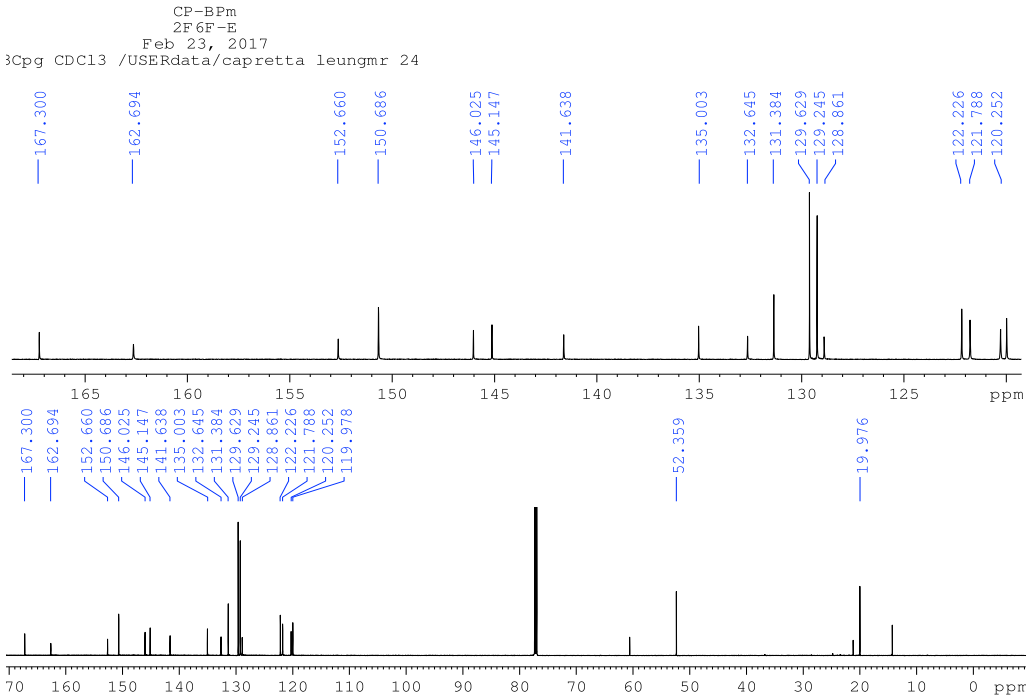

Figure S3-16. ^{13}C NMR of Methyl 5'-(2-Chloropyridine-4-Amido)-2'-Methyl-[1,1'-Biphenyl]-4-Carboxylate (**III-14**)

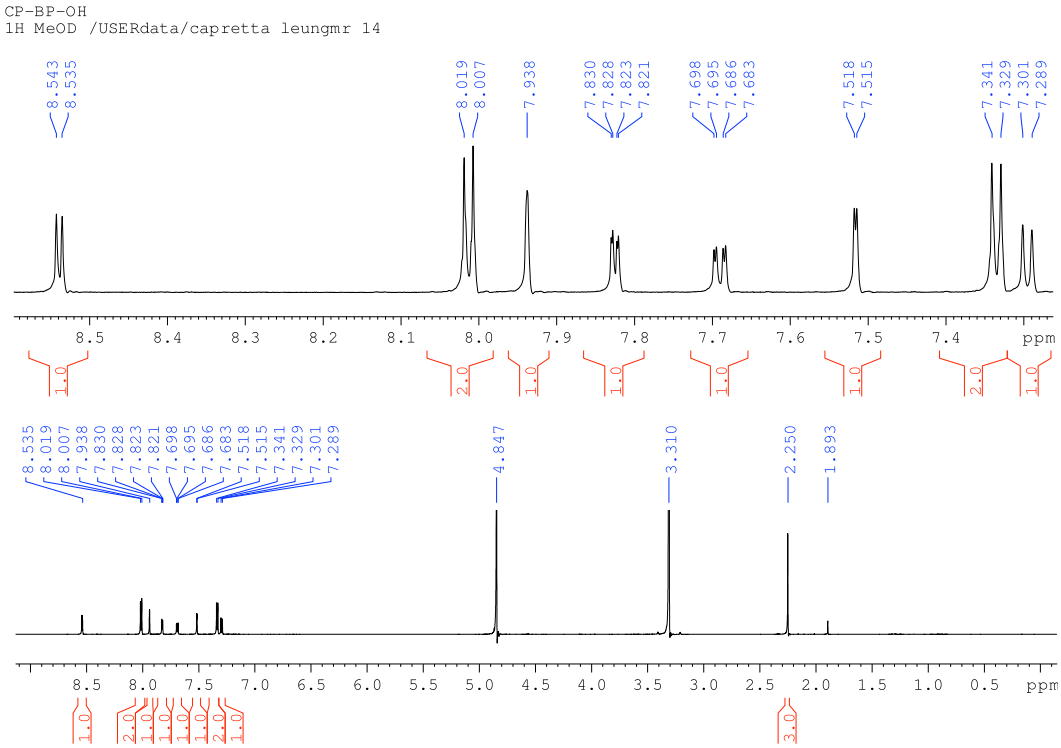

Figure S3-17. ^{1}H NMR of 5'-(2-Chloropyridine-4-Amido)-2'-Methyl-[1,1'-Biphenyl]-4-Carboxylic Acid (**III-15**)

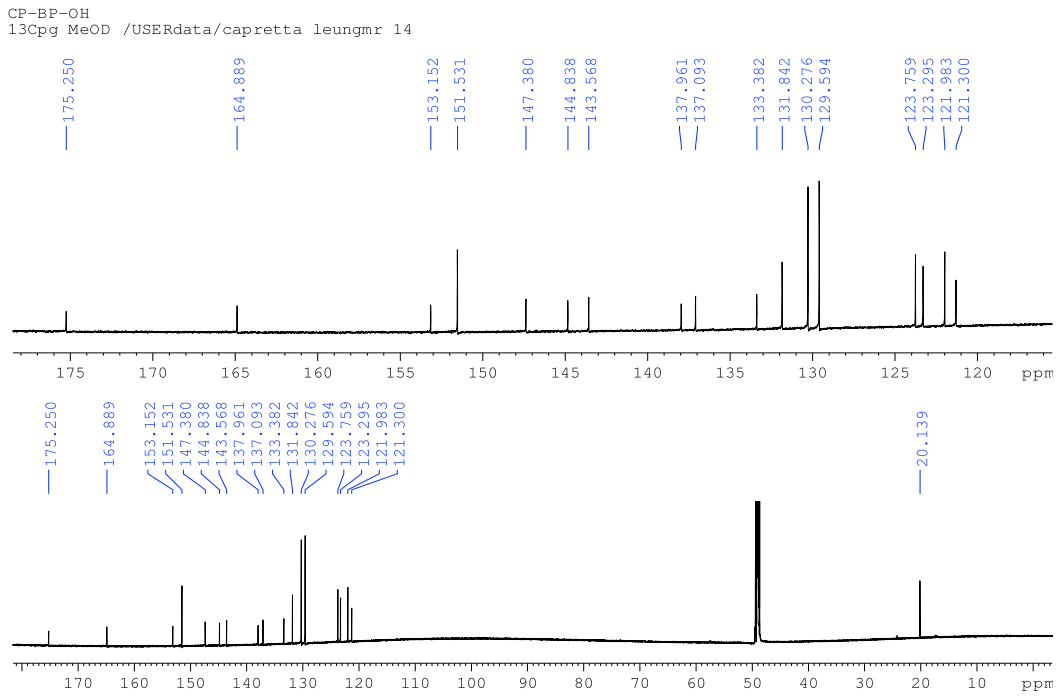

Figure S3-18. ^{13}C NMR of 5'-(2-Chloropyridine-4-Amido)-2'-Methyl-[1,1'-Biphenyl]-4-Carboxylic Acid (**III-15**)

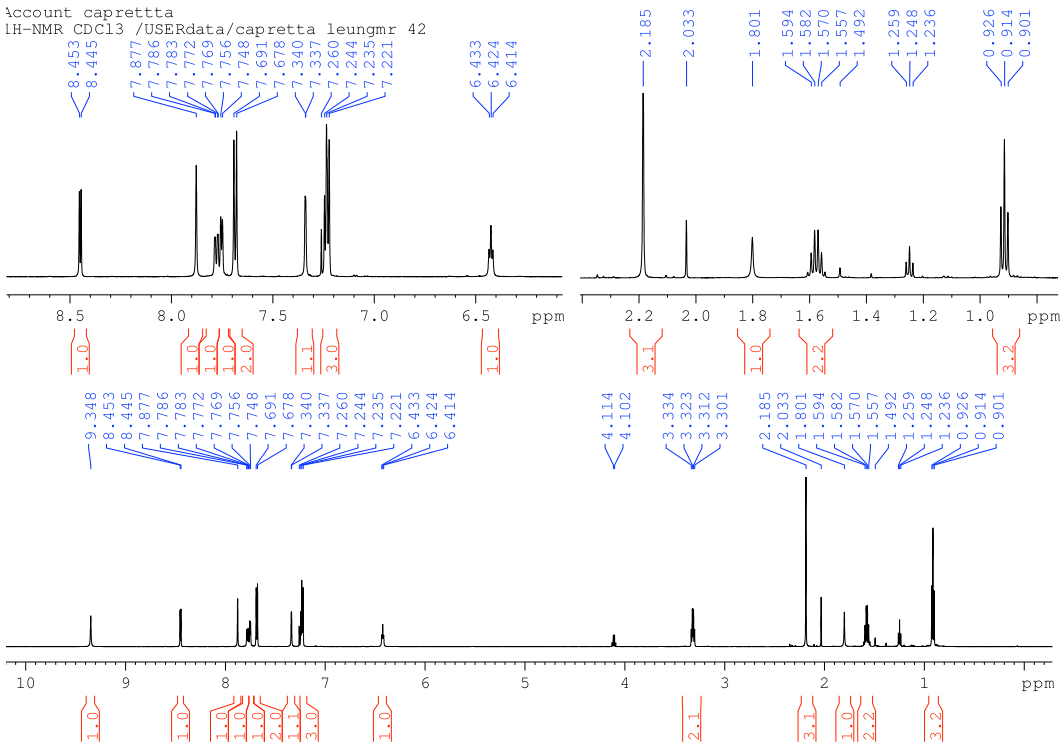

Figure S3-19. ^{1}H NMR of 2-Chloro-N-{6-Methyl-4'-(Propylcarbamoyl)-[1,1'-Biphenyl]-3-yl}Pyridine-4-Carboxamide (**III-27**)

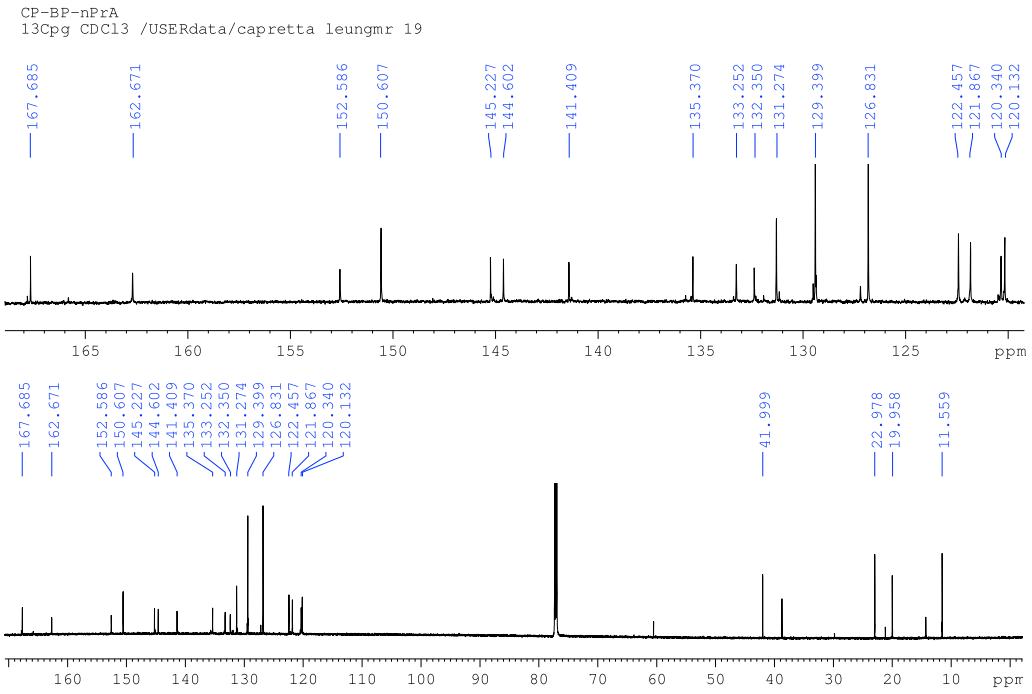

Figure S3-20. ^{13}C NMR of 2-Chloro-N-{6-Methyl-4'-(Propylcarbamoyl)-[1,1'-Biphenyl]-3-yl}Pyridine-4-Carboxamide (**III-27**)

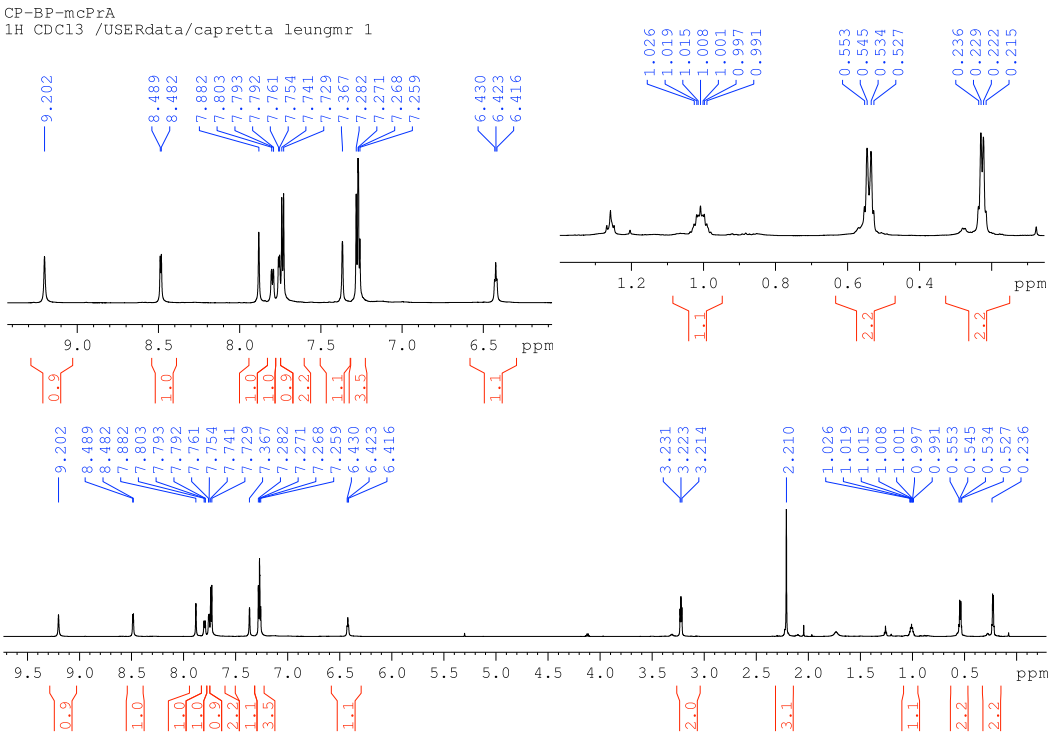

Figure S3-21. ^{1}H NMR of 2-Chloro-N-{4'-[(Cyclopropylmethyl)carbamoyl]-6-Methyl-[1,1'-Biphenyl]-3-yl}pyridine-4-Carboxamide (**III-18**)

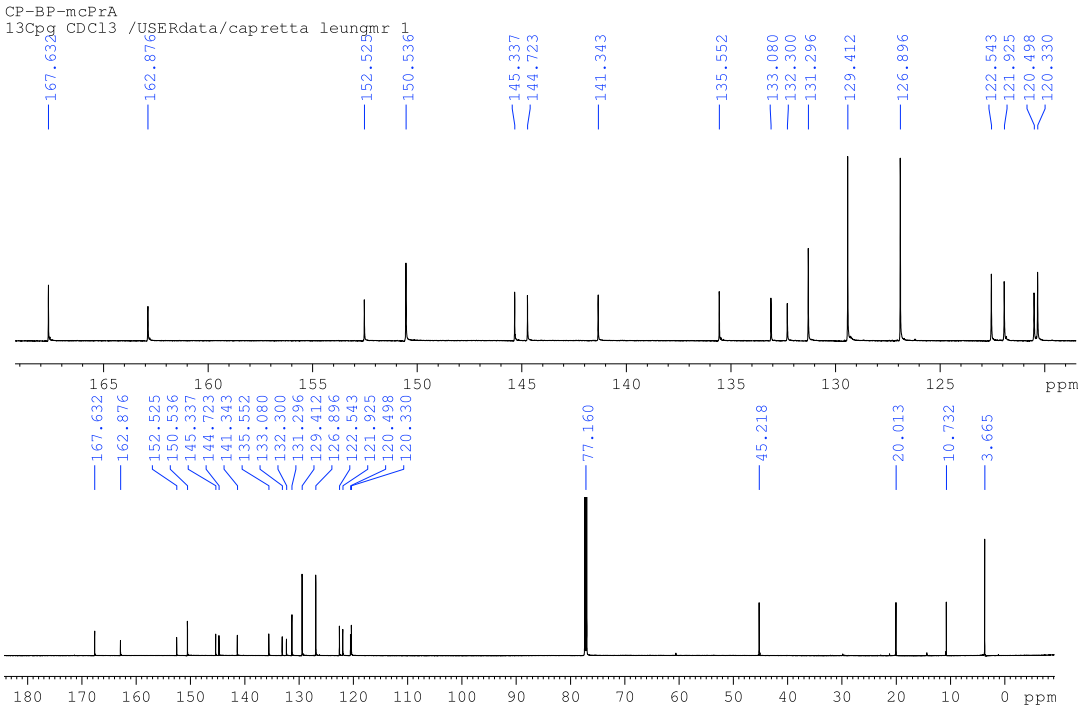

Figure S3-22. ^{13}C NMR of 2-Chloro-N-{4'-[(Cyclopropylmethyl)carbamoyl]-6-Methyl-[1,1'-Biphenyl]-3-yl}pyridine-4-Carboxamide (**III-18**)

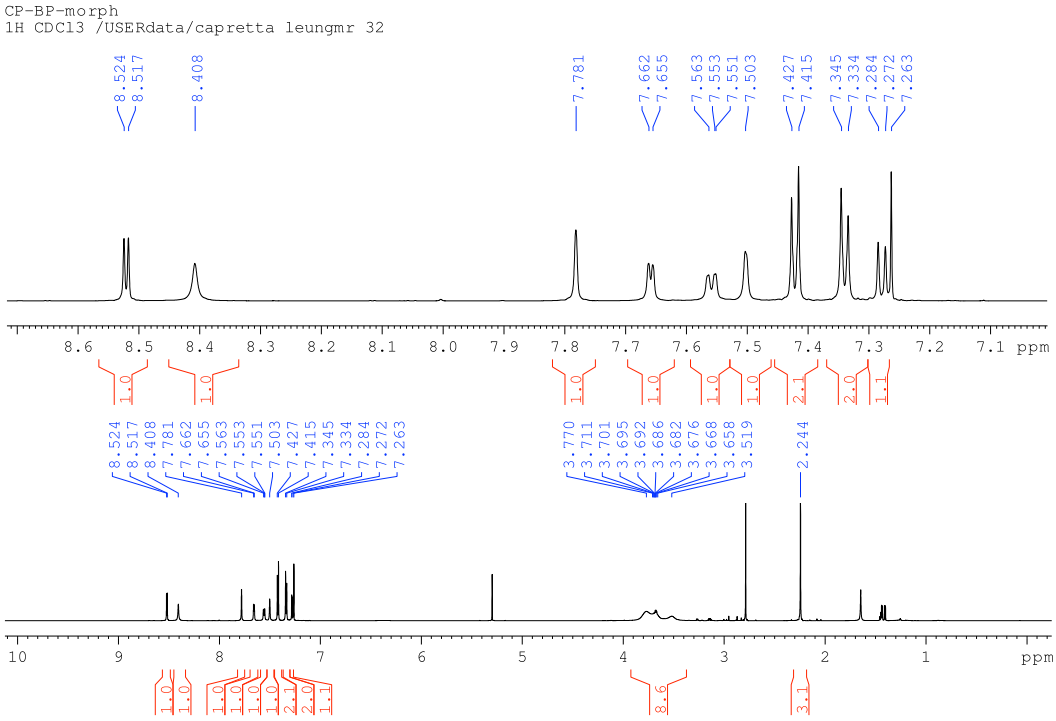

Figure S3-23. ^{1}H NMR of 2-Chloro-N-{6-Methyl-4'-(Morpholine-4-Carbonyl)-[1,1'-Biphenyl]-3-yl}pyridine-4-Carboxamide (**III-19**)

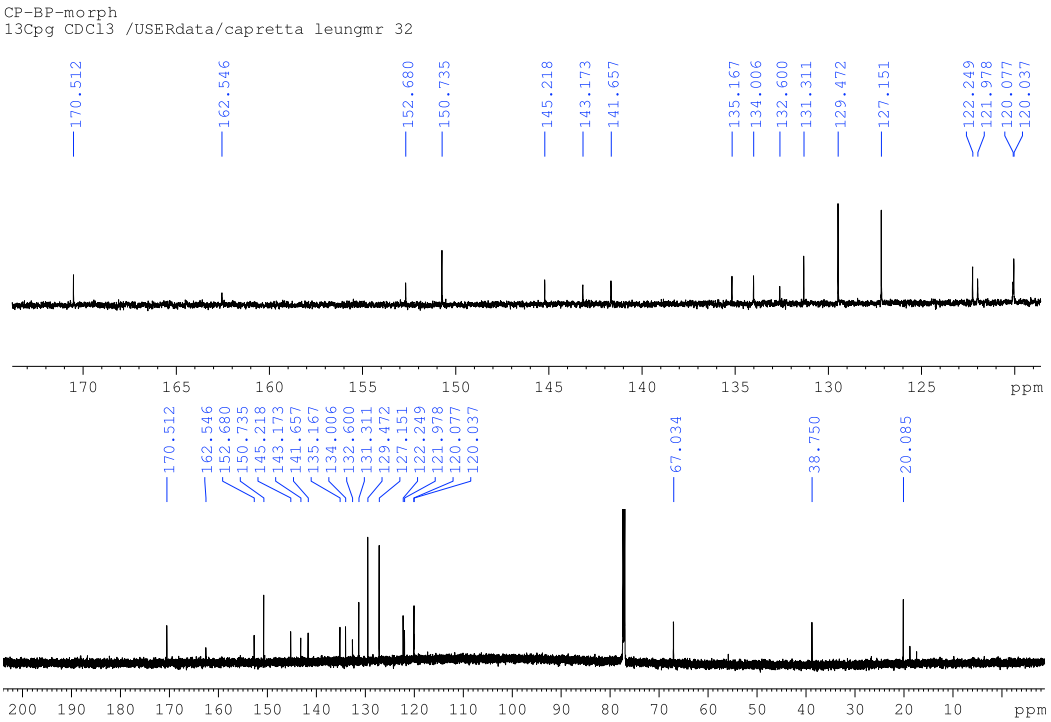

Figure S3-24. ^{13}C NMR of 2-Chloro-N-{6-Methyl-4'-(Morpholine-4-Carbonyl)-[1,1'-Biphenyl]-3-yl}pyridine-4-Carboxamide (**III-19**)

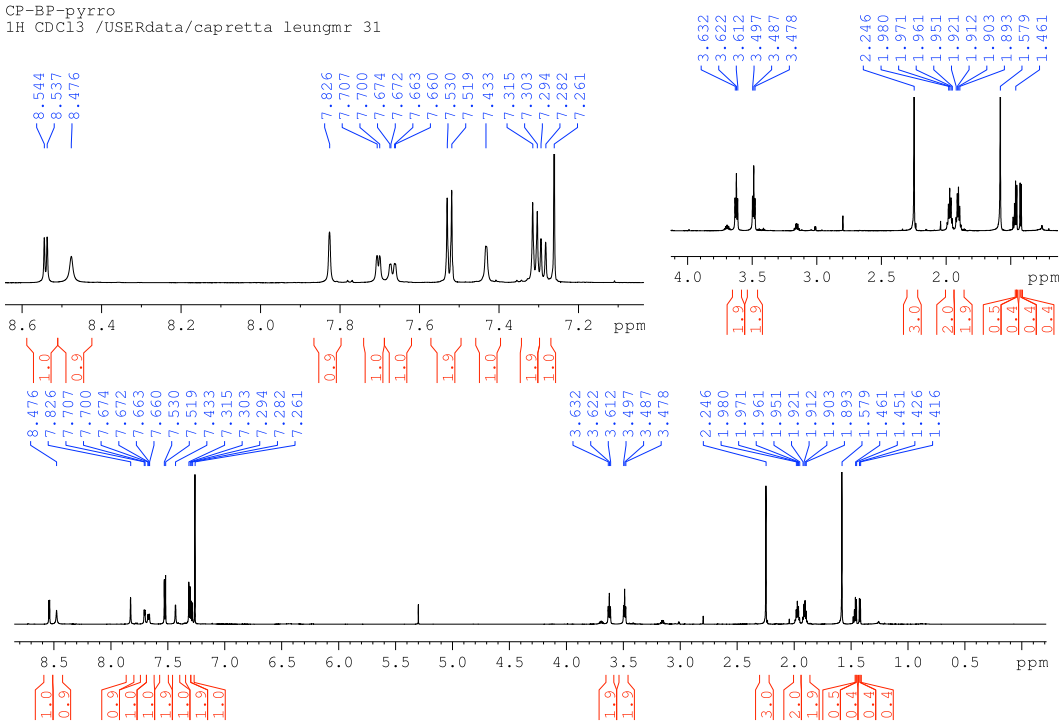

Figure S3-25. ^{1}H NMR of 2-Chloro-N-{6-Methyl-4'-(Pyrrolidine-1-Carbonyl)-[1,1'-Biphenyl]-3-yl}pyridine-4-Carboxamide (**III-28**)

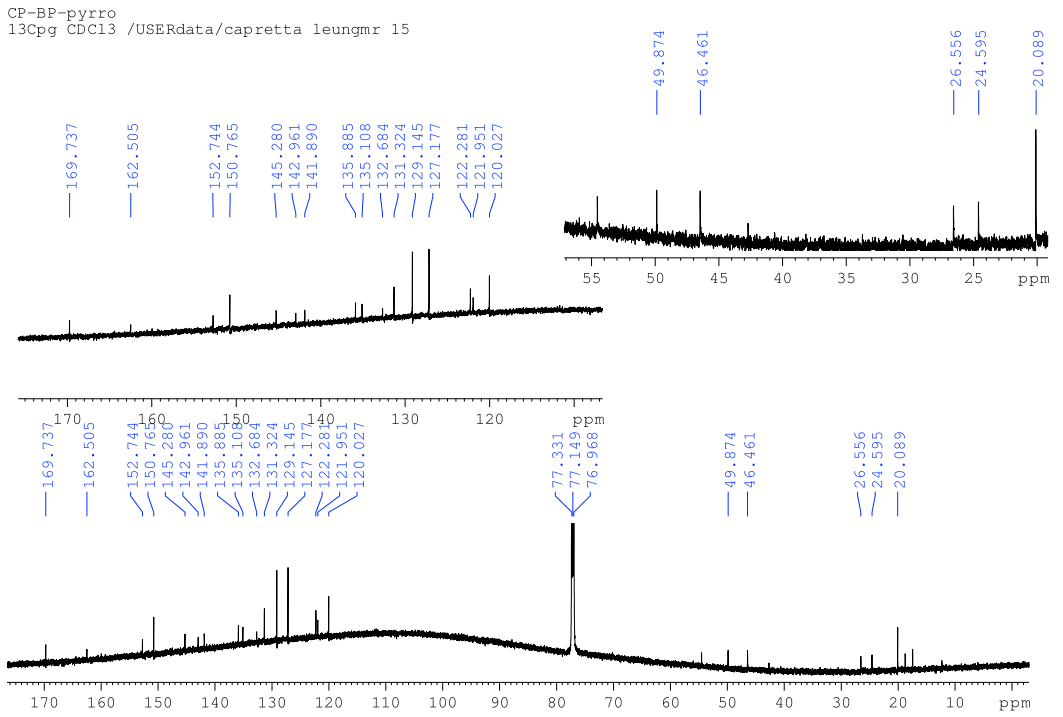

Figure S3-26. ^{13}C NMR of 2-Chloro-N-{6-Methyl-4'-(Pyrrolidine-1-Carbonyl)-[1,1'-Biphenyl]-3-yl}pyridine-4-Carboxamide (**III-28**)

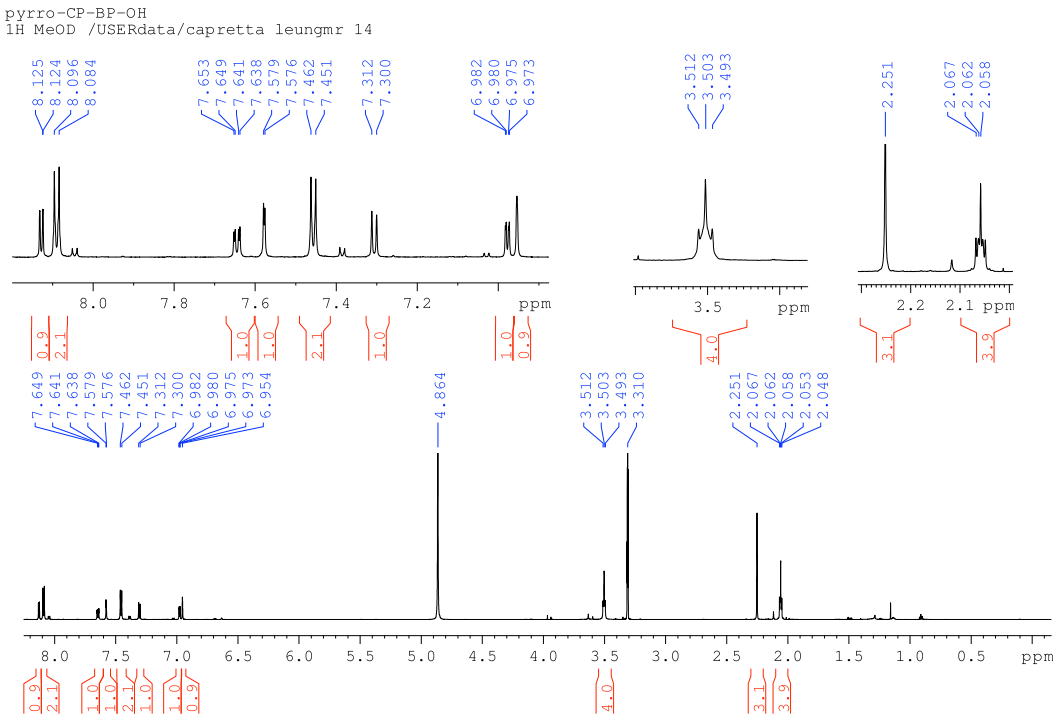

Figure S3-27. ^{1}H NMR of 2'-Methyl-5'-[(2-Pyrrolidin-1-yl)pyridine-Amido]-1,1'-Biphenyl-4-Carboxylic Acid (**III-23**)

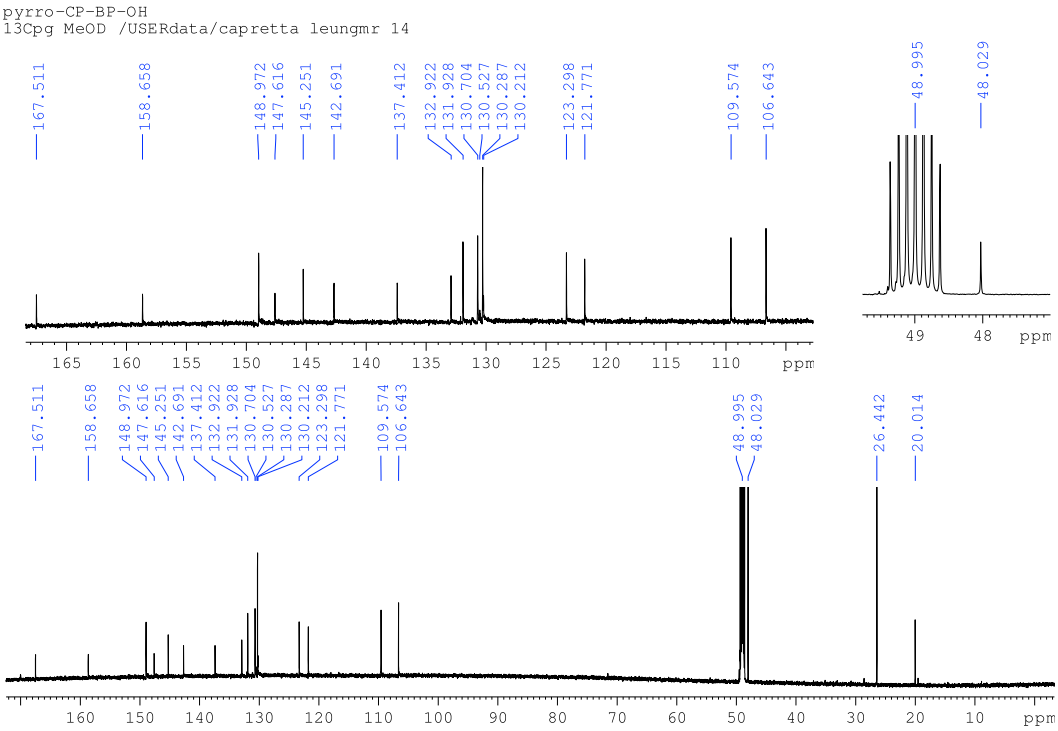

Figure S3-28. ^{13}C NMR of 2'-Methyl-5'-[(2-Pyrrolidin-1-yl)pyridine-Amido]-1,1'-Biphenyl-4-Carboxylic Acid (**III-23**)

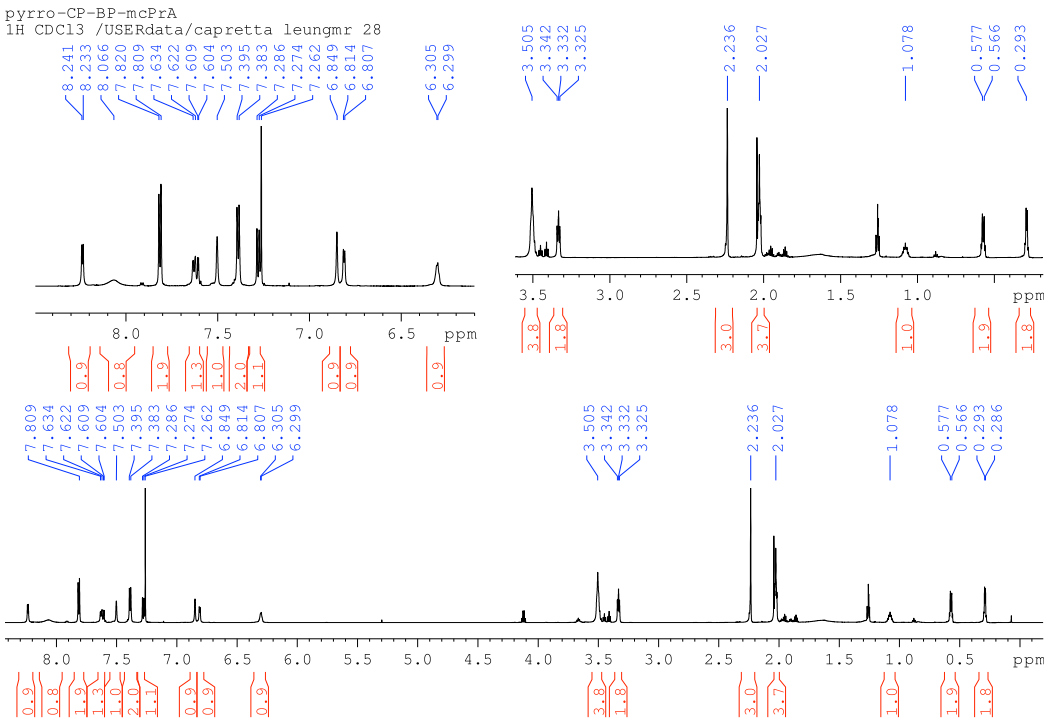

Figure S3-29. ^{1}H NMR of N-{4'-[(Cyclopropylmethyl)carbamoyl]-6-Methyl-[1,1'-Biphenyl]-3-yl}-2-(Pyrrolidin-1-yl)pyridine-4-Carboxamide (**III-1**)

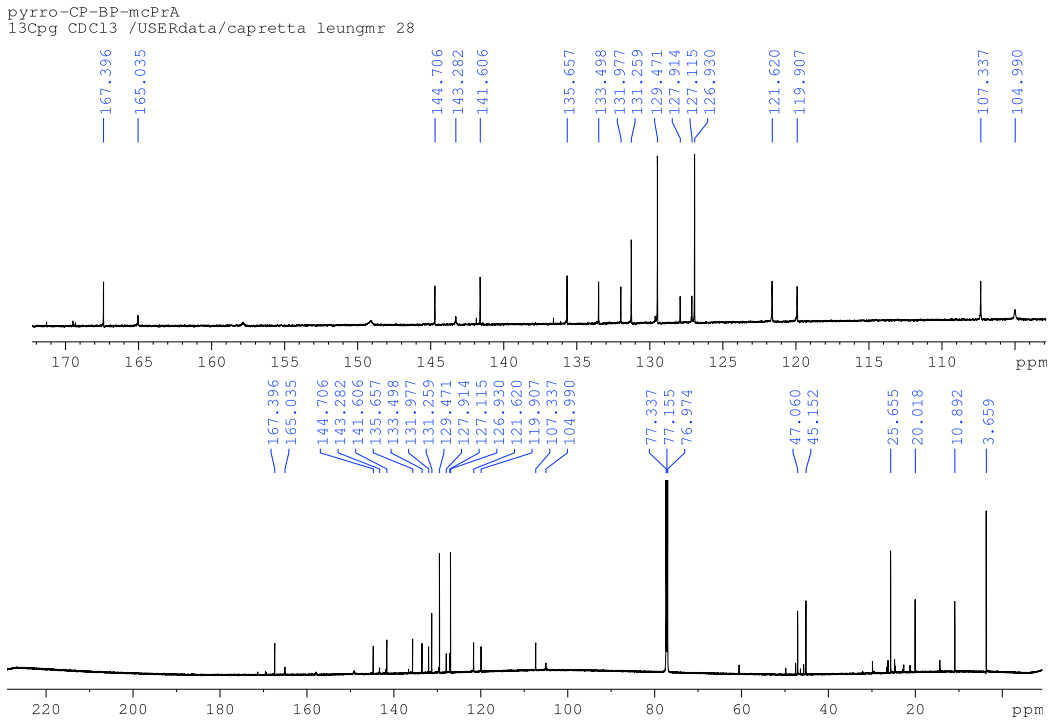

Figure S3-30. ^{13}C NMR of N-{4'-[(Cyclopropylmethyl)carbamoyl]-6-Methyl-[1,1'-Biphenyl]-3-yl}-2-(Pyrrolidin-1-yl)pyridine-4-Carboxamide (**III-1**)

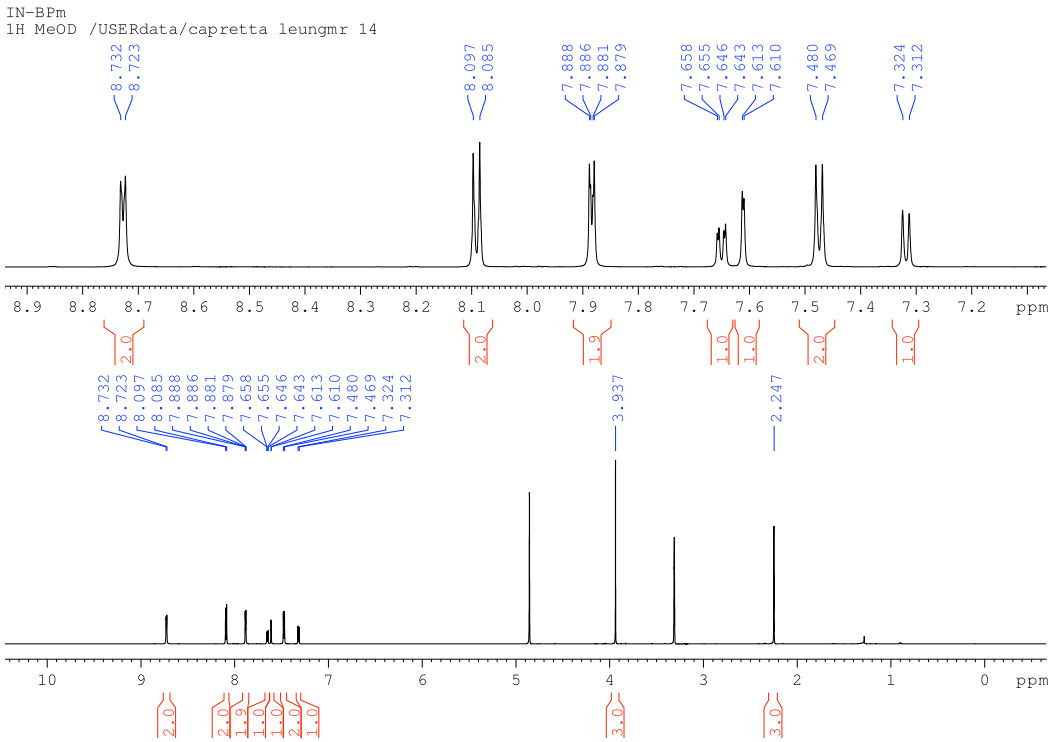

Figure S3-31. ^{1}H NMR of Methyl 2'-Methyl-5'-(Pyridine-4-Amido)-[1,1'-Biphenyl]-4-Carboxylate (**III-21**)

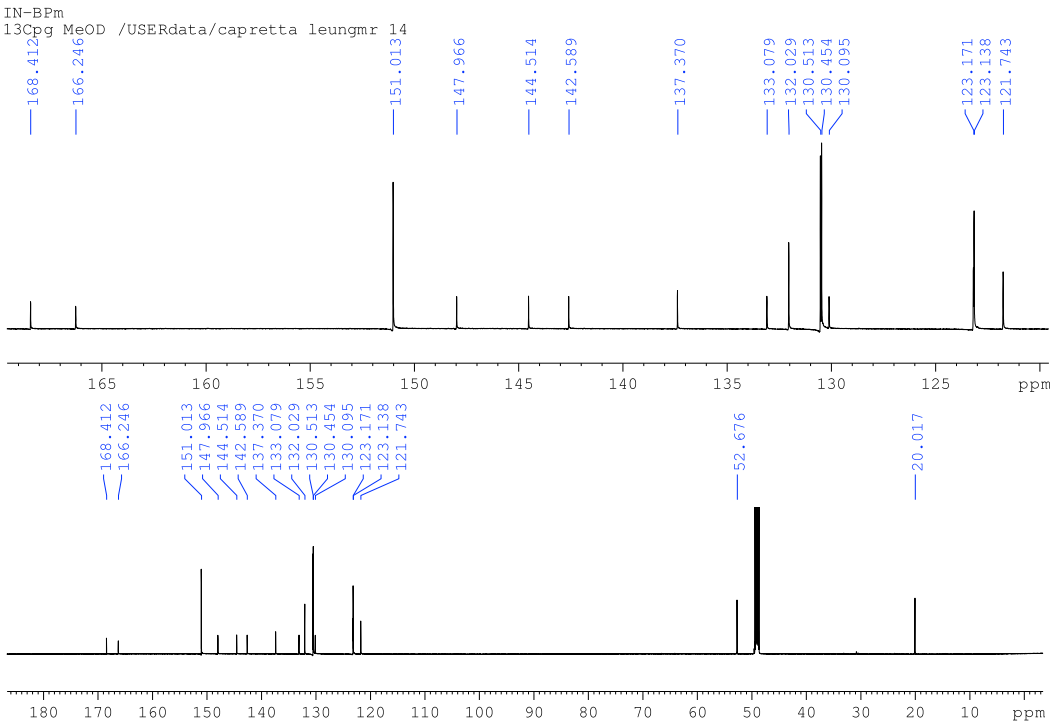

Figure S3-32. ^{13}C NMR of Methyl 2'-Methyl-5'-(Pyridine-4-Amido)-[1,1'-Biphenyl]-4-Carboxylate (**III-21**)

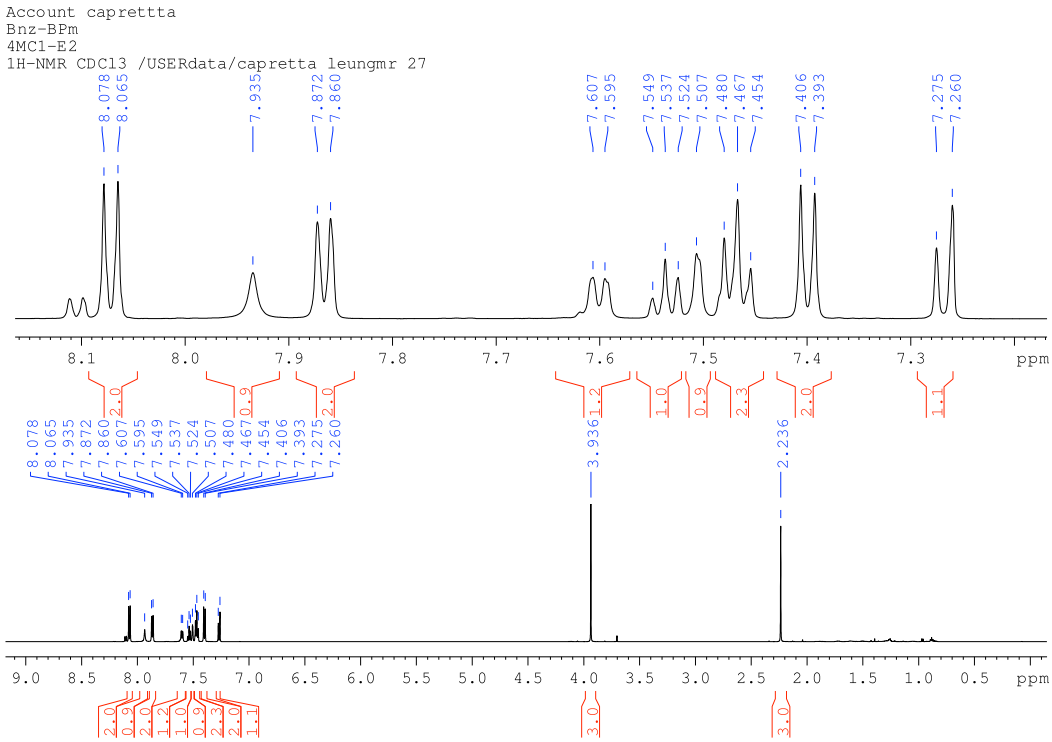

Figure S3-33. ^{1}H NMR of Methyl 5'-Benzamido-2'-Methyl-[1,1'-Biphenyl]-4-Carboxylate (**III-22**)

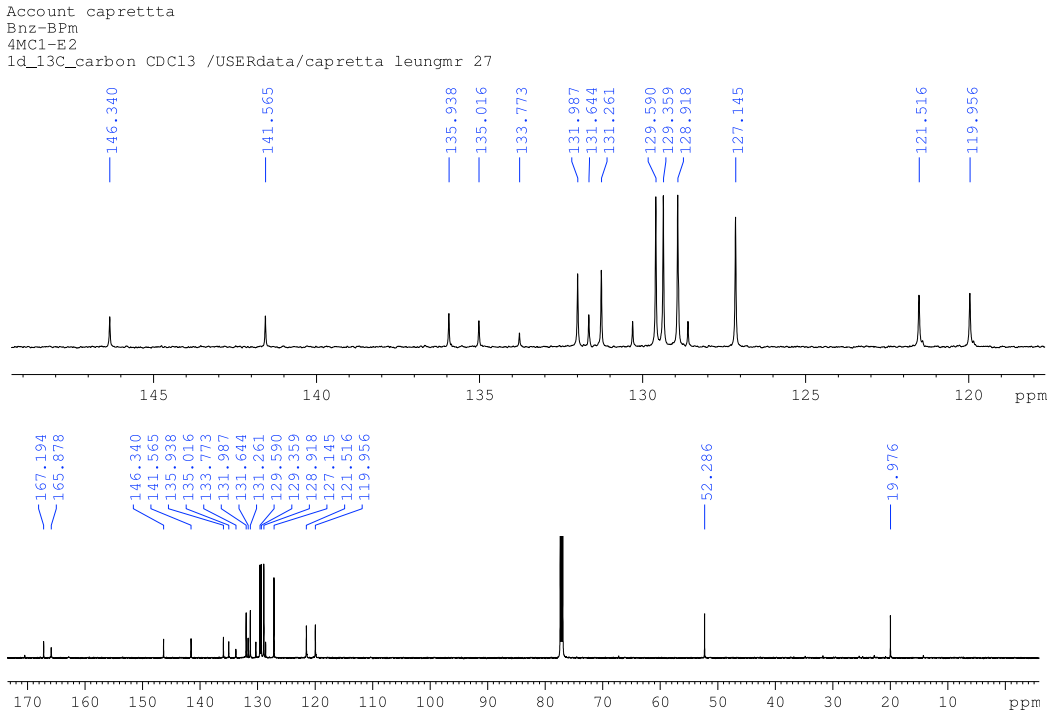

Figure S3-34. ^{13}C NMR of Methyl 5'-Benzamido-2'-Methyl-[1,1'-Biphenyl]-4-Carboxylate (**III-22**)

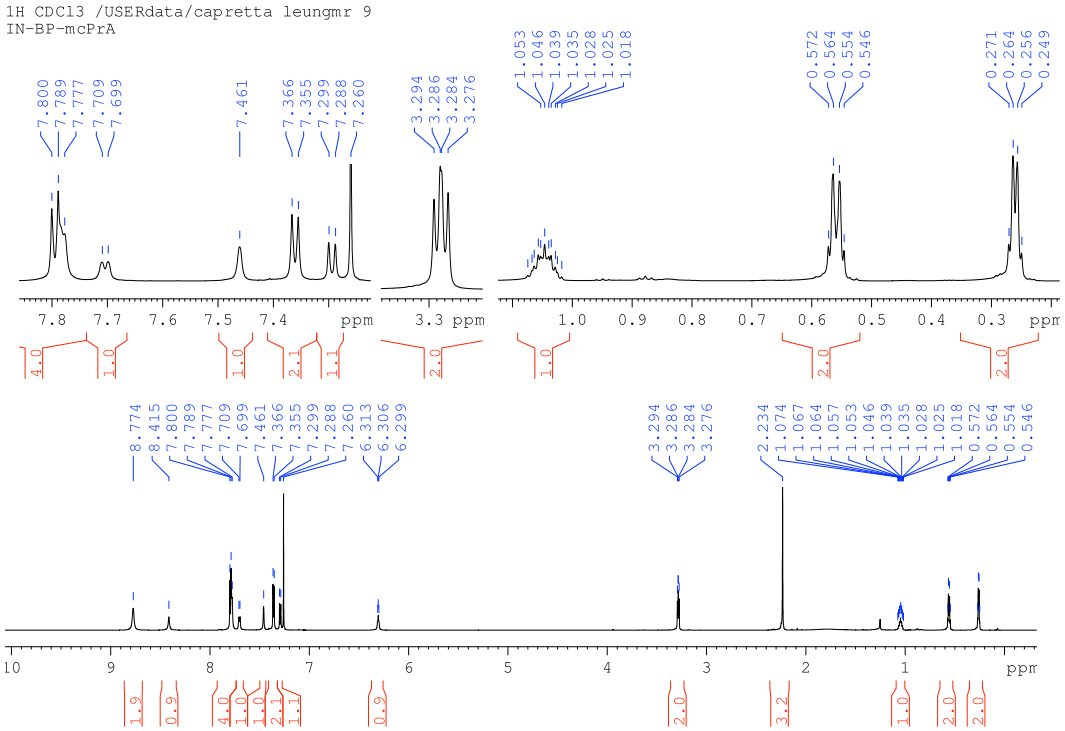

Figure S3-35. ^{1}H NMR of N-{4'-[(Cyclopropylmethyl)carbamoyl]-6-Methyl-[1,1'-Biphenyl]-3-yl}pyridine-4-Carboxamide (**III-29**)

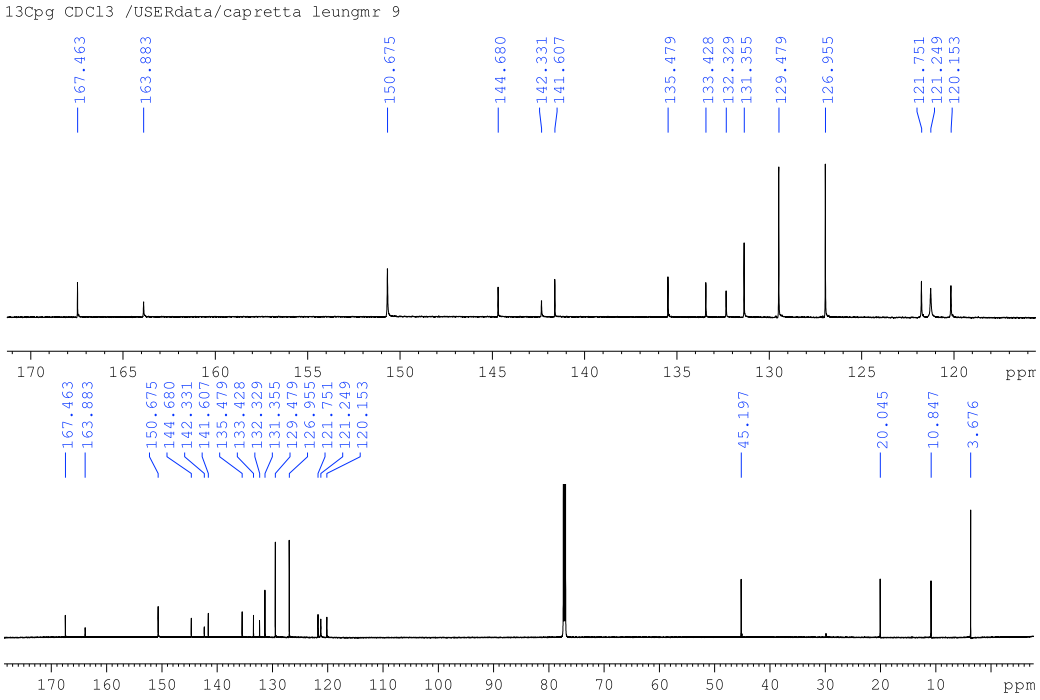

Figure S3-36. ^{13}C NMR of N-{4'-[(Cyclopropylmethyl)carbamoyl]-6-Methyl-[1,1'-Biphenyl]-3-yl}pyridine-4-Carboxamide (**III-29**)

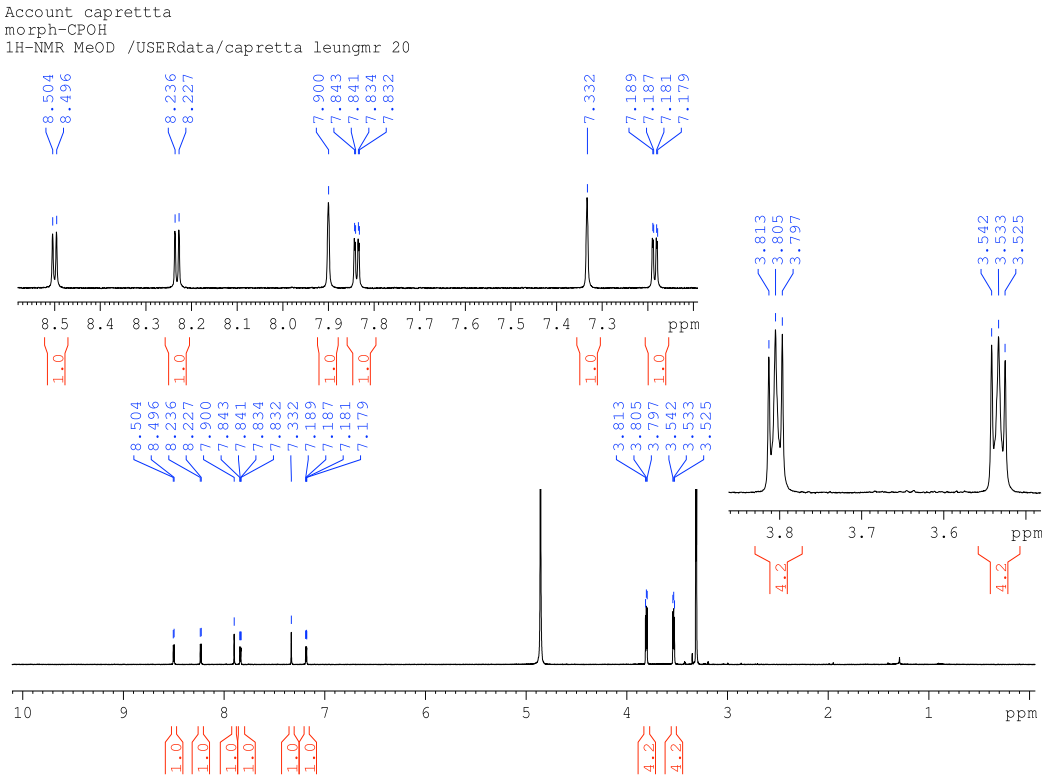

Figure S3-37. ^{1}H NMR of 2-(Morpholin-4-yl)pyridine-4-Carboxylic Acid (**III-25**)

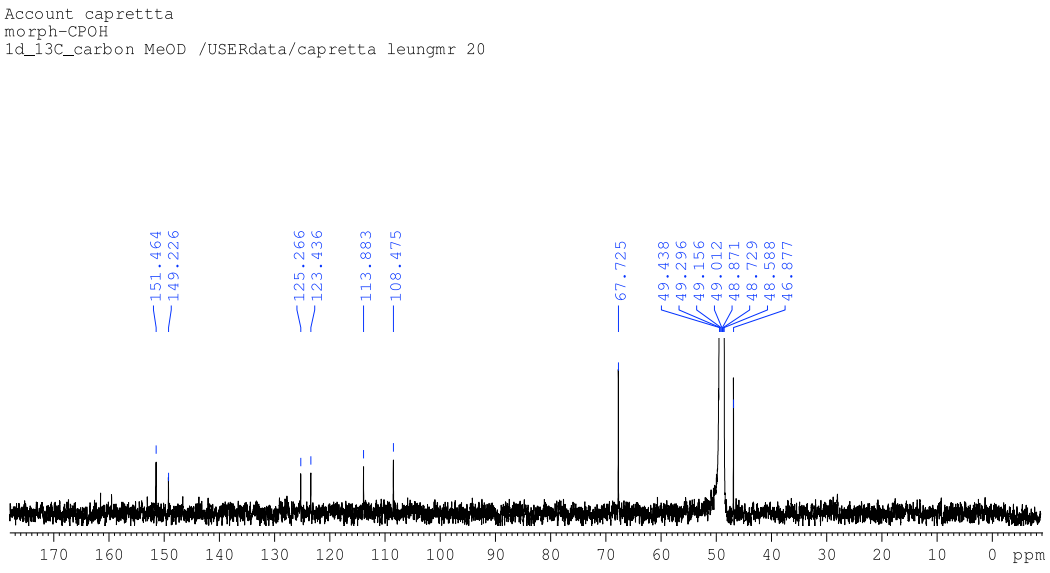

Figure S3-38. ^{13}C NMR of 2-(Morpholin-4-yl)pyridine-4-Carboxylic Acid (**III-25**)

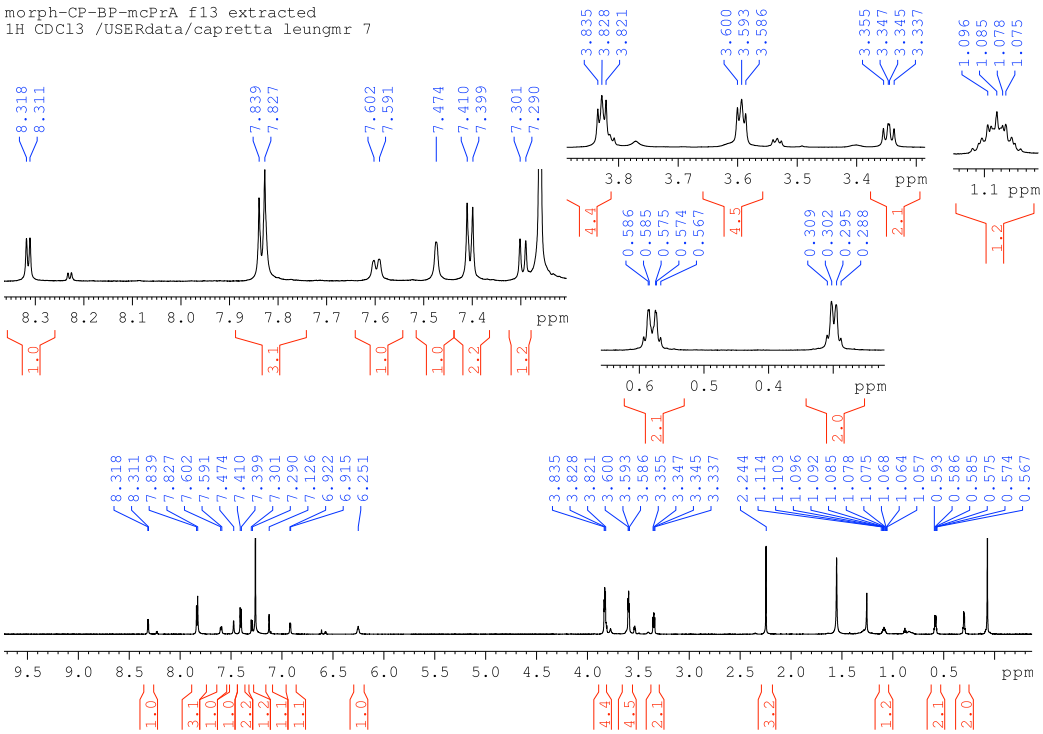

Figure S3-39. ^{1}H NMR of N-{4'-[(Cyclopropylmethyl)carbamoyl]-6-Methyl-[1,1'-Biphenyl]-3-yl}-2-(Morpholin-4-yl)pyridine-4-Carboxamide (**II-2**)

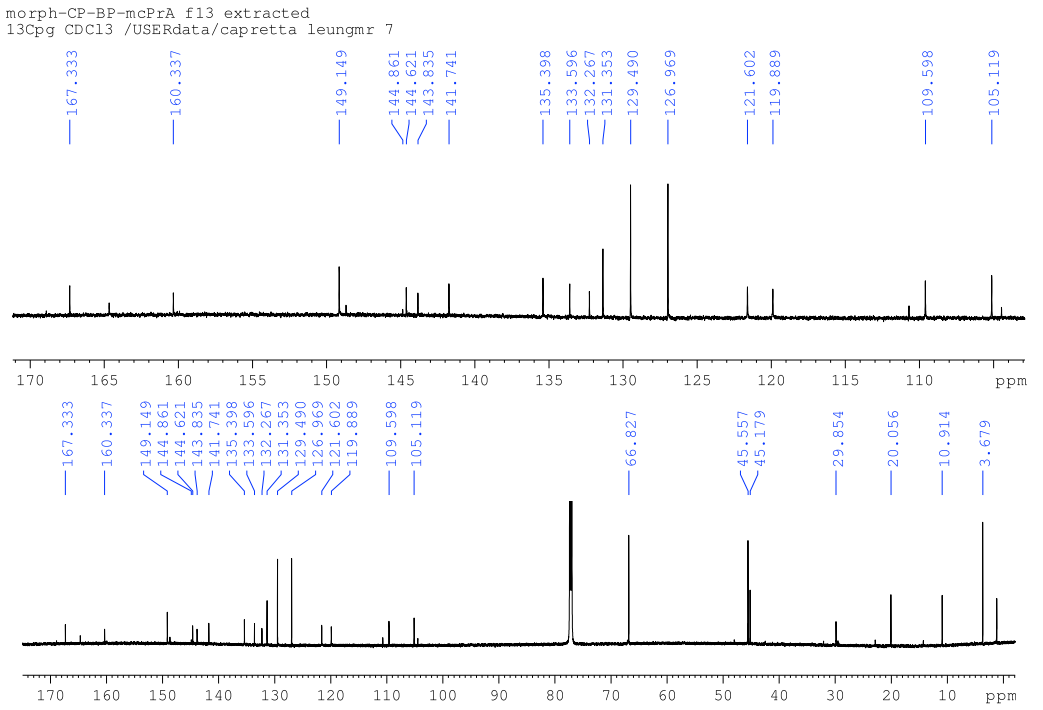

Figure S3-40. ^{13}C NMR of N-{4'-[(Cyclopropylmethyl)carbamoyl]-6-Methyl-[1,1'-Biphenyl]-3-yl}-2-(Morpholin-4-yl)pyridine-4-Carboxamide (**II-2**)

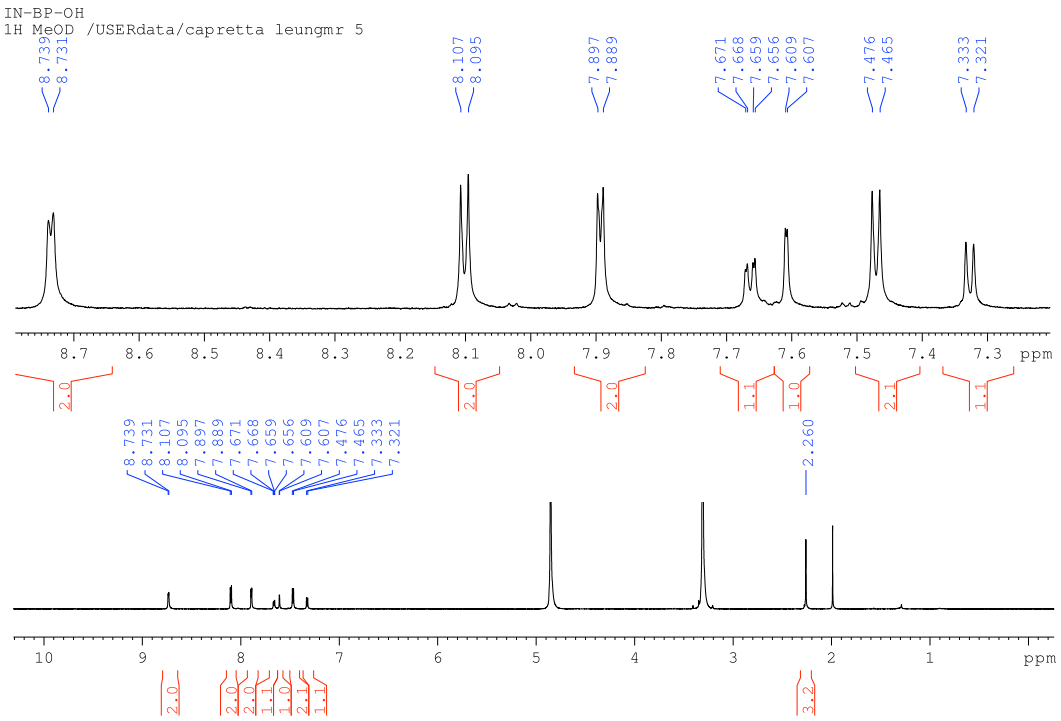

Figure S3-41. 1^{1}H NMR of 2'-Methyl-5'-(Pyridine-4-Amido)-[1,1'-Biphenyl]-4-Carboxylic Acid (**III-30**)

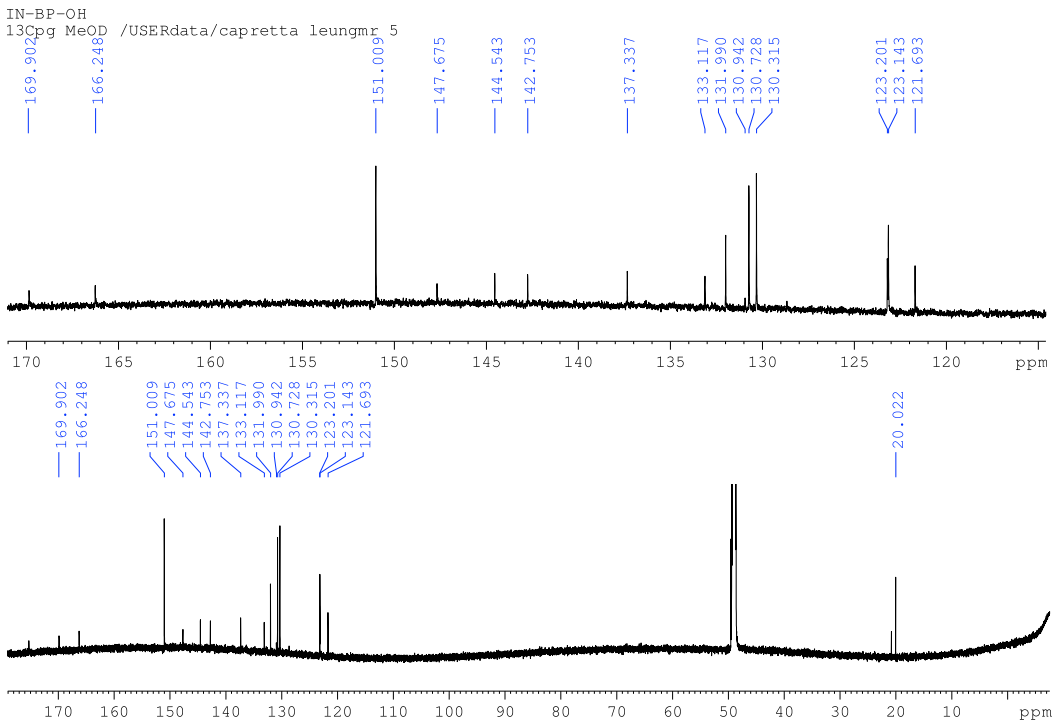

Figure S3-42. ^{13}C NMR of 2'-Methyl-5'-(Pyridine-4-Amido)-[1,1'-Biphenyl]-4-Carboxylic Acid (**III-30**)

4.0 Synthesis of Aspergillomarasmine A (AMA) Analogs as Inhibitors of the New Delhi Metallo-β-Lactamase 1 (NDM-1)

4.1 Background

Carbapenems play a critical role in the treatment of severe Gram-negative infections.[1–4] Their efficacy is threatened by the emergence of carbapenemases, particularly metallo-β-lactamases such as the New Delhi metallo-β-lactamases (NDMs).[3,5] The NDM carbapenemases are class B1 metallo-β-lactamases, which use two Zn^{2+} ions to position and activate water for nucleophilic attack on the β-lactam carbonyl .[3,5,6] In the decade since they were first described,[7] this family has emerged as a global threat, with at least 24 variants, and members are often co-acquired with aminoglycoside modifying enzymes, extended-spectrum β-lactamases, and other resistance mechanisms.[5,6,8] While there are several examples of serine-β-lactamase inhibitors, there are no metallo-β-lactamase inhibitors approved thus far.[3,9,10]

In 2014, a cell-based screen of natural product extracts identified aspergillomarasmine A (AMA, Figure 4-1) as an inhibitor of NDM-1.[11] AMA is a natural product produced by *Aspergillus versicolor* that has previously been investigated for inhibition of angiotensin-converting enzyme (ACE) and endothelin-converting enzyme (ECE).[12–14] It was able to rescue the activity of

meropenem both in *Acinetobacter*, *Enterobacter*, and *Pseudomonas* clinical strains and as well as in a murine model of *K. pneumonia* sepsis, and has a comparatively good safety profile.[11,14] AMA has since been advanced to preclinical safety and efficacy studies in rats and dogs.[15]

4.2 Previous Total Syntheses and SAR Analysis

While AMA can be obtained via fermentation,[11] a synthetic route is desirable for advancement through the drug development pathway. Analogs are needed to explore structure-activity relationships, and to improve physiochemical and pharmacokinetic properties. Often several iterations of analog libraries are tested in a bid to improve potency and selectivity. This is particularly important in the case of AMA, which has already been investigated for its effects on other enzymes and thus is expected to have cross-reactivity.[12,13] Furthermore, synthetic methods are more easily adapted to provide subsequent generation drugs, which is essential given the rapid evolution of NDM variants with superior zinc-binding properties.[5]

AMA can be retrosynthetically dissected into three modules: an aspartic acid and two serine analogs. Though initially the stereochemistry was reported as (*R,R,S*) it has since been reassigned as (*S,S,S*) through total synthesis efforts.[16–18]

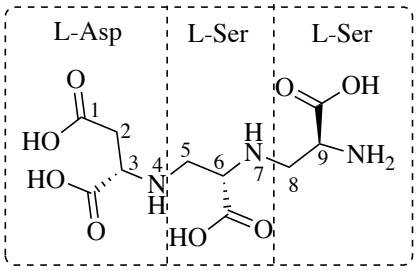

Figure 4-1. Deconstruction of Aspergillomarasmine A (AMA)

There are four reported syntheses of AMA. Koteva *et al*. used aziridines as serine equivalents in an 8-step synthesis with an overall yield of just over 1% (Figure 4-2).[17] Liao *et al*. coupled acetonide-protected diols by sequential reductive aminations to install the serine moieties (Figure 4-3, 15 steps, 4% overall yield).[18] Albu *et al*. completed the synthesis in 7 steps (Figure 4-4, 19% overall yield) using sulfamidates as activated serine equivalents,[19] while Zhang achieved 28% by combining the aziridine approach with the Mitsunobu amine alkylation (Figure 4-5, 6 steps).[20] Using these syntheses, a series of analogs have been made, permitting an introductory SAR analysis.

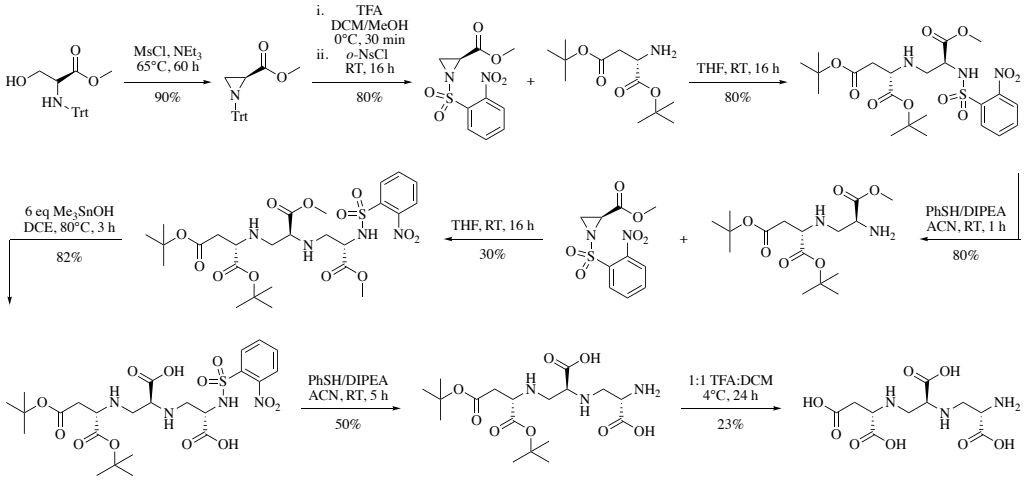

Figure 4-2. Koteva's Synthesis of AMA *via* Aziridine Ring-Opening Reactions[17]

AMA is generally considered to chelate zinc (from the second zinc binding site, Zn2, preferentially) through its four carboxylic acids and two backbone amines.[20,21] In keeping with this mechanism, it was shown that stereochemistry has minimal effect on activity, as *SRR*-, *SRS*-, *SSR*-, and *RSS*-AMA all have essentially

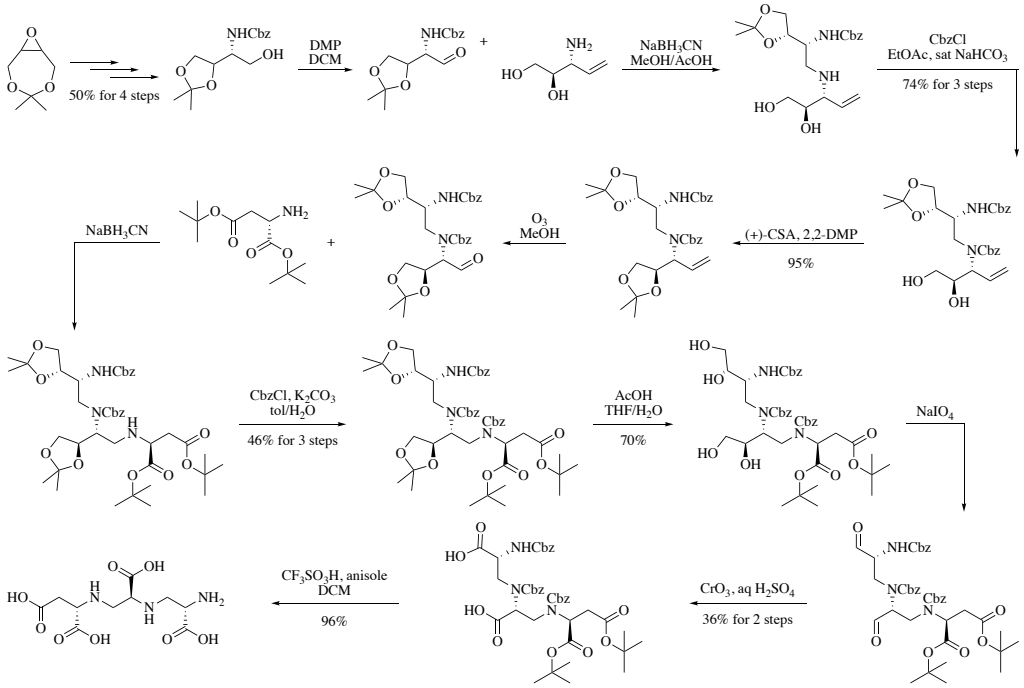

Figure 4-3. Liao's Synthesis of AMA *via* Reductive Amination of Acetonide-Diols[18]

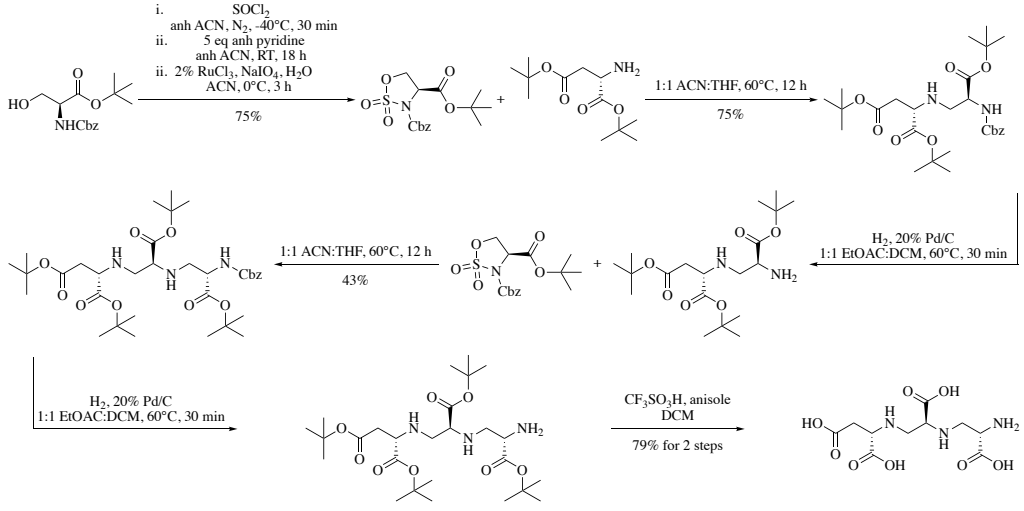

Figure 4-4. Albu's Synthesis of AMA *via* Sulfamidate Ring-Opening Reactions[19]

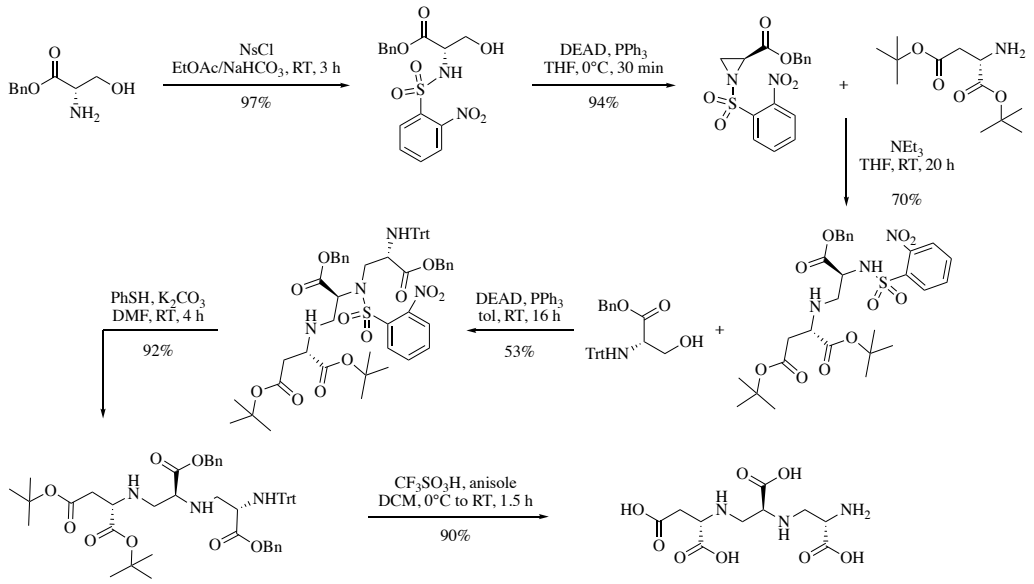

Figure 4-5. Zhang's Synthesis of AMA *via* Mitsunobu Couplings[20]

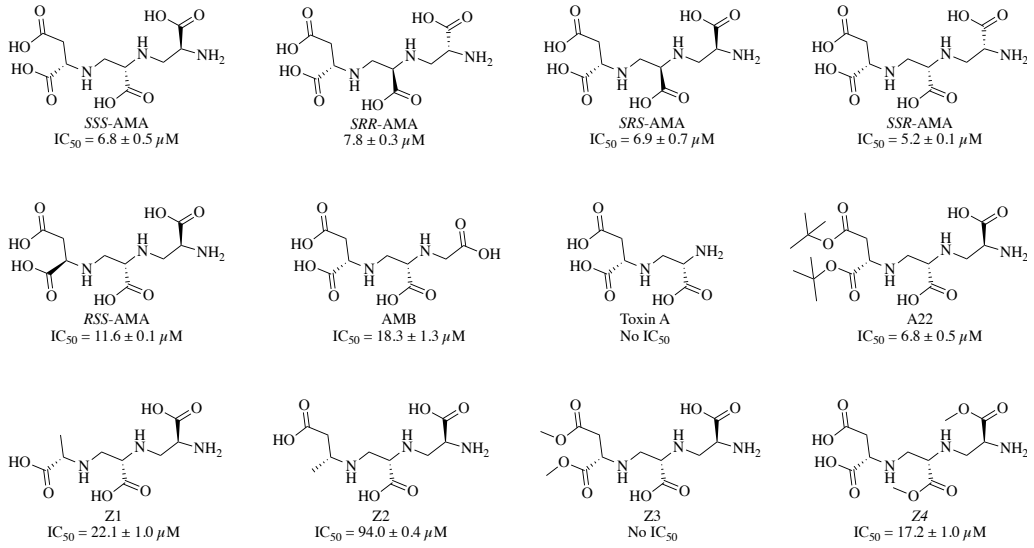

Figure 4-6. Summary of SAR Analysis of AMA Derivatives Performed by Koteva, Albu, and Zhang, and Colleagues[17,19,20]

identical IC_{50} values (Figure 4-6).[17,19,20] The amine at position 9 was similarly shown to have no effect as demonstrated by the retained activity of aspergillomarasmine B (AMB).[19] However, spatial separation is important, shown

by the loss of activity in Toxin A, which has available carboxylic acids at positions 2,3, and 6 but lacks the third unit.[19] Furthermore, while AMA is still the most effective inhibitor, having just two available carboxylic acids is generally sufficient for an analog to retain activity. Which two carboxylates is not certain: Zhang *et al* found that at least one of the carboxylic acids at positions 2 and 3 were essential (compare analogs **Z3** and **Z4**), and that loss at position 3 had a more pronounced effect (**Z1** vs **Z2**).[20] However, Albu *et al*. found that *tert*-butyl ester protection of these moieties was tolerated, so long as both carboxylic acids at positions 6 and 9 were present (**A22**).[19] The next logical step would be to determine the individual contributions of carboxylic acids 9 and especially 6. However, this has not been possible due to limitations in the ability of the current total syntheses to access position 6.

This chapter describes the development of a synthetic route to access the overlooked carboxylic moiety at position 6, using Garner's aldehyde to incorporate a 2-amino-3-hydroxy moiety as module 2 of AMA. In keeping with the overall synthetic approach to the AMA system, *tert*-butyl (4*S*)-4-formyl-2,2-dimethyl-1,3-oxazolidine-3-carboxylate (**IV-1**), or Garner's aldehyde, can be seen as another potential serine equivalent. The amino group and methylene alcohol group are protected by an acetonide to form the oxazolidine ring, while an aldehyde moiety replaces the carboxylic acid for ease in coupling. A versatile chiral building block widely used to introduce one or more stereocentres,[22,23] Garner's aldehyde contains a cloaked 2-amino-3-hydroxy moiety, which when coupled with the aspartic acid of module 1 by reductive amination installs a hydroxyl group in position 6. This 6-

hydroxy AMA analog is ideal for exploring the contributions of the carboxylic acid at that position, as it lacks the acid functionality but retains the associated hydroxyl group.

4.3 Synthetic Strategy to Access Position 6 of AMA

A synthetic approach was designed using commercially-available (*S*)-Garner's aldehyde as a serine equivalent and is presented in Figure 4-7. Garner's aldehyde (**IV-1**) is coupled to *tert*-butyl-protected *L*-aspartic acid (**IV-2**) by reductive amination to give **IV-3**. The *tert*-butyl protecting groups were chosen to take advantage of the triflic acid/anisole deprotection conditions reported by Liao *et al*.[18] After selective deprotection of the amine functionality, the resulting **IV-4** is coupled to an oxidized serine equivalent (the *tert*-butyl aziridine **IV-5** was chosen for ease of use). Compound **IV-6** is then deprotected to yield the 6-hydroxy analog (**IV-8**).

(*S*)-Garner's aldehyde was freshly-made from N-Boc-L-serine methyl ester in two steps according the published protocol due to concerns about racemization (Figure 4-7).[22] It was coupled to di-*tert*-butyl protected L-aspartic acid (**IV-4)**, and reduced with sodium triacetoxyborohydride (STAB). Attempts at purification by column chromatography were largely unsuccessful; however, recrystallization from methanol and water gave fine, needle-like crystals in of **IV-3** in 56% yield. At this stage, a sample of **IV-3** was submitted for X-ray crystallography. Surprisingly, the analysis showed the compound with (*S*,*R*) stereochemistry rather

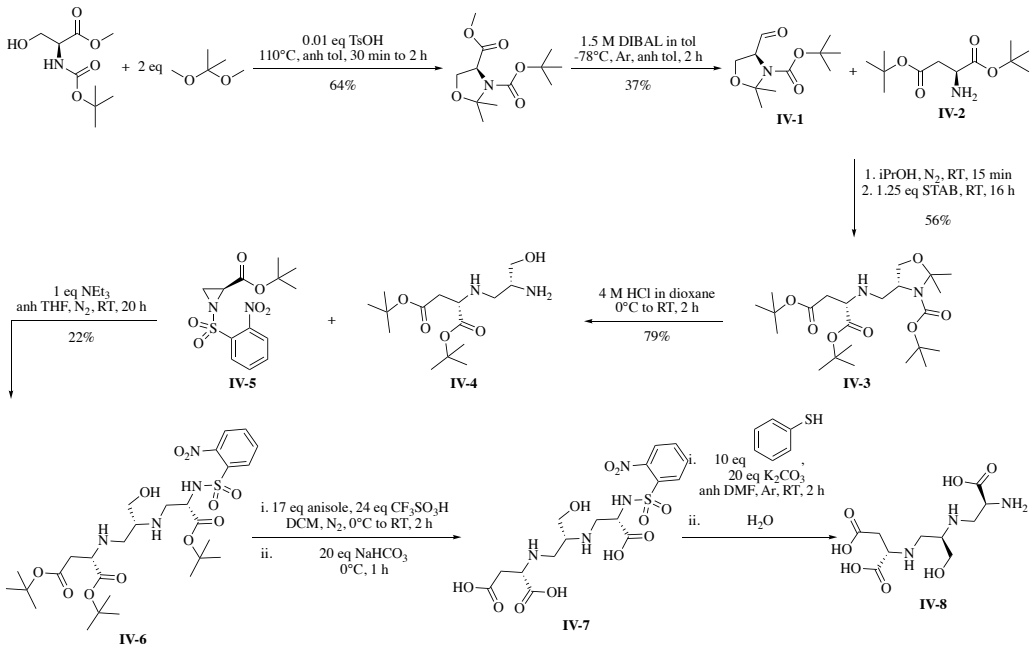

Figure 4-7. Synthetic Route to 6-Hydroxy AMA Analog **IV-8**

than the expected (*S*,*S*) stereochemistry. The epimerization at position 6 is discussed in section 4.5. The decision was made to continue the synthesis regardless.

Selective cleavage of the acetonide and Boc groups of 1,4-di-*tert*-butyl 2-[({3-[(*tert*-butoxy)carbonyl]-2,2-dimethyl-1,3-oxazolidin-4-yl}methyl)amino]butanedioate (**IV-3**) in the presence of *tert*-butyl protecting groups was challenging, as reagents such as TFA resulted in pan deprotection. This was further complicated by the poor resolution of reaction mixtures by TLC. It was found that 4 M hydrochloric acid in dioxane in anhydrous conditions at 0°C would preferentially remove the acetonide then N-Boc group in quantitative yield, although mixtures with loss of one or more *tert*-butyl groups were common.[24]

Reaction completion was monitored by LC-MS. The product was co-evaporated with anhydrous diethyl ether to remove residual hydrochloric acid, and the resulting 1,4-di-*tert*-butyl 2-[(-2-amino-3-hydroxypropyl)amino]butanedioate (**IV-4**) could be used in the next step without further purification.

Koteva's aziridine ring-opening reaction was used to attach the final serine module.[17] Compound **IV-4** and aziridine **IV-5** were dissolved in anhydrous tetrahydrofuran with triethylamine and stirred under nitrogen overnight. Purification by automated column chromatography yielded **IV-6** as a colourless oil which formed crystals upon addition of methanol.

The *tert*-butyl groups were removed by Liao's triflic acid/anisole deprotection conditions.[18,20] The resulting compound **IV-7** neutralized with and stored in sodium bicarbonate. Thiophenol and potassium carbonate was then used to remove the nosyl protecting group to yield 6-hydroxy analog **IV-8** following desalting by gel chromatography and purification by reverse-phase chromatography.[20] The product stains with ninhydrin, and is optically active (optical rotation of -4.0° in water). Mass spectrometry has fragmentation but shows the correct $[M+H]^+$ peak at m/z = 294. ^1H and ^{13}C NMR are consistent with 11 aliphatic protons and 7 aliphatic carbons respectively in D_2O; splitting pattern and correlation spectroscopy were used to assign connectivity.

4.4 ATTEMPTED TOTAL SYNTHESIS OF AMA USING GARNER'S ALDEHYDE

Compound **IV-4** is a linkage point between synthesis of the 6-hydroxy analog and another total synthesis of AMA (Figure 4-8). In this strategy, a second reductive amination of **IV-4** with Garner's aldehyde (**IV-1**) to yield **IV-9** could be followed by protection of the free nitrogen with a Boc group (**IV-10**). Jones reagent could simultaneously cleave the oxazolidine ring and oxidize the two hydroxyl groups to give **IV-11**. Universal deprotection with triflic acid/anisole would then yield AMA, in a total of 6 steps.

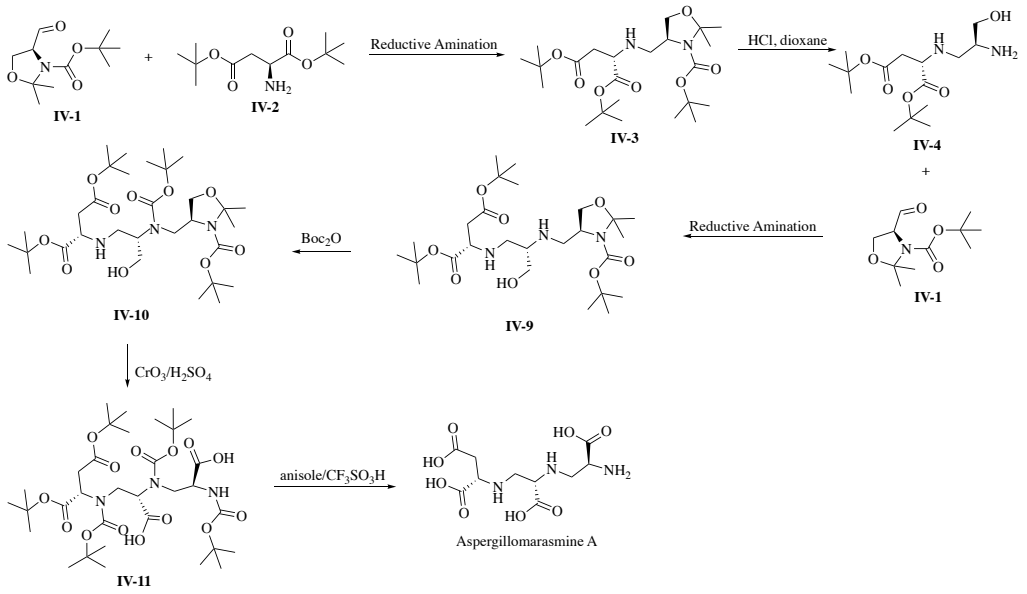

Figure 4-8. Planned Total Synthesis of Aspergillomarasmine A Using Garner's Aldehyde

Reductive amination with a second equivalent of Garner's aldehyde was therefore attempted, but steric hindrance prevented imine formation. Multiple conditions, including the use of titanium catalysts (titanium (IV) chloride and

titanium (IV) isopropoxide),[25–27] were tried unsuccessfully (Table 4-1), and resulted in degradation of the starting material.

Table 4-1. Reaction Conditions Tried for Second Reductive Amination

Amine	Lewis Acid	Reaction Conditions	Notes
IV-4	-	i. Anh iPrOH, N_2, RT, 15 min ii. STAB, RT, 16 h	No reaction
IV-4	-	i. Anh iPrOH, N_2, RT, 16 h ii. STAB, RT, 16 h	No reaction
IV-4	$TiCl_4$ (4.5 eq)	i. 3 eq NEt_3 Anh iPrOH, N_2, RT, 15 min ii. STAB, RT, 96 h	tBu cleavage
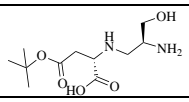	$Ti(OiPr)_4$ (1 eq)	i. Anh iPrOH, N_2, RT, 16 h ii. STAB, RT, 16 h	Product not detected
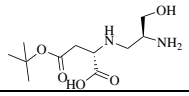	$TiCl_4$ (4.5 eq)	i. Anh iPrOH, N_2, RT, 16 h ii. STAB, RT, 16 h	Product not detected

4.5 KINETIC RESOLUTION OF (*S*,*R*)-STEREOISOMER

Compound **IV-3** was analyzed by X-ray crystallography and the resulting structure deposited in the Cambridge Crystallographic Data Centre (CCDC 1952742).[28] Analysis showed an orthorhombic crystal (a = 5.86 Å, b = 21.14 Å, c = 21.15 Å) with good resolution (R-factor of 4.5%). The crystal displayed $P2_12_12_1$ symmetry, with four atoms per unit cell. Surprisingly, however, it was shown to be exclusively the (3*S*,6*R*)-diastereomer (Figure 4-9, Flack parameter = -0.22 ± 18). This occurred whether racemic or optically-pure (*S*)-Garner's aldehyde was used.

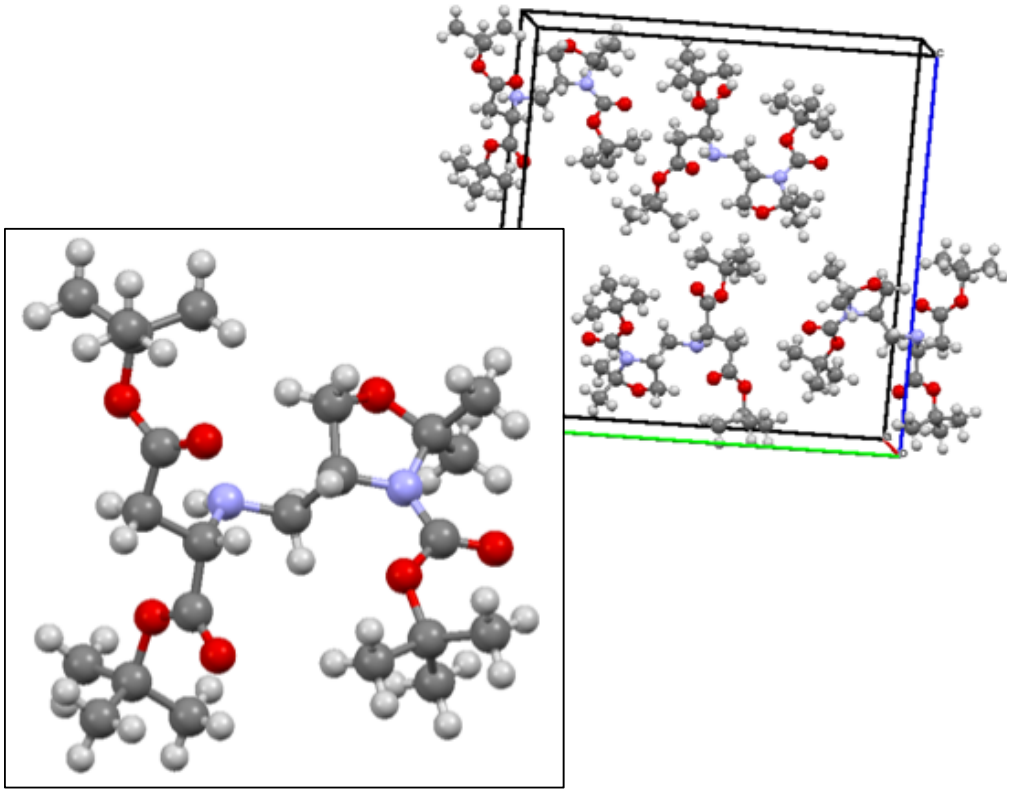

Figure 4-9. X-Ray Crystallographic Structure of **IV-3**

It is thought that the removal of acidic proton of the oxazolidine ring facilitated rearrangement into the ene-amine tautomer (Figure 4-10). This would have destroyed chirality at position 6, as the planar double bond could be protonated on either face to re-form the imine. Since there were now two imine species present (Imine A and Imine B), it was expected that subsequent reduction would result in a racemic mixture of (3*S*,6*S*)- and (3*S*,6*R*)-diastereomers. However, as only the (3*S*,6*R*)-diastereomer was formed, the reduction of Imine B must be favoured in some way. One possible explanation is that Imine B is much more stable than Imine A, so there is an excess of Imine B being present at equilibrium. However, there is no obvious reason for a difference in stability between the two imines, and one

would expect to see at least some (3*S,*6*S*)-product in that case. The more likely explanation is that only Imine B is reduced by STAB, and this irreversible step drives the equilibrium forward according to Le Chatelier's principle, resulting in the conversion of Imine A to Imine B. Thus, the choice of reducing agent could play a role in which (*S*)- or (*R*)-isomer is formed, and the relative ratios of the two. Imine-promoted chiral resolution through an keto-enol tautomerization has been previously been reported in the literature as a means to synthesize optically-pure CCK antagonist.[29] While SAR studies have shown that the stereochemistry of AMA have little influence on its ability to effectively sequester zinc, this phenomenon could prove useful as a means to obtain optically-pure products from racemic starting materials, especially if later NDM inhibitor leads do require a specific isomeric configuration.

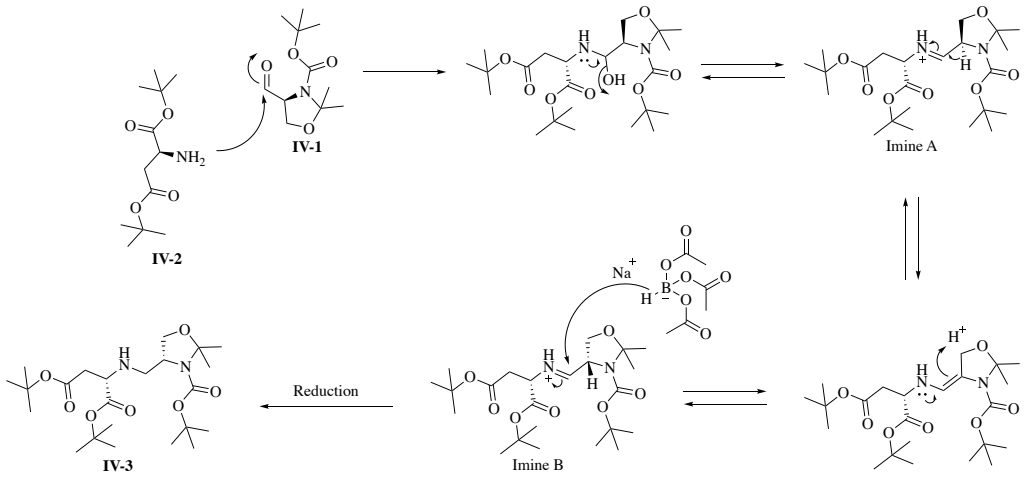

Figure 4-10. Possible Mechanism of Reductive Amination and Kinetic Resolution

4.6 Implications and Future Work

A synthetic strategy was developed that allows access to position 6 of AMA. The 6-hydroxyl analog **IV-8** produced by this methodology will be assayed for activity against NDM-1 in biochemical and cell-based assays in order to elucidate the contribution of the carboxylic acid at position 6 to activity. Cysteine can also be easily substituted for serine in the Garner's aldehyde ring, allowing the introduction of a thiol ligand, commonly seen in other metallo-β-lactamase inhibitors such as D-captopril.[6,30,31] 2,3-Diaminopropionic acid could similarly introduce an amine group.

A total synthesis of AMA using Garner's aldehyde as a serine equivalent was also attempted. Unfortunately, this was unsuccessful as steric hindrance prevented the formation, or subsequent reduction, of the imine needed for the second reductive amination. Further investigation into methods of imine formation is therefore warranted and may provide a solution to this problem.

Finally, a method of producing a single stereoisomer (3-*S*,6-*R*) from racemic starting materials was demonstrated. This should be followed up with a screen of various reducing conditions to see if this method can be applied to the resolution of the other stereoisomers.

4.7 Experimental

Materials and Instrumentation

Reactions were performed in a temperature-controlled oil bath. TLC was

performed on F-254 (0.25 mm) precoated silica gel (Merck) or F-254 (0.2 mm) precoated RP-18 (C18) modified silica gel (MilliporeSigma) and visualized under UV. Ninhydrin, bromocresol green, or anisaldehyde stains were used as needed. Flash column chromatography purifications were performed using a normal phase Teledyne Isco CombiFlash® Rf 200 with standard RediSep RF silica columns (4 g).

Compounds were characterized by ^{1}H NMR, ^{13}C NMR, DEPT Q, and LC-HRMS. NMR spectra were obtained from a Bruker AvanceIII 700 (700 MHz). Chemical shifts are reported as ppm, coupling constants in Hz, and peaks were calibrated to the solvent residual peak ($CDCl_3$ = 7.26 (^{1}H), 77.16 (^{13}C), D_2O = 4.79 (^{1}H), or MeOD = 3.31 (^{1}H), 49.00 (^{13}C)). The following LC gradient (a) was used: from 0 to 1 min isocratic 95% Solvent A (0.1% formic acid in water) and 5% Solvent B (acetonitrile), from 1 to 15 min linear gradient up to 95% Solvent B. Mass spectrometry was conducted with a MicrOTOF ESI-TOF coupled to an Agilent 1200 HPLC in either positive or negative ion mode. Optical rotation data are recorded as $[\alpha]_D^{20}$ (concentration in grams in 1 mL solution).

(-)- *tert*-Butyl (4S)-4-formyl-2,2-dimethyl-1,3-oxazolidine-3-carboxylate (IV-1). (-)- *tert*-butyl (4S)-4-formyl-2,2-dimethyl-1,3-oxazolidine-3-carboxylate (Garner's aldehyde) was synthesized from N-Boc-L-serine methyl ester according to the procedure reported in literature.[22] Anhydrous toluene was used instead of benzene with a standard distillation head at 150°C.

1,4-Di-*tert*-butyl (2*S*)-2-[({(4*R*)-3-[(*tert*-butoxy)carbonyl]-2,2-dimethyl-1,3-oxazolidin-4-yl}methyl)amino]butanedioate (IV-3). *L*-Aspartic acid di-*tert*-butyl ester hydrochloride (**IV-2**) (748.8 mg, 2.66 mmol) and Garner's aldehyde (**IV-1**) (624.2 mg, 2.72 mmol) were dissolved in 20 mL anhydrous isopropanol in a round bottom flask and stirred at room temperature under nitrogen for 15 minutes. Sodium triacetoxyborohydride (725.3 mg, 3.42 mmol) was added in two portions over 30 minutes, and the flask was sealed and stirred overnight. The reaction was quenched in 20 mL of water, then extracted in ethyl acetate (50 mL x 3), washed with brine (40 mL), and dried with sodium sulfate. The yellow oil was crystallized in methanol/water to yield needle-like crystals (689.6 mg, 56%). ^{1}H NMR (700 MHz; $CDCl_3$) δ3.90 (dd, J = 24.8 Hz, J = 9.1 Hz, 2H), 3.86 (tt, J = 52.8 Hz, J = 5.0 Hz, 1H), 3.48 (dt, J = 20.0 Hz, J = 14.2 Hz, 1H), 2.69 (ddd, 64.0 Hz, J = 54.1 Hz, J = 13.6 Hz, 1H), 2.58 (ddd, J = 83.7 Hz, J = 37.3 Hz, J = 11.2 Hz, 1 H), 2.56 (dd, J = 15.5 Hz, J = 4.5 Hz, 1H), 2.36 (dd, J = 15.4 Hz, J = 8.8 Hz, 1H), 1.80 (s, 1H, broad), 1.45 (m, 33H). Spectrum was processed with altered parameters to allow coupling constant determination. ^{13}C NMR (176 MHz; $CDCl_3$) δ173.44 (C), 170.31 (C), 151.84 (C), 93.94 (C), 81.68 (C), 80.99 (C),79.66 (C), 66.43 (CH), 66.04 (CH), 58.54 (CH_2), 58.23 (CH_2), 57.44 (CH_2), 56.86 (CH_2), 49.47 (CH), 48.93 (CH), 39.87 (CH_2), 28.64 (CH_3), 28.56 (CH_3), 28.22 (CH_3), 28.20 (CH_3), 27.66 (CH_3), 26.96 (CH_3), 24.61 (CH_3), 23.29 (CH_3). HRMS (ESI) for $C_{23}H_{42}N_2O_7$: Calculated $[M+H]^+$ 459.3064. Found $[M+H]^+$ 459.3044. R_t: 8.9 min (a). Optical rotation: -27.4° ($CHCl_3$, *c* 1%).

1,4-Di-*tert*-butyl (2*S*)-2-{[(2*R*)-2-amino-3-hydroxypropyl]amino}butanedioate (IV-4). To (2*S*)-2-[({(4*R*)-3-[(*tert*-butoxy)carbonyl]-2,2-dimethyl-1,3-oxazolidin-4-yl}methyl)amino]butanedioate (**IV-3**) (69.6 mg, 0.15 mmol) at 0°C under argon was added 1 mL of 4 M hydrochloric acid in dioxane. The reaction was stirred in an ice bath for 2 h, co-evaporated with ice-cold anhydrous ether (2 x 1 mL), and evaporated to an orange precipitate (38.1 mg, 79%). ^{1}H NMR (700 MHz; $CDCl_3$) δ4.22 (dt, J = 31.9 Hz, J = 6.1 Hz, 1H), 3.85 (dd, J = 8.3 Hz, J = 5.4 Hz, 2H), 3.69 (tt, 8.6 Hz, 1.5 Hz, 1H), 3.57 (ddd, J = 12.5 Hz, J = 4.1 Hz, J = 4.1 Hz, 1H), 3.41 (ddd, J = 40.3 Hz, J = 12.2 Hz, J = 4.4 Hz, 1H), 3.11 (ddd, J = 21.8 Hz, J = 10.2 Hz, J = 9.9 Hz, 1H), 3.05 (dd, J = 14.1 Hz, J = 6.7 Hz, 2H), 1.51 (m, 18H). Spectrum was processed with altered parameters to allow coupling constant determination. ^{13}C NMR (176 MHz; $CDCl_3$) δ170.94 (C), 85.94 (C), 83.85 (C), 61.35 (CH_2), 61.26 (CH), 59.13 (CH), 51.07 (CH^2), 43.55 (CH_2), 28.35 (CH_3), 28.13 (CH_3). HRMS (ESI) for $C_{15}H_{30}N_2O_5$: Calculated $[M+H]^+$ 319.2227. Found $[M+H]^+$ 319.2224. R_t: 6.0 min (a). Compound was converted to the free base to allow determination of optical rotation. Optical rotation: -7.0° ($CHCl_3$, *c* 0.5%).

1,4-Di-*tert*-butyl (2*S*)-2-{[(2*R*)-2-{[(2*S*)-3-(*tert*-butoxy)-2-(2-nitrobenzenesulfonamido)-3-oxypropyl]amino}-3-hydroxypropyl]amino}butanedioate (IV-6). 1,4-Di-*tert*-butyl (2*S*)-2-{[(2*R*)-2-amino-3-hydroxypropyl]amino}butanedioate (**IV-4**) (89.7 mg, 0.28 mmol) and *tert*-butyl (2*S*)-1-(2-nitrobenzenesulfonyl)aziridine-2-carboxylate (**IV-5**) (85.1 mg, 0.26 mmol) were dissolved in anhydrous tetrahydrofuran. Triethylamine (36 µL, 0.26 mmol) was added, and the reaction stirred at room temperature under nitrogen

for 20 min. Product was purified by combiflash to a clear oil that crystallized upon addition of methanol (36.3 mg, 22%). ^{1}H NMR (700 MHz; $CDCl_3$) δ8.09 (ddd, J = 4.7 Hz, J = 4.7 Hz, J = 3.6 Hz, 1H), 7.90 (ddd, J = 4.7 Hz, J = 4.7 Hz, J = 3.7 Hz, 1H), 7.71 (ddd, J = 4.5 Hz, J = 4.5 Hz, J = 3.6 Hz, 2H), 4.14 (t, J = 5.1 Hz, 1H), 3.62 (dd, J = 11.3 Hz, J = 4.2 Hz, 1H), 3.56 (dd, J = 11.2 Hz, J = 3.9 Hz, 1H), 3.43 (dd, J = 7.4 Hz, J = 5.2 Hz, 1H), 3.03 (ddd, J = 24.2 Hz, J = 12.7 Hz, J = 5.8 Hz, 2H), 2.90 (dd, J = 11.9 Hz, J = 4.9 Hz, 1H), 2.65 (tt, J = 12.2 Hz, J = 6.6 Hz, 1H), 2.54 (m, 3H), 1.45 (m, 18 H), 1.27 (s, 9H). ^{13}C NMR (176 MHz; $CDCl_3$) δ172.73 (C), 170.29 (C), 169.24 (C), 147.98 (C), 134.58 (C), 133.61 (CH), 132.89 (CH), 130.73 (CH), 125.63 (CH), 82.95 (C), 81.92 (C), 81.34 (C), 64.03 (CH_2), 58.94 (CH), 57.87 (CH), 57.76 (CH), 50.23 (CH_2), 49.25 (CH_2), 39.39 (CH_2), 28.21 (CH_3), 28.19 (CH_3), 27.87 (CH_3). HRMS (ESI) for $C_{28}H_{46}N_4O_{11}S$: Calculated $[M+H]^+$ 647.2957. Found $[M+H]^+$ 647.3053. R_t: 8.6 min (a). Optical rotation: -14.7° ($CHCl_3$, *c* 1%).

Sodium (2*S*)-2-{[(2*R*)-2-{[(2*S*)-2-carboxylato-2-(2-nitrobenzenesulfonamido)ethyl]amino}-3-hydroxypropyl]amido}butanedioate (IV-7). 1,4-Di-*tert*-butyl (2*S*)-2-{[(2*R*)-2-{[(2*S*)-3-(*tert*-butoxy)-2-(2-nitrobenzenesulfonamido)-3-oxypropyl]amino}-3-hydroxypropyl]amino}butanedioate (**IV-6**) was dissolved in 3 mL of dichloromethane under nitrogen and cooled to 0°C. Anisole (76 µL, 0.70 mmol) and triflic acid (62 µL, 1.01 mmol) were added and the reaction stirred on ice for 30 min. The reaction was allowed to warm to room temperature and stirred another 1.5 h. Sodium bicarbonate (71.0 mg, 0.85 mmol) in 4.5 mL of water at 0°C was

added and the reaction stirred for 1 h on ice. The product was washed with dichloromethane (3 x 6 mL), lyophilized, and used directly in the next step without further purification. HRMS (ESI) for $C_{16}H_{22}N_4O_{11}S$: Calculated $[M+H]^+$ 479.1079. Found $[M+H]^+$ 479.4394. R_t: 3.9 min (a).

(2*S*)-2-{[(2*R*)-2-{[(2*S*)-2-amino-2-carboxyethyl]amino}-3-hydroxypropyl]amino}butanedioic acid (IV-8). Crude sodium (2*S*)-2-{[(2*R*)-2-{[(2*S*)-2-carboxylato-2-(2-nitrobenzenesulfonamido)ethyl]amino}-3-hydroxypropyl]amido}butanedioate (**IV-7**) was dissolved in 1 mL of dimethylformamide under argon. Potassium carbonate (110.6 mg, 0.80 mmol) and thiophenol (39 μL, 0.38 mmol) were added and the reaction stirred at room temperature for 2.5 h. 4 mL of water was added, and the product was washed with dichloromethane (3 x 2.5 mL), evaporated, and purified by gel and reverse-phase chromatography. Yield was determined through ^{1}H NMR integration using pyridine as an internal standard (0.5 mg, 6%). ^{1}H NMR (700 MHz; D_2O) δ4.03 (t, J = 7.3 Hz, 1H), 3.79 (ddd, J = 20.4 Hz, J = 8.8 Hz, J = 4.2 Hz, 1H), 3.76 (dd, J = 11.6 Hz, J = 3.3 Hz, 1H), 3.70 (dd, J = 11.4 Hz, J = 3.3 Hz, 1H), 3.42 (m, 4H), 2.83 (m, 3H). ^{13}C NMR (176 MHz; D_2O) δ77.08 (CH_2), 62.70 (CH), 58.93 (CH), 58.01 (CH), 50.74 (CH_2), 48.97 (CH_2), 37.71 (CH_2). HRMS (ESI) for $C_{10}H_{19}N_3O_7$: Calculated $[M+H]^+$ 294.1296. Found $[M+H]^+$ 294.8639. R_t: 1.2 min (a). Optical rotation: -4.0° (H_2O, *c* 0.2%).

4.8 REFERENCES

(1) Schlecht, H. P.; Bruno, C. Overview of Antibacterial Drugs https://www.merckmanuals.com/en-ca/professional/infectious-diseases/bacteria-and-antibacterial-drugs/overview-of-antibacterial-drugs (accessed May 3, 2018).

(2) *The Merck Manual of Diagnosis and Therapy*, 19th ed.; Porter, R. S., Kaplan, J. L., Albert, R. K., Bowman, M. A., Braunstein, G. D., Cohen, S., Emanuel, L., Fawcett, J., Frenkel, E. P., Hendrix, S. L., et al., Eds.; Merck Sharp & Dohme Corp., A Subsidary of Merck & Co, Inc.: Whitehouse Station, NJ, 2011.

(3) Tooke, C. L.; Hinchliffe, P.; Bragginton, E. C.; Colenso, C. K.; Hirvonen, V. H. A.; Takebayashi, Y.; Spencer, J. β-Lactamases and β-Lactamase Inhibitors in the 21st Century. *J. Mol. Biol.* **2019**, https://doi.org/10.1016/j.jmb.2019.04.002.

(4) Exner, M.; Bhattacharya, S.; Christiansen, B.; Gebel, J.; Goroncy-Bermes, P.; Hartemann, P.; Heeg, P.; Ilschner, C.; Kramer, A.; Larson, E.; et al. Antibiotic Resistance: What Is so Special about Multidrug-Resistant Gram-Negative Bacteria? *GMS Hyg. Infect. Control* **2017**, *12*, Doc05.

(5) Wu, W.; Feng, Y.; Tang, G.; Qiao, F.; McNally, A.; Zong, Z. NDM Metallo-β-Lactamases and Their Bacterial Producers in Health Care Settings. *Clin. Microbiol. Rev.* **2019**, *32* (2), e00115-18.

(6) Linciano, P.; Cendron, L.; Gianquinto, E.; Spyrakis, F.; Tondi, D. Ten Years with New Delhi Metallo-β-Lactamase-1 (NDM-1): From Structural Insights to Inhibitor Design. *ACS Infect. Dis.* **2019**, *5*, 9–34.

(7) Yong, D.; Toleman, M. A.; Giske, C. G.; Cho, H. S.; Sundman, K.; Lee, K.; Walsh, T. R. Characterization of a New Metallo-Beta-Lactamase Gene, Bla(NDM-1), and a Novel Erythromycin Esterase Gene Carried on a Unique Genetic Structure in Klebsiella Pneumoniae Sequence Type 14 from India. *Antimicrob. Agents Chemother.* **2009**, *53* (12), 5046–5054.

(8) Kumarasamy, K. K.; Toleman, M. A.; Walsh, T. R.; Bagaria, J.; Butt, F.; Balakrishnan, R.; Chaudhary, U.; Doumith, M.; Giske, C. G.; Irfan, S.; et al. Emergence of a New Antibiotic Resistance Mechanism in India, Pakistan, and the UK: A Molecular, Biological, and Epidemiological Study. *Lancet. Infect. Dis.* **2010**, *10* (9), 597–602.

(9) Bush, K.; Bradford, P. A. β-Lactams and β-Lactamase Inhibitors: An Overview. *Cold Spring Harb. Perspect. Med.* **2016**, *6* (8), a025247.

(10) Wright, G. D. Antibiotic Adjuvants: Rescuing Antibiotics from Resistance.

Trends Microbiol. **2016**, *24* (11), 862–871.

(11) King, A. M.; Reid-Yu, S. A.; Wang, W.; King, D. T.; De Pascale, G.; Strynadka, N. C.; Walsh, T. R.; Coombes, B. K.; Wright, G. D. Aspergillomarasmine A Overcomes Metallo-β-Lactamase Antibiotic Resistance. *Nature* **2014**, *510* (7506), 503–506.

(12) Mikami, Y.; Suzuki, T. Novel Microbial Inhibitors of Angiotensin-Converting Enzyme, Aspergillomarasmines A and B. *Agric. Biol. Chem.* **1983**, *47* (ll), 2693–2695.

(13) Arai, K.; Ashikawa, N.; Nakakita, Y.; Matsuura, A.; Ashizawa, N.; Munekata, M. Aspergillomarasmine A and B, Potent Microbial Inhibitors of Endothelin-Converting Enzyme. *Biosci. Biotechnol. Biochem.* **1993**, *57* (11), 1944–1945.

(14) Matsuura, A.; Okumura, H.; Asakura, R.; Ashizawa, N.; Takahashi, M.; Kobayashi, F.; Ashikawa, N.; Arai, K. Pharmacological Profiles of Aspergillomarasmines as Endothelin Converting Enzyme Inhibitors. *Jpn. J. Pharmacol.* **1993**, *63* (2), 187–193.

(15) Dolgin, E. Inner Workings: Combating Antibiotic Resistance from the Ground Up. *Proc. Natl. Acad. Sci. U. S. A.* **2016**, *113* (42), 11642–11643.

(16) Haenni, A. L.; Robert, M.; Vetter, W.; Roux, L.; Barbier, M.; Lederer, E. Structure Chimique Des Aspergillomarasmines A et B. *Helv. Chim. Acta* **1965**, *48*, 729–750.

(17) Koteva, K.; King, A. M.; Capretta, A.; Wright, G. D. Total Synthesis and Activity of the Metallo-β-Lactamase Inhibitor Aspergillomarasmine A. *Angew. Chemie Int. Ed.* **2016**, *55* (6), 2210–2212.

(18) Liao, D.; Yang, S.; Wang, J.; Zhang, J.; Hong, B.; Wu, F.; Lei, X. Total Synthesis and Structural Reassignment of Aspergillomarasmine A. *Angew. Chemie Int. Ed.* **2016**, *55* (13), 4291–4295.

(19) Albu, S. A.; Koteva, K.; King, A. M.; Al-Karmi, S.; Wright, G. D.; Capretta, A. Total Synthesis of Aspergillomarasmine A and Related Compounds: A Sulfamidate Approach Enables Exploration of Structure-Activity Relationships. *Angew. Chemie Int. Ed.* **2016**, *55* (42), 13259–13262.

(20) Zhang, J.; Wang, S.; Bai, Y.; Guo, Q.; Zhou, J.; Lei, X. Total Syntheses of Natural Metallophores Staphylopine and Aspergillomarasmine A. *J. Org. Chem.* **2017**, *82* (24), 13643–13648.

(21) Bergstrom, A.; Katko, A.; Adkins, Z.; Hill, J.; Cheng, Z.; Burnett, M.; Yang, H.; Aitha, M.; Mehaffey, M. R.; Brodbelt, J. S.; et al. Probing the Interaction

of Aspergillomarasmine A with Metallo-β-Lactamases NDM-1, VIM-2, and IMP-7. *ACS Infect. Dis.* **2018**, *4* (2), 135–145.

(22) Garner, P.; Park, J. M. 1,1,-Dimethylethyl (S)- or (R)-4-Formyl-2,2-Dimethyl-3-Oxazolidinecarboxylate: A Useful Serinal Derivative. *Org. Synth.* **1992**, *70*, 18.

(23) Liang, X.; Andersch, J.; Bols, M. Garner's Aldehyde. *J. Chem. Soc. Perkin Trans. 1* **2001**, *0* (18), 2136–2157.

(24) Han, G.; Tamaki, M.; Hruby, V. J. Fast, Efficient and Selective Deprotection of the Tert-Butoxycarbonyl (Boc) Group Using HCl/Dioxane (4 M). *J. Pept. Res.* **2001**, *58* (4), 338–341.

(25) Leggio, A.; Le Pera, A.; Liguori, A.; Napoli, A.; Romeo, C.; Siciliano, C.; Sindona, G. Highly Stereoselective Synthesis of Optically Pure C-Aryl Imines from α-l-Amino Acid Methyl Esters. *Synth. Commun.* **2003**, *33* (24), 4331–4338.

(26) Balan, D.; Adolfsson, H. Titanium Isopropoxide as Efficient Catalyst for the Aza-Baylis−Hillman Reaction. Selective Formation of α-Methylene-β-Amino Acid Derivatives. *J. Org. Chem.* **2002**, *67* (7), 2329–2334.

(27) DiCesare, J. C.; White, C. E.; Rasmussen, W. E.; White, B. M.; McComas, C. B.; Craft, L. E. Modification of the Titanium(IV) Isopropoxide Reductive Amination Reaction: Application to Solid Phase Synthesis. *Synth. Commun.* **2005**, *35* (5), 663–668.

(28) Colden Leung, M. R.; Capretta, A. CCDC 1952742: Experimental Crystal Structure Determination https://www.ccdc.cam.ac.uk/structures/Search?Doi=10.5517%2Fccdc.csd.cc23jzpb&DatabaseToSearch=Published (accessed Sep 13, 2019).

(29) Reider, P. J.; Davis, P.; Hughes, D. L.; Grabowski, E. J. J. Crystallization-Induced Asymmetric Transformation: Stereospecific Synthesis of a Potent Peripheral CCK Antagonist. *J. Org. Chem.* **1987**, *52* (5), 955–957.

(30) Guo, Y.; Wang, J.; Niu, G.; Shui, W.; Sun, Y.; Zhou, H.; Zhang, Y.; Yang, C.; Lou, Z.; Rao, Z. A Structural View of the Antibiotic Degradation Enzyme NDM-1 from a Superbug. *Protein Cell* **2011**, *2* (5), 384–394.

(31) Rotondo, C. M.; Wright, G. D. Inhibitors of Metallo-B-Lactamases. *Curr. Opin. Microbiol.* **2017**, *39*, 96–105.

4.9 SUPPLEMENTARY DATA

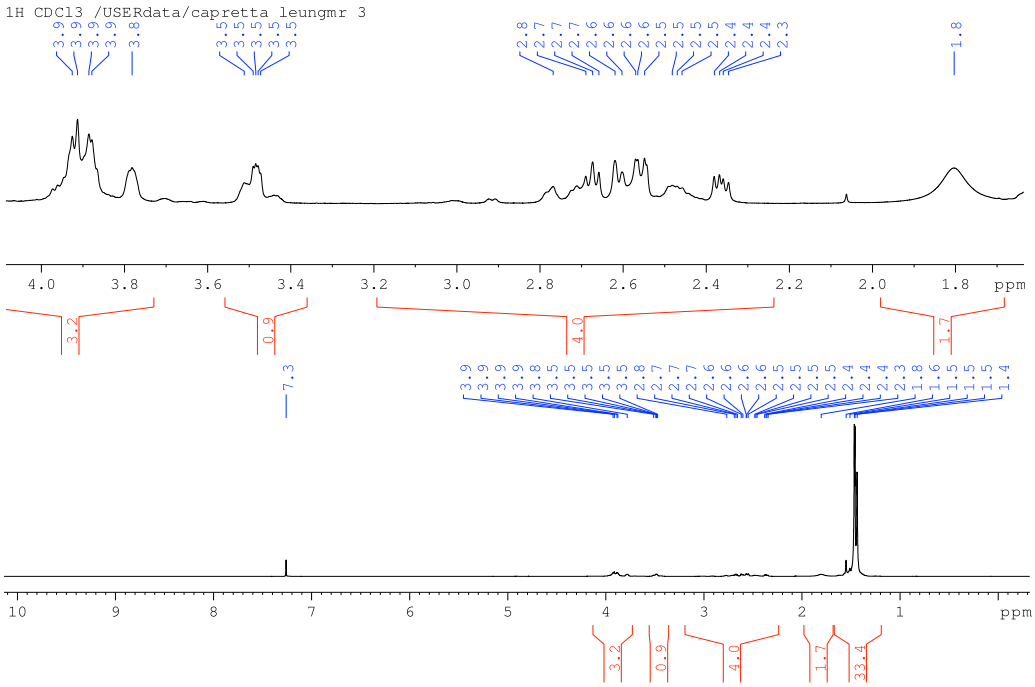

Figure S4-1. ^{1}H NMR of 1,4-Di-*tert*-Butyl (2*S*)-2-[({(4*R*)-3-[(*tert*-Butoxy)carbonyl]-2,2-Dimethyl-1,3-Oxazolidin-4-yl}methyl)amino]butanedioate (**IV-3**)

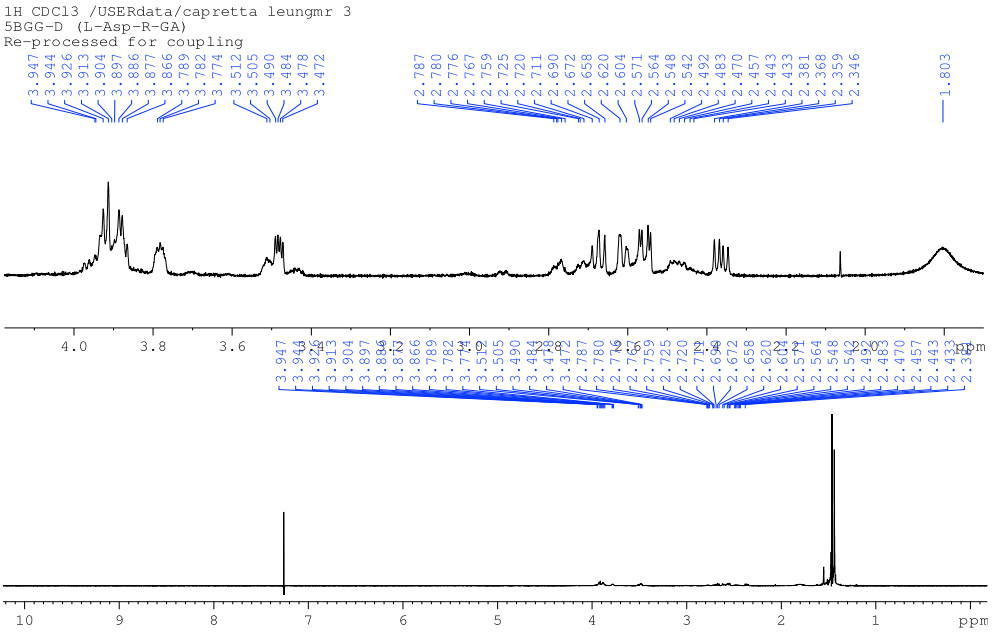

Figure S4-2. Re-processed ^{1}H NMR of (**IV-3**) for coupling constants

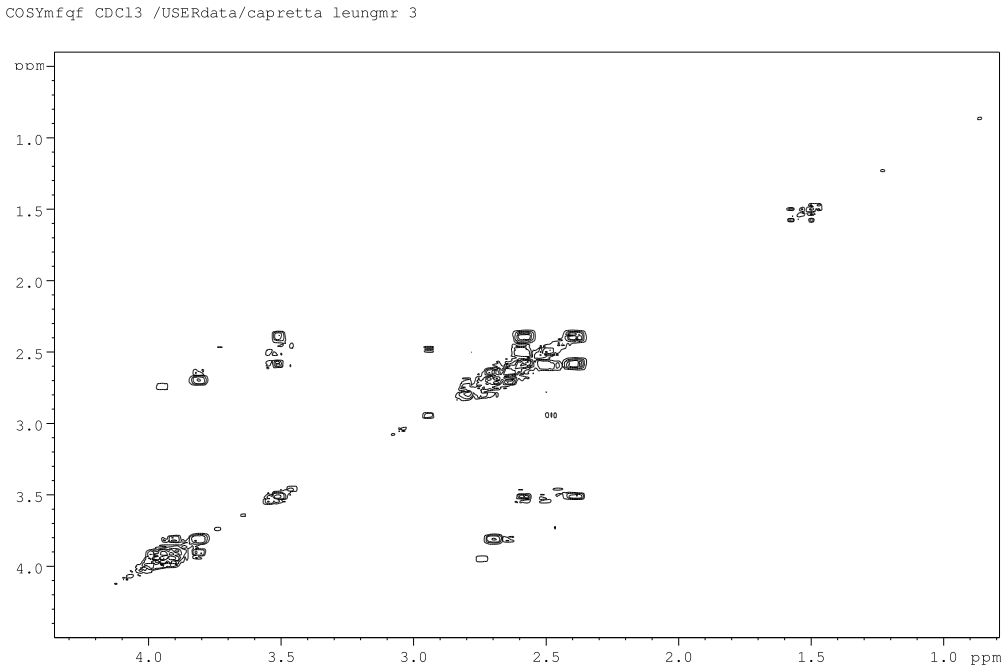

Figure S4-3. COSY of 1,4-Di-*tert*-Butyl (2*S*)-2-[({(4*R*)-3-[(*tert*-Butoxy)carbonyl]-2,2-Dimethyl-1,3-Oxazolidin-4-yl}methyl)amino]butanedioate (**IV-3**)

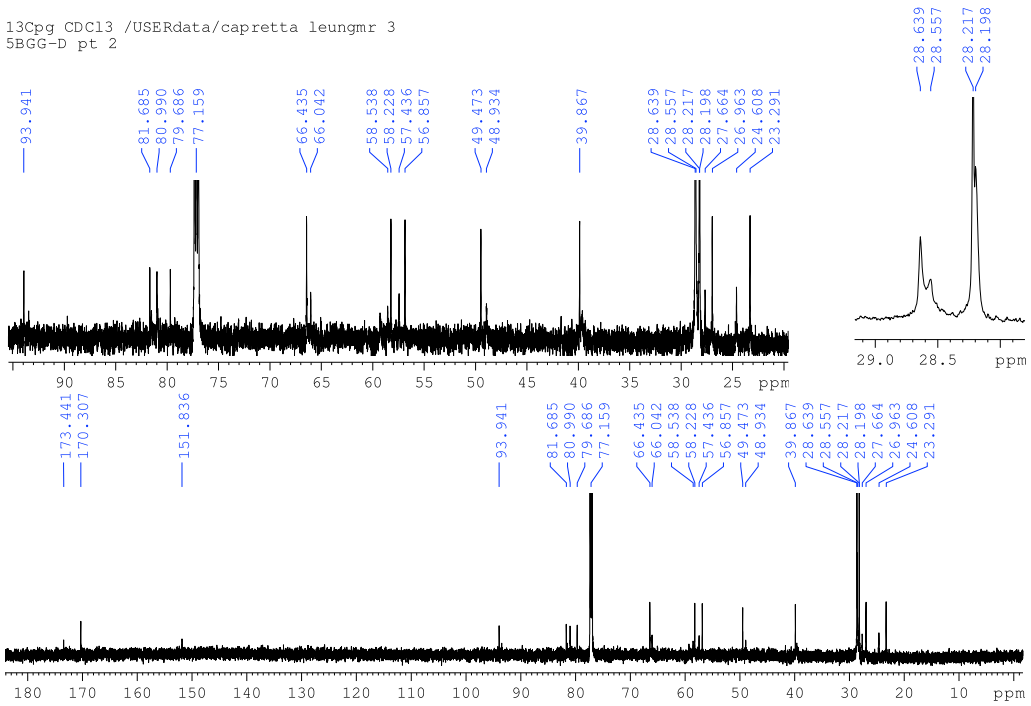

Figure S4-4. ^{13}C NMR of 1,4-Di-*tert*-Butyl (2*S*)-2-[({(4*R*)-3-[(*tert*-Butoxy)carbonyl]-2,2-Dimethyl-1,3-Oxazolidin-4-yl}methyl)amino]butanedioate (**IV-3**)

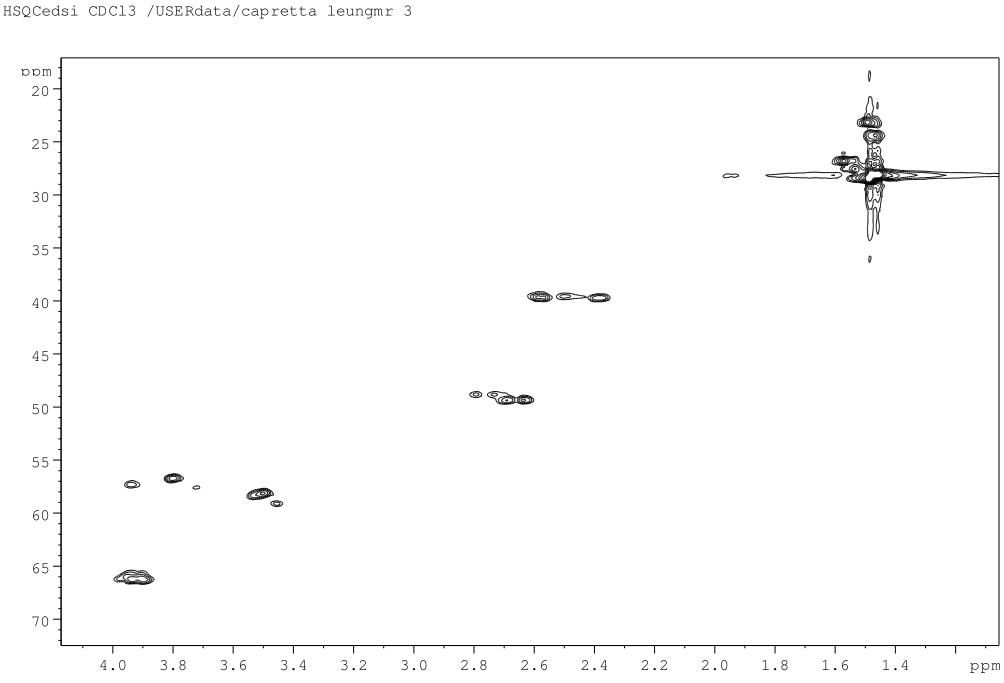

Figure S4-5. HSQC of 1,4-Di-*tert*-Butyl (2*S*)-2-[({(4*R*)-3-[(*tert*-Butoxy)carbonyl]-2,2-Dimethyl-1,3-Oxazolidin-4-yl}methyl)amino]butanedioate (**IV-3**)

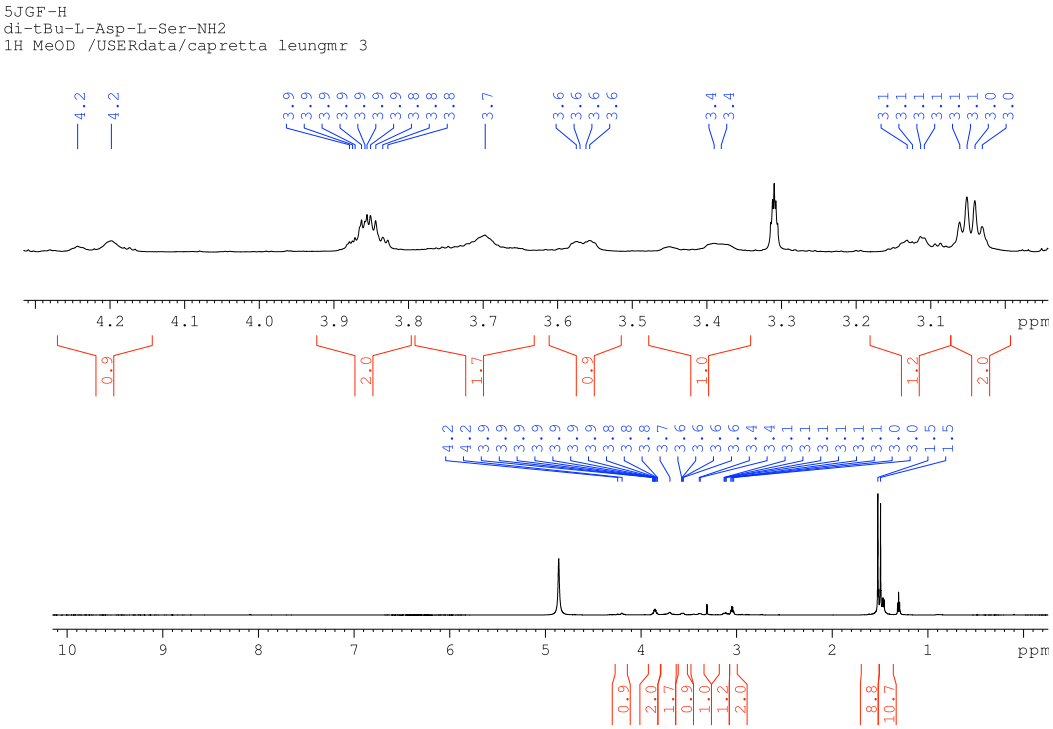

Figure S4-6. ^{1}H NMR of 1,4-Di-*tert*-Butyl (2*S*)-2-{[(2*R*)-2-Amino-3-Hydroxypropyl]amino}butanedioate (**IV-4**)

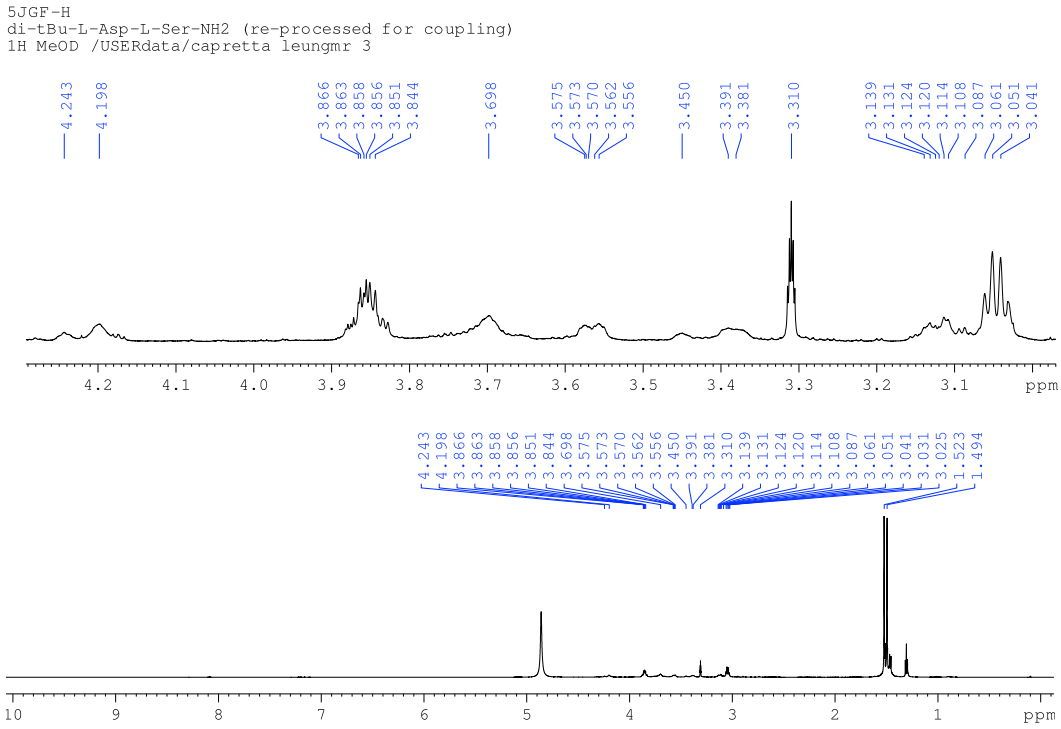

Figure S4-7. Re-processed ^{1}H NMR of (**IV-4**) for coupling constants

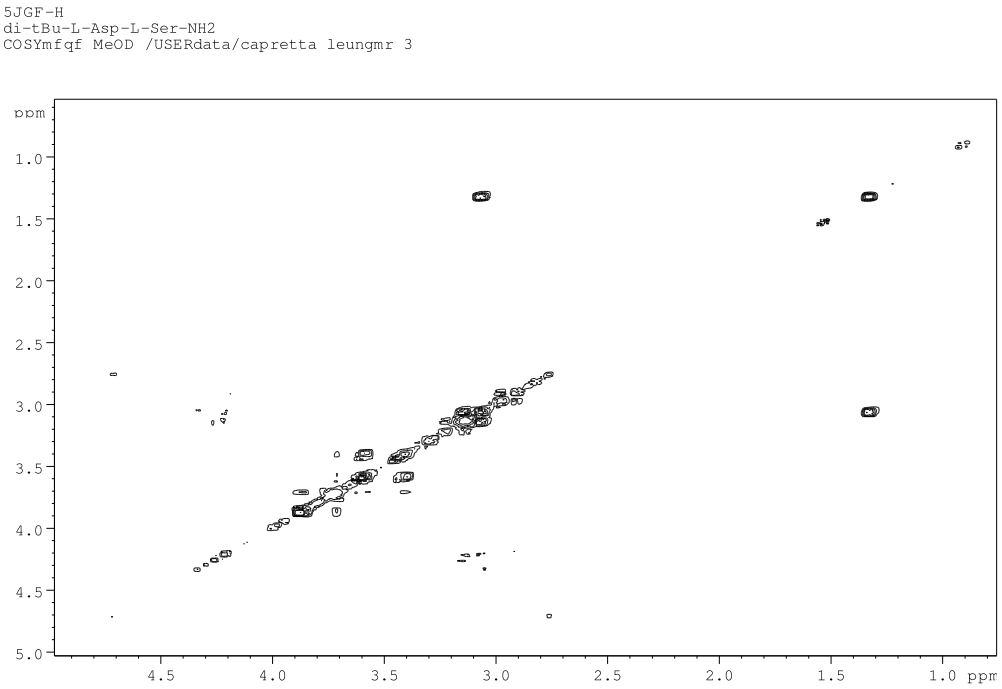

Figure S4-8. COSY of 1,4-Di-*tert*-Butyl (2*S*)-2-{[(2*R*)-2-Amino-3-Hydroxypropyl]amino}butanedioate (**IV-4**)

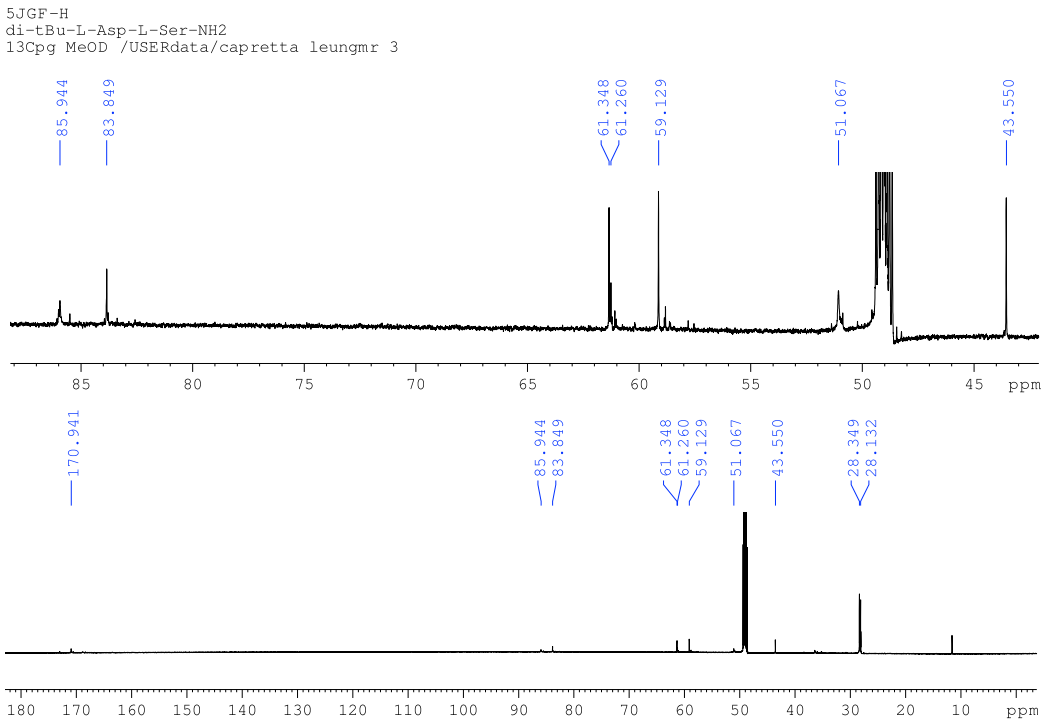

Figure S4-9. ^{13}C NMR of 1,4-Di-*tert*-Butyl (2*S*)-2-{[(2*R*)-2-Amino-3-Hydroxypropyl]amino}butanedioate (**IV-4**)

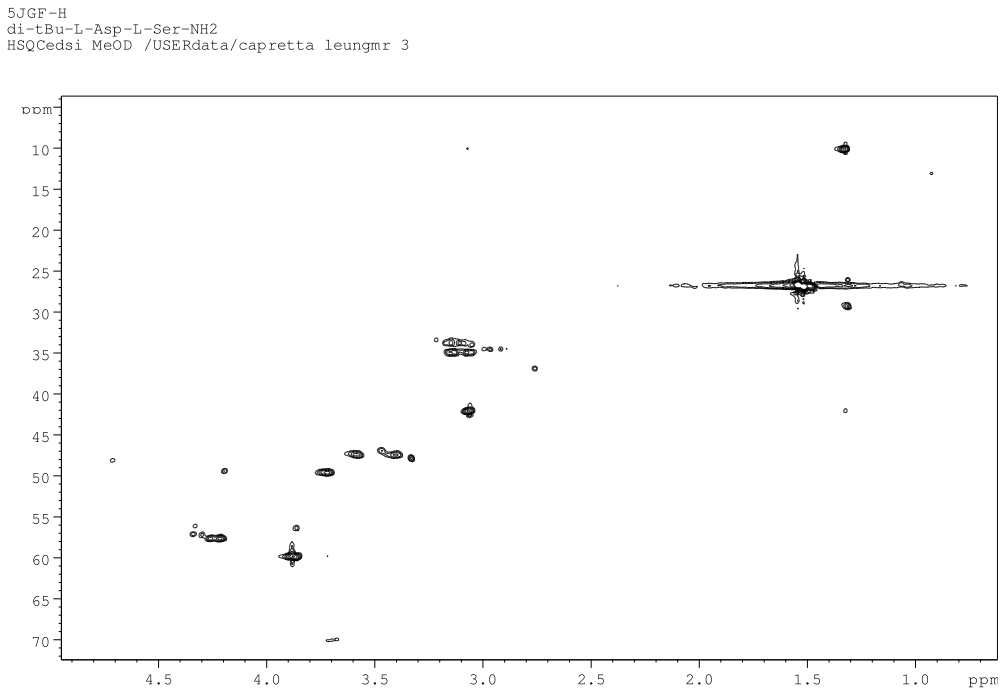

Figure S4-10. HSQC of 1,4-Di-*tert*-Butyl (2*S*)-2-{[(2*R*)-2-Amino-3-Hydroxypropyl]amino}butanedioate (**IV-4**)

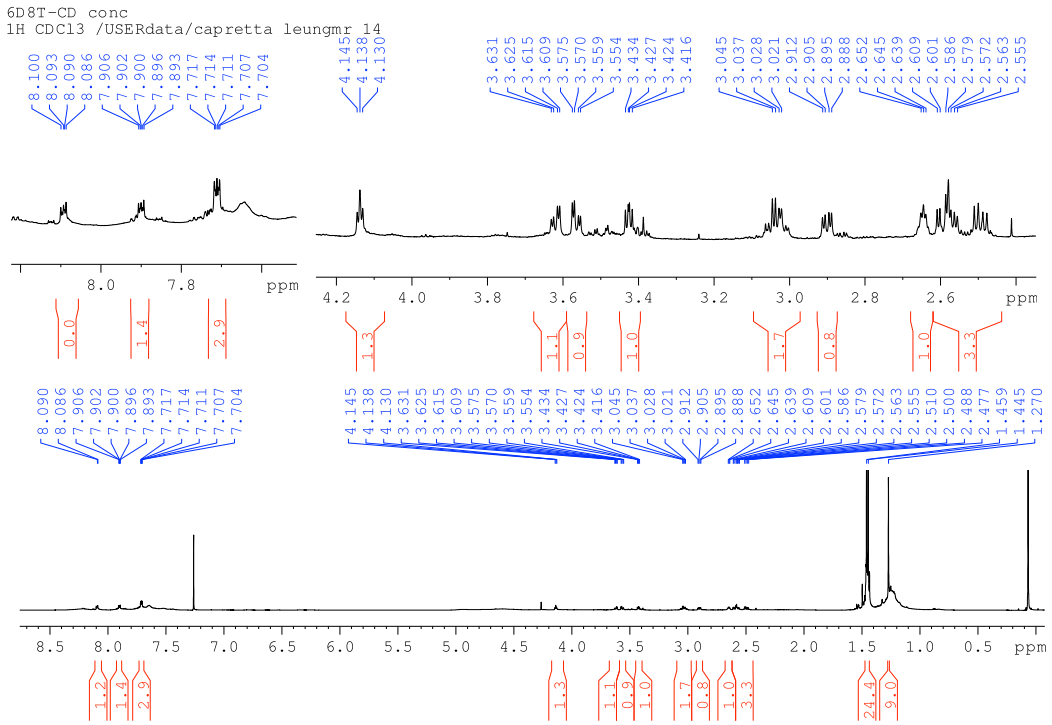

Figure S4-11. ^{1}H NMR of 1,4-Di-*tert*-Butyl (2*S*)-2-{[(2*R*)-2-{[(2*S*)-3-(*tert*-Butoxy)-2-(2-Nitrobenzenesulfonamido)-3-Oxypropyl]amino}-3-Hydroxypropyl]amino}butanedioate (**IV-6**)

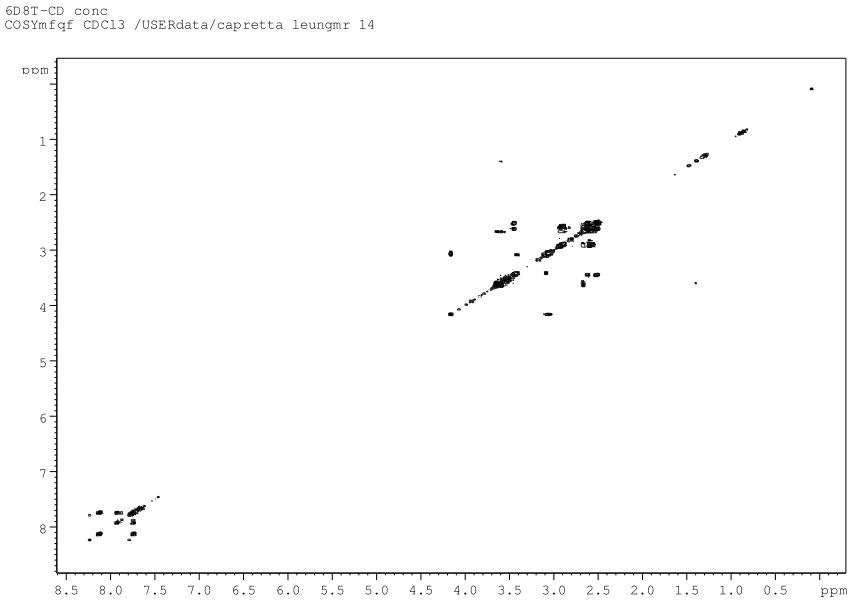

Figure S4-12. COSY of 1,4-Di-*tert*-Butyl (2*S*)-2-{[(2*R*)-2-{[(2*S*)-3-(*tert*-Butoxy)-2-(2-Nitrobenzenesulfonamido)-3-Oxypropyl]amino}-3-Hydroxypropyl]amino}butanedioate (**IV-6**)

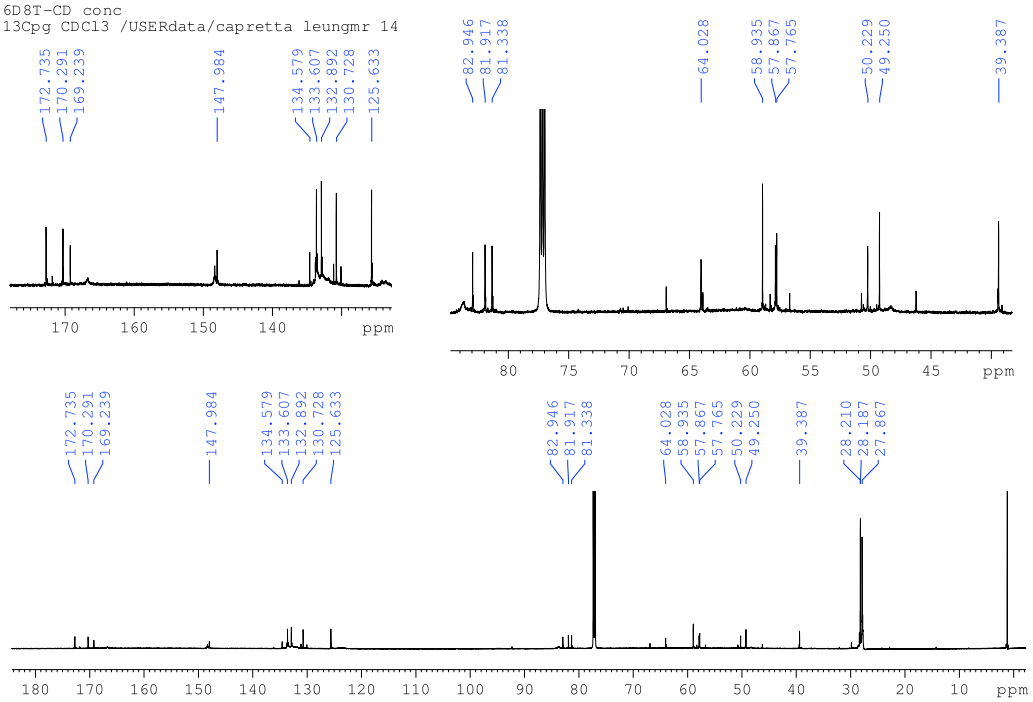

Figure S4-13. ^{13}C NMR of 1,4-Di-*tert*-Butyl (2*S*)-2-{[(2*R*)-2-{[(2*S*)-3-(*tert*-Butoxy)-2-(2-Nitrobenzenesulfonamido)-3-Oxypropyl]amino}-3-Hydroxypropyl]amino}butanedioate (**IV-6**)

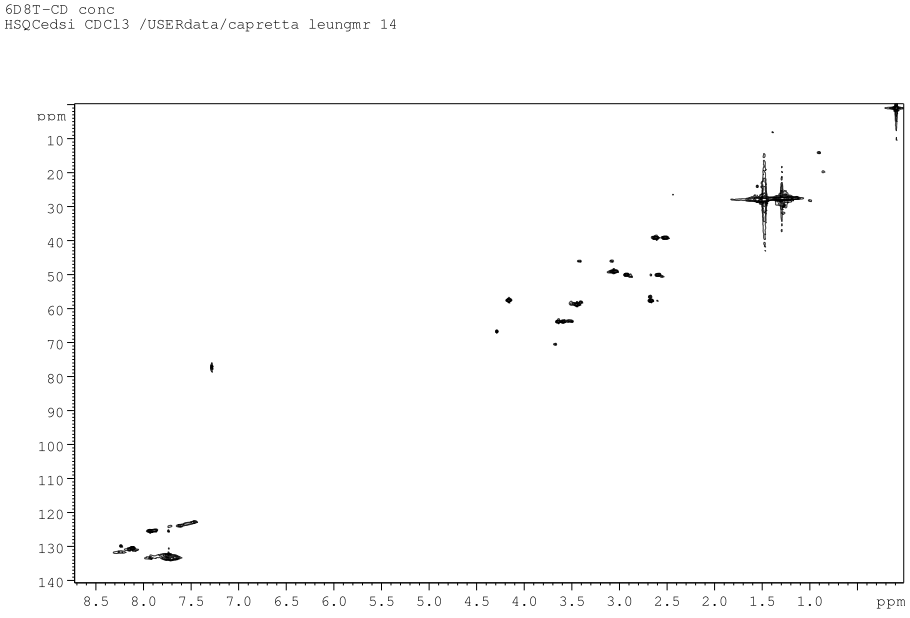

Figure S4-14. HSQC of 1,4-Di-*tert*-Butyl (2*S*)-2-{[(2*R*)-2-{[(2*S*)-3-(*tert*-Butoxy)-2-(2-Nitrobenzenesulfonamido)-3-Oxypropyl]amino}-3-Hydroxypropyl]amino}butanedioate (**IV-6**)

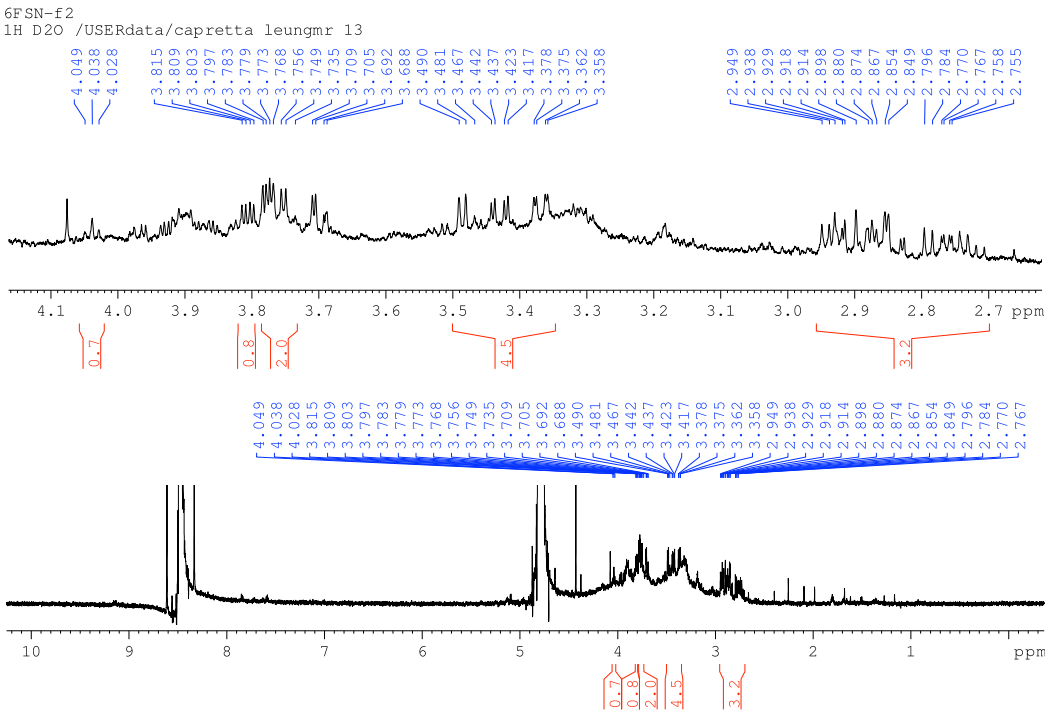

Figure S4-15. ^{1}H NMR of (2*S*)-2-{[(2*R*)-2-{[(2*S*)-2-Amino-2-Carboxyethyl]amino}-3-Hydroxypropyl]amino}butanedioic acid (**IV-8**)

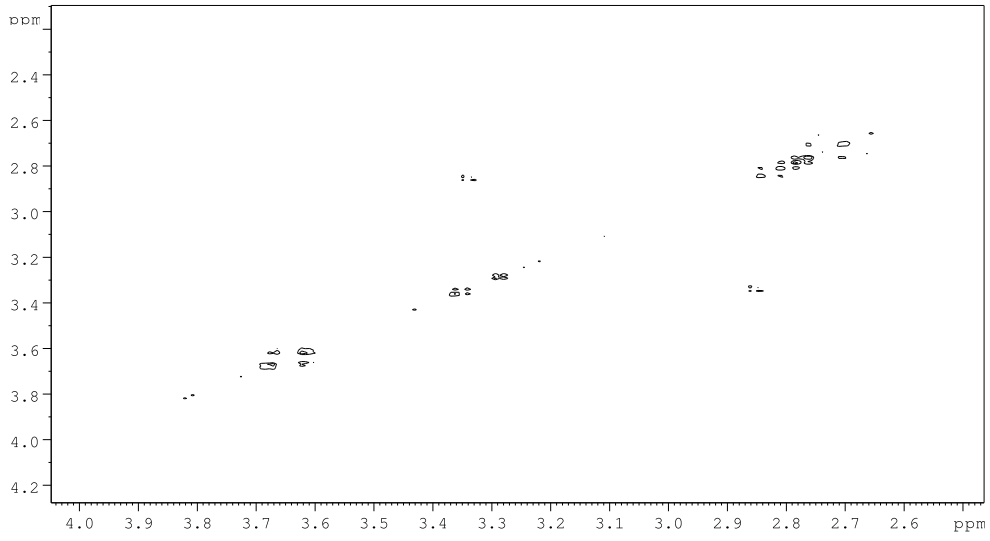

Figure S4-16. COSY of (2*S*)-2-{[(2*R*)-2-{[(2*S*)-2-Amino-2-Carboxyethyl]amino}-3-Hydroxypropyl]amino}butanedioic acid (**IV-8**)

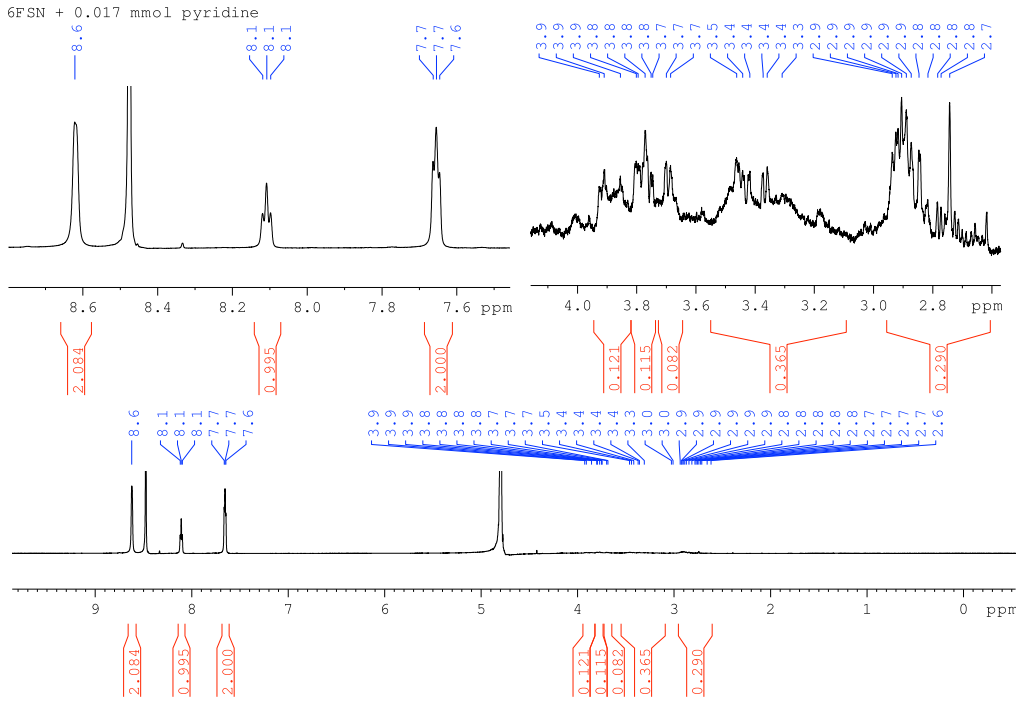

Figure S4-17. ^{1}H NMR of **IV-8** with pyridine as an internal standard for yield determination

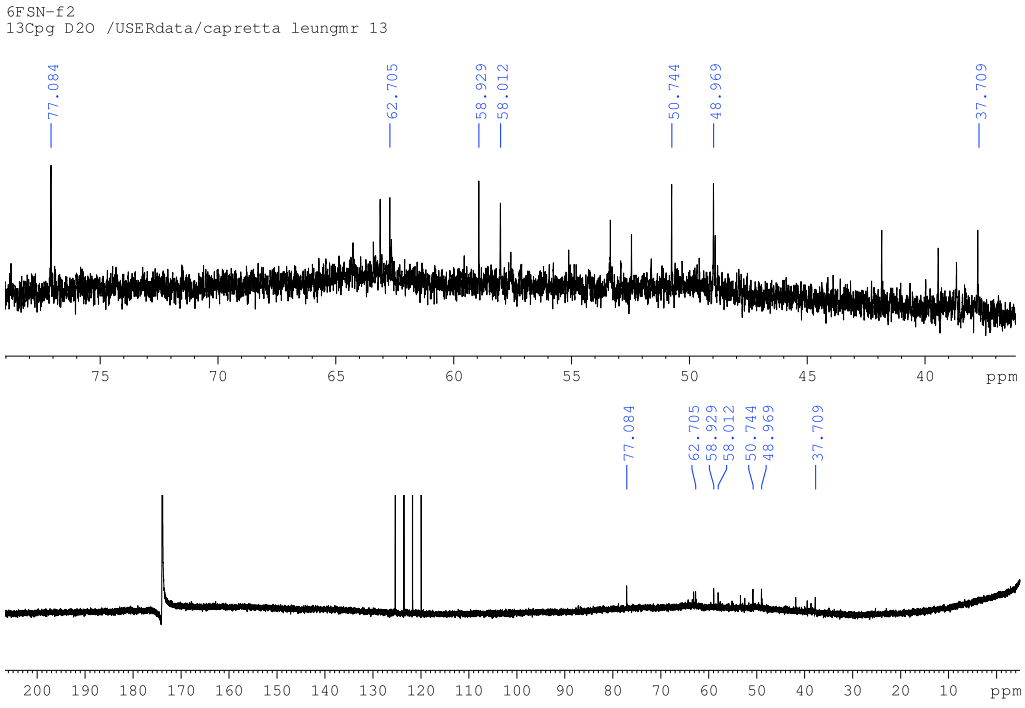

Figure S4-18. ^{13}C NMR of (2*S*)-2-{[(2*R*)-2-{[(2*S*)-2-Amino-2-Carboxyethyl]amino}-3-Hydroxypropyl]amino}butanedioic acid (**IV-8**)

5.0 Conclusions and Future Directions

Aminoglycoside N-acetyltransferase-3, aminoglycoside O-nucleotidyltransferase-2", and New Delhi metallo-β-lactamase-1 are three enzymes responsible for resistance in Gram negative pathogens. AAC(3) and ANT(2") interfere with the activity of aminoglycosides by covalent modifications with acetyl and adenylphosphate groups respectively,[1–5] while NDM-1 inactivates carbapenems by cleaving the β-lactam ring.[6–9] This thesis describes the development of inhibitors to these enzymes, which can be co-prescribed with these classes of antibiotics to suppress resistance and prolong clinical utility.

First, a high-throughput screen using cell- and enzyme-based assays identified the 3-benzylidene-2-indolinone scaffold as an inhibitor of AAC(3)-Ia. A focused library of 28 compounds was made around this scaffold using a Knoevenagel aldol condensation. Preliminary SAR using an Ellman-coupled assay was obfuscated by the poor solubility and high background absorbance of compounds, and lack of replicability in the enzyme purification protocol. Accordingly, a superior purification method using cobalt beads for AAC(3)-Ia was described, and a fluorescence-based biochemical assay was developed. Direct cleavage of the methyl ester at position 5 was attempted, but was not successful, so compound solubility was addressed by selecting polar indolinone building blocks, such as those containing hydroxyl or carboxylic acid groups.

SAR analysis using freshly purified enzyme and the newly-optimized fluorescent assay identified initial hit **II-1** as the best inhibitor (Figure 5-1).

Compound **II-1** has a methyl ester at position 5 and the 3,5-dibromo-4-hydroxybenzyl pharmacophore. Some variability was tolerated at position 5 (R = H, OH, or Br), though activity was affected. Similarly, some activity was retained with loss of the 4-hydroxy and 5-bromo substituents on the benzylidine ring; the 3-bromo group, however, was essential.

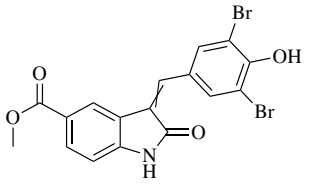

II-1

$IC_{50} = 4.3 \pm 1.4\ \mu M$

Figure 5-1. Lead AAC(3)-Ia Inhibitor **II-1**

These results will direct the assembly of another chemical library designed to improve *in vivo* activity. The 3,5-bromo-4-hydroxy pharmacophore will be retained, and analogs will be made with different substitutions around the 3-benzylidene-2-indolinone scaffold. In particular, analogs with charged and zwitterionic groups will be investigated, as these groups have been implicated in the cellular uptake of antibiotics in Gram-negative pathogens.[10–15]

Furthermore, as the majority of compounds were tested as a mixture of the (*E*)- and (*Z*)-isomers, work will be done to isolate the two isomers, either through selective synthesis or post-synthetic resolution, and test them individually. It is expected that only one isomer would be active due to restrictions within the enzyme's active site. Thus, isomeric resolution should result in an increase in potency, as the presence of the inactive isomer would have decreased the effective concentration. For **II-1**, which had a 2:1 *Z*/*E* ratio, if the (*Z*)-isomer is active, the IC_{50} would be expected to become 2-3 μM. If the (*E*)-isomer is active, the IC_{50} would drop to ~1 μM.

Secondly, kinase inhibitors with a biphenyl isonicotinamide scaffold were identified as inhibitors of ANT(2")-Ia through a previous whole-cell screen.[16] A parallel synthesis was developed, where core scaffold **III-17** was assembled *via* a Suzuki coupling and subsequent Boc and methyl ester deprotections followed by functionalization on either end through amide couplings (Figure 3-11). Further variation could be introduced on the Western end *via* S_NAr on 2-chloropyridine prior to coupling. Using this methodology, a small library was assembled and assayed for activity against *E. coli* BW25113 Δ*tolC* Δ*bamB* producing ANT(2")-Ia.

Remarkably, this extremely focused library (just 19 compounds) was sufficient for SAR analysis. While both original hits had functionalization at position 2 of the Western isonicotinamide, paring this down to the base pyridine ring resulted in superior activity against ANT(2")-Ia. Similarly, the Eastern amide was shown to be detrimental to inhibitory activity, and was replaced with either a carboxylic acid or methyl ester. The carboxylic acid **III-30** had the best activity against ANT(2")-Ia-producing cells (FIC = 0.4) and selectivity over the parent strand. This compound will form the basis of the next generation of ANT(2")-Ia inhibitors (Figure 5-2). Unfortunately, this compound was not shown to inhibit purified ANT(2")-Ia using the previously-reported EnzChek pyrophosphatase assay.[17,18] This may be due to solubility issues of the compound library, or the narrow detection window of the assay.

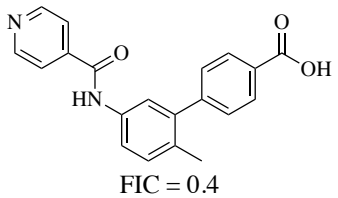

Figure 5-2. Lead ANT(2")-Ia Inhibitor **III-30**

Future work will address both of these issues. A second-generation library will be assembled based off of **III-30**, allowing exploration of substitutions around the ring system. In particular, the effect of polar substituents such as amines and hydroxyls will be investigated in an effort to improve solubility of the library. Other biochemical assays will also be investigated. For instance, a fluorescence-based assay is a more sensitive detection method and less prone to background noise, and thus would provide a larger inhibition detection window.

Finally, while previous AMA analog SAR analyses have explored the effect of stereochemistry, spatial arrangement, and loss of amine and carboxylic acid moieties, investigation into the essentiality of individual carboxylic acid groups was incomplete as previous synthetic strategies were unable to produce analogs lacking the carboxylic acid functionality at position 6.[19–21] A synthetic approach was therefore developed to access this position using Garner's aldehyde as a chiral building block (Figure 4-7). Reductive amination of Garner's aldehyde with *tert*-butyl-protected *L*-aspartic acid was followed by cleavage of the oxazolidine ring and subsequent coupling to an aziridine (an oxidized serine equivalent) to provide AMA analog **IV-8**, which has a hydroxyl group at position 6 in place of the carboxylic acid. A total synthesis of AMA *via* a second reductive amination with Garner's aldehyde was attempted, but unfortunately steric hindrance prevented formation of the imine intermediate.

A crystal structure of compound **IV-3** was obtained. Surprisingly, this showed complete epimerization to the (*S*,*R*)-isomer, despite the use of optically-pure (*S*)-starting materials. It is proposed that the rearrangement to the ene-amine

results in the presence of diastereomeric imines (Figure 4-10). One of these diastereomers is preferentially reduced, and the irreversibility of this step drives the consumption of the other. This method of kinetic resolution is a useful way of obtaining optically-pure products from racemic starting materials.

The next step for this project is to assemble a library of analogs using this methodology. For example, replacing serine with cysteine or 2,3-diaminopropionic acid in the Garner's aldehyde would introduce a thiol or amine group respectively, which could alter binding to zinc (Figure 5-3). These moieties could also be coupled to other functional groups to introduce further variation. This library would then be tested against NDM-1 and other variants to further investigate SAR.

There will also be further investigation into the reductive amination. If reaction conditions can be found to allow the second imine formation, the total synthesis of AMA may be completed *via* this approach. A screen of reducing agents will also be undertaken to identify one that will selectively form the (*S*)-isomer. This would allow stereospecific synthesis of AMA and its analogs from racemic

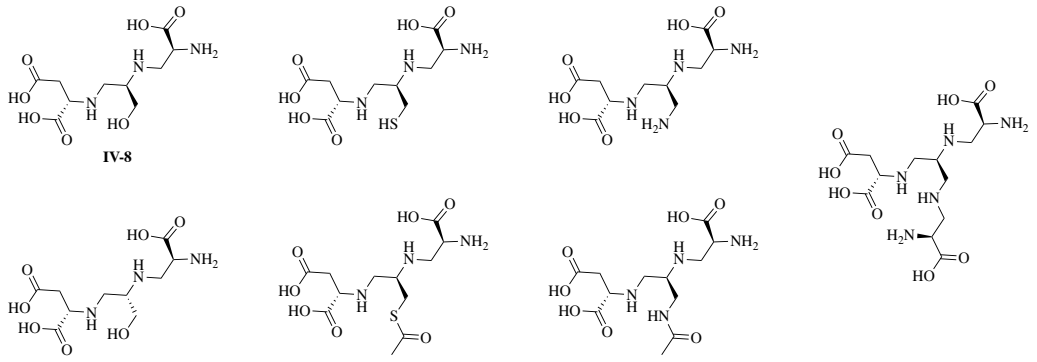

Figure 5-3. AMA Analog **IV-8** and Other Potential Analogs That Could Be Synthesized *via* Reductive Amination of Garner's Aldehyde-Like Building Blocks

starting materials, obviating the need for optically-pure serine equivalents. This imine-driven resolution of stereoisomers could also have applications in other total syntheses.

With a greater focus in recent years on antimicrobial stewardship, the use of adjuvants and other combination therapy strategies is becoming an increasingly attractive approach, giving older classes of antibiotics new life and allowing newer drugs to be reserved for the most desperate cases. There are ample targets against which this approach can be applied, including newer NDM variants with improved zinc affinity and ribosome methyltransferases such as *rmt*.[7,22,23] Furthermore, the techniques described in this thesis- combinatorial and total synthesis, assay development, and structure-activity relationship analysis, are fundamental components of the drug discovery process, both antimicrobial and otherwise. And while primitive remedies have been around since ancient times, modern medicine is dependent on the continued influx of new and improved therapies to alleviate suffering.

5.1 REFERENCES

(1) Shaw, K. J.; Rather, P. N.; Hare, R. S.; Miller, G. H. Molecular Genetics of Aminoglycoside Resistance Genes and Familial Relationships of the Aminoglycoside-Modifying Enzymes. *Microbiol. Rev.* **1993**, *57* (1), 138–163.

(2) Gonzalez, U. S.; Spencer, J. P. Aminoglycosides: A Practical Review. *Am. Fam. Physician* **1998**, *58* (8), 1811–1820.

(3) Wright, G. D.; Thompson, P. R. Aminoglycoside Phosphotransferases: Proteins, Structure, and Mechanism. *Front. Biosci.* **1999**, *4*, 9–21.

(4) Labby, K. J.; Garneau-Tsodikova, S. Strategies to Overcome the Action of Aminoglycoside-Modifying Enzymes for Treating Resistant Bacterial Infections. *Future Med. Chem.* **2013**, *5* (11), 1285–1309.

(5) Cox, G.; Stogios, P. J.; Savchenko, A.; Wright, G. D. Structural and Molecular Basis for Resistance to Aminoglycoside Antibiotics by the Adenylyltransferase ANT(2″)-Ia. *MBio* **2015**, *6* (1), e02180-14.

(6) Yong, D.; Toleman, M. A.; Giske, C. G.; Cho, H. S.; Sundman, K.; Lee, K.; Walsh, T. R. Characterization of a New Metallo-Beta-Lactamase Gene, Bla(NDM-1), and a Novel Erythromycin Esterase Gene Carried on a Unique Genetic Structure in Klebsiella Pneumoniae Sequence Type 14 from India. *Antimicrob. Agents Chemother.* **2009**, *53* (12), 5046–5054.

(7) Wu, W.; Feng, Y.; Tang, G.; Qiao, F.; McNally, A.; Zong, Z. NDM Metallo-β-Lactamases and Their Bacterial Producers in Health Care Settings. *Clin. Microbiol. Rev.* **2019**, *32* (2), e00115-18.

(8) Linciano, P.; Cendron, L.; Gianquinto, E.; Spyrakis, F.; Tondi, D. Ten Years with New Delhi Metallo-β-Lactamase-1 (NDM-1): From Structural Insights to Inhibitor Design. *ACS Infect. Dis.* **2019**, *5*, 9–34.

(9) Tooke, C. L.; Hinchliffe, P.; Bragginton, E. C.; Colenso, C. K.; Hirvonen, V. H. A.; Takebayashi, Y.; Spencer, J. β-Lactamases and β-Lactamase Inhibitors in the 21st Century. *J. Mol. Biol.* **2019**, https://doi.org/10.1016/j.jmb.2019.04.002.

(10) Bryskier, A.; Aszodi, J.; Chantot, J.-F. Parenteral Cephalosporin Classification. *Expert Opin. Investig. Drugs* **1994**, *3* (2), 145–171.

(11) O'Shea, R.; Moser, H. E. Physicochemical Properties of Antibacterial Compounds: Implications for Drug Discovery. *J. Med. Chem.* **2008**, *51* (10), 2871–2878.

(12) Delcour, A. H. Outer Membrane Permeability and Antibiotic Resistance. *Biochim. Biophys. Acta* **2009**, *1794* (5), 808–816.

(13) Hancock, R. E. W.; Bell, A. Antibiotic Uptake into Gram-Negative Bacteria. *Eur. J. Clin. Microbiol. Infect. Dis* **1988**, *7* (6), 713–720.

(14) Trimble, M. J.; Mlynárčik, P.; Kolář, M.; Hancock, R. E. W. Polymyxin: Alternative Mechanisms of Action and Resistance. *Cold Spring Harb. Perspect. Med.* **2016**, *6* (10), a025288.

(15) Taber, H. W.; Mueller, J. P.; Miller, P. F.; Arrow, A. S. Bacterial Uptake of Aminoglycoside Antibiotics. *Microbiol. Rev.* **1987**, *51* (4), 439–457.

(16) Cox, G.; Sieron, A.; King, A. M.; De Pascale, G.; Pawlowski, A. C.; Koteva, K.; Wright, G. D. A Common Platform for Antibiotic Dereplication and Adjuvant Discovery. *Cell Chem. Biol.* **2017**, *24* (1), 98–109.

(17) Hirsch, D. R.; Cox, G.; D'Erasmo, M. P.; Shakya, T.; Meck, C.; Mohd, N.; Wright, G. D.; Murelli, R. P. Inhibition of the ANT(2″)-Ia Resistance Enzyme and Rescue of Aminoglycoside Antibiotic Activity by Synthetic α-Hydroxytropolones. *Bioorg. Med. Chem. Lett.* **2014**, *24* (21), 4943–4947.

(18) *EnzChek® Pyrophosphate Assay Kit (E-6645)*.

(19) Koteva, K.; King, A. M.; Capretta, A.; Wright, G. D. Total Synthesis and Activity of the Metallo-β-Lactamase Inhibitor Aspergillomarasmine A. *Angew. Chemie Int. Ed.* **2016**, *55* (6), 2210–2212.

(20) Albu, S. A.; Koteva, K.; King, A. M.; Al-Karmi, S.; Wright, G. D.; Capretta, A. Total Synthesis of Aspergillomarasmine A and Related Compounds: A Sulfamidate Approach Enables Exploration of Structure-Activity Relationships. *Angew. Chemie Int. Ed.* **2016**, *55* (42), 13259–13262.

(21) Zhang, J.; Wang, S.; Bai, Y.; Guo, Q.; Zhou, J.; Lei, X. Total Syntheses of Natural Metallophores Staphylopine and Aspergillomarasmine A. *J. Org. Chem.* **2017**, *82* (24), 13643–13648.

(22) Hidalgo, L.; Hopkins, K. L.; Gutierrez, B.; Ovejero, C. M.; Shukla, S.; Douthwaite, S.; Prasad, K. N.; Woodford, N.; Gonzalez-Zorn, B. Association of the Novel Aminoglycoside Resistance Determinant RmtF with NDM Carbapenemase in Enterobacteriaceae Isolated in India and the UK. *J. Antimicrob. Chemother.* **2013**, *68* (7), 1543–1550.

(23) Cox, G.; Ejim, L.; Stogios, P. J.; Koteva, K.; Bordeleau, E.; Evdokimova, E.; Sieron, A. O.; Savchenko, A.; Serio, A. W.; Krause, K. M.; et al. Plazomicin Retains Antibiotic Activity against Most Aminoglycoside Modifying Enzymes. *ACS Infect. Dis.* **2018**, *4* (6), 980–987.